The role of the *Bacillus subtilis* ParABS system in DNA replication and segregation

Alan Koh Soon Chai

Thesis submitted in partial fulfilment of the requirements of the regulation for the degree of Doctor of Philosophy

Newcastle University

Faculty of Medical Sciences

Institute of Cell and Molecular Biosciences

9th February 2015

Abstract

The partitioning of low-copy number plasmids into daughter cells requires the plasmid encoded ParA and ParB proteins acting on centromeric sites termed *parS*. Bioinformatics approaches have shown that bacterial chromosome also encodes the ParABS system (Livny et al., 2007). In *B. subtilis* the majority of the chromosomally encoded *parS* sites are located near the replication origin region where they are bound by Spo0J (ParB), forming a set of nucleoprotein complexes that colocalizes with *oriC* (Breier and Grossman, 2007; Graham et al., 2014; Lin and Grossman, 1998; Livny et al., 2007; Murray et al., 2006). SMC complex (condensin) localization at *oriC* is dependent on Spo0J and is required for chromosome origin segregation (Gruber and Errington, 2009; Sullivan et al., 2009; Wang et al., 2014b). In addition Spo0J regulates Soj (ParA), which in turn controls the master DNA replication initiation protein DnaA (Murray and Errington, 2008; Scholefield et al., 2012; Scholefield et al., 2011). Therefore, I hypothesized that the localization of *parS* sites proximal to the replication origin might be important for the regulation of Soj by Spo0J.

In this thesis I have constructed a range of genetically modified strains that differ in the number and location of *parS* sites. I have found that a single Spo0J:*parS* nucleoprotein complex is necessary and sufficient for effective regulation of Soj activity, and that this regulation is independent of the genetic context of the *parS* site. In contrast chromosome organization and origin region segregation were affected when Spo0J (and presumably condensin) was redistributed to ectopic locations. Finally, I provide evidence that Soj interacts with Spo0J:*parS* nucleoprotein complexes to promote DNA segregation and dictate chromosome orientation. I propose a model that integrates the roles of

Soj as a regulator of DNA replication initiation and chromosome origin segregation.

Acknowledgement

Firstly, I would like to thank Dr Heath Murray for giving me the opportunity to work on this exciting PhD project and his infectious enthusiasm for science is beyond words. His unflagging support and advice throughout these years have made me both a better scientist and a person.

I would like to thank all past and present members in the Centre for Bacterial Cell biology for their friendship and making the lab as warm and cosy as possible. A special thanks to Mr Ian Selmes for the seamless running of the day to day operation in the lab.

A really big thank you to all my friends especially Nadia Rostami, David Forest, David Adams, Declan Gray, David Roberts, Guan Thee, Hazel Chow, and Hua Khee for never letting me doubt myself and for reminding me there is a world outside of my PhD.

Last but not least, to my family at home, Mom, Dad, Mama, Brandon, Desmond, Ting Ting, Groover and Chicky Baby for their continuous love and undying support for my dreams! You guys made me into who I am.

Finally to everyone, I have finally made it! To infinity and beyond!

Publication

Murray, H., and Koh, A. (2014). Multiple regulatory systems coordinate DNA replication with cell growth in Bacillus subtilis. Plos Genet *10*, e1004731.

Table of Contents

Chapter 1: Introduction

Replication and segregation of chromosomal DNA must be tightly regulated to ensure the viability of all organisms, and mutations that affect this regulation often lead to defects in cell growth. Although different organisms use a variety of complex molecular mechanisms to precisely control replication, organisms across the domains of life share the basic machinery consisting of initiator proteins (the origin replication complex (ORC) in eukaryotes and DnaA in prokaryotes) that interact with specialized genomic regions called replication origins to initiate DNA synthesis. Subsequently the newly replicated DNA molecules are organized to facilitate accurate segregation prior to cell division. The focus of this thesis is the regulation of chromosome replication and segregation in the Gram-positive bacterium *Bacillus subtilis* (Figure 1.0.1). Bacteria, with their relatively simple and well characterised structure and physiology, are ideal systems with which to study these mechanisms because they are readily amenable to genetic manipulation.

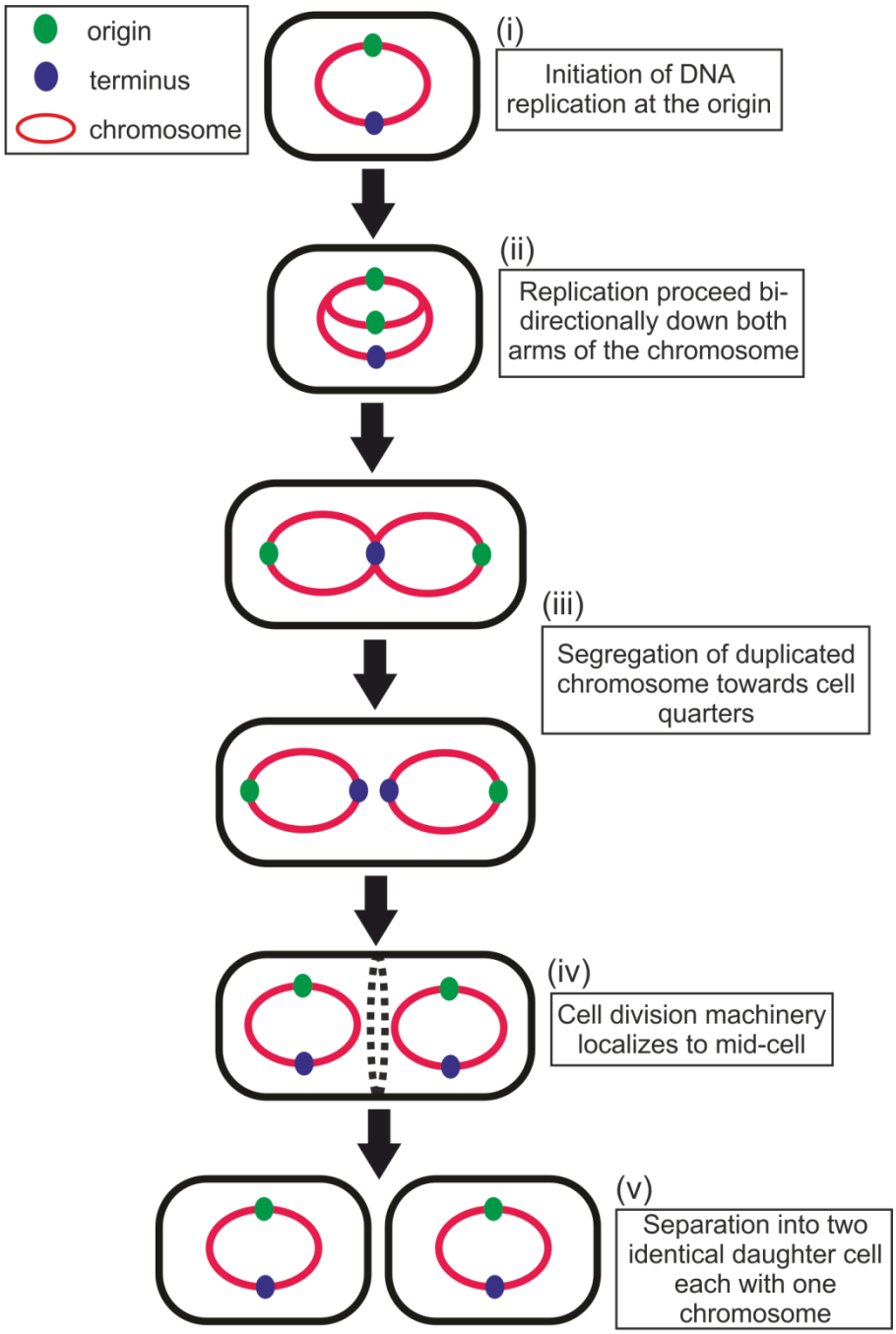

Figure 1.0.1: Overview of *B. subtilis* cell cycle

Cartoon representation of *B. subtilis* cell cycle. (i) Initiation of DNA replication occur at the origin on the circular chromosome. (ii) Replication proceeds bi-directionally down both arms of the chromosome. (iii) Duplicated origins are segregated towards the cell quarters. (iv) The cell division machinery localizes at mid-cell and the subsequent formation of the new cell pole. (v) Two identical daughter cells, each containing one complete circular chromosome.

1.1 DnaA, the master initiator of DNA replication in bacteria

DnaA is the ubiquitous master bacterial DNA replication initiation protein that promotes opening of the DNA duplex and the deposition of the DNA replication machinery. DnaA is a 50 kDa multi-domain protein (446 amino acids) belonging to the AAA+ family of ATPases. It is comprised of four distinct functional domains (Figure 1.1.1). Domain IV, located at the C-terminus of the protein, contains both the helix-turn-helix motif that contacts the major groove and the unique basic loop that mediates contact with the minor groove of the double stranded DNA after binding to specific DnaA-box located within the *oriC* (Erzberger et al., 2002; Fujikawa et al., 2003). Domain III contains the unique initiator specific motifs that are characteristic of the AAA+ protein superfamily forming the αβα base and an α helical bundle called the lid (Iyer et al., 2004). The structure consists of a Walker A (P-loop) motif required for ATP binding; a Walker B motif involved in ATP hydrolysis and magnesium ion interaction with ATP; Sensor I and II motifs involved in ATP binding and hydrolysis, and located at the bottom of the AAA+ module and at the tip of the lid, respectively; the BoxVII arginine finger that contacts the γ-phosphate of the nucleotide and is required for DnaA oligomerization; and finally, the α3/α4 and α5/α6 helices that bind to single stranded DNA. Together these form a bipartite ATP binding site (Duderstadt et al., 2011; Erzberger et al., 2006; Felczak and Kaguni, 2004; Kawakami et al., 2005; Kawakami et al., 2006; Nishida et al., 2002). Domain IV is connected to domain III by an amphipathic region that interacts with membrane phospholipids and facilitates nucleotide exchange, which has been shown to increase the amount of ATP-bound DnaA (DnaA-ATP) in *Escherichia Coli* (*E. coli*). However, it is worth noting that the affinity of DnaA for nucleotide varies in different bacterial species and the half-life of the *B. subtilis* DnaA with

nucleotide is 10 times longer than that of the *E. coli* protein, suggesting that the majority of DnaA in *B. subtilis* is always bound to the more abundant ATP (Erzberger et al., 2006; Garner and Crooke, 1996; Kurokawa et al., 2009). Linking domain I with domains III-IV is the flexible and poorly conserved domain II that may be involved in positioning of domain I and effectively exposing the helicase interaction site (Abe et al., 2007; Molt et al., 2009). Domain I at the N-terminus interacts with additional proteins to facilitate the loading of helicase, DnaA dimerization, and it may also stabilize the open complex by interacting weakly with single stranded DNA (Abe et al., 2007; Seitz et al., 2000; Simmons et al., 2003).

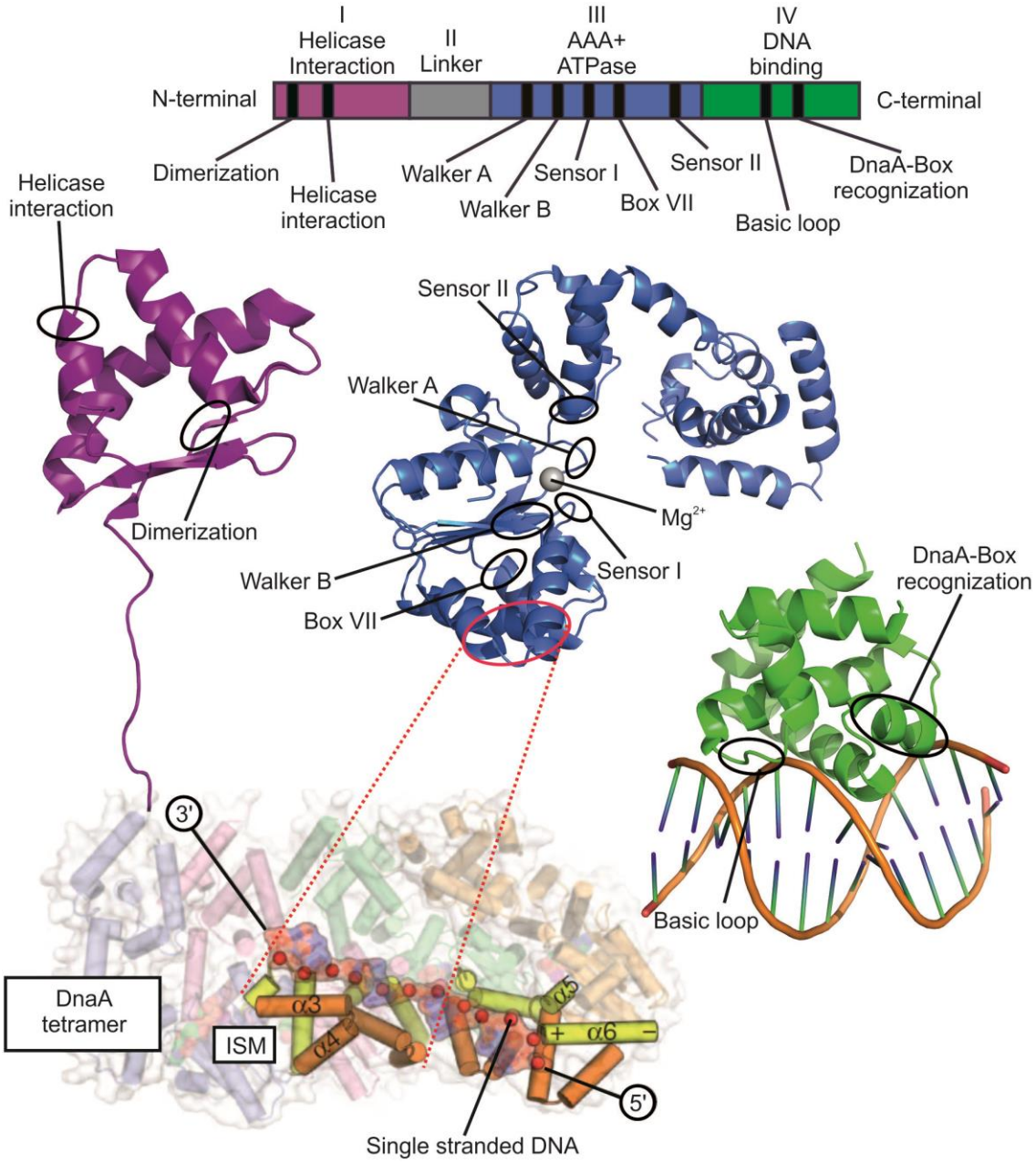

Figure 1.1.1: Structural domains of DnaA

Schematic diagram showing the four functional domains of DnaA with their corresponding crystal structures. The functional regions in each domain are indicated by black ovals. DnaA domains were obtained from the protein data bank (PDB ID; domain I – 2E0G, domain III – 2HCB, domain IV – IJIV). DnaA tetramer image adapted from (Duderstadt et al., 2011).

1.2 Initiation of DNA replication by DnaA at *oriC*

The accurate synthesis of bacterial chromosomes requires precise coordination and regulation of DnaA assembly at the replication origin (*oriC*). Based largely on work using *E. coli* as the model organism, the minimal *oriC* consists of two functional regions with different types of binding sites.

Bacterial replication origins contain multiple DnaA-boxes (consensus sequence of 5'-TTATCCACA-3') that are specifically recognized by domain IV of DnaA and are bound with different affinities (Mott, 2007). The number and orientation of DnaA-boxes within species vary, making it difficult to formulate a universal mechanism for bacterial origin activity (Messer, 2002). However, it is clear that to initiate DNA replication, DnaA-ATP binds to the high affinity DnaA-boxes (Figure 1.2.1i) to promote oligomerization and assembly into a helical filament (Figure 1.2.1ii) (McGarry et al., 2004; Miller et al., 2009; Rozgaja et al., 2011; Scholefield et al., 2012; Scholefield and Murray, 2013).

The formation of the DnaA helix at *oriC* is thought to stretch one strand of the DNA duplex to promote opening of the intrinsically unstable AT-rich DNA unwinding element (DUE) (Figure 1.2.1iii) (Bramhill and Kornberg, 1988a, b). Following DNA duplex unwinding by DnaA in *B. subtilis*, DnaC (helicase) is loaded onto the single stranded DNA by DnaI (helicase loader). Here this reaction is facilitated by two other essential replication initiation proteins, DnaB and DnaD (Rokop et al., 2004). DnaD interacts with DnaA to enhance duplex unwinding of the DUE region and recruits DnaB (Ishigo-Oka et al., 2001; Zhang et al., 2008), which in turn interacts physically with DnaI to form a pair of helicase loaders that load DnaC onto the DNA (Velten et al., 2003). Therefore, in *B. subtilis* these factors are recruited to the origin in the following linear fashion DnaA → DnaD → DnaB → DnaI:DnaC , loading the replicative helicase

and forming the prepriming complex (Figure 1.2.1iv) (Smits et al., 2010). Following enlargement of the DUE by helicase, DNA primase and DNA polymerase coupled with the DNA sliding clamp mediate the synthesis of primer RNA and complementary DNA, respectively, to initiate DNA synthesis (Figure 1.2.1v).

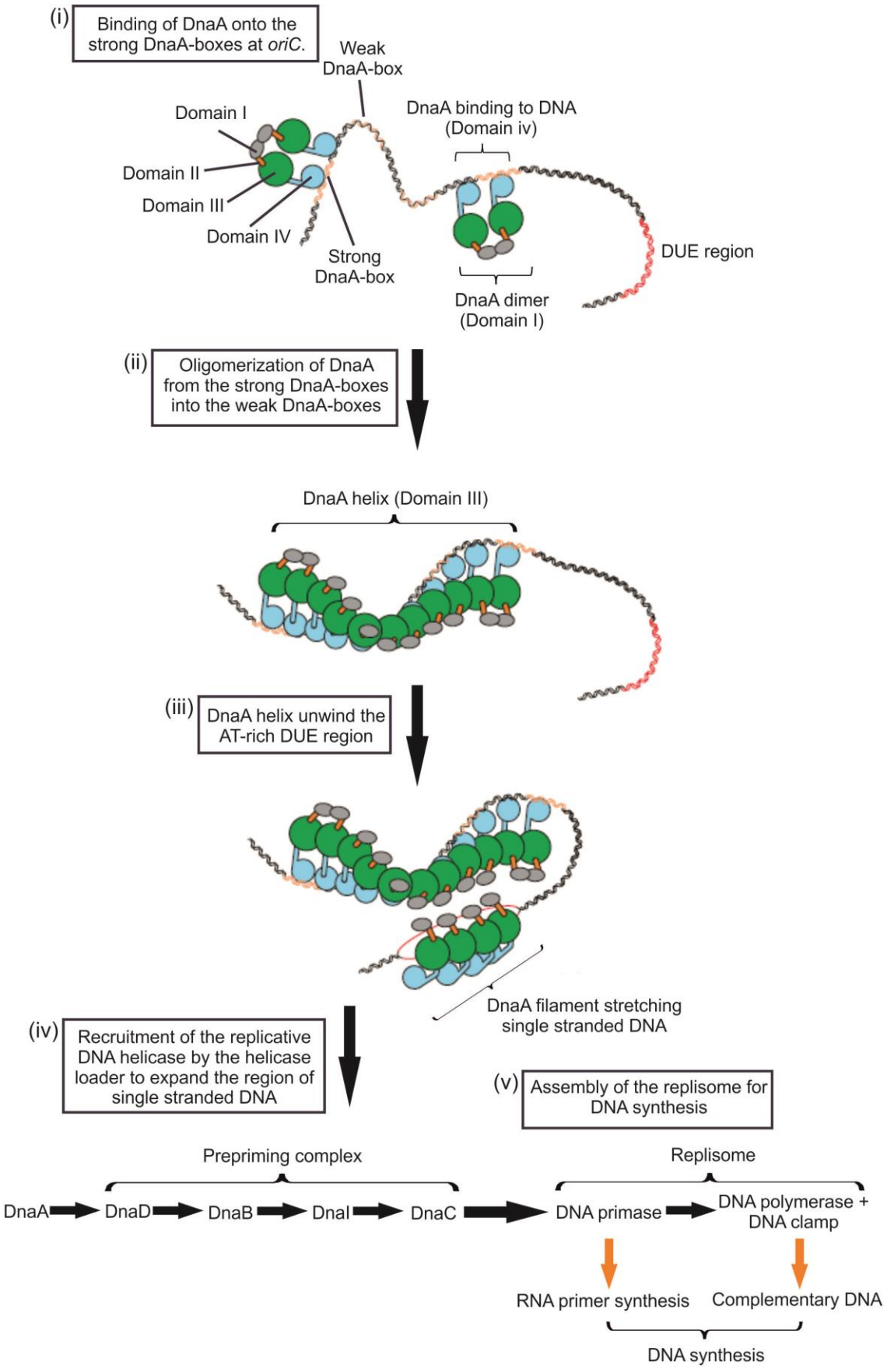
(i) Binding of DnaA onto the strong DnaA-boxes at oriC.
Weak DnaA-box
Domain I
Domain II
Domain III
Domain IV
DnaA binding to DNA (Domain iv)
Strong DnaA-box
DUE region
DnaA dimer (Domain I)
(ii) Oligomerization of DnaA from the strong DnaA-boxes into the weak DnaA-boxes
DnaA helix (Domain III)
(iii) DnaA helix unwind the AT-rich DUE region
DnaA filament stretching single stranded DNA
(iv) Recruitment of the replicative DNA helicase by the helicase loader to expand the region of single stranded DNA
(v) Assembly of the replisome for DNA synthesis
Prepriming complex
Replisome
DnaA
DnaD
DnaB
DnaI
DnaC
DNA primase
DNA polymerase + DNA clamp
RNA primer synthesis
Complementary DNA
DNA synthesis

Figure 1.2.1: DnaA at the origin of replication

Cartoon representation of the formation of the DnaA helix at *oriC*. (i) DnaA binds to strong DnaA-boxes located at *oriC* throughout the cell cycle. (ii) DnaA helix formation leads to DnaA spreading away from the strong DnaA-boxes towards the weaker DnaA-boxes. (iii) Unwinding of the DUE region by the DnaA helix and stabilization of the open complex formation by DnaA. (iv) Recruitment of downstream replication initiation proteins to form the prepriming complex. (v) Assembly of the replisome leads to DNA synthesis. Figure modified from (Scholefield et al., 2012).

1.3 Regulation of initiation in *B. subtilis* during vegetative growth

The assembly of DnaA at *oriC* must be tightly regulated to promote timely initiation during the cell cycle and to avoid aberrant initiation events that could be detrimental to cell viability. During vegetative growth *B. subtilis* employs several mechanisms that control the activity of DnaA at *oriC*. Regulatory mechanisms include: (i) prevention of DnaA helix formation at *oriC* by Soj, YabA and DnaD through interactions with domain III of DnaA; (ii) YabA sequestering DnaA away from *oriC* by tethering DnaA to the replisome; (iii) autoregulation by DnaA expression; (iv) redistribution of DnaA to DnaA-box clusters that are located away from *oriC* (Figure 1.3.1).

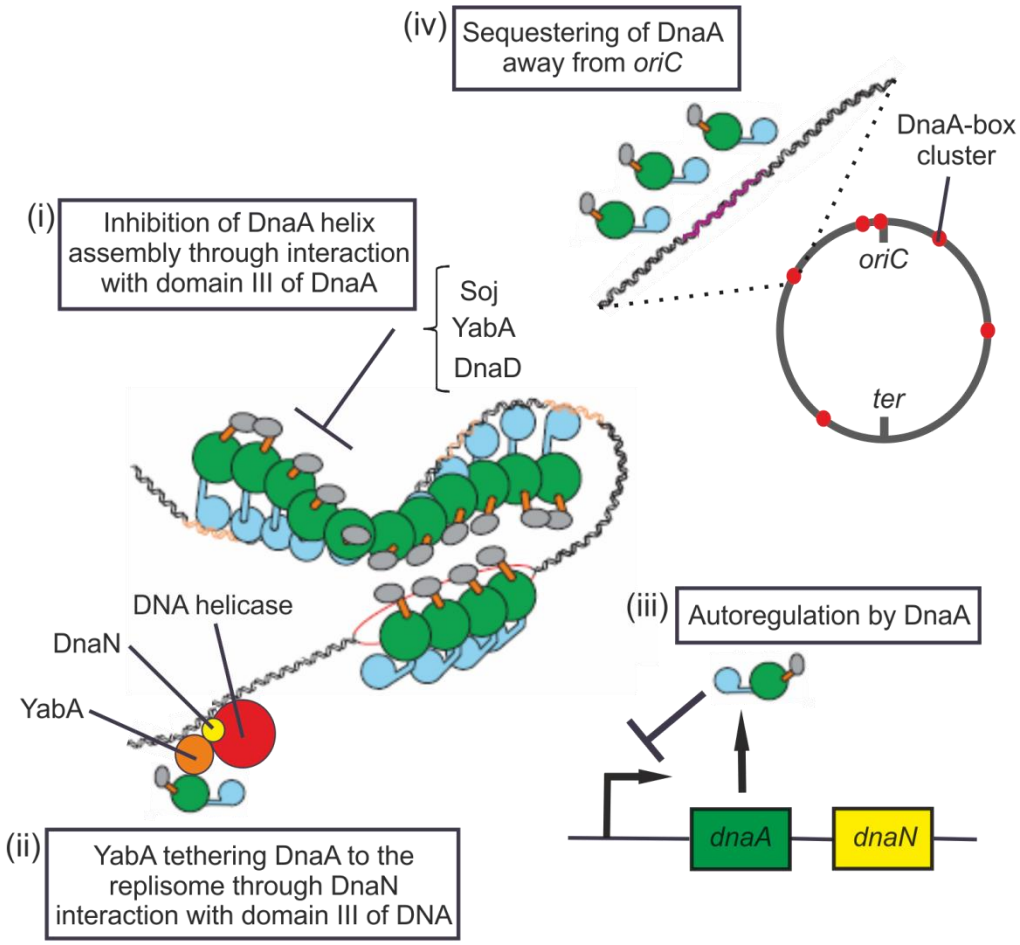

Figure 1.3.1: Regulation of initiation in *B. subtilis* during vegetative growth

Cartoon representation showing regulators of DNA replication initiation during vegetative growth. (i) Inhibition of DnaA helix formation at *oriC* by Soj, YabA and DnaD through interactions with domain III of DnaA. (ii) YabA sequestering DnaA away from *oriC* by tethering DnaA to the replisome. (iii) Autoregulation by DnaA. (iv) Redistribution of DnaA to DnaA-box clusters located away from *oriC*.

1.3.1 Soj controls DNA replication initiation by preventing DnaA helix formation

Soj (ParA) is a Walker-type ATPase that contains a P-loop motif for ATP binding and hydrolysis (Leonard et al., 2005). A *soj* null mutant overinitiates DNA replication, indicating that Soj is primarily an inhibitor of DNA replication initiation (Murray and Errington, 2008). However, overexpression of Soj (or deletion of *spo0J*) leads to an increase in replication initiation (Ogura et al., 2003), suggesting that Soj can undergo a switch in its regulatory activities. Biochemical analysis of Soj revealed that it forms an ATP dependent sandwich dimer (Leonard et al., 2005; Murray and Errington, 2008; Scholefield et al., 2011), and it was subsequently shown that the regulatory activity of Soj on DNA replication initiation is dictated by its nucleotide-bound state (Figure 1.3.1.1) (Scholefield et al., 2011). Monomeric Soj (either apo or ADP-bound) inhibits DNA replication initiation by directly interacting with domain III of DnaA and specifically preventing DnaA oligomerization (Figure 1.3.1i) (Scholefield et al., 2012). However, in the presence of ATP, Soj forms a dimer that binds to DNA and stimulates DnaA-dependent replication initiation (Figure 1.3.1.2) (although the mechanism of activation by Soj has not yet been elucidated).

Spo0J (ParB) is the regulator of Soj and contains a classical helix-turn-helix motif that is required for DNA binding (Leonard et al., 2004). Spo0J binds to centromere-like sequences (*parS* sites) clustered around the replication origin to form large nucleoprotein complexes that extend away from the *parS* nucleation sites (Breier and Grossman, 2007; Lin and Grossman, 1998; Livny et al., 2007; Murray et al., 2006). Spo0J contains two lysine residues within its flexible N-terminal region that stimulate Soj ATPase activity to regulate the nucleotide bound state of Soj (Scholefield et al., 2011). This regulation appears

to be conserved amongst the superfamily of ParA/ParB proteins, as it was originally shown that ParG (an analogue of ParB) of plasmid TP228 contains an arginine residue within its N-terminal region that is essential for stimulating the ATPase activity of ParF (ParA) (Ah-Seng et al., 2009; Barilla et al., 2007).

Besides having been implicated to regulate DNA replication, Soj and Spo0J are also involved in chromosome segregation (Figure 1.3.1.2, dotted box), which will be discussed in Chapter 1.8.1 and 1.9.

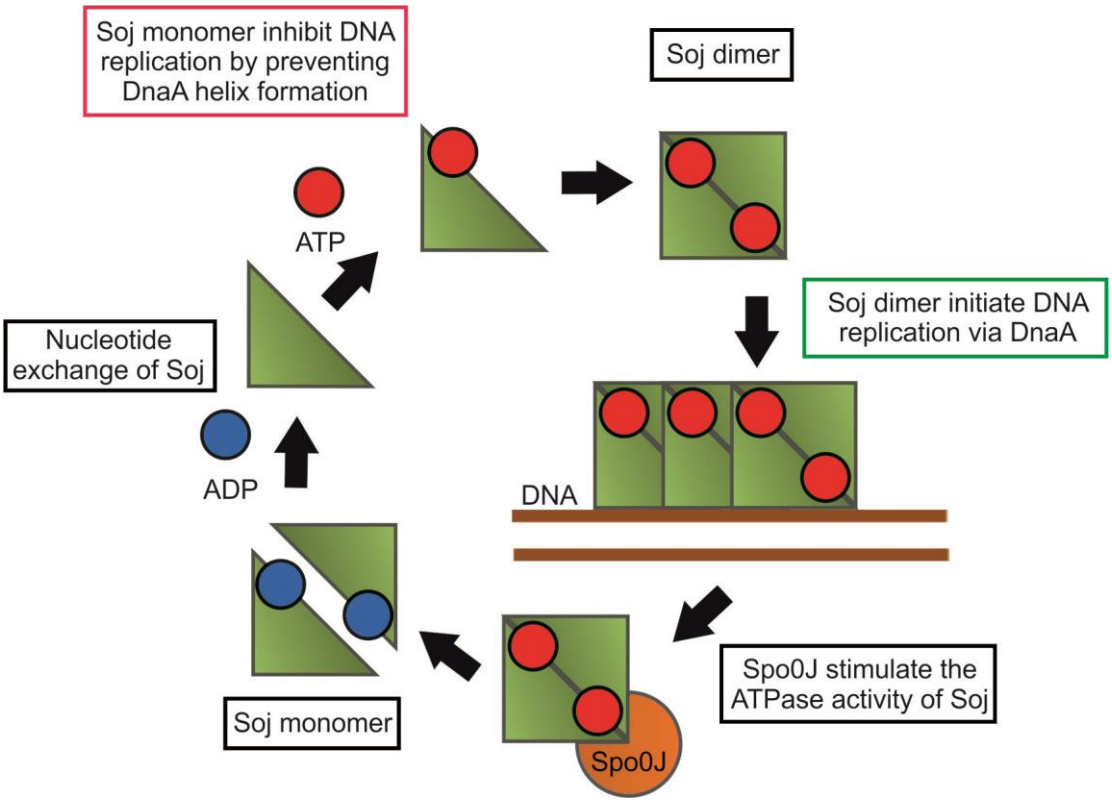

Figure 1.3.1.1: Soj activity cycle

Cartoon representation showing Soj activity cycle. Soj undergo a nucleotide switch that dictate its activity and is regulated by Spo0J. Soj dimer initiates DNA replication via DnaA, while Soj monomer inhibits DNA replication by preventing DnaA helix formation.

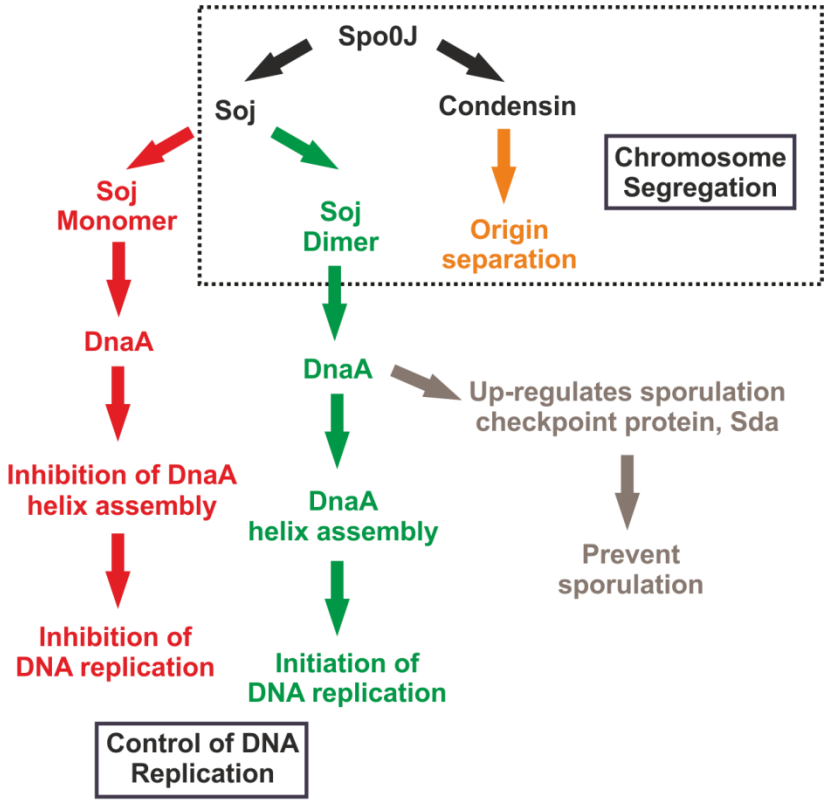

Figure 1.3.1.2: Overview of Spo0J, Soj and condensin in chromosome segregation and DNA replication

Schematic diagram showing the functions of Spo0J, Soj and condensin. Spo0J regulation of Soj leads to either activation (green) or inhibition (red) of DNA replication initiation by regulating the formation of the DnaA helix at the origin. DnaA indirectly regulates sporulation by regulating the expression of the sporulation checkpoint protein, Sda (brown). Spo0J recruits condensin to *oriC* and together with dimeric Soj, is required for proper chromosome segregation and organization (dotted box).

1.3.2 YabA prevents DnaA helix formation and titrates DnaA away from the origin via DnaN

YabA is another negative regulator of DNA replication initiation that controls DnaA by inhibiting its activity through two mechanisms. Firstly, YabA interacts with domain III of DnaA at *oriC* and prevents assembly of the DnaA helix that is necessary for DNA duplex unwinding (Figure 1.3.1i) (Cho et al., 2008; Scholefield and Murray, 2013). Secondly, YabA connects DnaA with DnaN, the sliding clamp component of the replisome. Approximately 500 DnaN protein dimers accumulate on the lagging strand behind the replisome during replication elongation (Su'etsugu and Errington, 2011). YabA binds to these DnaN proteins to sequester DnaA away from *oriC* when the replisome moves along the chromosome, thereby lowering the number of free DnaA proteins at *oriC* (Figure 1.3.1ii) (Merrikh and Grossman, 2011; Noirot-Gros et al., 2002; Noirot-Gros et al., 2006; Soufo et al., 2008). Deletion of *yabA* leads to a severe overinitiation phenotype, supporting the notion that the multiple regulatory activities of YabA are critical for replication control (Noirot-Gros et al., 2002).

1.3.3 DnaD controls DNA replication initiation by preventing DnaA helix formation

The replication initiation protein DnaD appears to play both positive and negative roles during DNA replication initiation. In addition to its essential activity recruiting the DNA helicase loader DnaB, it is also a negative regulator of the initiation event. Biochemical experiments have revealed that when DnaD is recruited to *oriC* by DnaA, it inhibits initiation by preventing DnaA helix formation without affecting ATP binding or hydrolysis activities (Figure 1.3.1i) (Bonilla and Grossman, 2012; Ishigo-Oka et al., 2001; Scholefield and Murray, 2013; Smits et al., 2011). The opposing activities of DnaD may help to precisely coordinate DNA duplex unwinding with helicase loading.

1.3.4 DnaA autoregulation and sequestering of DnaA by DBCs

Transcription of the *dnaA-dnaN* operon is autoregulated by DnaA binding to DnaA-boxes flanking the *dnaA* promoter within *oriC* (Figure 1.3.1iii) (Ogura et al., 2001). Furthermore, DnaA also binds to six other DnaA box clusters (DBCs) located away from the origin (Ishikawa et al., 2007; Smits et al., 2011). Deletion of all six DBCs lead to overinitiation of DNA replication and can be partially restored by an ectopic DBC whose effectiveness depends on the DBC proximity to the origin and its copy number (Figure 1.3.1iv) (Okumura et al., 2012).

1.4 Regulation of DNA replication initiation in *B. subtilis* during sporulation

Upon conditions of nutrient deprivation, *B. subtilis* can initiate a developmental program leading to the production of a stress-resistant dormant spore. During sporulation the bacterium undergoes an asymmetric cell division process to produce a large compartment (mother cell) and a small compartment (forespore) joined together by the division septum. As sporulation proceeds, the smaller cell will be engulfed by the mother cell where it will develop into an endospore. Following lysis of the mother cell, the spore will be released into the environment where it will remain dormant until it encounters favourable environmental conditions that promote germination and vegetative growth (Higgins and Dworkin, 2012). Critically, during sporulation each cell-type requires one copy of the genome to accomplish the developmental program, and multiple regulatory systems act to coordinate DNA replication with the sporulation-specific cell cycle.

The master developmental transcriptional regulator Spo0A directly governs the expression of 121 sporulation genes by binding to Spo0A-boxes (5’ TGTCGAA 3’) and recruiting RNA polymerase (Fujita et al., 2005). The activation of Spo0A requires phosphorylation and this is mediated by a multicomponent phosphorelay system. The phosphorelay consists of five histidine kinases (KinA-E) that autophosphorylate in response to different environmental conditions and two phosphotransfer proteins, Spo0F and Spo0B (Higgins and Dworkin, 2012; LeDeaux et al., 1995). The phosphate group from the histidine kinases are transferred from Spo0F→Spo0B and finally to Spo0A, leading to an accumulation of phosphorylated Spo0A that will activate genes required for sporulation (Figure 1.4.1A) (Burbulys et al., 1991).

In order to ensure that cells are able to replicate two copies of the genome prior to the initiation of sporulation, *B. subtilis* inhibits the spore developmental pathway at the onset of DNA replication. The checkpoint protein Sda (suppressor of *dnaA*) is a negative regulator of sporulation and interacts directly with KinA and KinB to prevent autophosphorylation and the transfer of the phosphate group to Spo0F (Figure 1.4.1A) (Burkholder et al., 2001; Cunningham and Burkholder, 2009). Expression of *sda* is controlled by DnaA binding to DnaA-boxes upstream of the *sda* promoter and is specifically up-regulated in conjunction with initiation of DNA replication (Figure 1.3.1.2,brown) (Breier and Grossman, 2009; Burkholder et al., 2001; Cunningham and Burkholder, 2009; Ishikawa et al., 2007; Veening et al., 2009). This burst of Sda expression delays sporulation and allows time for the replication machinery to duplicate the genome. Subsequently, because Sda is an intrinsically unstable protein, its abundance in the cell rapidly decreases, thereby allowing sporulation to proceed towards the end of the replication cycle.

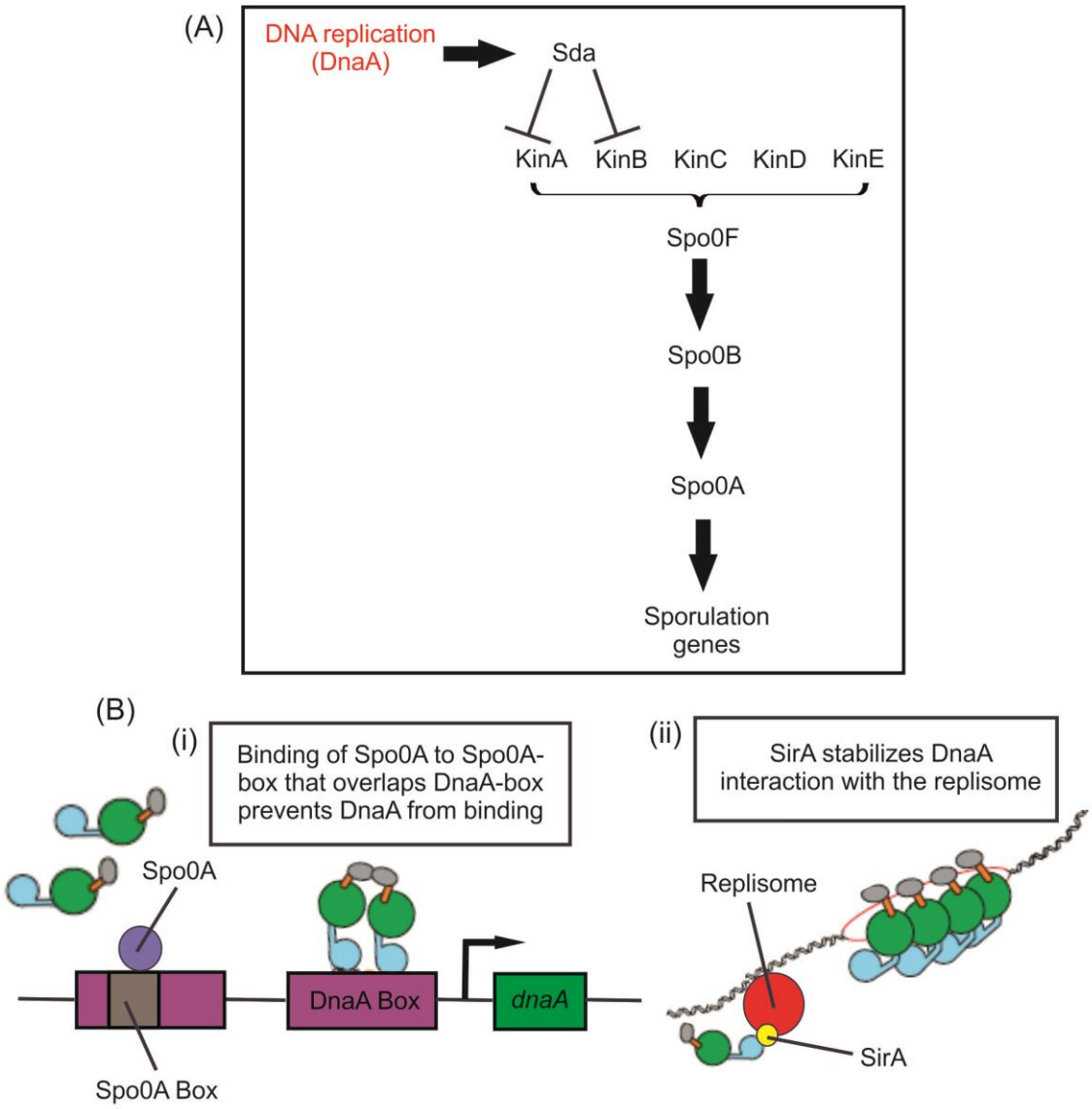

Figure 1.4.1: Regulation of initiation in *B. subtilis* during sporulation

(A) Schematic diagram showing the sporulation phosphorelay channel. **(B)** Cartoon representation of the various regulators of DNA replication initiation during sporulation. (i) Binding of Spo0A to Spo0A-boxes prevents DnaA from binding to DnaA-boxes at *oriC*. (ii) Sequestering of DnaA away from *oriC* via tethering to the replisome.

1.4.1 Spo0A binding to origin region affects chromosome copy number

To achieve maximal spore fitness, a developing *B. subtilis* cell requires precisely two copies of the chromosome, one for the forespore and the other for the mother cell (Veening et al., 2009). This control of chromosome copy number is achieved by Spo0A acting both directly at *oriC* and indirectly through expression of the DnaA inhibitory protein SirA.

Spo0A-boxes (5' TGTCGAA 3') share sequence homology with DnaA-boxes (5' TGTGGATAA 3') and several of these sites overlap one another at *oriC* (Boonstra et al., 2013). Spo0A bound to Spo0A-boxes blocks open complex formation at *oriC in vitro* (Figure 1.4.1Bi) (Castilla-Llorente et al., 2006). *In vivo* mutants with disrupted Spo0A-boxes showed a modest increase in DNA replication initiation and this effect was more prominent in a *sda*/*sirA* double mutant background when cells are growing rapidly (Boonstra et al., 2013).

1.4.2 SirA interferes with DnaA *oriC* binding

SirA is a sporulation-induced protein identified as an inhibitor of DNA replication that is important for maintaining diploidy. SirA interacts with domain I of DnaA and inhibits reinitiation following the onset of the developmental process (Figure 1.4.1Bii) (Jameson et al., 2014; Rahn-Lee et al., 2009; Rahn-Lee et al., 2011; Wagner et al., 2009). Artificially inducing SirA in vegetative growing cells interferes with DnaA binding to the origin and leads to lethality (Rahn-Lee et al., 2011; Wagner et al., 2009). Native expression of SirA during sporulation stabilizes DnaA at the replisome away from *oriC* and has been proposed to inhibit DnaA origin localization through sequestration (Jameson et al., 2014).

1.5 Regulation of initiation in *E. coli*

The half-life of *E. coli* DnaA-ATP/ADP is approximately 10-fold higher than *B. subtilis* (Chapter 1.1); therefore, the majority of mechanisms employed by *E. coli* to regulate DnaA are aimed at regulating the overall availability of DnaA-ATP within the cell. These mechanisms includes: (i) autoregulation of *dnaA*; (ii) sequestering of DnaA by *datA*; (iii) Hda stimulating the nucleotide hydrolysis of DnaA; (iv) interfering with DnaA binding to DnaA-boxes (Figure 1.5.1).

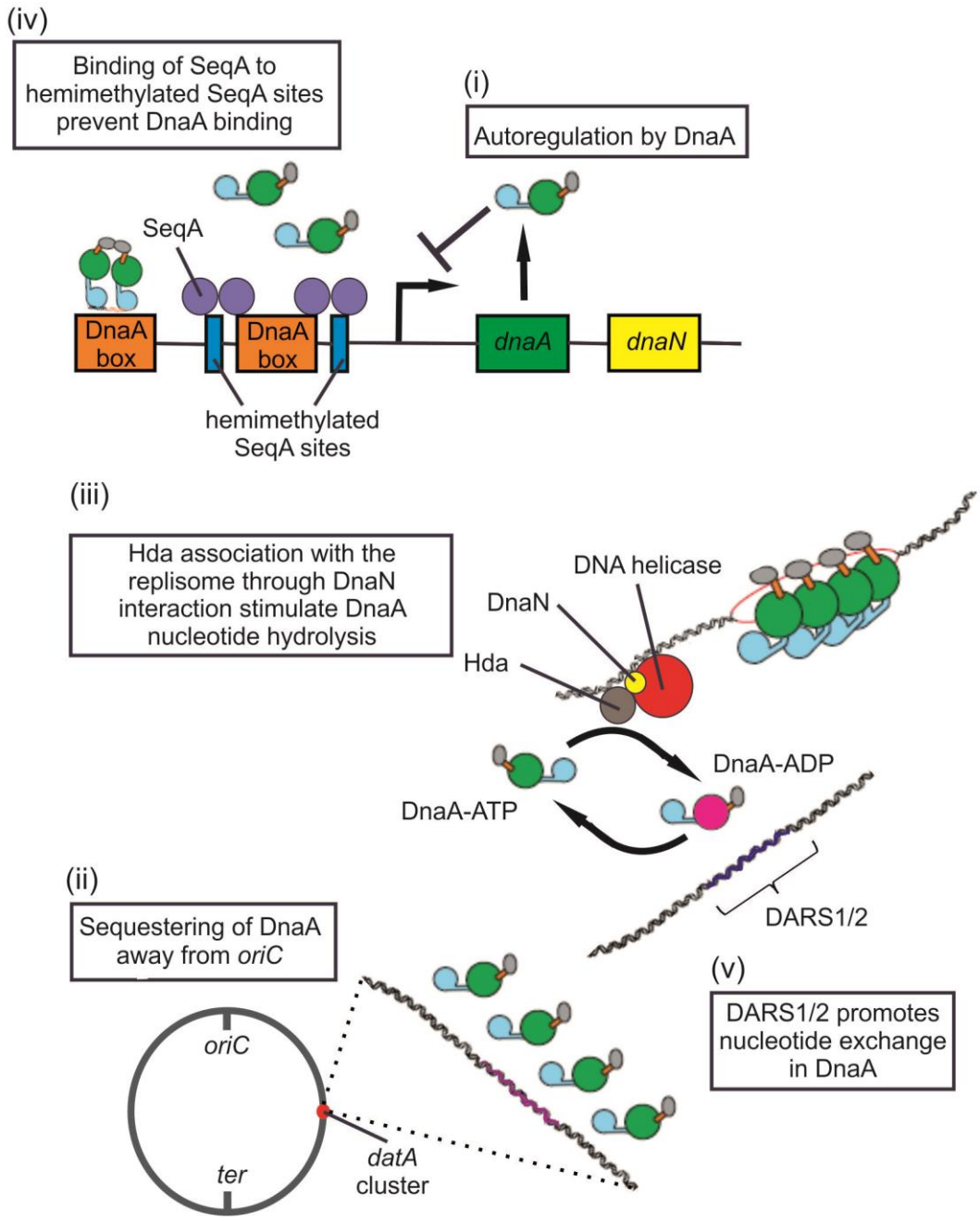

Figure 1.5.1: Regulation of initiation in *E. coli*

Cartoon representation of regulators of DNA replication initiation during vegetative growth. (i) Autoregulation by DnaA. (ii) Sequestering of DnaA away from *oriC* by *datA.* (iii) Hda associates with the replisome via DnaN to stimulate DnaA nucleotide hydrolysis. (iv) SeqA blocking DnaA from binding to DnaA-boxes at *oriC*. (v) DAR1/2 promotes nucleotide exchange in DnaA.

1.5.1 DnaA autoregulation and sequestering of DnaA by *datA*

Similarly to *B. subtilis* (Chapter 1.3.4), transcription of the *dnaA*-*dnaN* operon is autoregulated by DnaA binding to DnaA-boxes flanking the *dnaA* promoter within *oriC* (Figure 1.5.1i) (Braun et al., 1985). In a similar fashion to DBCs in *B. subtilis* (Chapter 1.3.4), *datA* is a region of DNA that contains DnaA-boxes that sequester large amount of DnaA away from *oriC*. *datA* null mutant leads to an overinitiation phenotype that can be suppressed by a plasmid containing *datA* (Figure 1.5.1ii) (Kitagawa et al., 1998; Nozaki et al., 2009).

1.5.2 Controlling the availability of DnaA-ATP for DNA replication initiation

The *E. coli* regulatory inactivation of DnaA (RIDA) system consists of the protein Hda forming a complex with the replisome via the DNA clamp and stimulating the ATP hydrolysis activity of DnaA (Figure 1.5.1iii) (Kato and Katayama, 2001; Su'etsugu et al., 2005). This couples inactivation of DnaA to the functional assembly of the replisome. Interestingly, although both Hda and YabA appear to form a trimeric complex with DnaA and DnaN, the mechanism in which they regulate DnaA is different (Chapter 1.3.2).

DARS1/2 (DnaA-reactivating sequence 1/2) are sequences on the chromosome that are required to increase the level of DnaA-ATP by promoting the exchange of ADP for ATP, although the precise mechanism is unknown (Figure 1.5.1v) (Fujimitsu et al., 2009).

1.5.3 SeqA interferes with DnaA *oriC* binding and transcription

Initiation of DNA replication is delayed by SeqA binding with high affinity to hemimethylated 5’-GATC-3’ sites that overlap DnaA-boxes within *oriC* and are transiently present following DNA synthesis of a daughter strand. Binding to hemimethylated DNA inhibits DnaA binding to DnaA-boxes and inhibits both transcription of the *dnaA* gene and oligomerization of DnaA (Figure 1.5.1iv) (Lu et al., 1994; Nievera et al., 2006; Waldminghaus and Skarstad, 2009).

1.6 Regulation of initiation in *Caulobacter crescentus*

C. crescentus undergoes asymmetric cell division, yielding a swarmer cell that is unable to initiate DNA replication and a stalked cell that strictly replicates its chromosome once per cell cycle. Similarly to *E.coli* and *B. subtilis*, multiple regulatory mechanisms regulate DnaA activity in *C. crescentus* (Gorbatyuk and Marczynski, 2001). These systems include: (i) CtrA interfering with DnaA binding to *cori*; (ii) controlling DnaA and CtrA levels by ClpXP proteases; (iii) RIDA mediated by HdaA (Figure 1.6.1).

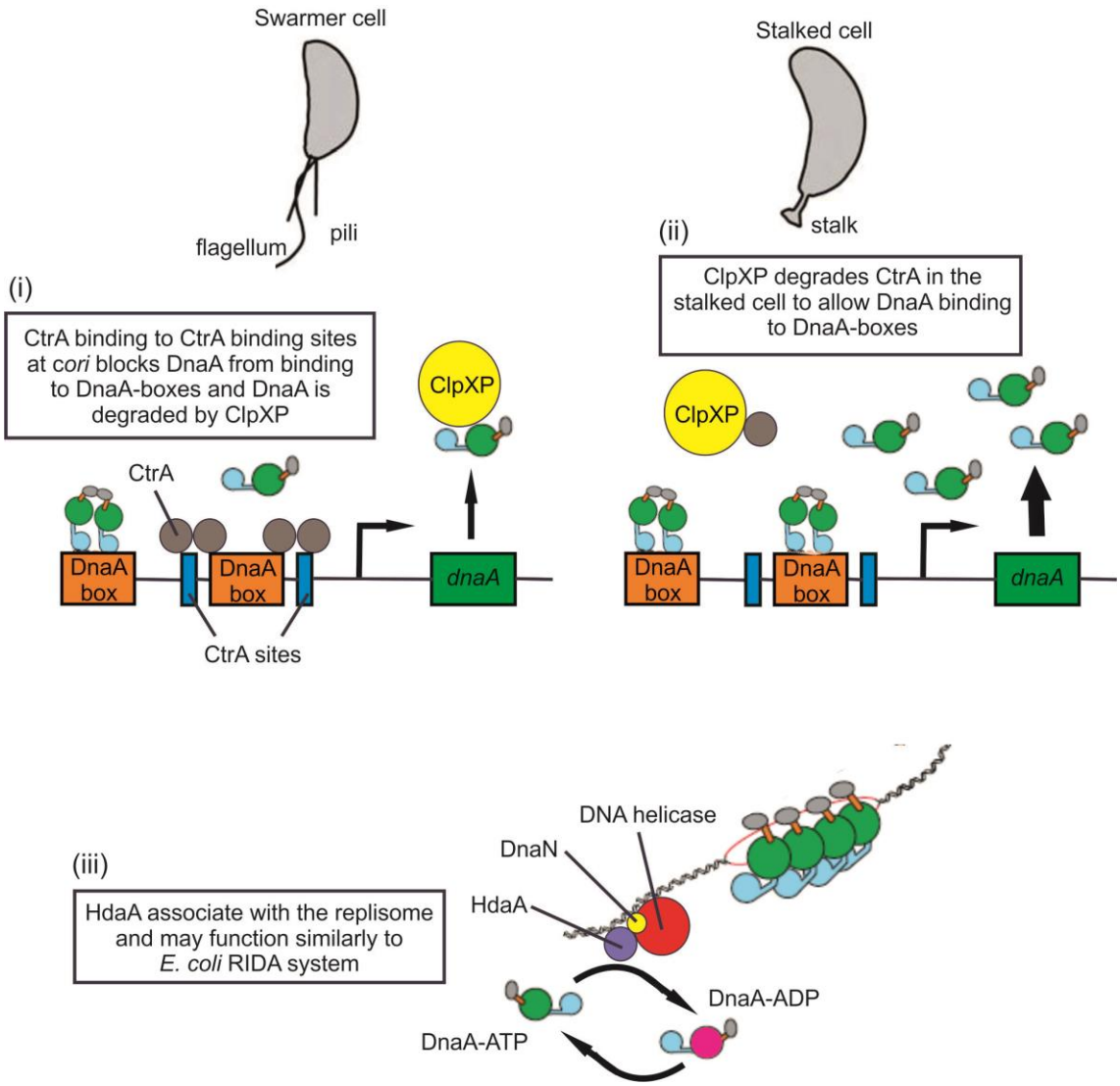

Figure 1.6.1: Regulation of initiation in *C. crescentus* during vegetative growth

Cartoon representation of regulators of DNA replication initiation during vegetative growth. (i) In the non-replicating swarmer cell, increased level of CtrA block DnaA from binding to the DnaA-boxes at *cori* and DnaA gets degraded by ClpXP. (ii) In the replication competent stalked cell, CtrA gets degraded by ClpXP to allow DnaA to bind at *cori* to initiate DNA replication. (iii) HdaA associates with the replisome in a manner that is similar to *E. coli* RIDA system.

1.6.1 Controlling the level of DnaA-ATP levels

The *C. crescentus* genome encodes the *hdaA* gene that is a homologue of the *E. coli hda* gene. HdaA localizes with the replisome and is necessary to prevent overinitiation of DNA replication, strongly suggesting a mechanism that may be similar to the RIDA system in *E. coli* (Figure 1.6.1iii) (Chapter 1.5.2). Interestingly, *C. crescentus hdaA* transcription is regulated by DnaA, creating a negative feedback loop (Collier and Shapiro, 2009).

DnaA protein levels within *C. crescentus* are tightly coordinated with the cell cycle and proteins are rapidly degraded after the initiation of DNA replication by the ClpXP protease (Figure 1.6.1i) (Gorbatyuk and Marczynski, 2005). Furthermore, during carbon starvation (p)ppGpp synthesis by SpoT regulates DnaA protein level via the ClpXP protease (Jonas et al., 2013; Lesley and Shapiro, 2008).

1.6.2 CtrA interferes with DnaA *oriC* binding

CtrA is an abundant global transcriptional regulator that accumulates in *C. crescentus* swarmer cells and directly regulates ~95 genes. It has been shown that CtrA binds to five sites within the replication origin (*cori*) that overlap with DnaA-boxes (Figure 1.6.1i) (Laub et al., 2002; Quon et al., 1998). In a mechanism reminiscent of*E. coli* SeqA (Chapter 1.5.3) and *B. subtilis* Spo0A (Chapter 1.4.1), CtrA binding to these sites represses replication in the swarmer cell. Upon development into a replication competent stalked cell, CtrA is degraded by the ClpXP protease to allow DnaA to initiate DNA replication at *cori* (Figure 1.6.1ii) (Gorbatyuk and Marczynski, 2005; McGrath et al., 2006; Quon et al., 1998).

1.7 Bacterial chromosome segregation

To ensure propagation of the genetic material, DNA replication must be followed by accurate segregation of the genome. Eukaryotes undergo distinct phases during the cell cycle, such as the S phase where the chromosomes are duplicated and then mitosis where the replicated genome is compacted and segregated. Here chromosome segregation is mediated by a bipolar mitotic spindle made up of microtubules that capture and align the chromosomes before facilitating segregation using movement generated either by molecular motors or microtubule polymer dynamics (Gatlin and Bloom, 2010).

Prokaryotes on the other hand do not undergo such distinct cycles and instead segregate sister chromosomes immediately as replication proceeds. In the original model for bacterial DNA segregation proposed by Francois Jacob and colleagues in 1963, they suggested a passive process in which the two newly replicated DNA molecules were segregated by tethering to the cell membrane at mid cell followed by cell elongation to physically separate the replicated genome into individual chromosome located within opposite cell halves (Jacob et al., 1963). However, inconsistences in the model came from studies that show that the bipolar movement of the replicated origins away from the mid cell position are faster than the rate of cell elongation (Fiebig et al., 2006; Viollier et al., 2004). Therefore, in contrast to the original passive segregation hypothesis, recent studies in a variety of diverse organisms have provided evidence indicating that bacterial DNA segregation is highly dynamic and requires active processes, which will be discussed in the following sections.

1.7.1 Plasmid segregation

Low-copy number bacterial plasmids have long been utilized as a model system to study DNA segregation, and indeed much of the thinking regarding bacterial chromosomes is based on the founding work with plasmids. The plasmid partitioning (Par) systems are one of the best characterized systems for bacterial DNA segregation, where pairs or clusters of plasmids are separated into opposite regions of a cell. This system is generally comprised of three essential components, (i) a polymerizing motor/movement protein that requires nucleotide, (ii) a DNA binding adapter protein, and (iii) a centromeric binding site on the DNA that is recognised by the adapter protein. The plasmid partitioning systems have been classified into three main categories (type I, II, III) described below.

The type I partitioning system is the most common and consists of (i) a Walker-type ATPase such as ParA found in pB171 and P1 or SopA encoded in F plasmid, (ii) a DNA binding protein ParB or SopB, and (iii) a *cis*-acting DNA sequence *parS* or *sopC* (Yamaichi and Niki, 2000). The type I plasmid system is closely related to the chromosomally encoded ParABS system described in Chapter 1.3.1. Plasmid ParB/SopB proteins bind to *parS*/*sopC* sites and spread several kilobases into neighbouring DNA to form large nucleoprotein complexes. When bound to ATP, ParA/SopA proteins interact with ParB/SopB:*parS/sopC* complexes to promote plasmid segregation. In addition ParB/SopB proteins stimulate the ATPase activity of their cognate ParA/SopA proteins. Interestingly, although the ParG protein (encoded by *parFGH* of plasmid TP288) appears to be unrelated to ParB/SopB, the mechanism by which ParG binds to *parH* and stimulates ParF ATPase activity appear to be similar, suggesting a common mechanism among bacteria for the interaction

between type I partitioning proteins (Barilla et al., 2007; Barilla and Hayes, 2003; Barilla et al., 2005; Hayes, 2000).

In vivo, ParA/SopA forms a comet like cloud that assembles over the nucleoid and appears to pull plasmids as it oscillates (Ebersbach and Gerdes, 2001, 2004; Hatano et al., 2007; Lim et al., 2005; Ringgaard et al., 2009). Recent studies using a cell free reconstituted system coupled with computer stimulation have shown that SopA forms a gradient on DNA and interacts with the SopB:*sopC* partitioning complex to generate cargo motion. This motion is generated from the combination of ParB:*parS* complex binding to ParA on the flexible DNA that allows movement upon hydrolysis of ParA coupled with the physical confinement of the complex to the DNA (Figure 1.7.1.1i) (Lim et al., 2014; Vecchiarelli et al., 2014).

The type II partitioning system consists of actin like ATPases, such as ParM encoded by the *parMRC* operon of the low-copy R1 plasmid. This system uses a search and capture model, where ParM assembles into unstable filaments that are constantly polymerizing and depolymerizing. The ParR:*parC* complex caps and stabilizes the growing end of the ParM filament to allow addition of new ParM subunits. By assembling into an antiparallel pair of filaments, the ParM proteins are able to push two plasmids toward opposite cell poles (Figure 1.7.1.1ii) (Campbell and Mullins, 2007; Garner et al., 2004; Garner et al., 2007; Gayathri et al., 2012; Moller-Jensen et al., 2003; Moller-Jensen et al., 2002).

Finally, the type III partitioning system consists of FtsZ/tubulin-like proteins such as the *tubZRC* operon from pBtoxis (Tang et al., 2006). The TubR:*tubC* partitioning complex interacts with a TubZ filament that contain a distinct plus and minus end. Addition of TubZ subunit into the filament will

threadmill the plasmid along the cell membrane and release the plasmid at the curved surface of the cell (Figure 1.7.1.1iii) (Aylett and Lowe, 2012; Aylett et al., 2010; Chen and Erickson, 2008; Larsen et al., 2007; Montabana and Agard, 2014; Ni et al., 2010).

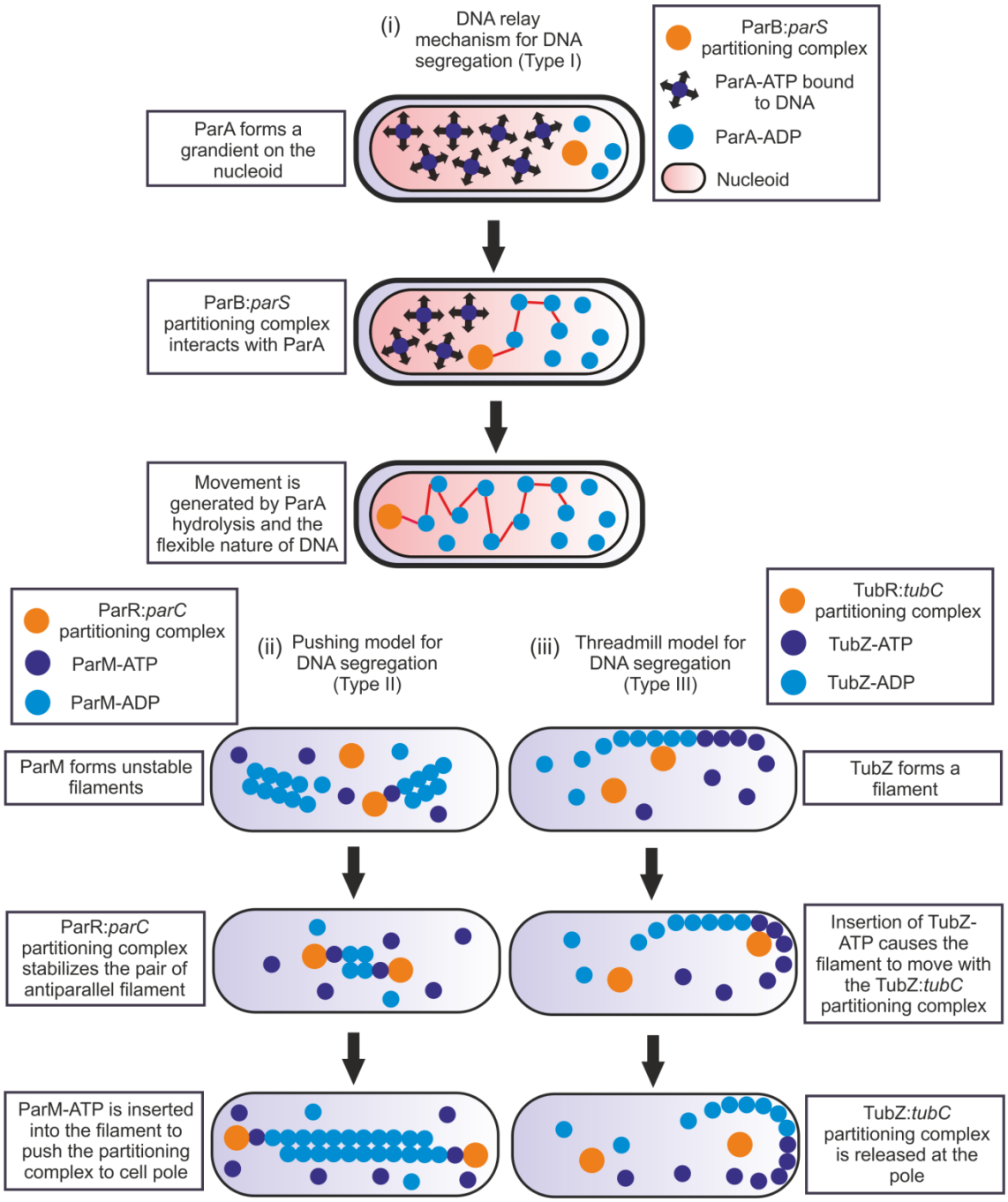

Figure 1.7.1.1: Plasmid segregation

Cartoon representation of the various mechanisms of plasmid segregation. (i) Type I plasmid segregation using the DNA relay mechanism. (ii) Type II plasmid segregation using the pushing model. (iii) Type III plasmid segregation using the threadmill model.

1.8 Chromosome ParABS system in segregation and organization

Chromosome segregation and organization often involve one of the following general features; motor/movement proteins that drive the segregation of replicated chromosome origin domains and a site at the cell pole that could subsequently either capture or provide positional information to the segregation systems. The chromosomally encoded ParABS system, condensin (SMC complexes), nucleoid associated proteins (NAPs) and topoisomerase (Topo IV) have been found to play critical roles for DNA partitioning and organization within many bacterial species, and these provide the framework for our understanding of bacterial chromosome segregation.

The role of Par systems in segregating low-copy number plasmids have been well established (Chapter 1.7.1). However, their role in bacterial chromosome segregation has been controversial because the disruption of *par* genes often produced either only a mild segregation defect or a range of diverse phenotypes (e.g. altered development, increased DNA replication). Bioinformatics analyses of sequenced bacterial genomes have shown that over 65% contained a chromosomally encoded *par* locus. These chromosomally encoded genes are usually located within the origin proximal region of the chromosome (Livny et al., 2007). Similarly to the plasmid encoded *par* loci, ParB is a DNA binding protein that recognizes and binds to palindromic sequences known as *parS* sites that typically flank the origin of replication, and the ParB/*parS* complexes directly stimulates the ATPase activity of ParA.

1.8.1 *Bacillus subtilis*

During vegetative growth of *B. subtilis*, newly replicated chromosomes adopt an *ori-ter* pattern, where the origins are located towards the cell pole, the termini rest near mid-cell, and the two chromosome arms are arranged in parallel between them (Figure 1.8.1Aii) (Lee et al., 2003; Teleman et al., 1998; Wang et al., 2014a). Immediately after DNA replication initiates near the cell pole, the duplicated origins move to mid-cell and adopt a left-*ori*-right conformation (Figure 1.8.1Ai) before they are actively separated from one another and move towards opposite cell poles (Wang et al., 2014a). This oscillation between two distinct patterns of chromosome origin localization depends upon the Par system and condensin (Wang et al., 2014a).

B. subtilis possesses chromosomally encoded homologues of ParA and ParB called Soj (27kDa) and Spo0J (32 kDa), respectively. Deletion of *spo0J* leads to an increase in anucleate cell production (Ireton et al., 1994) and newly replicated origins are impaired in separation and located closer together, leading to their mis-positioning within the cell. A string of recent studies have revealed that Spo0J recruits the chromosome organization complex condensin (SMC) to the origin region and that this is required for accurate origin segregation (see additional information on condensin below) (Gruber and Errington, 2009; Gruber et al., 2014; Sullivan et al., 2009; Wang et al., 2014b). Furthermore, Spo0J alone has been found to compact DNA through lateral spreading and long-range bridging activities, suggesting that Spo0J may play a direct role in chromosome organization to facilitate DNA segregation (Graham et al., 2014; Lee and Grossman, 2006; Lee et al., 2003; Murray et al., 2006).

A *soj* null mutant shows no significant defect in chromosome segregation, although separation of duplicated origin regions is affected (Ireton

et al., 1994; Lee and Grossman, 2006; Wang et al., 2014a). These results indicate that in *B. subtilis* the Par system affects chromosome segregation predominantly through the interaction of Spo0J:*parS* nucleoprotein complexes with condensin, and the Soj-Spo0J:*parS* system plays a secondary supporting role. Furthermore, Soj plays a role regulating the master DNA replication initiation protein DnaA (Chapter 1.3.1), suggesting that Soj may coordinate DNA replication with chromosome segregation (Figure 1.3.1.2).

Under conditions of nutrient limitation *B. subtilis* undergoes a differentiation process that involves the formation of a stress resistant spore. This process requires the formation of an asymmetric septum near one pole, leading to the formation of a larger mother cell and a smaller forespore. As described in Chapter 1.4, sporulation requires two chromosomes, one for each cellular compartment. Following DNA replication the origin region is segregated towards the cell pole where it becomes anchored to the membrane by the sporulation induced DNA binding protein RacA. RacA directly recognizes ~25 *racA* sites near the replication origin and forms a bridge between the chromosome and the cell pole through interaction with the membrane bound DivIVA protein (Ben-Yehuda et al., 2005; Ben-Yehuda et al., 2003; Lenarcic et al., 2009; Wu and Errington, 2003). Formation of the asymmetric septum near one cell pole leads to the entrapment of the origin region (Figure 1.8.1Aiii) (Wu and Errington, 1994). The remaining chromosome is then pumped into the forespore by the septum localized membrane protein, SpoIIIE (Bath et al., 2000; Wu and Errington, 1994, 1997).

Spo0J and Soj are important for chromosome origin trapping during sporulation. Either deletion of *spo0J* or recruitment of Spo0J to ectopic *parS* sites leads to a significant defect in the trapping of the correct region of the

chromosome in the forespore, and this is likely related to altered localization of condensin away from the origin (Sullivan et al., 2009; Wu and Errington, 2002). Deletion of *soj* produces a modest defect in chromosome origin trapping during sporulation. However the effect is exacerbated in combination with a *racA* mutant, suggesting a partially redundant role for both proteins (Ireton et al., 1994; Sharpe and Errington, 1996; Sullivan et al., 2009; Wu and Errington, 2003)

1.8.2 *Caulobacter crescentus*

The dimorphic bacterium *C. crescentus* replicates its chromosome only once per cell cycle and here the Par system is essential for viability. The *C. crescentus* chromosome contains two *parS* sites near *cori* and like *B. subtilis* the *parS* sequences serve as ParB binding sites (Figure 1.8.1C) (Livny et al., 2007; Mohl and Gober, 1997; Toro et al., 2008). The chromosome adopts an *ori-ter* orientation, similar to *B. subtilis* during sporulation, although here the origin region is anchored to the cell pole by the ParB:*parS* complex interacting with the membrane protein PopZ (Figure 1.8.1C) (Bowman et al., 2008; Ebersbach et al., 2008; Toro et al., 2008; Viollier et al., 2004). Following initiation of DNA replication at the old pole, the ParB:*parS* complex translocates the newly replicated chromosome origin by progressing towards a gradient of dimeric ParA proteins spread across the nucleoid. As ParB:*parS* moves along the ParA gradient, it stimulates ParA ATPase activity to drive ParA dimers into monomers. The ParA monomers then become enriched at the new pole through an interaction with the polar localization protein TipN, thereby promoting unidirectional motion of ParB:*parS* (Ptacin et al., 2014; Ptacin et al., 2010; Schofield et al., 2010; Shebelut et al., 2010; Toro et al., 2008). Here the

ParABS system plays a dominant role in chromosome segregation, and indeed relocating *parS* sites to a origin distal location in the genome leads to reorganization of the chromosome within the cell, with the ectopic *parS* region anchored at the cell pole and the origin region reoriented towards mid cell (Umbarger et al., 2011).

1.8.3 *Vibrio cholera*

The Gram-negative *V. cholerae* genome is divided into two chromosomes, a large chromosome (ChrI) that encodes ParABI with three origin proximal *parS*I sites, while the smaller plasmid-like replicon (ChrII) encodes ParABII with nine *parS*II sites (Figure 1.8.1D) (Yamaichi et al., 2007b). Unlike the Par system of *C. crescentus,* ParABI is not essential for ChrI segregation. To translocate the newly replicated ChrI across the long axis of the cell, ParAI forms a cloud-like structure that pulls the ParBI/*parSI* complex to the new pole and is anchored at the pole by the cell anchoring protein, HubP, in an *ori-ter* linear conformation (Figure 1.8.1D) (David et al., 2014; Fogel and Waldor, 2006; Yamaichi et al., 2012). Similarly to *C. crescentus*, the orientation of the ChrI is dictated by *parS*, because insertion of *parS* at ectopic position leads to reorganization of the chromosome (David et al., 2014). Conversely, ParABSII, unlike ParABSI, is essential for ChrII maintenance, segregation and subcellular localization at mid cell and is able to stabilize an unstable mini-F plasmid, suggesting an important role in chromosome partitioning (Fogel and Waldor, 2005; Yamaichi et al., 2007a; Yamaichi et al., 2007b).

1.8.4 *Sulfolobus solfataricus*

The discovery of the *segAB* operon of *S. solfataricus* has provided the first insight into archaeal chromosome segregation. The *segAB* operon is a partitioning locus and indeed SegA has substantial sequence similarity to bacterial ParA. However, the DNA binding protein SegB does not appear to be related to ParB proteins, although it appears to function in an analogous manner by binding to centromeric elements upstream of the operon. In the presence of nucleotide, SegA polymerizes into a filament *in vitro,* and this activity is enhanced by SegB. Furthermore, disrupting the balance of SegAB *in vivo* leads to anucleate cell formation, strongly suggesting a direct and important role in chromosome segregation, perhaps related to either the type I or type II plasmid partitioning systems (Kalliomaa-Sanford et al., 2012).

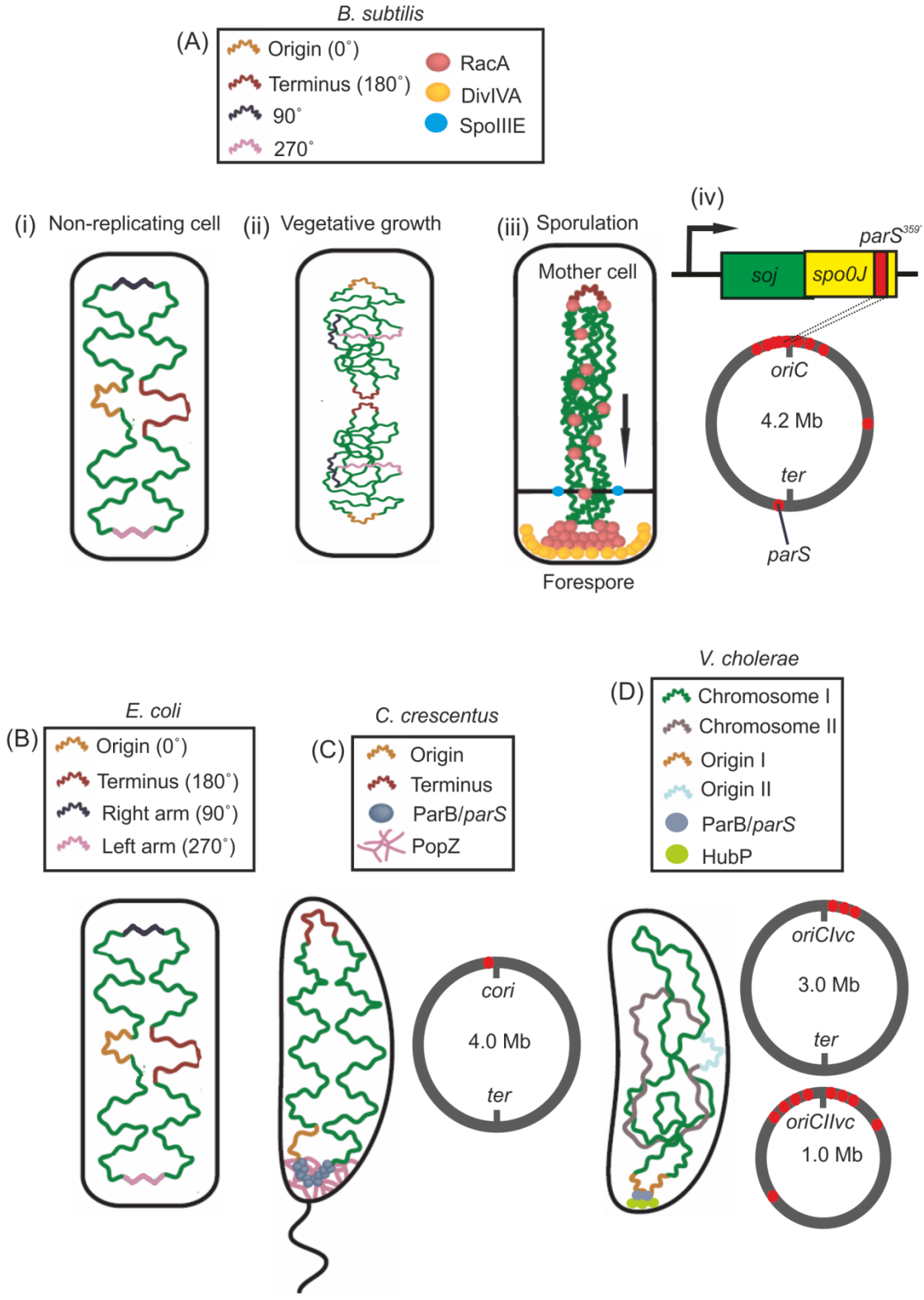
B. subtilis
(A)
Origin (0˚)
Terminus (180˚)
90˚
270˚
RacA
DivIVA
SpoIIIE
(i) Non-replicating cell
(ii) Vegetative growth
(iii) Sporulation
Mother cell
Forespore
(iv)
parS359'
soj
spo0J
oriC
4.2 Mb
ter
parS
E. coli
(B)
Origin (0˚)
Terminus (180˚)
Right arm (90˚)
Left arm (270˚)
C. crescentus
(C)
Origin
Terminus
ParB/parS
PopZ
cori
4.0 Mb
ter
V. cholerae
(D)
Chromosome I
Chromosome II
Origin I
Origin II
ParB/parS
HubP
oriCIvc
3.0 Mb
ter
oriCIIvc
1.0 Mb

Figure 1.8.1: Chromosome organization in the various organisms

Cartoon representation showing the organization of chromosome in various organisms. **(A)** Chromosome organization in the different developmental stages of *B. subtilis*. (i) The chromosome is organized into the left-*ori*-right formation in a single non-dividing cell. (ii) During vegetative growth, the chromosome adopts an *ori-ter* pattern where the origin is located at the cell quarter and the terminus at mid cell, with the two replication arms between them. (iii) During sporulation the origin is tether to the forespore by RacA binding to DivIVA with the arrow showing the direction of chromosome movement (only the entraped chromosome is shown here). (iv) The *soj-spo0J* operon located at 359˚. **(B)** *E. coli* chromosome adopts a left-*ori*-right formation. **(C)** *C. crescentus* chromosome is organized in a linear fashion with the origin anchored to the cell pole by the ParB:*parS* complex with PopZ. **(D)** *V. cholera* chromosome I is anchored to the pole by HubP interaction with the ParB:*parS* complex in a linear fashion and chromosome II is localized at mid cell. Figures are modified from (Toro and Shapiro, 2010).

1.9 Structural Maintenance of Chromosome (SMC), nucleoid associated proteins (NAPs) and topoisomerase IV in segregation and organization

The proper organization of DNA requires three classes of proteins: (i) Structural Maintenance of Chromosome (SMC) complexes; (ii) Nucleoid Associated Proteins (NAPs); (iii) Topoisomerase IV (Topo IV).

The Structural Maintenance of Chromosome (SMC) complexes, also known as condensin and cohesin in eukaryote, are ubiquitous in all three domains of life. Their architecture generally consists of Walker A and Walker B motifs at the N-terminus and C-terminus, respectively, which are separated by a long coiled-coil domain that adopts an antiparallel conformation, forming a rod-like central domain with an ATP-binding head at one end and a hinge domain on the other. The hinge domain allows binding of two monomers to form the SMC V-shaped molecule. To complete the SMC ring complex, a kleisin protein associated with a second non-SMC protein is needed to bridge the SMC dimer (Figure 1.9.1A) (Nolivos and Sherratt, 2014).

In eukaryotes, SMC complexes are involved in mitotic chromosome condensation and sister chromatid cohesion, and there are at least six different SMC proteins, ranging from SMC 1-6 that form heterodimers with several non-SMC subunits (Figure 1.9.1A). SMC1-SMC3 forms cohesin that meditates sister chromatid cohesion, while SMC2-SMC4 forms condensin that is necessary for chromosome assembly and segregation. Interestingly, although both cohesin and condensin are structurally similar, their conformations are slightly different, likely reflecting their distinct activities (Nolivos and Sherratt, 2014).

Genes encoding SMC complex homologues have been found in nearly all Gram-positive bacteria and archaea, although many Gram-negative bacteria appear to utilize the analogous MukBEF complex (Soppa, 2001). *B. subtilis* and

C. crescentus SMC complex and *E. coli* MukBEF adopts the same structure as eukaryotes, and the SMC/MukB dimer is bridged by ScpA/MukE (kleisin subunit) and ScpB/MukF (non-kleisin subunit) (Figure 1.9.1B and 1.9.1C) (Nolivos and Sherratt, 2014).

B. subtilis SMC complexes associate with DNA and are recruited to the replication origin region by Spo0J (Gruber and Errington, 2009; Sullivan et al., 2009). In contrast, *C. crescentus* SMC complexes form multiple foci depending on the cell cycle stage, which may be required for holding the chromosome arms together (Jensen and Shapiro, 2003; Le et al., 2013; Schwartz and Shapiro, 2011). In addition, *E. coli* MukB foci colocalize with the origin and repletion experiments have suggested that MukBEF complexes position the origin at the cell quarter positions (Badrinarayanan et al., 2012; Danilova et al., 2007). Null mutants in any of the genes encoding the SMC/MukBEF complex leads to impairment in growth in rich medium, which can be alleviated by growth in conditions that lowers replication fork velocity. Furthermore, these mutants lead to anucleate cell formation with mis-positioned origins and the nucleoid structure appears to be grossly perturbed, consistent with the bacterial condensin having a critical role in chromosome organization and segregation (Badrinarayanan et al., 2012; Britton et al., 1998; Danilova et al., 2007; Gruber and Errington, 2009; Gruber et al., 2014; Jensen and Shapiro, 1999, 2003; Niki et al., 1991; Schwartz and Shapiro, 2011; Sullivan et al., 2009; Tadesse et al., 2005; Wang et al., 2014b).

The Nucleoid Assoicated Proteins (NAPs) such as HU, H-NS, IHF and FIS binds throughout the genome and mediate nucleoid compaction through DNA bending and bridging and acts in concert with MukBEF in *E. coli* (Figure 1.9.2A) (Ali et al., 2001; Dame et al., 2000; Skoko et al., 2006; Wang et al.,

2013). In contrast, *B. subtilis* only possess one NAP called HBsu and is essential for cell viability (Micka and Marahiel, 1992).

In addition, topoisomerase IV (TopoIV) which belongs to the type II family of topoisomerase has been implicated in DNA segregation by decatenating newly replicated daughter chromosome together with DNA gyrase to alleviate positive coiling as DNA replication proceed caused by DNA being unwound by helicase (Figure 1.9.2B) (Crisona et al., 2000; Higgins et al., 1978; Wang et al., 2013). In *E. coli*, MukBEF stimulates the activity of Topo IV and like the SMC complex of *C. crescentus*, recruits Topo IV to the replication origins and works in concert to promote decatenation and positioning of newly replicated origins (Li et al., 2010; Nicolas et al., 2014; Wang and Shapiro, 2004). Indeed, overproduction of Topo IV in *B. subtilis* rescues SMC deletion strain by restoring cell growth and nucleoid organization, but is not necessary to resolve replicated origins, suggesting a redundancy in these systems (Tadesse et al., 2005; Wang et al., 2014b).

.

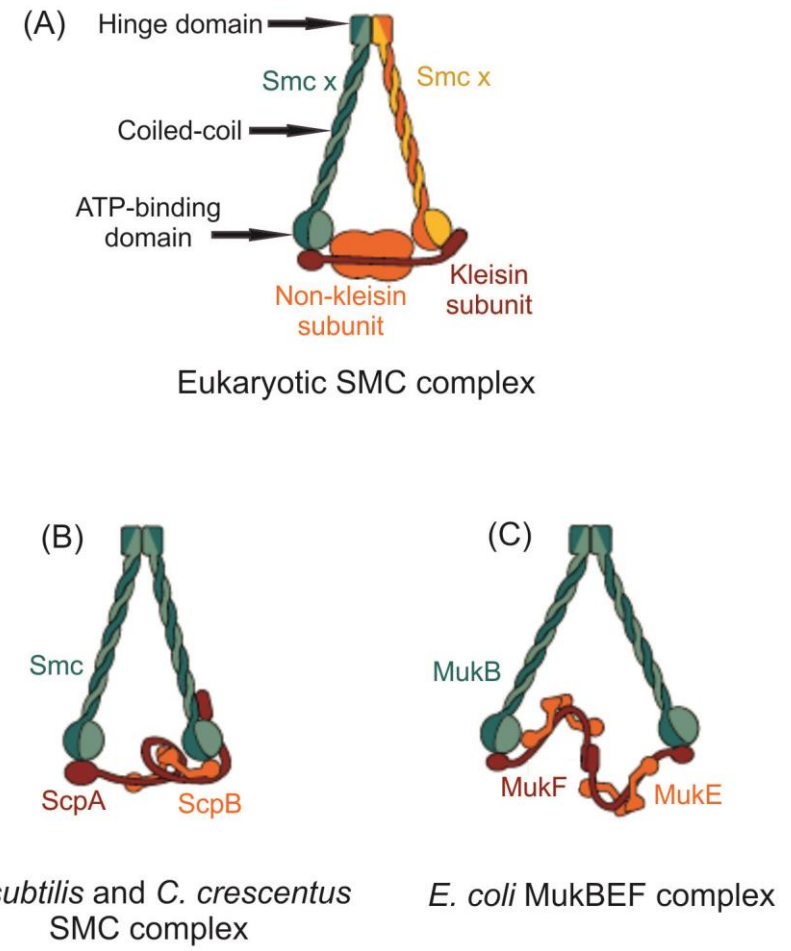

Figure 1.9.1: Architecture of SMC complexes

The SMC protein consists of three distinct components, an ATPase head domain that is connected to the flexible dimerization hinge domain by a long coiled-coil. The SMC protein dimer is bridged by a kleisin subunit (red) that is associated with a non-kleisin subunit (orange). **(A)** Eukaryotic SMC complex. **(B)** *B. subtilis* and *C. crescentus* SMC complex. **(C)** *E. coli* MukBEF complex. Figures modified from (Nolivos and Sherratt, 2014).

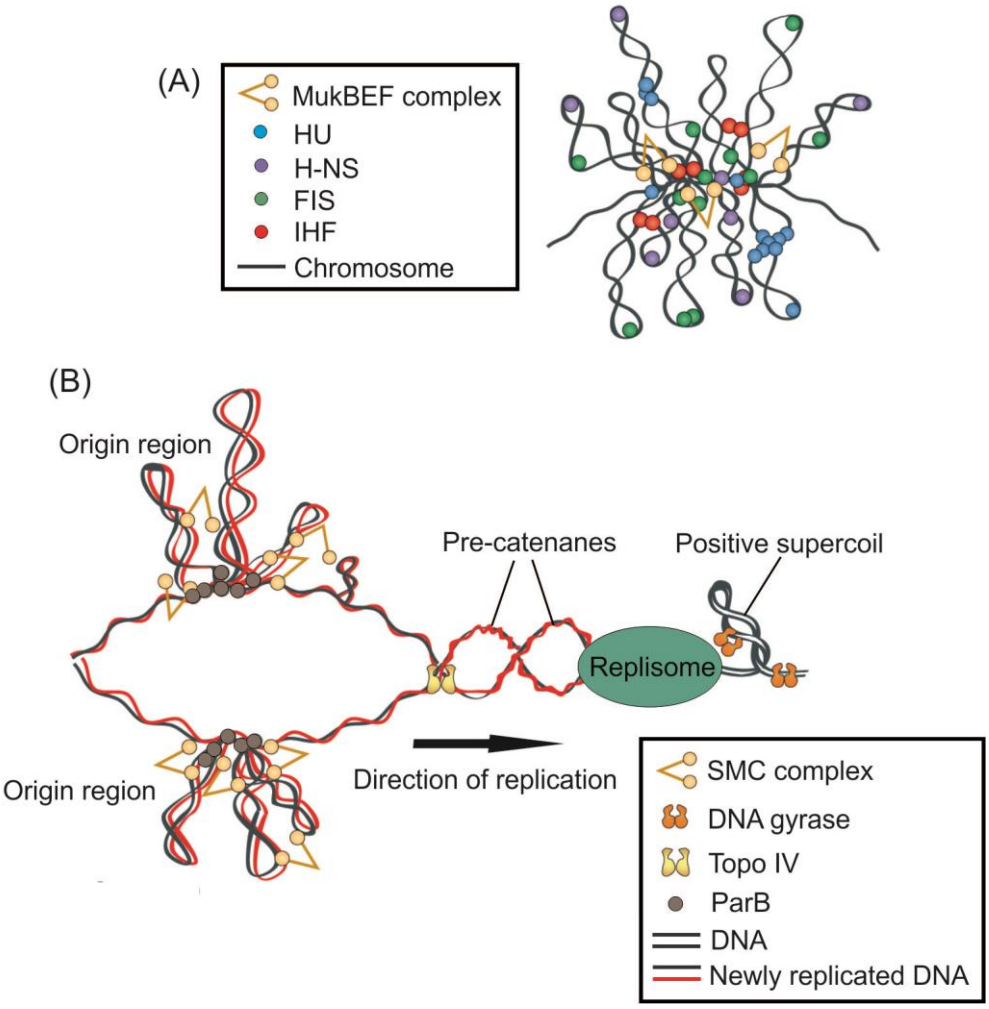

Figure 1.9.2: Organization of the chromosome

(A) Cartoon representation showing MUKBEF complex of *E. coli* in concert with NAPs to bend and bridge DNA for chromosome maintainance. **(B)** Cartoon representation showing compaction of the replicated origins in *B. subtilis* by SMC complex. Pre-catenanes and positive supercoil is generated as the replisome moves along the DNA and this is relieved by Topo IV and DNA gyrase. Figures modified from (Wang et al., 2013).

Chapter 2: Materials and Methods

2.1 Maintenance and growth of strains

Nutrient agar (Oxoid) was used for routine selection and maintenance of both *B. subtilis* and *E. coli* strains. Supplements were added as required: chloramphenicol (5 µg/ml), erythromycin (1 µg/ml), kanamycin (2 µg/ml), spectinomycin (50 µg/ml), tetracycline (10 µg/ml), zeomycin (10 µg/ml), ampicillin (200 µg/ml). For experiments in *B. subtilis* cells were grown either in Luria-Bertani LB or in defined minimal medium base (Spizizen minimal salts supplemented with Fe-NH_4-citrate (1 µg/ml), $MgSO_4$ (6 mM), $CaCl_2$ (100 µM), $MnSO_4$ (130 µM), $ZnCl_2$ (1 µM), thiamine (2 µM)) supplemented with casein hydrolysate (200 µg/ml) and/or various carbon sources (succinate (2.0%), glucose (2.0%)). Supplements were added as required: tryptophan (20 µg/ml), erythromycin (1 µg/ml), spectinomycin (50 µg/ml). Unless otherwise stated all chemicals and reagents were obtained from Sigma-Aldrich.

For plasmid expression and selection in *E. coli* cells were grown in LB medium and supplemented with ampicillin (200 µg/ml).

2.2 General DNA manipulation techniques

2.2.1 Synthesis of oligonucleotides

Oligonucleotides used in this study are listed in Table 2.3 and were designed using clone manager and purchased from Eurogentec. All oligonucleotides were dissolved in water to give a 10 μM stock solution and stored at -20˚C.

2.2.2 Polymerase chain reaction (PCR) amplification

PCR amplification was used to amplify DNA fragments from plasmids or chromosomal DNA templates. PCR reaction was carried out in a tube made up of 0.02 U/μl of Q5 DNA polymerase (NEB), 1x of Q5 buffer, 200 μM of dNTPs (Promega), 0.5 μM of each primers, < 1000 ng of DNA template and topped up to a final volume of 50 μl with water. PCR was carried out in a PCR machine (Techne) with a typical reaction cycle of: 98˚C for 30 sec (initial denaturation) followed by 25 cycles of: 98˚C for 10 sec (denaturation), 55˚C for 20 sec (annealing) and 72˚C for 1 kb per min (extension) and finished with a final extension of 72˚C for 2 min.

2.2.3 PCR purification

PCR purification was performed using QiAquick PCR purification kit (Qiagen) and was used according to the manufacturer's protocol.

2.2.4 Agarose gel electrophoresis

DNA samples were mixed with DNA loading dye (Qiagen) and loaded onto1% agarose (Sigma-Aldrich) gel and DNA fragments were separated by molecular weight in 1x TBE buffer (90 mM Tris-borate and 2 mM EDTA). Gels were stained with ethidium bromide (Invitrogen) and visualized with a UV transilluminator and molecular sizes were estimated using either a 1 kb or 100 bp ladder (NEB).

2.2.5 DNA gel extraction

DNA gel extraction was performed using QiAquick gel extraction kit (Qiagen) and was used according to the manufacturer's protocol.

2.2.6 Restriction endonuclease digestion

Restriction endonucleases (Promega, Qiagen or NEB) were used to digest DNA according to manufacturer's protocol. DNA were digested either for 3 h at 37˚C or overnight at 30˚C and purified using the QiAquick PCR purification kit (Qiagen).

2.2.7 Ligation of DNA fragments

Linearized plasmids were treated for 2 h at 37˚C with 0.01 u/µg of calf intestinal alkaline phosphatase (Promega) after restriction endonuclease digestion and purified using the QiAquick PCR purification kit (Qiagen). The DNA fragments were then ligated together in a tube made up of 1 µl of T4 DNA ligase (Promega), 1x of ligase buffer, 50 ng of plasmid backbone, 37.5 ng of

DNA fragment and topped up to a final volume of 10 µl water. The ligation reactions were then incubated overnight at 15˚C.

2.2.8 DNA sequencing

Plasmids and DNA fragments were sequenced using the DNA sequencing service provided by the University of Dundee.

2.3 *E. coli* experimental methods

2.3.1 Transformation of *E. coli*

E. coli strains DH5α were made competent using the method as described by (Hanahan, 1985). A range of plasmid concentration (10-50 ng) were then transformed into 200 µl of competent DH5α cells on ice for 30 min before subjected to heat shock at 42˚C for 90 sec and finally incubated on ice for a further 2 min. Competent DH5α were then incubated in 1 ml of LB at 30˚C for 1 h and subsequently plated onto NA plates supplemented with ampicillin (200 µg/ml).

2.3.2 Isolation of plasmid DNA

Overnight cultures containing 5ml of LB supplemented with ampicillin (200 µg/ml) were grown at 37˚C and plasmids were isolated using the QIAprep Spin Miniprep kit (Qiagen) according to the manufacturer's protocol. Plasmid DNA was then stored at -20˚C.

2.4 *B. subtilis* experimental methods

2.4.1 Transformation of *B. subtilis*

Starter culture of strains were grown in 2 ml of minimal media (Spizizen minimal salts supplemented with Fe-NH_4-citrate (0.01 mg/ml), $MgSO_4$ (6 mM), casein hydrolysate (200 µg/ml), glucose (0.5%), tryptophan (0.02 mg/ml) overnight at 37˚C. The next morning, 300 µl of cultures were diluted into 5 ml of fresh MM media and allowed to grow for 4 h at 37˚C. 5 ml of prewarmed starvation media (SMM and glucose (0.5%)) were then added to the cultures and allowed for a further growth of 2 h. A range of DNA/plasmid concentration (100-600 ng) was then incubated together with the competent cells for 1 h at 37˚C to allow DNA/plasmid to be uptaken. Transformed cells were then subsequently plated onto NA plates supplemented with the appropriate antibiotics.

2.4.2 Isolation of chromosomal DNA (Quick Prep)

Starter culture of strains were grown overnight at 37˚C in LB. The next morning, cultures were diluted into fresh LB (1:50) and allowed to grow to OD_{600} 0.8. 1 ml of each culture was then mixed with 1 ml of SSC buffer and centrifuged. The cell pellets were resuspended in 950 µl of SSC buffer and 50 µl of lysozyme and incubated at 37˚C for 30 min to lyse the cell. Finally 1 ml of NaCl (4 M) was added to the cell mixture and subsequently sterile filtered through a Millipore filter (0.45 µm). Chromosomal DNA was then stored at -20˚C.

2.4.3 Isolation of chromosomal DNA (DNeasy Blood and Tissue Kit (Qiagen))

Strains were growth overnight in 5 ml of LB at 37˚C. The next morning, DNeasy Blood and Tissue Kit (Qiagen) was used according to the manufacturer's protocol to isolate chromosomal DNA. Chromosomal DNA was then stored at -20˚C.

2.5 Marker frequency analysis

To obtain chromosomal DNA, starter cultures were grown at 30˚C or 37˚C in SMM based medium supplemented with tryptophan (20 µg/ml), casein hydrolysate (200 µg/ml), succinate (2.0%) and antibiotic (as indicated) overnight, then diluted 1:100 into fresh medium supplemented with succinate (2.0%) to reduce multi-fork replication and antibiotic (as indicated) and allowed to achieve early exponential growth (OD_{600} 0.3-0.4). Sodium azide (0.5%; Sigma) was added to exponentially growing cells to prevent further metabolism. Chromosomal DNA was isolated using a DNeasy Blood and Tissue Kit (Qiagen). Either Rotor-Gene SYBR Green (Qiagen) or GoTaq (Promega) qPCR mix was used for PCR reactions. Q-PCR was performed in a Rotor-Gene Q Instrument (Qiagen). For quantification of the origin, the intergenic region between *dnaA* and *dnaN* was amplified using primers 5'-GATCAATCGGGGAAAGTGTG-3' and 5'-GTAGGGCCTGTGGATTTGTG-3'. For quantification of the terminus, the region downstream of *yocG* was amplified using primers 5'-TCCATATCCTCGCTCCTA CG-3' and 5'-ATTCTGCTGATGTGCAATGG-3'. By use of crossing points (C_T) and PCR efficiency a relative quantification analysis ($\Delta\Delta C_T$) was performed using Rotor-Gene Software version 2.0.2 (Qiagen) to determine the *ori/ter* ratio of each

sample. These results were normalized to the *ori/ter* ratio of a DNA sample from *B. subtilis* spores which only contain one chromosome and thus have an *ori/ter* ratio of 1.

2.6 Microscopy

To visualize cells during exponential growth, starter cultures were grown overnight and then diluted 1:100 into fresh medium and allowed to achieve at least three doublings before observation as described for marker frequency analysis. Cells were mounted on ~1.2% agar pads (0.25x minimal medium base) and a 0.13-0.17 mm glass coverslip (VWR) was placed on top. To visualize individual cells the cell membrane was stained with 0.4 µg/ml FM5-95 (Molecular Probes). Microscopy was performed on an inverted epifluorescence microscope (Nikon Ti) fitted with a Plan-Apochromat objective (Nikon DM 100x/1.40 Oil Ph3). Light was transmitted from a 300 Watt xenon arc-lamp through a liquid light guide (Sutter Instruments) and images were collected using a CoolSnap HQ^2 cooled CCD camera (Photometrics). All filters were Modified Magnetron ET Sets from Chroma and details are available upon request. Digital images were acquired and analysed using METAMORPH software (version V.6.2r6).

Visualization of GFP-Soj and DAPI staining was conducted in minimal medium supplemented with 2% glucose at 37˚C because optimal GFP and DAPI signal was achieved at this condition.

Visualization of Spo0J-GFP, TetR-GFP and LacI-YFP was conducted using the same conditions as stated in the marker frequency analysis.

2.7 Western blot analysis

To detect protein in strains, starter cultures were grown overnight and then diluted 1:100 into fresh medium and allowed to achieve at least three doublings before 1 ml of cultures were centrifuged to remove supernatant and the cell pellet quick freeze in liquid nitrogen. The pellets were then resuspended in 104 µl of sonication buffer (PBS supplemented with Roche mini-complete tablet and 1 mM of EDTA) and sonicated twice (15 sec at lowest setting). 4x of Laemmli buffer (Invitrogen) and 10x of reducing agent (Invitrogen) were added to the sonicated cells and heated for 10 min at 80˚C to disrupt the protein disulphide bonds. Cell debris were spun down and 10 µl of samples were loaded into a NuPAGE 4-12% Bis-Tris gradient gel in MES buffer (Life technologies) containing antioxidant (Invitrogen) and separated by electrophoresis at 150 V for 45-60 min. The proteins were then transferred to a Hybond-P PVDF membrane (GE Healthcare) with transfer buffer (20% methanol in 0.5x MES buffer) using a semi dry apparatus (Hoefer Scientific Instruments). The transferred membrane was then blocked in blocking buffer (0.1% Tris and 7.5% of skimmed milk powder in PBS) for 2 h and rinsed twice for 5 min in PBST. Polyclonal primary antibodies (1:5000 for α-Spo0J, 1:2500 for α-Soj and 1:5000 for α-DivIVA) were added to the buffer (5 ml of blocking buffer in 20 ml of PBST) and incubated for 2 h to probe for the protein of interest. The membrane was washed twice for 5 min in PBST and anti-rabbit horseradish peroxidase-linked secondary antibody (2 µl if HRP in 5 ml of blocking buffer and 20 ml of PBST) was incubated for 1 h and again the membrane was rinsed twice in PBST for 5 min. An ImageQuant LAS 4000 mini digital imaging system (GE Healthcare) was used to detect the protein of interest.

2.8 Sporulation assays

To induce sporulation in *B. subtilis*, cells were grown in 2 ml of hydrolysed casein (CH) media overnight at 30˚C. The starter culture were then diluted back into CH media to an OD_{600} 0.1 and allowed to grow until OD_{600} 0.9 to 1.0 at 37˚C. The cultures were then centrifuged and resuspended in 2 ml of SM media and allowed to grow for a further 24 h at 37˚C. The next day, 50 µl of the cultures were diluted into 450 µl of LB to form two sets. Set A will be heat shocked at 80˚C for 25 min to kill cells, while set B will not be heat shock and will serve as the total viable cell counts. 10-fold serial dilutions of both sets were done and 50 µl of culture from each sets were plated onto NA plates and incubated overnight at 37˚C. The next day, colonies were counted and sporulation frequencies were determined as the ratio of heat resistant colony forming units (80˚C for 20 min) to total colony forming units.

2.9 Measurement of focus position within cells with two foci

For each cell, the focus closest to a pole was designated (Near), and the other focus was designated (Far). Three measurements were made: (i) the distance from the pole to the center of focus (near); (ii) the distance from the same pole to the center of focus (far); and (iii) the distance between the two poles (cell length).

To determine the distance of the focus (near) from the cell pole, the measured distance was divided by cell length, and multiplied by 100 to give the focus position as a percentage of cell length. To determine the distance of the focus (far) from the cell pole, the measured distance (far) was subtracted from the cell length and multiplied by 100 to give the focus position as a percentage

of cell length. These numbers were averaged for all cells in a sample. The 95% confidence intervals for the mean were calculated

Interfocal distance was calculated by subtracting focus (near) from focus (far), divided by cell length, and multiplied by 100 to give the focus distance as a percentage of cell length. These numbers were averaged for all cells in a sample. The 95% confidence intervals for the mean were calculated.

2.10 Strain list

Table 1: Strain list

Strain	Genotype	Reference
168CA	*Wild-type trpC2*	(Kunst et al., 1997)
AH3159	*spo0j*ΩpGR112 (*spo0j-gfp cat*)	(Real et al., 2005)
AK47	*trpC2 yycR*::(*tetO*$_{25}$ *erm*) *amyE*::($P_{spac(c)}$-*tetR-gfp spc*)	(Murray and Koh, 2014)
AK83	*trpC2 cotS*::(*parS*^{16} *cat*)	This work. PSL23 transformed into 168CA
AK87	*trpC2 spo0J*::*neo spo0J*::*neo yycR*::(*tetO*$_{25}$ *erm*) *amyE*::($P_{spac(c)}$-*tetR-gfp spc*) *yheH*::(*parS*^{16} *tet*) *cotS*::(*parS*^{16} *cat*)	This work. AK83 transformed into AK99
AK89	*trpC2* Δ*soj*::*neo yycR*::(*tetO*$_{25}$ *erm*) *amyE*::($P_{spac(c)}$-*tetR-gfp spc*) yheH::(*parS*^{16} *tet*) *cotS*::(*parS*^{16} *cat*)	This work. HM766 transformed into AK97
AK91	*trpC2 yheH*::(*parS*^{16} *cat*)	This work. PSL25 transformed into 168CA
AK93	*trpC2 yheH*::(*parS*^{16} *tet*)	This work. Pcat:tet transformed into AK91
AK95	*trpC2 yycR*::(*tetO*$_{25}$ *erm*) *amyE*::($P_{spac(c)}$-*tetR-gfp spc*) *yheH*::(*parS*^{16} *tet*)	This work. AK93 transformed into AK47

AK97	*trpC2 yycR*::(*tetO*$_{25}$ *erm*) *amyE*::(P$_{spac(c)}$-*tetR-gfp spc*) *yheH*::(*parS*^{16} *tet*) *cotS*::(*parS*^{16} *cat*)	This work. AK83 transformed into AK95
AK99	*trpC2 spo0J*::*neo yycR*::(*tetO*$_{25}$ *erm*) *amyE*::(P$_{spac(c)}$-*tetR-gfp spc*) *yheH*::(*parS*^{16} *tet*)	This work. HM765 transformed into AK95
AK123	*trpC2* Δ*spo0J*::*neo yycR*::(*tetO*$_{25}$ *erm*) *amyE*::(P$_{spac(c)}$-*tetR-gfp spc*) *yheH*::(*parS*^{16} *tet*) *cotS*::(*parS*^{16} *cat*)	This work. HM907 transformed into AK97
AK150	*trpC2 yheH*::(*parS*^{16} *tet*) *cotS*::(*parS*^{16} *cat*)	This work. AK83 transformed into AK91
AK153	*trpC2 spo0J-gfp*::*neo yheH*::(*parS*^{16} *tet*) *cotS*::(*parS*^{16} *cat*)	This work. HM756 transformed into Ak150
AK169	*yycR*::(*tetO*$_{25}$ *erm*) *amyE*::(P$_{spac(c)}$-*tetR-gfp spc*)	This work. BKM865 transformed into BKM918
AK171	Δ8*parS yycR*::(*tetO*$_{25}$ *erm*) *amyE*::(P$_{spac(c)}$-*tetR-gfp spc*)	This work. PCR fragment of (oAK7/8) & (oAK5/6) transformed into BNS1657
AK177	Δ8*parS neo*(*soj-spo0j)* *yycR*::(*tetO*$_{25}$ *erm*) *amyE*::(P$_{spac(c)}$-*tetR-gfp spc*)	This work. pHM309 transformed into AK171

AK179	Δ8*parS* Δ*spo0J*::*neo yycR*::(*tetO*$_{25}$ *erm*) *amyE*::(P$_{spac(c)}$-*tetR-gfp spc*)	This work. pHM456 transformed into AK171
AK181	*neo*(*soj-spo0j*) *yycR*::(*tetO*$_{25}$ *erm*) *amyE*::(P$_{spac(c)}$-*tetR-gfp spc*)	This work. pHM422 transformed into AK169
AK183	Δ*spo0J*::*neo yycR*::(*tetO*$_{25}$ *erm*) *amyE*::(P$_{spac(c)}$-*tetR-gfp spc*)	This work. HM907 transformed into AK169
AK199	*trpC2 gfp-soj*::*neo yheH*::(*parS*16 *tet*) *cotS*::(*parS*16 *cat*)	This work. HM740 transformed into AK150
AK205	Δ9*parS*	This work. pAK09 transformed into BNS1657
AK207	Δ9*parS neo*(*soj-spo0j*) *yycR*::(*tetO*$_{25}$ *erm*) *amyE*::(P$_{spac(c)}$-*tetR-gfp spc*)	This work. pAK09 transformed into AK177
AK209	Δ9*parS* Δ*spo0J*::*neo yycR*::(*tetO*$_{25}$ *erm*) *amyE*::(P$_{spac(c)}$-*tetR-gfp spc*)	This work. pAK09 transformed into AK179
AK213	Δ9*parS*	This work. pAK23 transformed into BNS1657
AK215	Δ10*parS*	This work. pAK23 transformed into AK205
AK225	Δ10*parS neo*(*soj-spo0j*) *yycR*::(*tetO*$_{25}$ *erm*) *amyE*::(P$_{spac(c)}$-*tetR-gfp spc*)	This work. pAK23 transformed into AK207
AK227	Δ10*parS* Δ*spo0J*::*neo yycR*::(*tetO*$_{25}$ *erm*) *amyE*::(P$_{spac(c)}$-*tetR-gfp spc*)	This work. pAK23 transformed into AK209

AK239	*neo*(*soj-spo0j*)	This work. pAK26 transformed into PY79
AK241	Δ*spo0J*::*neo*	This work. pAK28 transformed into PY79
AK243	Δ10*parS neo*(*soj-spo0j*)	This work. pAK32 transformed into AK215
AK245	Δ10*parS* Δ*spo0J*::*neo*	This work. pAK30 transformed into AK215
AK249	*spo0J*^{R149A}::*neo*	This work. pAK38 transformed into PY79
AK251	*spo0J*^{G77S}::*neo*	This work. pAK44 transformed into PY79
AK259	Δ9*parS*$^{+359}$ *neo*(*soj-spo0j*)	This work. pAK26 transformed into AK215
AK261	Δ9*parS*$^{+359}$ Δ*spo0J*::*neo*	This work. pAK28 transformed into AK215
AK277	*gfp-soj*::*neo*	This work. pHM23 transformed into PY79
AK279	(*gfp-soj* Δ*spo0J*)*::neo*	This work. pHM33 transformed into PY79
AK281	Δ10*parS gfp-soj*::*neo*	This work. pAK48 transformed into AK215
AK283	Δ10*parS* (*gfp-soj* Δ*spo0J*)::*neo*	This work. pAK50 transformed into AK215

AK305	Δ9*parS*$^{+359}$ *gfp-soj*::*neo*	This work. pHM23 transformed into AK215
AK307	Δ9*parS*$^{+359}$ (*gfp-soj* Δ*spo0J*) ::*neo*	This work. pHM33 transformed into AK215
AK315	Δ9*parS*$^{+90}$	This work. pAK56 transformed into AK205
AK323	Δ9*parS*$^{+90}$ *neo*(*soj-spo0j*)	This work. pAK32 transformed into AK315
AK325	Δ9*parS*$^{+90}$ Δ*spo0J*::*neo*	This work. pAK30 transformed into AK315
AK367	*spo0J-gfp*::*neo*	This work. pAK82 transformed into PY79
AK369	Δ10*parS spo0J-gfp*::*neo*	This work. pAK83 transformed into AK215
AK373	Δ9*parS*$^{+90}$ *spo0J-gfp*::*neo*	This work. pAK83 transformed into AK315
AK399	Δ9*parS*$^{+90}$ *gfp-soj*::*neo*	This work. pAK48 transformed into AK315
AK405	Δ9*parS*$^{+90}$ *yycR*::(*tetO*$_{25}$ *erm*) *amyE*::($P_{spac(c)}$-*tetR-gfp spc*)	This work. pAk56 transformed into AK207
AK417	Δ9*parS*$^{+90}$ *spo0J*^{R149A}::*neo*	This work. pAK42 transformed into AK315
AK419	Δ9*parS*$^{+90}$ *spo0J*^{G77S}::*neo*	This work. pAK46 transformed into AK315

AK421	(Δ*soj spo0J-gfp*)::*neo*	This work. pAK102 transformed into PY79
AK425	Δ9*parS*$^{+90}$ (Δ*soj spo0J-gfp*)::*neo*	This work. pAK103 transformed into AK315
AK427	*neo*(*soj-spo0j*) (pLOSS *parS*$^{+}$)	This work. pAK92 transformed into AK239
AK429	*neo*(*soj-spo0j*) (pLOSS *parS*$^{-}$)	This work. pAK97 transformed into AK239
AK431	Δ*spo0J*::*neo* (pLOSS *parS*$^{+}$)	This work. pAK92 transformed into AK241
AK433	Δ*spo0J*::*neo* (pLOSS *parS*$^{-}$)	This work. pAK97 transformed into AK241
AK435	Δ10*parS neo*(*soj-spo0j*) (pLOSS *parS*$^{+}$)	This work. pAK92 transformed into AK243
AK437	Δ10*parS neo*(*soj-spo0j*) (pLOSS *parS*$^{-}$)	This work. pAK97 transformed into AK243
AK439	Δ10*parS* Δ*spo0J*::*neo* (pLOSS *parS*$^{+}$)	This work. pAK92 transformed into Ak245
AK441	Δ10*parS* Δ*spo0J*::*neo* (pLOSS *parS*$^{-}$)	This work. pAk97 transformed into AK245
AK455	*spo0J-gfp*::*neo* (pLOSS *parS*$^{+}$)	This work. pAK104 transformed into AK367
AK457	*spo0J-gfp*::*neo* (pLOSS *parS*$^{-}$)	This work. pAK106 transformed into AK367

AK459	Δ10*parS spo0J-gfp*::*neo* (pLOSS *parS*$^{+}$)	This work. pAK104 transformed into AK369
AK461	Δ10*parS spo0J-gfp*::*neo* (pLOSS *parS*$^{-}$)	This work. pAK106 transformed into AK369
AK463	*gfp-soj*::*neo* (pLOSS *parS*$^{+}$)	This work. pAK92 transformed into AK277
AK465	*gfp-soj*::*neo* (pLOSS *parS*$^{-}$)	This work. pAK97 transformed into AK277
AK467	(*gfp-soj* Δ*spo0J*)::*neo* (pLOSS *parS*$^{+}$)	This work. pAK92 transformed into AK279
AK469	(*gfp-soj* Δ*spo0J*)::*neo* (pLOSS *parS*$^{-}$)	This work. pAK97 transformed into AK279
AK471	Δ10*parS gfp-soj*::*neo* (pLOSS *parS*$^{+}$)	This work. pAK92 transformed into AK281
AK473	Δ10*parS gfp-soj*::*neo* (pLOSS *parS*$^{-}$)	This work. pAK97 transformed into AK281
AK475	Δ10*parS* (*gfp-soj* Δ*spo0J*)::*neo* (pLOSS *parS*$^{+}$)	This work. pAK92 transformed into AK283
AK477	Δ10*parS* (*gfp-soj* Δ*spo0J*)::*neo* (pLOSS *parS*$^{-}$)	This work. pAK97 transformed into AK283
AK519	Δ9*parS yycR*::(*tetO*$_{25}$ *erm*) *amyE*::($P_{spac(c)}$-*tetR-gfp spc*)	This work. pAK23 transformed into AK171
AK521	Δ10*parS yycR*::(*tetO*$_{25}$ *erm*) *amyE*::($P_{spac(c)}$-*tetR-gfp spc*)	This work. pAK09 transformed into AK519

AK547	*trpC2* (*gfp-soj* Δ*spo0J*)::*neo*	This work. HM13 transformed into 168CA
AK553	Δ9*parS*$^{+90}$ Δ(*soj-spo0J*)::*neo*	This work. pAK100 transformed into AK315
AK555	Δ9*parS*$^{+90}$ Δ*soj*::*neo*	This work. pAK101 transformed into AK315
AK557	Δ*soj*::*neo*	This work. pAK98 transformed into PY79
AK559	Δ(*soj-spo0J*)::*neo*	This work. pAK99 transformed into PY79
AK561	Δ9*parS*$^{+359}$ Δ(*soj-spo0J*)::*neo*	This work. pAK99 transformed into AK215
AK563	Δ10*parS* Δ(*soj-spo0J*)::*neo*	This work. pAK100 transformed into AK215
AK569	*trpC2* (*gfp-soj* Δ*spo0J*)::*neo* (plasmid *parS*$^{-}$)	This work. pHM430 transformed into AK547
AK571	*trpC2* (*gfp-soj* Δ*spo0J*)::*neo* (plasmid *parS*$^{+}$)	This work. pHM432 transformed into AK547
AK573	*trpC2* Δ(*soj-spo0J*)::*neo* *yycR*::(*tetO*$_{25}$ *erm*) *amyE*::($P_{spac(c)}$-*tetR-gfp spc*)	This work. HM749 transformed into AK47
AK575	*trpC2* Δ(*soj-spo0J*)::*neo* *yycR*::(*tetO*$_{25}$ *erm*) *amyE*::($P_{spac(c)}$-*tetR-gfp spc*) *yheH*:: (*parS*^{16} *tet*) *cotS*::(*parS*^{16} *cat*)	This work. HM749 transformed into AK97

AK577	*trpC2* (*gfp-soj* Δ*spo0J*)::*neo* *yheH*::(*parS*^{16} *tet*) *cotS*::(*parS*^{16} *cat*)	This work. AK547 transformed into AK150
AK585	*trpC2* (Δ*soj* Δ*spo0J tetO*$_{array}$)::*neo* *cgeD*::(P$_{pen(mutTTAG)}$-*tetR-yfp tet*)	This work. HM194 transformed into 168CA
AK587	*trpC2* (Δ*soj* Δ*spo0J tetO*$_{array}$)::*neo* *cgeD*::(P$_{pen(mutTTAG)}$-*tetR-yfp tet*) (plasmid *parS*$^{-}$)	This work. pHM430 transformed into AK585
AK589	*trpC2* (Δ*soj* Δ*spo0J tetO*$_{array}$)::*neo* *cgeD*::(P$_{pen(mutTTAG)}$-*tetR-yfp tet*) (plasmid *parS*$^{+}$)	This work. pHM432 transformed into AK585
AK591	Δ9*parS*$^{+359}$ *yycR*::(*tetO*$_{25}$ *erm*) *amyE*::(P$_{spac(c)}$-*tetR-gfp spc*)	This work. pAK26 transformed into AK521
AK593	Δ9*parS*$^{+359}$ *spo0J-gfp*::*neo*	This work. pAK82 transformed into AK215
AK595	Δ10*parS* (Δ*soj spo0J-gfp*)::*neo*	This work. pAK103 transformed into AK215
AK597	Δ9*parS*$^{+270}$ *spo0J-gfp*::*neo*	This work. pAK180 transformed into AK369
AK599	Δ9*parS*$^{+270}$ *gfp-soj*::*neo*	This work. pAK180 transformed into AK281
AK601	Δ9*parS*$^{+270}$ (*gfp-soj* Δ*spo0J-gfp*) ::*neo*	This work. pAK180 transformed into AK283
AK603	Δ9*parS*$^{+270}$ (*soj-spo0j*)::*neo*	This work. pAK180 transformed into AK243

AK605	Δ9*parS*$^{+270}$ Δ*spo0J*::*neo*	This work. pAK180 transformed into AK245
AK607	Δ9*parS*$^{+270}$ Δ(*soj-spo0J)*::*neo*	This work. pAK180 transformed into AK563
AK615	Δ9*parS*$^{+90}$ Δ*spo0J*::*neo* *yycR*::(*tetO*$_{25}$ *erm*) *amyE*::(P$_{spac(c)}$-*tetR-gfp spc*)	This work. pAK56 transformed into AK209
AK617	Δ10*parS* Δ*soj*::*neo*	This work. pAK101 transformed into AK215
AK619	Δ*soj*::*neo* (pLOSS *parS*$^{+}$)	This work. pAK92 transformed into AK557
AK621	Δ*soj*::*neo* (pLOSS *parS*$^{-}$)	This work. pAK97 transformed into AK557
AK623	Δ(*soj-spo0J*)::*neo* (pLOSS *parS*$^{+}$)	This work. pAK92 transformed into AK559
AK625	Δ(*soj-spo0J*)::*neo* (pLOSS *parS*$^{-}$)	This work. pAK97 transformed into AK559
AK627	Δ10*parS* Δ(*soj-spo0J*)::*neo* (pLOSS *parS*$^{+}$)	This work. pAK92 transformed into AK563
AK629	Δ10*parS* Δ(*soj-spo0J*)::*neo* (pLOSS *parS*$^{-}$)	This work. pAK97 transformed into AK563
AK631	Δ10*parS* Δ*soj*::*neo* (pLOSS *parS*$^{+}$)	This work. pAK92 transformed into AK617
AK633	Δ10*parS* Δ*soj*::*neo* (pLOSS *parS*$^{-}$)	This work. pAK97 transformed into AK617

AK639	Δ9*parS*$^{+359}$ Δspo0J::*neo* yycR::(*tetO*$_{25}$ *erm*) *amyE*::(P$_{spac(c)}$-*tetR-gfp spc*)	This work. pAK28 transformed into AK521
AK641	Δ9*parS*$^{+359}$ (Δ*soj spo0J-gfp*)::*neo*	This work. pAK102 transformed into AK215
AK643	Δ9*parS*$^{+270}$ (Δ*soj spo0J-gfp*)::*neo*	This work. pAK180 transformed into AK595
AK649	Δ9*parS*$^{+270}$ Δ*soj*::*neo*	This work. pAK180 transformed into AK617
AK665	Δ9*parS* Δ*soj*::*tet*	This work. pHM59 transformed into AK205
AK667	Δ8*parS*$^{+359}$ Δ*soj*::*neo*	This work. pHM160 transformed into AK665
AK669	Δ9*parS*$^{+359}$ Δ*soj*::*neo*	This work. AK213 transformed into AK667
BKM865	*yycR*::(*tetO*$_{25}$ *erm*) *amyE*::(P$_{spac(c)}$-*tetR-gfp spc*)	(Wagner et al., 2009)
BKM918	*yycR*::(*tetO*$_{25}$ *erm*)	(Wagner et al., 2009)
BNS1657	Δ8*parS*	(Sullivan et al., 2009)
DCL484	Δ6*parS*	(Lin and Grossman, 1998)
HM4	*trpC2 gfp-soj*::*neo*	(Murray and Errington, 2008)
HM13	*trpC2* (*gfp-soj* Δ*spo0J*)::*neo*	(Murray and Errington, 2008)
HM34	*trpC2 spo0J*::*neo*	(Murray and Errington, 2008)
HM61	*trpC2 spo0J-gfp*::*neo*	(Leaver et al., 2009)

HM130	*trpC2* (*spo0J* $tetO_{150}$)::neo *cgeD*::($P_{pen(mutTTAG)}$-*tetR-yfp tet*)	(Murray and Errington, 2008)
HM168	*trpC2* (Δ*spo0J* $tetO_{150}$)::*neo* *cgeD*::($P_{pen(mutTTAG)}$-*tetR-yfp tet*)	(Murray and Errington, 2008)
HM171	*trpC2* (Δ*soj* $tetO_{150}$)::*neo* *cgeD*::($P_{pen(mutTTAG)}$-*tetR-yfp tet*)	(Murray and Errington, 2008)
HM183	*trpC2* Δ(*soj-spo0J*)::*neo*	(Scholefield et al., 2011)
HM194	*trpC2* (*Δsoj Δspo0J* $tetO_{150}$)::*neo* *cgeD*::($P_{pen(mutTTAG)}$-*tetR-yfp tet*)	(Murray and Errington, 2008)
HM226	*trpC2 pheA Δspo0J*::*neo*	(Murray and Errington, 2008)
HM227	*trpC2 pheA Δsoj*::*neo*	(Murray and Errington, 2008)
HM740	*trpC2 gfp-soj*::*neo*	This work. HM4 transformed into 168CA
HM747	*trpC2 spo0J*::*neo*	This work. HM34 transformed into 168CA
HM748	*trpC2 Δsoj*::*neo*	This work. HM227 transformed into 168CA
HM749	*trpC2 Δ(soj-spo0J)*::*neo*	This work. HM183 transformed into 168CA
HM754	*trpC2 Δspo0J*::*neo*	This work. HM226 transformed into 168CA
HM756	*trpC2 spo0J-gfp*::*neo*	This work. HM61 transformed into 168CA
HM765	*trpC2 spo0J*::*neo yycR*::(*$tetO_{25}$ erm*) *amyE*::($P_{spac(c)}$-*tetR-gfp spc*)	This work. HM747 transformed into AK47

HM766	*trpC2* Δ*soj*::*neo yycR*::(*tetO*$_{25}$ *erm*) *amyE*::(P$_{spac(c)}$-*tetR-gfp spc*)	This work. HM748 transformed into AK47
HM821	*trpC2 spo0J-gfp*::*neo* (plasmid *parS*$^{-}$)	This work. pHM430 transformed into HM756
HM823	*trpC2 spo0J-gfp*::*neo* (plasmid *parS*$^{+}$)	This work. pHM432 transformed into HM756
HM831	*trpC2* (*Δspo0J tetO*$_{150}$)::*neo* *cgeD*::(P$_{pen(mutTTAG)}$-*tetR-yfp tet*)	This work. HM168 transformed into 168CA
HM832	*trpC2* (Δ*soj tetO*$_{150}$)::*neo* *cgeD*::(P$_{pen(mutTTAG)}$-*tetR-yfp tet*)	This work. HM171 transformed into 168CA
HM834	*trpC2* (Δ*spo0J tetO*$_{150}$)::*neo*) *cgeD*::(P$_{pen(mutTTAG)}$-*tetR-yfp tet*) (plasmid *parS*$^{-}$)	This work. pHM430 transformed into HM831
HM835	*trpC2* (Δ*soj tetO*$_{150}$)::*neo* *cgeD*::(P$_{pen(mutTTAG)}$-*tetR-yfp tet*) (plasmid *parS*$^{-}$)	This work. pHM430 transformed into HM832
HM837	*trpC2* (Δ*spo0J tetO*$_{150}$)::*neo* *cgeD*::(P$_{pen(mutTTAG)}$-*tetR-yfp tet*) (plasmid *parS*$^{+}$)	This work. pHM432 transformed into HM831
HM838	*trpC2* (Δ*soj tetO*$_{150}$)::*neo* *cgeD*::(P$_{pen(mutTTAG)}$-*tetR-yfp tet*) (plasmid *parS*$^{+}$)	This work. pHM432 transformed into HM832
HM853	*trpC2* (*spo0J tetO*$_{150}$)::*neo* *cgeD*::(P$_{pen(mutTTAG)}$-*tetR-yfp tet*)	This work. HM130 transformed into 168CA

HM855	*trpC2* (*spo0J tetO*$_{150}$):: *neo* *cgeD*::(P$_{pen(mutTTAG)}$-*tetR-yfp tet*) (plasmid *parS*$^{-}$)	This work. pHM430 transformed into HM853
HM856	*trpC2* (*spo0J tetO*$_{150}$)::*neo* *cgeD*::(P$_{pen(mutTTAG)}$-*tetR-yfp tet*) (plasmid *parS*$^{+}$)	This work. pHM432 transformed into HM853
HM870	*trpC2 gfp-soj*::*neo* (plasmid *parS*$^{-}$)	pHM430 transformed into HM740
HM871	*trpC2 gfp-soj*::*neo* (plasmid *parS*$^{+}$)	pHM432 transformed into HM740
HM907	*trpC2* Δ*spo0J*::neo *yycR*::(*tetO*$_{25}$ *erm*) *amyE*::(P$_{spac(c)}$-*tetR-gfp spc*)	HM754 transformed into AK47
JH693	*spo0J*^{G77S}	(Hoch and Mathews, 1973; Hranueli et al., 1974)
PSL23	*trpC2* Δ6*parS spo0J-gfp* *cotS*::(*parS*^{16} *cat*)	(Lee et al., 2003)
PSL25	*trpC2* Δ6*parS spo0J-gfp* *yheH*::(*parS*^{16} *cat*)	(Lee et al., 2003)
PY79	Wild-type prototroph	(Youngman et al., 1983)

2.11 Plasmid list

Table 2: Plasmid list

Plasmid	Genotype	Construction	Reference
pCat::Tet	*cat*::*tet*		(Steinmetz and Richter, 1994)
pAK05	*bla cat 'sigX* Δ*parS*^{206}::*zeo*	*'sigX* (oAK17/oAK18) ligated into pHM457 (HindIII-Asp718I)	This work
pAK09	*bla cat 'sigX* Δ*parS*^{206}::*zeo resE'*	*resE'* (oAk15/oAK16) ligated into pAK05 (SacI-SacII)	This work
pAK11	*bla cat pheo*	*Pheo* from pIC22 subcloned into pHM01 (BamHI)	This work
pAK13	*bla* cat *'yhaX*^{parS90} *pheo*	Site directed mutagenesis of *'yhaX*^{parS90} (oAK38 /oAK39) ligated into pAK11 (SacI-SacII)	This work
pAK14	*bla cat pheo hemZ'*	*hemZ'* (oAK40/oAK41) ligated into pAK11 (XhoI-Asp718I)	This work

pAK15	*bla cat 'yhaX*$^{-parS90}$ *::pheo hemZ'*	*yhaX*$^{-parS90}$ (pAK13) subcloned into pAK14 (SacI-SacII)	This work
pAK23	*bla cat 'yhaX*$^{-parS90}$*::tet hemZ'*	*Tet* (oAK47/oAK51) from pBEST309 ligated into pAK15 (BamHI-PstI)	This work
pAK26	*bla cat 'soj-spo0J::neo yyaC'*	*'soj-spo0J-neo* (oAK55/oGJS431) from pHM48 ligated into pHM23 (BlnI-NotI)	This work
pAK28	*bla cat 'soj-*Δ*spo0J::neo yyaC'*	*'soj-*Δ*spo0J-neo* (oAK55/oGJS431) from pHM52 ligated into pHM23 (BlnI-NotI)	This work
pAK30	*bla cat 'soj-*Δ*spo0J-parS*$^{-}$ *::neo*	*'soj-*Δ*spo0J-parS*$^{-}$*neo* (oAK55/oGJS431) from pHM456 ligated into pHM23 (BlnI-NotI)	This work

pAK32	*bla cat 'soj-spo0J-parS*$^{-}$ ::*neo yyaC'*	*'soj-spo0J-parS*$^{-}$ (oAK52/oAK53) from pHM142 ligated into pAK26 (SacII-XbaI)	This work
pAK38	*bla cat 'soj-spo0J*^{R149A}::*neo yyaC'*	*spo0J*^{R149A} mutation (oHM76/oGJS149) from pSG4616 ligated into pAK26 (NdeI-HindIII)	This work
pAK42	*bla cat 'soj-spo0J*^{R149A}-*parS*$^{-}$::*neo yyaC'*	*spo0J*^{R149A} mutation (oHM76/oGJS149) from pSG4616 ligated into pAK32 (NdeI-HindIII)	This work
pAK44	*bla cat 'soj-spo0J*^{G77S}::*neo yyaC'*	*spo0J*^{G77S} mutation (oAK52/oGJS149) from JH693 ligated into pAK26 (NdeI-HindIII)	This work
pAK46	*bla cat 'soj- spo0J*^{G77S}-*parS*$^{-}$::*neo yyaC'*	*spo0J*^{G77S} mutation (oAK52/oGJS149) from Spo0J93 ligated into pAK32 (NdeI-HindIII)	This work

pAK48	*bla cat* '*yyaB* P_{soj}-*gfp-soj-spo0J-parS*$^-$::*neo yyaC'*	'*soj-spo0J-parS*$^-$ (oAK52/oAK53) from pHM309 ligated into pHM23 (SacII-XbaI)	This work
pAK50	*bla cat* '*yyaB* P_{soj}-*gfp-soj-*Δ*spo0J-parS*$^-$::*neo yyaC'*	'*soj-*Δ*spo0J-parS*$^-$ (oAK52/oAK53) from pHM456 ligated into pHM23 (SacII-XbaI)	This work
pAK56	*bla cat* '*yhaX*^{parS90}::*tet parS*$^+$ *hemZ*'	'*soj-parS*$^+$*-spo0J*' (oAK61/oAK62) from pHM48 ligated into pAK23 (NotI)	This work
pAK82	*bla cat 'soj-spo0J-gfp*::*neo yyaC'*	'*spo0J-gfp* (pHM110) subcloned into pAK26 (XcmI-XbaI)	This work
pAK83	*bla cat 'soj-spo0J-gfp-parS*$^-$::*neo yyaC'*	'*spo0J-gfp* (pHM110) subcloned into pAK32 (XcmI-XbaI)	This work
pAK92	*spc parS*$^+$	'*spo0J-parS*$^+$*-spo0J*' (oAK61/oAK62) from pHM48 ligated into pAK97 (NotI)	This work
pAK97	*spc*	pLOSS renamed to pAK97	(Claessen et al., 2008)

pAK98	*bla cat 'Δsoj-spo0J::neo yyaC'*	'Δ*soj* (oAK58/oHM20) from pHM160 ligated into pAK26 (KpnI-SacII)	This work
pAK99	*bla cat 'Δ(soj-spo0J)::neo yyaC'*	'Δ*soj* (oAK58/oHM20) from pHM160 ligated into pAK28 (KpnI-SacII)	This work
pAK100	*bla cat '(Δsoj-spo0J-parS⁻)::neo*	'Δ*soj* (oAK58/oHM20) from pHM160 ligated into pAK30 (KpnI-SacII)	This work
pAK101	*bla cat 'Δsoj-spo0J-parS⁻::neo yyaC'*	'Δ*soj* (oAK58/oHM20) from pHM160 ligated into pAK32 (KpnI-SacII)	This work
pAK102	*bla cat 'Δsoj-spo0J-gfp::neo yyaC'*	'Δ*soj* (oAK58/oHM20) from pHM160 ligated into pAK82 (KpnI-SacII)	This work
pAK103	*bla cat 'Δsoj-spo0J-gfp-parS⁻::neo yyaC'*	'Δ*soj* (oAK58/oHM20) from pHM160 ligated into pAK83 (KpnI-SacII)	This work

pAK104	*spc tetO*$_{array}$ *parS*$^{+}$	*tetO*$_{array}$ from pLAU44 subcloned into pAK92 (SacI)	This work
pAK106	*spc tetO*$_{array}$	*tetO*$_{array}$ from pLAU44 subcloned into pAK97 (SacI)	This work
pAK128	*bla cat 'ytcC*::*zeo*	*'ytcC* (oAK191/oAK192) ligated into pHM457 (SacI-SacII)	This work
pAK130	*bla cat zeo ytxO*'	*ytxO*' (oAK189/oAK190) ligated into pHM457 (KpnI-XhoI)	This work
pAK136	*bla cat 'ytcC*::*zeo ytxO*'	*ytxO*' from pAK130 subcloned into pAK128 (KpnI-XhoI)	This work
pAK178	*bla cat 'ytcC*::*erm ytxO*'	*erm* (oAK227/oAK257) from pHM432 ligated into pAK136 (BamHI-XhoI)	This work

pAK180	*bla cat 'ytcC*::*erm parS*$^{+}$ *ytxO*'	'*soj-spo0J-parS*$^{-}$ (oAK216/oAK217) from pHM422 ligated into pAK178 (XbaI)	This work
pBEST309	*bla tet*		(Itaya, 1992)
pIC22	*bla phleo*		(Steinmetz and Richter, 1994)
pSG4616	*bla cat spo0J*^{R149A}		(Autret et al., 2001)
pHM01	*bla cat*		(Murray et al., 2006)
pHM16	*bla cat* P_{soj}-*soj-spo0J*::*neo yyaC'*		(Murray et al., 2006)
pHM23	*bla cat* '*yyaB*-P_{soj}-*gfp-soj-spo0J*::*neo yyaC'*		(Murray and Errington, 2008)
pHM33	*bla cat* '*yyaB*-P_{soj}-*gfp-soj* Δ*spo0J*::*neo yyaC'*		(Murray and Errington, 2008)
pHM48	*bla cat* P_{soj}-*soj-spo0J*::*neo yyaC'*		(Murray and Errington, 2008)

pHM52	*bla cat* P_{soj}-*soj*-Δ*spo0J*::*neo yyaC'*		(Murray and Errington, 2008)
pHM59	*bla cat* '*yyaB*-P_{soj}::*tet yyaC'*		(Murray and Errington, 2008)
pHM109	*bla cat* '*yyaB* P_{soj}-*soj-spo0J*::*neo yyaC'*	P_{soj}-*soj-spo0J*::*neo yyaC'* from pHM16 subcloned into pOU82 (NcoI-SacI)	This work
pHM110	*bla cat* '*yyaB* P_{soj}-*soj-spo0J-gfp*::*neo yyaC'*	Linker replaced the stop codon of *spo0J* and *gfp* (oHM79/oHM80) from AH3159 ligated into pAK109 (SacII-XbaI)	This work
pHM142	*bla cat* P_{soj}-*soj-spo0J-parS*$^{-}$::*neo yyaC'*	*'spo0J-parS*$^{-}$*-spo0J*' (oHM11/oHM76) from DCL484 ligated into pHM16 (EcoRI-HindIII)	This work
pHM160	*bla cat* P_{soj}-Δ*soj-spo0J*::*neo yyaC'*		(Murray and Errington, 2008)

pHM309	*bla cat* Δ*soj-spo0J-parS*⁻ ::*neo yyaC'*	*'spo0J-parS*⁻*-spo0J*' from pHM142 subcloned into pHM160 (EcoRI-HindIII)	This work
pHM430	*erm*	pNZ8907 renamed to pAK97	(Bongers et al., 2005)
pHM432	*Erm* '*spo0J-parS*⁺*-spo0J*'	'*spo0J-parS*⁺*-spo0J*' (oAK61/oAK62) from pHM48 ligated into pHM432 (NotI)	This work
pHM445	*erm*	pAPNC-*erm* renamed to pHM445	Lab strain
pHM456	*bla cat* P_{soj}-*soj*-Δ*spo0J-parS*⁻::*neo*	*'spo0J-parS*⁻*-spo0J*' from pHM142 subcloned into pHM52 (EcoRI-HindIII)	This work
pHM457	*bla cat zeo*	*Zeo* subcloned into pHM01 (EcoRI)	This work
pLAU44	*bla gm* $tetO_{array}$		(Lau et al., 2003)
pOU82	*bla*		(Gerdes et al., 1985)

2.12 Primer list

Table 3: Primer list

Primer	Sequence	Construction
oAK15	5’-AATTTAATTTCCGCGGATTCAGACTCGATTTTACCGTTTTG-3’	pAK05
oAK16	5’-AATTTAATTTGAGCTCAGCTGAGAACACCGATCTCCATG-3’	pAK05
oAK17	5’-AATTTAATTTGGTACCAGTACTTTGAGCCCTCTGTG-3’	pAK09
oAK18	5’-AATTTAATTTAAGCTTACATTAATAAAATTTAAGGATATGTTAATAT-3’	pAK09
oAK38	5’-AATTTAATTTGAGCTCCTGCTTCGGTCGAACGGGAAG-3’	pAK13
oAK39	5’-AATTTAATTTCCGCGGTTACACTCTCTTCATATGAAATTTATCAAGAAATCCTTTTCGCTGCTG-3’	pAK13
oAK40	5’-AATTTAATTTCTCGAGAAAAGCCGCTCGCGCCCTGACAG-3’	pAK14
oAK41	5’-AATTTAATTTGGTACCGATTGATGCTGATCCGATCAATGTC-3’	pAK14
oAK47	5’-AATTTAATTTCTGCAGCTCCCAAAGTTGATCCCTTAACG-3’	pAK23
oAK51	5’-AATTTAATTTGGATCCCAGAGATCTCCCATATTGTTG-3’	pAK23

oAK52	5’-AAGGGAAGGGCCGCGGTCAAGAGGTGCGGAAGTATATTTAG-3’	pAK44/pAK48/pAK50
oAK53	5’-AAGGGAAGGGTCTAGAACTAGTGGATCCCCCGGGCTGC-3’	pAK48/pAK50
oAK55	5’-AATTTAATTTCCTAGGTAAGGAAAAATCATAGCAATTACGAAC-3’	pAK26
oAK58	5’-CTTTATGCTTCCGGCTCGTATG-3’	pAK98
oAK61	5’-AATTTAATTTGCGGCCGCGACTGCTGACACTGCCAG-3’	pAK56/pAK92
oAK62	5’-AATTTAATTTGCGGCCGCCATTTATGATTCTCGTTCAGAC-3’	pAK56/pAK92
oAK189	5’-AAGGGAATTCTCGAGGTGACTTTATGCCTTGCGCTTTAC-3’	pAK130
oAK190	5’-AAGGGAATTGGTACCGCCTCTATTTCTAAACTGGATCTCGAC-3’	pAK130
oAK191	5’-AAGGGAATTTGAGCTCGTGGTTCAGCGATGACAG-3’	pAK128
oAK192	5’-AAGGGAATTTCCGCGGTTTGCAACACGAGCTGTAGG-3’	pAK128
oAK216	5’-AAGGGAATTTCTAGAGACTGCTGACACTGCC-3’	pAK180
oAK217	5’-AAGGGAATTTCTAGACATTTATGATTCTCGTTCAGAC-3’	pAK180
oAK227	5’-AAGGGAATTGGATCCGACTCATAGAATTATTTCCTCCCG-3’	pAK178

oAK257	5’-AATTTAATTTCTCGAGTATCACGAGGCCCTTTCGTCTTCAAGAATTGATCC-3’	pAK178
oGJS149	5’-GGAGATAGGATTCCCGTTCTTTTAG-3’	pAK38/pAK44
oGJS431	5’-GGTGGTCCCGCGGCATCTTCGTTTGAAAGATGCGGC-3’	pAK26
oHM11	5’-CCGAATTCTGGGCGCATATAAAATAAAAACCATC-3’	pHM142
oHM20	5’-TTTTCTTGGCTGATAAGGATTAGGGCGTAAATCG-3’	pAK98
oHM76	5’-TCGAGCGGCAAAGCTGGCAGGTTTAGATAC-3’	pAK38/pHM142
oHM79	5’-GGGAATTCGCCACCATGAGTAAAGGAGAAGAACTTTTCAC-3’	pHM110
oHM80	5’- GCTCTAGATTATTTGTATAGTTCATCCATG-3’	pHM110

2.13 Western blot analysis of strains

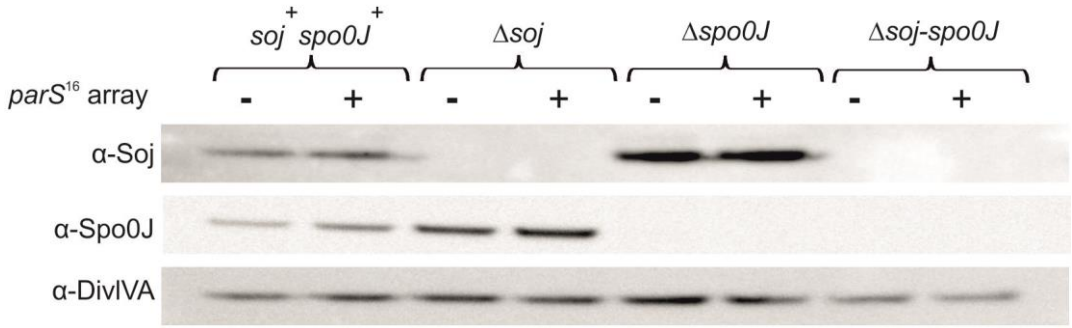

Figure 2.13.1: Western blot for Chapter 3 strain constructions (*parS*^{16} arrays on the chromosome)

Western blot analysis of the various *parS* mutants. Cells were grown in 2% succinate minimal media at 37˚ until early exponential phase. Cells were lysed and Soj and Spo0J proteins were detected using Western blot analysis (DivIVA protein was likewise detected and used as a loading control). *soj*$^{+}$ *spo0J*$^{+}$ (HM765), *soj*$^{+}$ *spo0J*$^{+}$ *parS*^{16} array (90˚ & 270˚) (AK87), Δ*spo0J* (HM907), Δ*spo0J parS*^{16} array (90˚ & 270˚) (AK123), Δ*soj* (HM766), Δ*soj parS*^{16} array (90˚ & 270˚) (AK89), Δ*soj-spo0J* (AK573), Δ*soj-spo0J parS*^{16} array (90˚ & 270˚) (AK575).

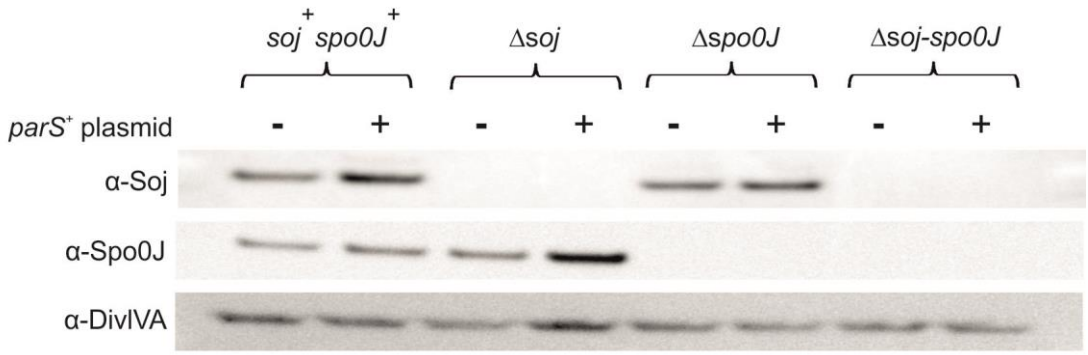

Figure 2.13.2: Western blot for Chapter 3 strain constructions (*parS* on the multi-copy plasmid)

Western blot analysis of the various *parS* mutants. Cells were grown in 2% succinate minimal media at 37˚ until early exponential phase. Cells were lysed and Soj and Spo0J proteins were detected using Western blot analysis (DivIVA protein was likewise detected and used as a loading control). *soj*$^{+}$ *spo0J*$^{+}$ *parS*$^{-}$ (HM855), *soj*$^{+}$ *spo0J*$^{+}$ *parS*$^{+}$ (HM856), Δsoj *parS*$^{-}$ (HM835), Δsoj *parS*$^{+}$ (HM838), Δspo0J *parS*$^{-}$ (HM834), Δ*spo0J parS*$^{+}$ (HM837), Δ*soj-spo0J parS*$^{-}$ (AK587), Δ*soj-spo0J parS*$^{-}$ (AK589).

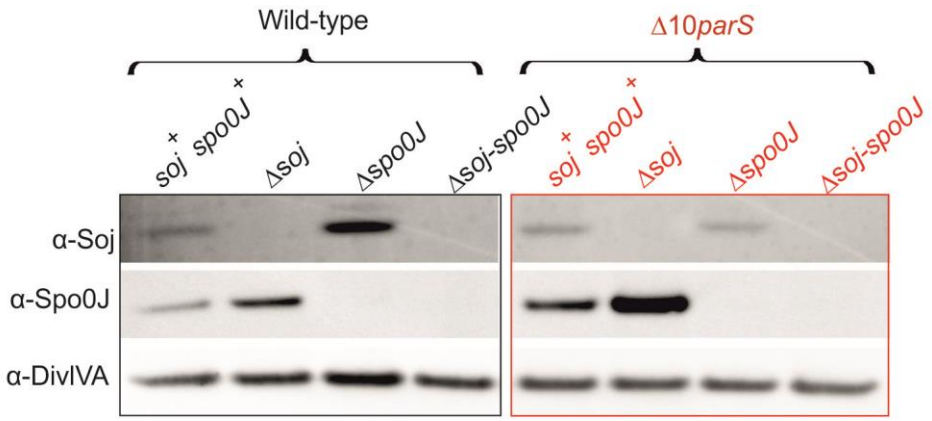

Figure 2.13.3: Western blot for Chapter 4 strain constructions

Western blot analysis of the various *parS* mutants. Cells were grown in 2% succinate minimal media at 37˚ until early exponential phase. Cells were lysed and Soj and Spo0J proteins were detected using Western blot analysis (DivIVA protein was likewise detected and used as a loading control). *soj*$^{+}$ *spo0J*$^{+}$ (AK239), *soj*$^{+}$ *spo0J*$^{+}$ Δ10*parS* (AK243), Δ*spo0J* (AK241), Δ*spo0J* Δ10*parS* (AK245), Δ*soj-spo0J* (AK559), Δ*soj-spo0J* Δ10*parS* (AK563), Δ*soj* (AK557), Δ*soj* Δ10*parS* (AK617).

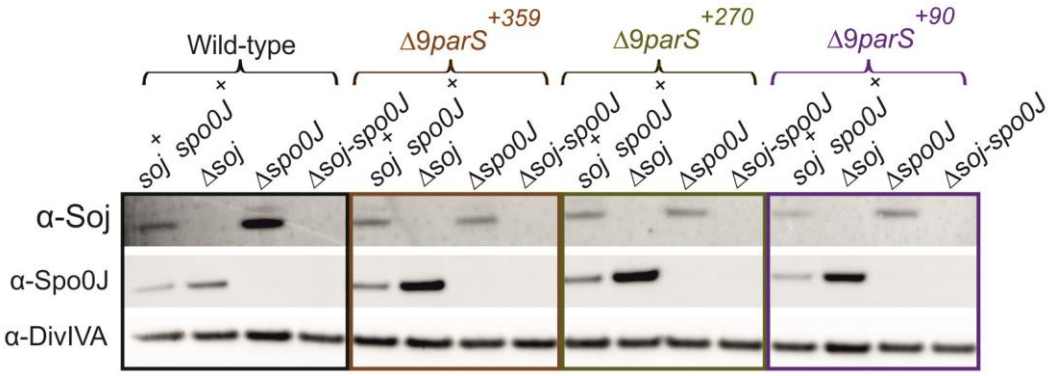

Figure 2.13.4: Western blot for Chapter 5 strain constructions (*parS* on the chromosome)

Western blot analysis of the various *parS* mutants. Cells were grown in 2% succinate minimal media at 37˚ until early exponential phase. Cells were lysed and Soj and Spo0J proteins were detected using Western blot analysis (DivIVA protein was likewise detected and used as a loading control). *soj*$^{+}$ *spo0J*$^{+}$ (AK239), *soj*$^{+}$ *spo0J*$^{+}$ *parS*^{90} (AK323), *soj*$^{+}$ *spo0J*$^{+}$ *parS*^{270} (AK603), *soj*$^{+}$ *spo0J*$^{+}$ *parS*^{359} (AK259), Δ*spo0J* (AK241), Δ*spo0J parS*^{90} (AK325), Δ*spo0J parS*^{270} (AK605), Δ*spo0J parS*^{359} (AK261), Δ*soj-spo0J* (AK559), Δ*soj-spo0J parS*^{90} (AK553), Δ*soj-spo0J parS*^{270} (AK607), Δ*soj-spo0J parS*^{359} (AK561), Δ*soj* (AK557), Δ*soj parS*^{90} (AK555), Δ*soj parS*^{270} (AK649), Δ*soj parS*^{359} (AK653).

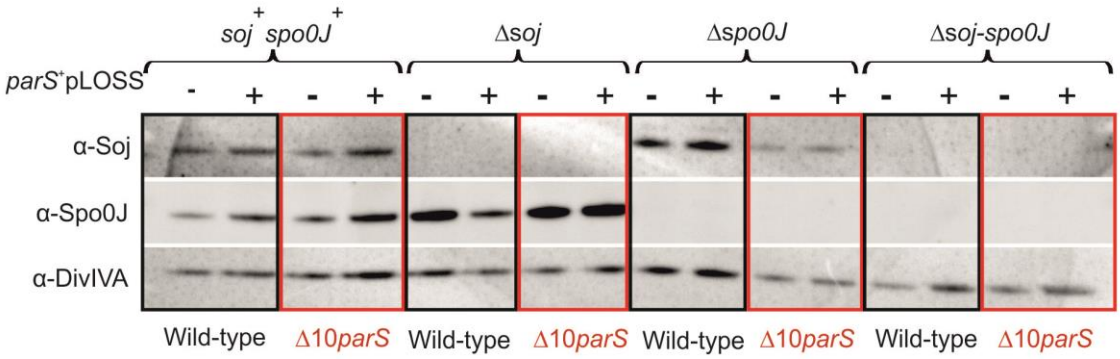

Figure 2.13.5: Western blot for Chapter 5 strain constructions (*parS* on the low-copy plasmid)

Western blot analysis of the various *parS* mutants. Cells were grown in 2% succinate minimal media at 37˚ until early exponential phase. Cells were lysed and Soj and Spo0J proteins were detected using Western blot analysis (DivIVA protein was likewise detected and used as a loading control). *parS*$^-$ pLOSS wild-type (AK429), *parS*$^-$ pLOSS Δ10*parS* (AK437), *parS*$^+$ pLOSS wild-type (AK427), *parS*$^+$ pLOSS Δ10*parS* (AK435), Δspo0J *parS*$^-$ pLOSS wild-type (AK433), Δspo0J *parS*$^-$ pLOSS Δ10*parS* (AK441), Δspo0J *parS*$^+$ pLOSS wild-type (AK431), Δspo0J *parS*$^+$ pLOSS Δ10*parS* (AK439), Δ*soj-spo0J parS*$^-$ pLOSS wild-type (AK625), Δ*soj-spo0J parS*$^-$ pLOSS Δ10*parS* (AK629), Δ*soj-spo0J parS*$^+$ pLOSS wild-type (AK623), Δ*soj-spo0J parS*$^+$ pLOSS Δ10*parS* (AK627), Δ*soj parS*$^-$ pLOSS wild-type (AK621), Δ*soj parS*$^-$ pLOSS Δ10*parS* (AK633), Δ*soj parS*$^+$ pLOSS wild-type (AK619), Δ*soj parS*$^+$ pLOSS Δ10*parS* (AK631).

Chapter 3: Redistribution of Spo0J away from *oriC* affects chromosome origin segregation but not regulation of Soj

Chapter 3 Introduction

Coordination of DNA replication with chromosome segregation is crucial to ensure accurate inheritance of the genetic material. As described in detail in Chapter 1, the *B. subtilis* Par system is important for both of these essential cell cycles. First, Spo0J promotes proper chromosome segregation by recruiting condensin to *parS* sites flanking the replication origin region (Gruber and Errington, 2009; Sullivan et al., 2009; Wang et al., 2014b). Second, Spo0J controls the oligomeric form of Soj by regulating Soj ATPase activity, which in turn dictates whether monomeric Soj inhibits DnaA or dimeric Soj activates DnaA at *oriC* (Murray and Errington, 2008; Scholefield et al., 2012; Scholefield et al., 2011).

The location of *parS* sites near *oriC* has been shown to be functionally significant because recruitment of condensin is required for origin segregation following the initiation of DNA replication. Based on this finding, I hypothesized that the origin-proximal localization of *parS* sites could be important for the control of Soj by Spo0J, and therefore in turn for the proper regulation of the DNA replication initiation protein DnaA by Soj.

To investigate the importance of Spo0J:*parS* nucleoprotein complex localization near the replication origin for efficient regulation of Soj, additional *parS* were introduced away from *oriC*. Two complementary experimental approaches were employed to recruit Spo0J away from the origin: (1) inserting arrays of *parS* sites into the chromosome at positions 90˚ and 270˚ or (2) introducing a multi-copy plasmid containing a *parS* site. As expected the

redistribution of Spo0J away from the origin proximal *parS* sites perturbed chromosome origin segregation. However, data from multiple Soj activity assays showed that redistribution of Spo0J away from *oriC* did not affect control of Soj by Spo0J.

Chapter 3 Results

3.1 Insertion of *parS* arrays into ectopic regions of the chromosome

To construct a strain with additional *parS* sites integrated into the chromosome away from the origin, two *parS* arrays were inserted along the chromosome arms at 90˚ and 270˚ (Figure 3.1.1A, green bars). Each *parS* array contains 16 tandem *parS* repeats with the consensus sequence 5'-TGTTCCACGTGAAACA-3' as first described by (Lee et al., 2003).

To probe whether the inserted *parS* arrays were functional, a *spo0J-gfp* fusion was expressed from its native promoter and the number of Spo0J-GFP foci within single cells was determined using epifluorescence microscopy. Under the growth conditions utilized the majority of wild-type cells contained a pair of Spo0J-GFP foci located towards the cell poles, consistent with Spo0J localizing at the origin (Figure 3.1.1Bi-C) (Glaser et al., 1997; Lin et al., 1997; Teleman et al., 1998). In the strain that harbours the additional *parS* arrays, there was an increase in the number of Spo0J-GFP foci per cell (Figure 3.1.1Bii-C).This is consistent with the idea that increasing the number of *parS* sites on the chromosome generates more Spo0J nucleoprotein complexes and supporting the notion that Spo0J-GFP were titrated away from its endogenous *parS* sites to the ectopic locations (Breier and Grossman, 2007). However it is possible that the increase in Spo0J-GFP foci in the presence of the ectopic *parS* arrays could be due to an increase in initiation of DNA replication. To test this possibility, marker frequency analysis will be employed and will be discussed in Chapter 3.3.

Soj activity can be determined using a number of different assays. Soj localization can be determined using a GFP fusion and it has been shown that

the monomeric form of Soj has a cellular distribution that is distinct from the dimeric form of the protein. Furthermore, Soj is a regulator of the DNA replication initiator protein DnaA, and therefore Soj activity can be inferred by measuring either the rate of DNA replication initiation or the DnaA-dependent expression of the sporulation checkpoint protein Sda. In the following sections all of these assays were utilized to determine the effect of additional *parS* sites on Spo0J regulation of Soj.

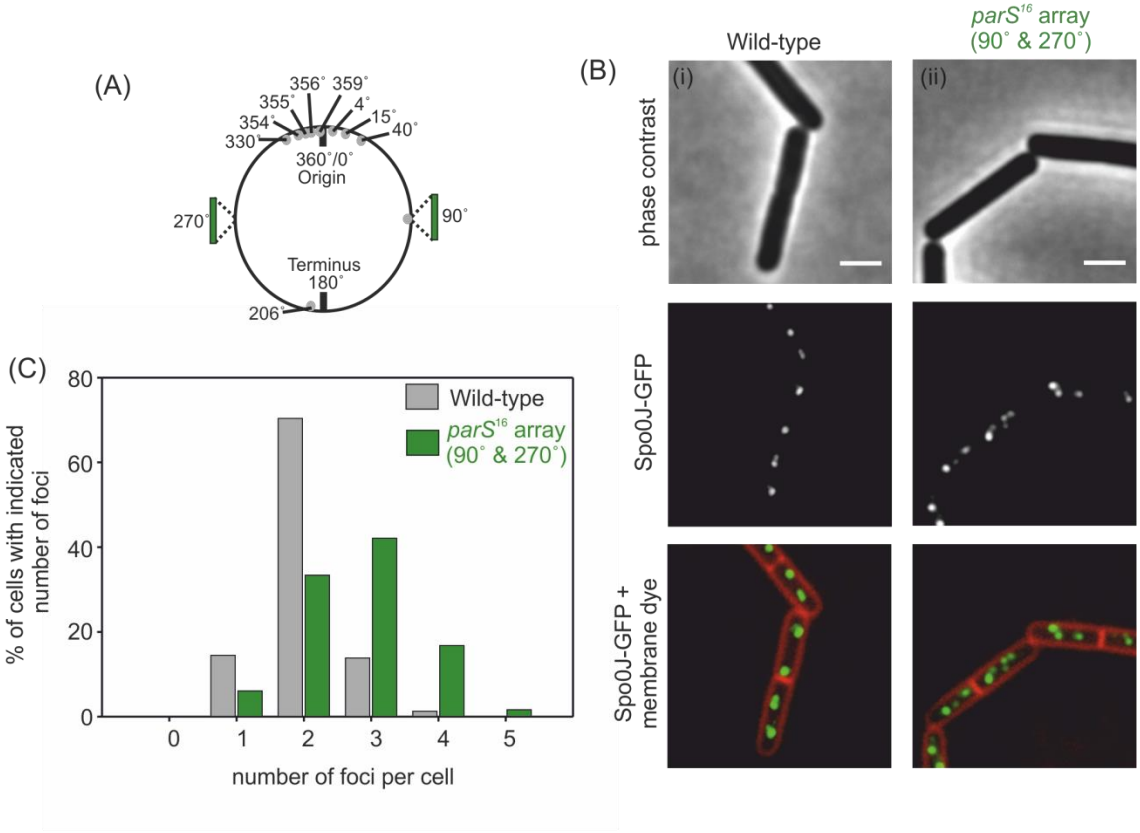

Figure 3.1.1: Spo0J localization and foci number in wild-type cells and in the strain containing two arrays of *parS* sites on the chromosome

(A) Schematic diagram showing the locations of the *parS* sites in *B. subtilis* chromosome, which are labelled as grey dots (4˚, 15˚, 40˚, 90˚, 206˚, 330˚, 354˚, 355˚, 356˚ and 359˚). *parS* arrays are shown as green bars. **(B)** Spo0J-GFP foci formation in wild-type and strains harbouring *parS* arrays. Cells were grown in 2% succinate minimal media at 37˚ until early exponential phase. Cell membranes were stained with FM-595 dye to distinguish individual cells and the number of fluorescent Spo0J-GFP foci per cell was determined using epifluorescence microscopy (Scale bar = 3 μm). (i) *spo0J-gfp* (HM756), (ii) *spo0J-gfp parS*^{16} array (90˚ & 270˚) (AK153). **(C)** Quantification of Spo0J-GFP foci per cell. Approximately 500 cells were counted for each strain. *spo0J-gfp* (HM756), *spo0J-gfp parS*^{16} array (90˚ & 270˚) (AK153).

3.2 Ectopic *parS* arrays do not alter the localization pattern of Soj

To directly assess Soj activity within the cell, Soj localization was determined in single cells in the presence and absence of *parS* arrays. The *soj* gene was fused to *gfp* under the control of its native promoter and GFP-Soj was visualized using epifluorescence microscopy. Previous work has shown that in the presence of Spo0J, GFP-Soj is likely monomeric and forms both DnaA-dependent foci at *oriC* (Figure 3.2.1.i, asterisk) and localizes to septa (Figure 3.2.1.i, arrow). In a Δ*spo0J* mutant, GFP-Soj colocalizes with the nucleoid (Figure 3.2.1ii, circle), consistent with the idea that the dimeric form of Soj binds to DNA (Autret et al., 2001; Marston and Errington, 1999; Murray and Errington, 2008; Quisel et al., 1999; Scholefield et al., 2011). The pattern of GFP-Soj localization in the presence of *parS* arrays was indistinguishable from the parent strain (Figure 3.2.1iii-iv), indicating that additional Spo0J:*parS* complexes formed on the chromosome away from the replication origin region do not affect the regulation of Soj by Spo0J. However, one of the caveats of fusing GFP to Soj is that the resulting chimera is not fully functional (Heath Murray, personal communication). Therefore, to further determine whether Soj activity was affected by the redistribution of Spo0J away from *oriC*, the activity of DnaA was determined using marker frequency analysis to detect the frequency of DNA replication initiation and using sporulation assay to detect the activation of Sda expression.

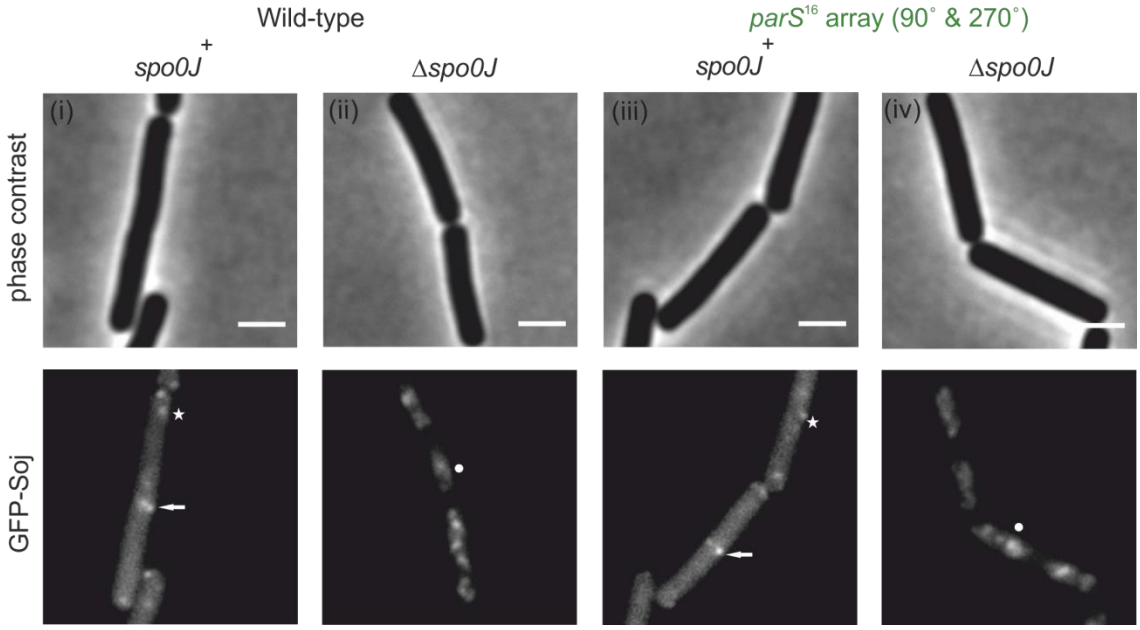

Figure 3.2.1: Soj localization was not affected by *parS* arrays

GFP-Soj localization in wild-type and *parS* arrays strains in the presence and absence of Spo0J. Cells were grown in 2% glucose minimal media at 37˚ until early exponential phase. GFP-Soj localization was determined by epifluorescence microscopy. An arrow (→) denotes localization at a septum, an asterisk (*) indicates localization as a focus and a circle (●) denotes nucleoid binding (Scale bar = 3 μm). Approximately 500 cells were visualized for each strain and typical cells are shown. (i) *gfp-soj* (HM740), (ii) *gfp-soj* Δ*spo0J* (AK547), (iii) *gfp-soj parS*^{16} array (90˚ & 270˚) (AK199), (iv) *gfp-soj* Δ*spo0J* *parS*^{16} array (90˚ & 270˚) (AK577).

3.3 Control of DNA replication initiation by Soj was not affected by *parS* arrays

To investigate whether ectopic *parS* arrays influenced the rate of DNA replication initiation, quantitative PCR was used to measure the amount of DNA near the replication origin and terminus. This marker frequency analysis did not detect any change in the frequency of DNA replication initiation when the *parS* arrays were present (Figure 3.3.1). It was possible that the results obtained could be due to Soj becoming non-functional in the presence of the arrays. To test this hypothesis *spo0J* was deleted. In the absence of Spo0J, Soj normally accumulates as a dimer that activates DnaA, leading to an increase in DNA replication initiation (Lin and Grossman, 1998; Murray and Errington, 2008; Ogura et al., 2003; Scholefield et al., 2011). Using the strain containing the *parS* arrays, an increase in the initiation frequency was observed when a Δ*spo0J* mutation was introduced. This effect was Soj-dependent because in the Δ(*soj-spo0J)* double mutant, the initiation frequency returned to a level near wild-type (and equal to the Δ*soj* mutant; Figure 3.3.1). Western blot and PCR analysis confirmed deletion of *soj* and *spo0J* genes in the strains containing *parS* arrays (Figure 2.13.1 and data not shown). These results indicate that Soj remains competent to regulate DnaA in the presence of the *parS* arrays, but that the redistributed Spo0J retains the capacity to inhibit this activity.

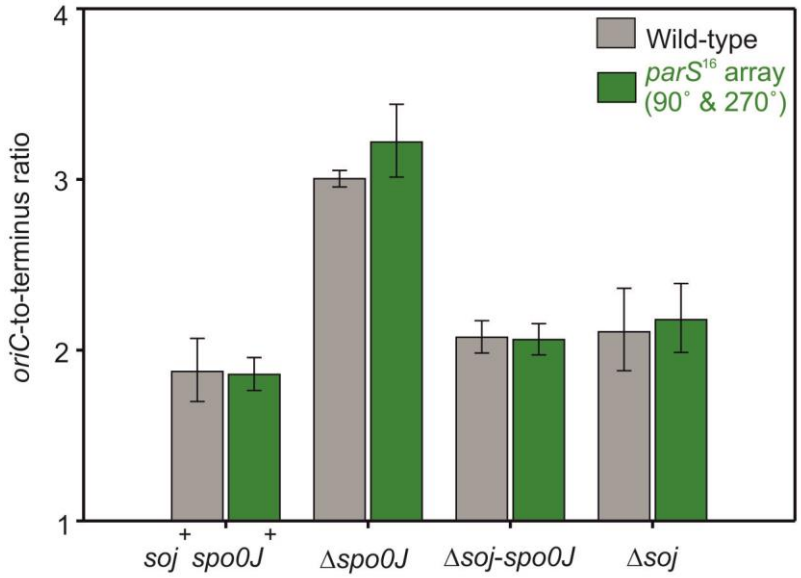

Figure 3.3.1: DNA replication initiation was not affected by ectopic *parS* arrays

The rate of replication initiation was not affected by increasing the number of *parS* sites on the chromosome. Cells were grown in 2% succinate minimal media at 37˚ until early exponential phase. Genomic DNA was harvested from cells and the *oriC*-to-terminus ratio of each mutant in a wild-type strain (grey) and in a *parS*^{16} array (90˚ & 270˚) strain (green) was determined using marker frequency analysis. The results are shown as the average ± standard deviation from three technical replicates. *soj*$^{+}$ *spo0J*$^{+}$ (HM765), *soj*$^{+}$ *spo0J*$^{+}$ *parS*^{16} array (90˚ & 270˚) (AK87), Δ*spo0J* (HM907), Δ*spo0J parS*^{16} array (90˚ & 270˚) (AK123), Δ*soj* (HM766), Δ*soj parS*^{16} array (90˚ & 270˚) (AK89), Δ*soj-spo0J* (AK573), Δ*soj-spo0J parS*^{16} array (90˚ & 270˚) (AK575).

3.4 Sporulation was not affected by *parS* arrays

To further test whether ectopic *parS* arrays affect the ability of Spo0J to regulate the activity of Soj, sporulation efficiency was determined in the presence and absence of the *parS* arrays. Recall that in a Δ*spo0J* mutant, Soj stimulates DnaA to activate the expression of the *sda* checkpoint protein and thereby inhibits sporulation (Chapter 1.4). This sporulation defect is suppressed by a Δ*soj-spo0J* double mutation, (Figure 3.4.1; black), in congruence with the stimulation of DnaA activity at *oriC* and consistent with the idea that the ATP-bound dimeric form of Soj activates DnaA (Murray and Errington, 2008). In strains containing *parS* arrays, the pattern of sporulation was unperturbed (Figure 3.4.1; green). These results are in agreement with the marker frequency analysis (Figure 3.3.1) and taken together they suggest that redistribution of Spo0J away from replication origins is insufficient to affect the regulation of Soj (and hence its regulation of DnaA).

	Strain	Genotype	# Colonies/ml	# Spores/ml	% Sporulation
Wild-type	HM765	*soj*$^+$ *spo0J*$^+$	1.3×10^8	1.1×10^8	83
	HM907	Δ*spo0J*	6.8×10^6	6.0×10^2	0.009
	AK573	Δ*soj-spo0J*	1.2×10^8	9.4×10^7	78
	HM766	Δ*soj*	1.5×10^8	1.1×10^8	73
parS^{16} array (90˚ & 270˚)	AK87	*soj*$^+$ *spo0J*$^+$	1.0×10^8	8.0×10^7	80
	AK123	Δ*spo0J*	8.0×10^6	8.0×10^2	0.010
	AK575	Δ*soj-spo0J*	1.0×10^8	8.0×10^7	80
	AK89	Δ*soj*	1.5×10^8	1.0×10^8	67

Figure 3.4.1: *parS* arrays do not affect sporulation

Sporulation frequency was not affected by the addition of extra *parS* sites on the chromosome. The sporulation frequencies were determined by calculating the ratio of heat-resistance colony-forming units (80°C for 25 min) to the total colony-forming units. *soj*$^+$ *spo0J*$^+$ (HM765), *soj*$^+$ *spo0J*$^+$ *parS*^{16} array (90˚ & 270˚) (AK87), Δ*spo0J* (HM907), Δ*spo0J parS*^{16} array (90˚ & 270˚) (AK123), Δ*soj* (HM766), Δ*soj parS*^{16} array (90˚ & 270˚) (AK89), Δ*soj-spo0J* (AK573), Δ*soj-spo0J parS*^{16} array (90˚ & 270˚) (AK575).

3.5 Multi-copy plasmid containing a *parS* site

The experiments with chromosomal *parS* arrays indicated that increasing the number of Spo0J binding sites away from the replication origin did not affect Spo0J regulation of Soj. However, I wondered whether the *parS* arrays were insufficient to redistribute the majority of Spo0J away from the origin. Consistent with this possibility, Spo0J-GFP still appeared to localize near *oriC* even in the presence of the *parS* arrays (Figure 3.1.1B).

To test this hypothesis a multi-copy plasmid containing a single consensus *parS* site was constructed (Figure 3.5.1A). To judge whether the plasmid was functional, Spo0J-GFP localization was examined by epifluorescence microscopy. In the presence of the *parS*$^{+}$ plasmid, Spo0J-GFP displayed a patchy distribution that appears to be associated with the nucleoid, reminiscent of type I plasmid localization over the DNA mass (Figure 3.5.1Bii) (Ebersbach and Gerdes, 2001, 2004; Ringgaard et al., 2009). More importantly, this is consistent with the idea that the plasmid is present at high copy number and significantly increases the number of Spo0J binding sites within the cell. A control plasmid lacking a *parS* site had no effect on Spo0J-GFP localization (Figure 3.5.1Bi).

In order to further assess Soj activity in the presence of greater number of Spo0J binding sites, we will be using similar assays as mentioned in the earlier sections to determine its activity.

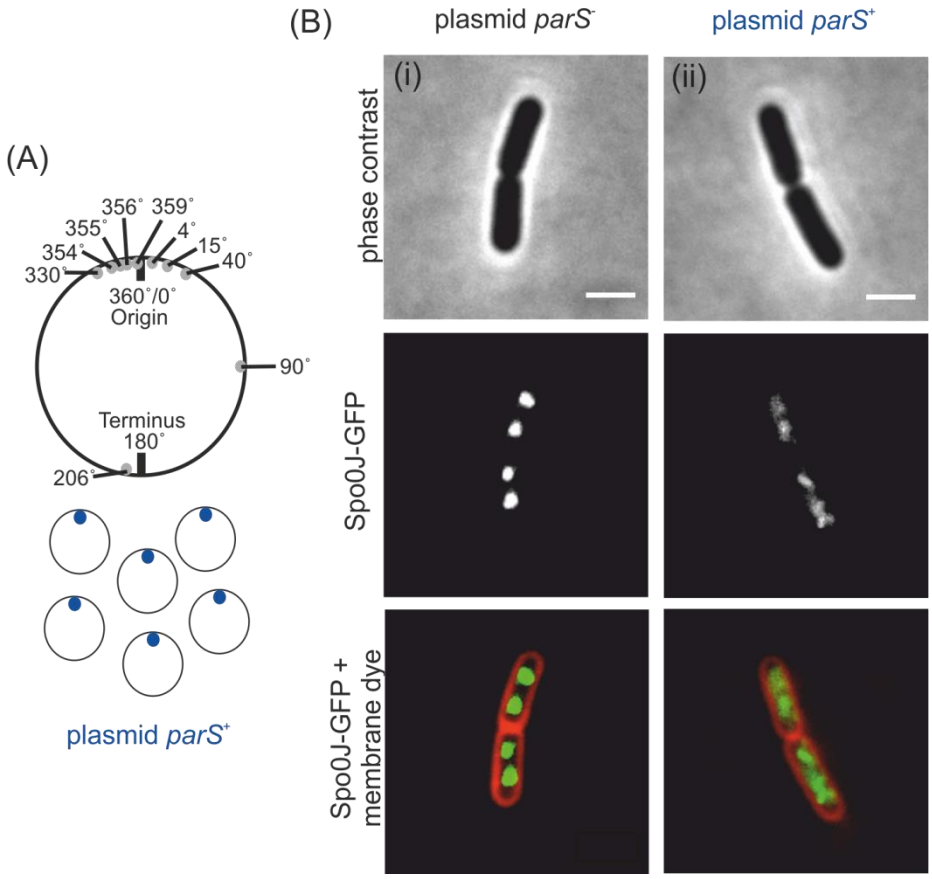

Figure 3.5.1: Multi-copy plasmid containing a single *parS* in the cell

(A) Schematic diagram showing a multi-copy plasmid harbouring a single *parS* site in a strain with all ten endogenous *parS* as shown by grey dots (4˚, 15˚, 40˚, 90˚, 206˚, 330˚, 354˚, 355˚, 356˚ and 359˚). **(B)** Spo0J-GFP foci formation in strain harbouring the control or *parS*$^{+}$ plasmids. Cells were grown in 2% succinate minimal media at 30˚ supplemented with erythromycin (1 µg/ml) until early exponential phase. Cell membranes were stained with FM-595 dye to distinguish individual cells and Spo0J-GFP localization was determined using epifluorescence microscopy (Scale bar = 3 µm). Approximately 500 cells were visualized for each strain and typical cells are shown. (i) *spo0J-gfp parS*$^{-}$ (HM821), (ii) *spo0J-gfp parS*$^{+}$ (HM823).

3.6 A *parS* site on a multi-copy plasmid does not perturb the regulation of Soj by Spo0J

As before with the chromosomal *parS* arrays, a battery of assays were utilized to investigate Soj activity in strains harbouring the *parS*$^{+}$ plasmids. Consistent with the previous findings using *parS* arrays, redistribution of Spo0J away from the replicating origin region affected neither GFP-Soj localization (Figure 3.6.1) nor the regulation of DnaA by Soj (marker frequency analysis Figure 3.6.2; sporulation frequency Figure 3.6.3). Taken together, these results show that redistributing Spo0J away from the origin does not affect Soj regulation.

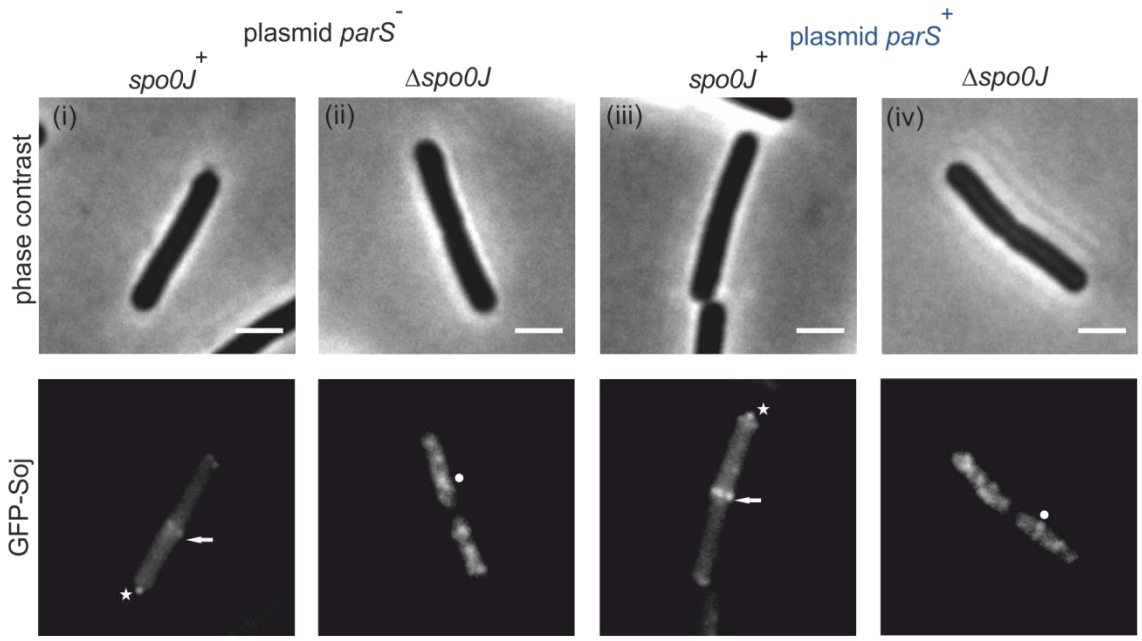

Figure 3.6.1: Soj localization was not affected by ectopic *parS* arrays

GFP-Soj localization in the wild-type and Spo0J mutant in the presence of the control or *parS*$^+$ plasmids. Cells were grown in 2.0% glucose minimal media at 37˚ supplemented with erythromycin (1 µg/ml) until early exponential phase. GFP-Soj localization was determined by epifluorescence microscopy. An arrow (→) denotes localization at a septum, an asterisk (*) indicates localization as a focus and a circle (●) denotes nucleoid binding (Scale bar = 3 µm). Approximately 500 cells were visualized for each strain and typical cells are shown. (i) *gfp-soj parS*$^-$ (HM870), (ii) *gfp-soj* Δ*spo0J parS*$^-$ (AK569), (iii) *gfp-soj parS*$^+$ (HM871), (iv) *gfp-soj* Δ*spo0J parS*$^+$ (AK571).

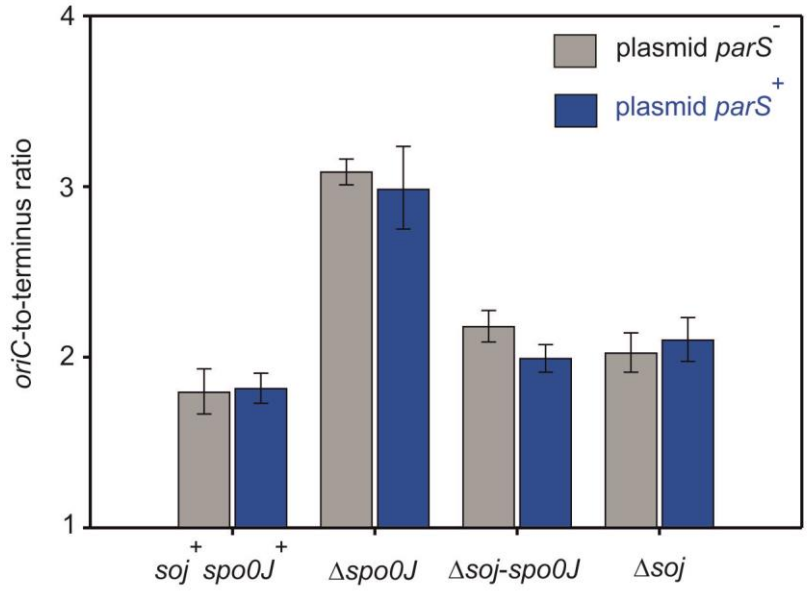

Figure 3.6.2: DNA replication initiation was not affected by ectopic *parS* arrays

The rate of replication initiation was not affected by the multi-copy plasmid. Cells were grown in 2% succinate minimal media at 30˚ supplemented with erythromycin (1 µg/ml) until early exponential phase. Genomic DNA was harvested from cells and the *oriC*-to-terminus ratio of each mutant containing *parS*$^-$ plasmid strain (grey bars) or *parS*$^+$ plasmid strain (blue bars) was determined using marker frequency analysis. The results are shown as the average ± standard deviation from three technical replicates. *soj*$^+$ *spo0J*$^+$ *parS*$^-$ (HM855), *soj*$^+$ *spo0J*$^+$ *parS*$^+$ (HM856), Δ*soj parS*$^-$ (HM835), Δ*soj parS*$^+$ (HM838), Δ*spo0J parS*$^-$ (HM834), Δ*spo0J parS*$^+$ (HM837), Δ*soj-spo0J parS*$^-$ (AK587), Δ*soj-spo0J parS*$^-$ (AK589).

	Strain	Genotype	# Colonies/ml	# Spores/ml	% Sporulation
plasmid - *parS*	HM855	*soj*$^+$ *spo0J*$^+$	2.0×10^8	1.5×10^8	75
	HM834	Δ*spo0J*	1.5×10^7	7.8×10^3	0.052
	AK587	Δ*soj-spo0J*	2.0×10^8	1.5×10^8	75
	HM835	Δ*soj*	4.8×10^8	3.4×10^8	71
plasmid + *parS*	HM856	*soj*$^+$ *spo0J*$^+$	1.4×10^8	1.0×10^8	71
	HM837	Δ*spo0J*	1.9×10^7	4.2×10^3	0.022
	AK589	Δ*soj-spo0J*	1.9×10^8	1.3×10^8	68
	HM838	Δ*soj*	7.2×10^8	4.6×10^8	67

Figure 3.6.3: Sporulation was not affected by ectopic *parS* arrays

Sporulation frequency was not affected by the multi-copy plasmid. The sporulation frequencies were determined by calculating the ratio of heat-resistance colony-forming units (80°C for 25 min) to the total colony-forming units. *soj*$^+$ *spo0J*$^+$ *parS*$^-$ (HM855), *soj*$^+$ *spo0J*$^+$ *parS*$^+$ (HM856), Δ*soj parS*$^-$ (HM835), Δ*soj parS*$^+$ (HM838), Δ*spo0J parS*$^-$ (HM834), Δ*spo0J parS*$^+$ (HM837), Δ*soj-spo0J parS*$^-$ (AK587), Δ*soj-spo0J parS*$^-$ (AK589).

3.7 Origin separation was affected by redistributing Spo0J away from the origin

To confirm that the methodologies used to redistribute Spo0J were sufficient to affect chromosome segregation, the origin region was visualized by marking it with an array of *tetO* operators that were bound by a fluorescent TetR reporter protein (Murray and Errington, 2008; Wagner et al., 2009) (Figure 3.7.1A; TetR-GFP or Figure 3.7.2A; TetR-YFP). The majority of wild-type cells contained two fully separated origins (Figure 3.7.1Bi; grey bar and Figure 3.7.2Bi; grey bar). In contrast, the presence of additional *parS* sites resulted in a significant increase in the number of cells containing only a single focus, indicating a defect in chromosome origin segregation (Figure 3.7.1Bi; green bar and Figure 3.7.2Bi; blue bar). In a Δ*spo0J* mutant the number of origins per cell greatly increased, consistent with the notion that the effect on origin segregation was Spo0J-dependent and with previous results showing that DNA replication initiation is stimulated via activation of DnaA by Soj (Figure 3.7.1Bii and 3.7.2Bii) (Lee et al., 2003; Murray and Errington, 2008; Ogura et al., 2003).

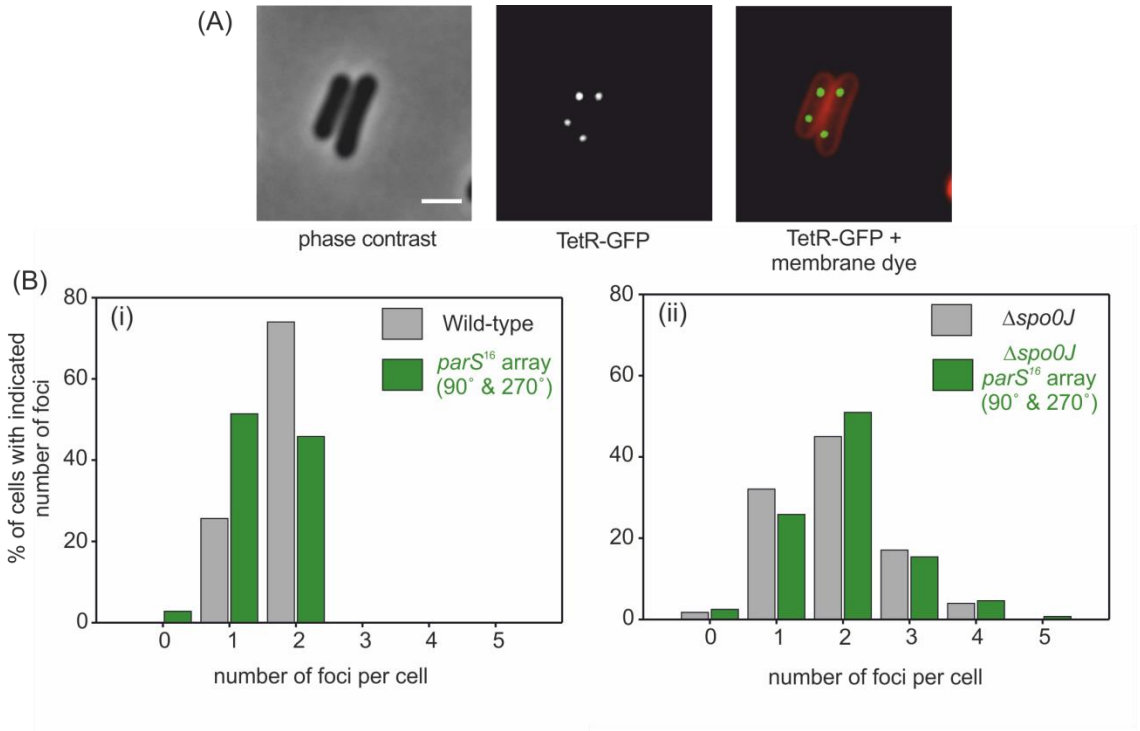

Figure 3.7.1: Chromosome segregation was affected in strains that contain *parS* arrays on the chromosome

(A) Origin localization in wild-type *B. subtilis.* The *oriC* region was labelled with an array of *tetO* operators bound by TetR-GFP. *soj*$^{+}$ *spo0J*$^{+}$ (HM765) (Scale bar = 3 μm). **(B)** Origin counting in wild-type and *parS* arrays mutant in the presence and absence of Spo0J. Cells were grown in 2% succinate minimal media at 37˚C until early exponential phase. Cell membranes were stained with FM-595 dye to distinguish individual cells and the number of fluorescent TetR-GFP foci per cell was determined using epifluorescence microscopy. Bar charts showing the results from chromosome origin counts. The strain information is shown in the top right hand corner of each graph. An approximate of 500 cells was counted for each strain. (i) *soj*$^{+}$ *spo0J*$^{+}$ (HM765), *soj*$^{+}$ *spo0J*$^{+}$ *parS*^{16} array (90˚ & 270˚) (AK87), (ii) Δ*spo0J* (HM907), Δ*spo0J parS*^{16} array (90˚ & 270˚) (AK123).

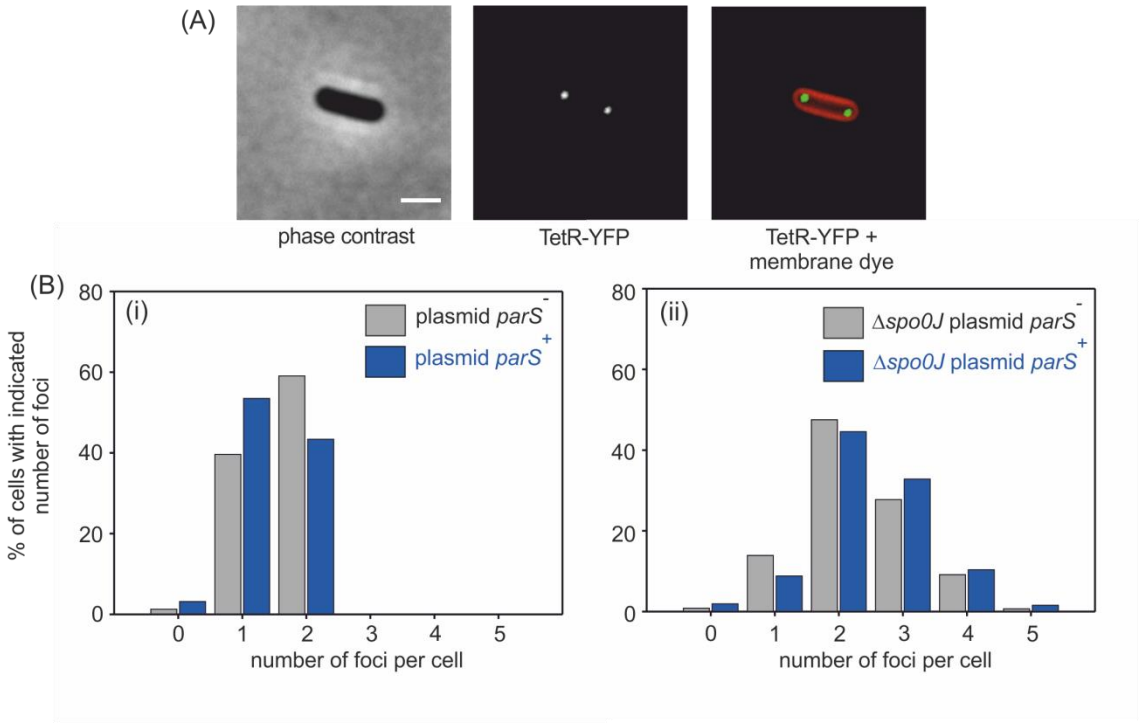

Figure 3.7.2: Chromosome segregation was affected in strains that harbour the multi-copy plasmid with a *parS* site

(A) Origin localization in wild-type *B. subtilis.* The *oriC* region was labelled with an array of *tetO* operators bound by TetR-YFP. *soj*$^{+}$ *spo0J*$^{+}$ *parS*$^{-}$ (HM855) (Scale bar = 3 μm). **(B)** Origin counting of wild-type and *spo0J* mutant in the presence of the control or *parS*$^{+}$ plasmids. Cells were grown in 2% succinate minimal media at 30˚C supplemented with erythromycin (1 μg/ml) until early exponential phase. Cell membranes were stained with FM-595 dye to distinguish individual cells and the number of fluorescent TetR-YFP foci per cell was determined using epifluorescence microscopy. Bar charts showing the results from chromosome origin counts. The strain information is shown in the top right hand corner of each graph. An approximate of 500 cells was counted for each strain. (i) *soj*$^{+}$ *spo0J*$^{+}$ *parS*$^{-}$ (HM855), *soj*$^{+}$ *spo0J*$^{+}$ *parS*$^{+}$ (HM856), (ii) Δ*spo0J parS*$^{-}$ (HM834), Δ*spo0J parS*$^{+}$ (HM837).

3.8 Chapter 3 Discussion

3.8.1 Soj interaction with Spo0J:*parS* complexes

It has been shown that recruitment of condensin by *oriC*-flanking Spo0J:*parS* complexes is required for accurate origin region segregation (Gruber and Errington, 2009; Sullivan et al., 2009; Wang et al., 2014b). Because Spo0J also regulates the DNA replication initiation regulator Soj, I hypothesized that Spo0J localization might be important to coordinate DNA replication with chromosome segregation. Two approaches were used to test this possibility by redistributing Spo0J away from *oriC*; integrating arrays of *parS* sites into chromosome arms and placing a *parS* site into a multi-copy plasmid. Although both approaches appeared to successfully redistribute Spo0J away from *oriC,* as functionally judged by Spo0J-GFP localization and defects in chromosome origin separation (see below), neither approach was sufficient to alter Soj activity.

However, because the endogenous *parS* sites remain near the replication origin in these experiments, it is possible that low levels of Spo0J binding to these sites is sufficient to elicit proper regulation of Soj. Alternatively, Spo0J localization near *oriC* may not be necessary for the regulation of Soj. To address these possibilities I constructed a strain where all ten endogenous *parS* sites were removed and the ability of Spo0J to regulate Soj activity was determined (see Chapter 4).

3.8.2 Formation of ectopic Spo0J:*parS* complexes away from the origin affected proper chromosome segregation

Spo0J localization near *oriC* was shown to be important for recruiting condensin, which in turn promotes proper replication origin organization and facilitates accurate chromosome origin segregation (Gruber and Errington, 2009; Sullivan et al., 2009; Wang et al., 2014b). The findings that *oriC*-distal *parS* sites inhibit chromosome origin separation are consistent with previous data, and it is assumed that the ectopic Spo0J:*parS* complexes are recruiting condensin to these regions and away from *oriC*. These ectopic Spo0J:*parS* complexes could interfere with chromosome origin segregation either by depleting condensin from chromosome origins or creating inappropriate organizational structures that interfere with origin-bound complexes, or both. Additionally, the activity of Soj as a secondary factor driving origin segregation could be impaired under conditions where Spo0J is redistributed away from *oriC* (Lee et al., 2003; Sullivan et al., 2009).

3.9 Chapter 3 Future work

3.9.1 ChIP-seq to investigate titration of Spo0J away from the origin

Increasing the number of *parS* sites generated either more Spo0J-GFP foci in the presence of the *parS* arrays (Figure 3.1.1Bii) or a patchy distribution in the presence of the *parS*$^{+}$ plasmid (Figure 3.5.1Bii). And the increase in Spo0J-GFP foci are not due to overinitiation of DNA replication leading to the availability of more origin proximal *parS* sites (Figure 3.3.1 and Figure 3.6.2).

These results suggest that although Spo0J-GFP was forming additional nucleoprotein complexes at the ectopic *parS* arrays, it is still possible that it is the unbound Spo0J-GFP within the cell that made up these foci and not the origin proximal Spo0J-GFP being titrated to these ectopic locations. Or in the case of the *parS*$^{+}$ plasmid, the high level of background signal caused by the multi-copy *parS*$^{+}$ plasmids within the cytoplasm, may have masked the detection of Spo0J-GFP foci.

Therefore to test whether Spo0J-GFP was successfully titrated away from the origin, ChIP-seq will be performed to analyse the amount of Spo0J enrichment around the origin region, *parS* at 90˚ and 206˚ in the strains that harbour the *parS*$^{+}$ plasmid and in the case of the *parS* arrays, enrichment at the origin, *parS* at 206˚ and the *parS* arrays at 90˚ and 270˚.

Chapter 4: Spo0J:*parS* nucleoprotein complexes are required to regulate Soj

Chapter 4 Introduction

I have shown in Chapter 3 that increasing the number of ectopic Spo0J:*parS* complexes either on the chromosome or on a multi-copy plasmid did not affect Soj activity as judged directly by the GFP-Soj localization pattern and indirectly by measuring DnaA activity (the rate of DNA replication initiation and sporulation frequency). However, because the endogenous *parS* sites remain near the replication origin in these experiments, it is possible that low levels of Spo0J binding to these sites is enough to elicit proper regulation of Soj. Alternatively, Spo0J localization near *oriC* may not be necessary for the regulation of Soj.

Therefore, to understand the relationship between origin-proximal Spo0J nucleoprotein complexes with regards to Soj regulation, a strain was constructed with all ten *parS* sites deleted (Δ10*parS*). It was found that in the absence of *parS* sites, Spo0J was unable to efficiently regulate Soj activity, consistent with the model that *parS*-dependent Spo0J nucleoprotein complexes are required to regulate Soj activity. Unexpectedly, overall chromosome organization and segregation appears to remain largely unaffected in the absence of origin proximal Spo0J:*parS* complexes.

Chapter 4 Results

4.1 Removing all ten endogenous *parS* on the chromosome

To begin construction of the Δ10*parS* mutant (Figure 4.1.1Aii), a strain lacking the eight origin proximal *parS* sites (Δ8*parS*) was obtained (Figure 4.1.1Ai) (Sullivan et al., 2009). I then proceeded with removing the remaining two *parS* located at 90˚ and 206˚ on the circular chromosome. $parS^{206}$ lies within the noncoding sequence between two genes, therefore a plasmid was constructed that could integrate into the chromosome by double-crossover and replace $parS^{206}$ with an antibiotic cassette (Figure 4.1.1B). $parS^{90}$ is found within the coding sequence of the *yhaX* gene. A plasmid was constructed that contained the *yhaX* gene and its endogenous surrounding sequences flanking an antibiotic cassette to allow integration into the chromosome by double-crossover. Site directed mutagenesis was then used to mutate the $parS^{90}$ sequence while maintaining the amino acid coding sequence for the YhaX protein (Figure 4.1.1C). Plasmids were sequenced to ensure that construction was correct. The plasmids were then integrated into the Δ8*parS* mutant to obtain the Δ10*parS* mutant.

Construction of the Δ10*parS* mutant was confirmed by PCR and DNA sequencing (data not shown) followed by localization of Spo0J-GFP using epifluorescence microscopy. It should be noted that the $parS^{359}$ site is located within *spo0J.* Therefore, in order to create a *spo0J-gfp* fusion expressed from its native promoter at the endogenous locus without reintroducing the $parS^{359}$ site, a *spo0J-gfp* integration plasmid was constructed where the $parS^{359}$ sequence was mutated while maintaining the amino acid coding sequence for the Spo0J protein. The plasmid was then sequenced to check for any unwanted mutation

in the coding sequence and was subsequently integrated into the Δ10*parS* strain.

In a wild-type strain, Spo0J-GFP binds to multiple *parS* sites and forms a fluorescent focus at the replication origin (Figure 4.1.2i). In the Δ10*parS* mutant, Spo0J-GFP was delocalized and was observed as a diffuse signal, weakly associated with the nucleoid (Figure 4.1.2ii). This result is consistent with the idea that Spo0J is a DNA binding protein that requires *parS* to form specific nucleoprotein complexes.

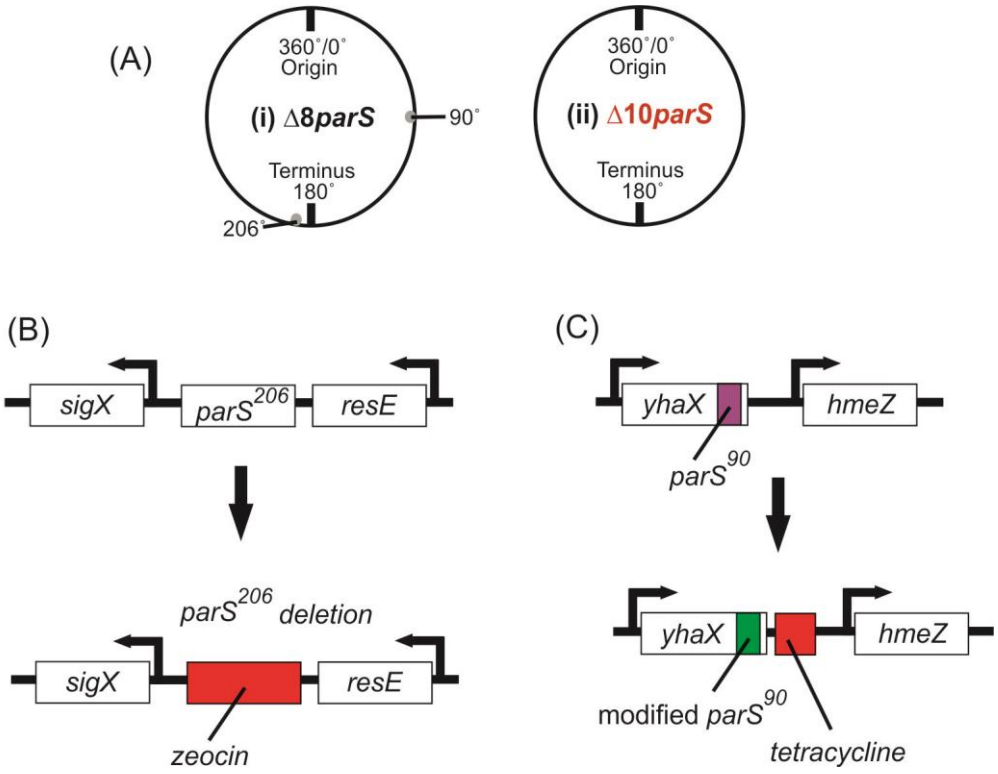

Figure 4.1.1: Removal of ten endogenous *parS* on the chromosome

(A) Schematic diagram showing a (i) Δ8*parS* strain with remaining *parS* at 90˚ and 206˚, (ii) Δ10*parS* strain. **(B)** Schematic diagram showing the deletion of $parS^{206}$ in the Δ8*parS* strain. Chromosomal $parS^{206}$ was replaced by the insertion of the antibiotic resistance cassette (zeocin; red bar) between *sigX* and *resE*. **(C)** Schematic diagram showing the mutation of $parS^{90}$ in the Δ9*parS* strain. Chromosomal $parS^{90}$ was modified by site directed mutagenesis linked to an antibiotic resistance cassette (tetracycline; red bar) within the *yhaX* gene.

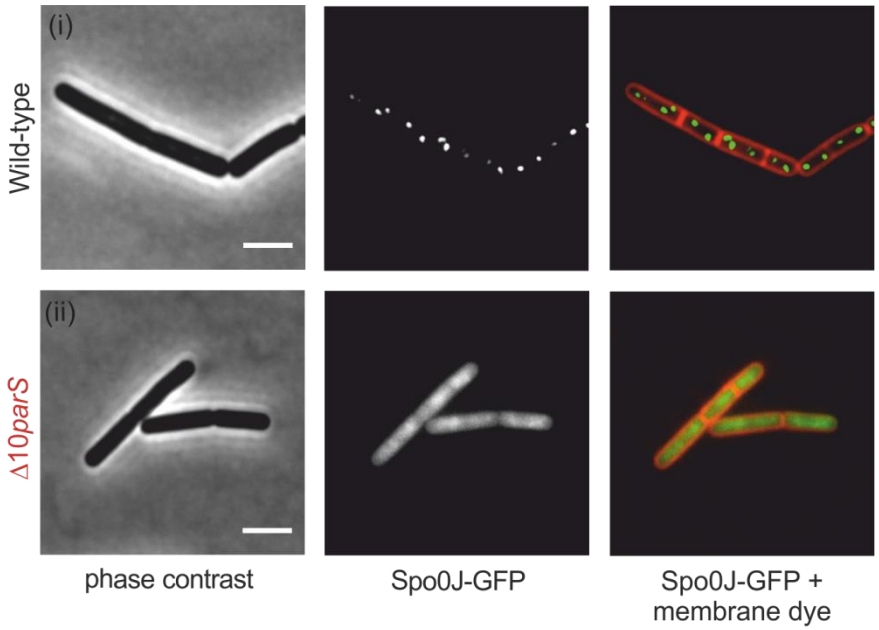

Figure 4.1.2: Spo0J localization requires *parS* site

Spo0J-GFP localization in a wild-type strain and the Δ10*parS* mutant. Cells were grown in 2% succinate minimal media at 37˚ until early exponential phase. Cell membranes were stained with FM-595 dye to distinguish individual cells and fluorescent Spo0J-GFP foci per cell were determined using epifluorescence microscopy (Scale bar = 3 μm). Approximately 500 cells were visualized for each strain and typical cells are shown. (i) *spo0J-gfp* (AK367), (ii) *spo0J-gfp* Δ10*parS* (AK369).

4.2 GFP-Soj localization is altered in the Δ10*parS* mutant

Soj localization was determined in single cells to directly assess Soj activity. The *soj* gene was fused to *gfp* under the control of its native promoter and GFP-Soj was visualized using epifluorescence microscopy. Note that plasmids used to integrated *gfp-soj* into the chromosome (replacing the endogenous gene) contained either the entire *spo0J* gene or a fragment (for Δ*spo0J*), and in both cases the *parS*^{359} site was substituted as described above.

Wild-type GFP-Soj colocalizes with the origin as a faint focus (Figure 4.2.1i, asterisk) in a DnaA-dependent manner, as well as binding to the septa (Figure 4.2.1i, arrow). This localization pattern is dependent upon Spo0J (Figure 4.2.1.ii, circle) and in a Δ*spo0J* mutant, GFP-Soj is able to form a stable dimer that binds DNA non-specifically. Strikingly, in the Δ10*parS* mutant, GFP-Soj appears to be predominantly associated with the nucleoid (Figure 4.2.1iii, red circle) even in the presence of Spo0J. Semi-quantitative analysis of this localization pattern reveals that GFP-Soj appears to associate with the nucleoid less efficiently than in the complete absence of *spo0J,* as judged by the different level of GFP intensity (Figure 4.2.1iii and 4.2.1iv). In addition, close examination of GFP-Soj in the Δ10*parS* strain revealed that weak septal localization and faint foci could be observed, suggesting that some residual capability of Spo0J to regulate Soj likely remained (Figure 4.2.1iii, red arrow and red asterisk respectively).

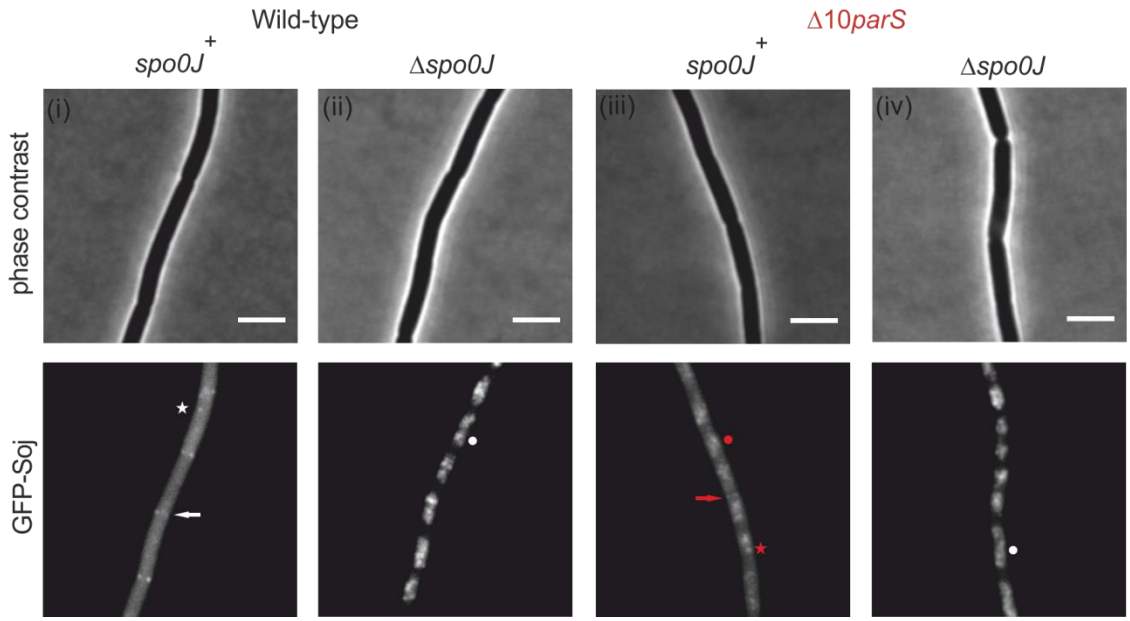

Figure 4.2.1: Soj localization in the absence of *parS* sites

GFP-Soj localization in the wild-type and Δ10*parS* strain in the presence and absence of Spo0J. Cells were grown in 2% glucose minimal media at 37˚ until early exponential phase. GFP-Soj localization was determined by epifluorescence microscopy. An arrow (→) denotes localization at a septum, an asterisk (*) indicates localization as a focus and a circle (●) denotes nucleoid binding (Scale bar = 3 μm). Approximately 500 cells were visualized for each strain and typical cells are shown. (i) *soj*$^{+}$ *spo0J*$^{+}$ (AK277), (ii) Δ*spo0J* (AK279), (iii) *soj*$^{+}$ *spo0J*$^{+}$ Δ10*parS* (AK281), (iv) Δ*spo0J* Δ10*parS* (AK283).

4.3 Control of DNA replication initiation is perturbed in the absence of *parS* sites

To further analyse Soj activity in the Δ10*parS* mutant, marker frequency analysis was used to determine the effect of Soj on DnaA (Figure 4.3.1). These experiments showed that the frequency of DNA replication initiation increased in the Δ10*parS* mutant and that this increase was Soj-dependent, indicating that Soj was accumulating as a dimer to activate DnaA. Western blot and PCR analysis confirmed the correct construction of each mutant (Figure 2.13.3 and data not shown).

Interestingly, the degree of overinitiation in the absence of *parS* sites was not as severe as in the Δ*spo0J* mutant, consistent with the GFP-Soj localization data that suggested some residual Spo0J activity remains in this strain (Figure 4.2.1). In further support of this interpretation, sporulation efficiency was unaffected in the Δ10*parS* mutant (Figure 4.3.2). Intriguingly, a similar pattern of lower degree in overinitiation was observed in the absence of *parS* sites and Spo0J.

Nevertheless, the localization and activity studies suggest that in order for Spo0J to properly regulate Soj, Spo0J has to interact with *parS* sites to form a Spo0J:*parS* nucleoprotein complex. This is compatible with *in vitro* data where a *parS* site is necessary for maximal stimulation of Soj ATPase activity by Spo0J (Scholefield et al., 2011).

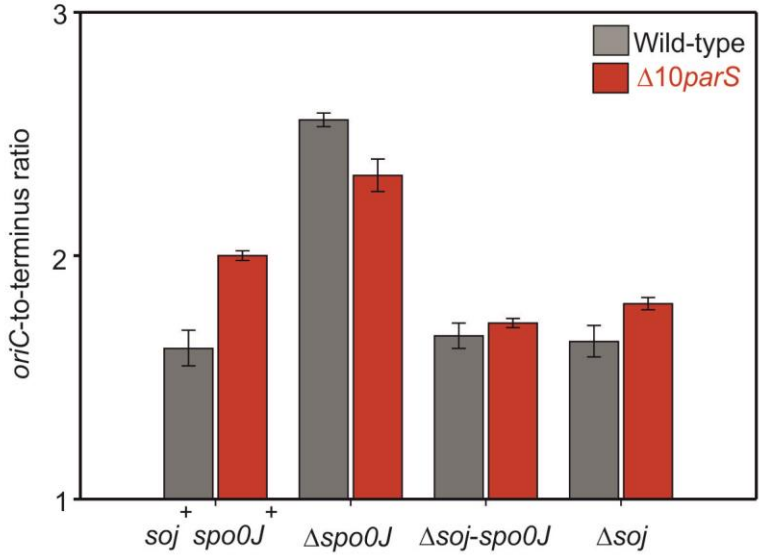

Figure 4.3.1: Control of DNA replication was affected in the Δ10*parS* strain

The rate of replication initiation was affected by deleting *parS* sites from the chromosome. Cells were grown in 2% succinate minimal media at 37˚ until early exponential phase. Genomic DNA was harvested from cells and the *oriC*-to-terminus ratio of each mutant in a wild-type strain (grey bars), in the Δ10*parS* strain (red bars) was determined using marker frequency analysis. The results are shown as the average ± standard deviation from three technical replicates. *soj*$^{+}$ *spo0J*$^{+}$ (AK239), *soj*$^{+}$ *spo0J*$^{+}$ Δ10*parS* (AK243), Δ*spo0J* (AK241), Δ*spo0J* Δ10*parS* (AK245), Δ*soj-spo0J* (AK559), Δ*soj-spo0J* Δ10*parS* (AK563), Δ*soj* (AK557), Δ*soj* Δ10*parS* (AK617).

	Strain	Genotype	# Colonies/ml	# Spores/ml	% Sporulation
Wild-type	AK239	*soj*$^+$ *spo0J*$^+$	3.7×10^8	3.2×10^8	86
	AK241	Δ*spo0J*	2.2×10^6	2.2×10^3	0.1
	AK559	Δ*soj-spo0J*	2.6×10^8	2.2×10^8	85
	AK557	Δ*soj*	2.7×10^8	2.3×10^8	85
Δ10*parS*	AK243	*soj*$^+$ *spo0J*$^+$	3.3×10^7	2.7×10^7	82
	AK245	Δ*spo0J*	2.2×10^6	1.2×10^4	0.5455
	AK563	Δ*soj-spo0J*	2.8×10^8	2.4×10^8	86
	AK617	Δ*soj*	2.3×10^8	2.1×10^8	91

Figure 4.3.2: Sporulation was not affected in the Δ10*parS* strain

Sporulation frequency was not affected by the deletion of *parS* sites from the chromosome. The sporulation frequencies were determined by calculating the ratio of heat-resistance colony-forming units (80°C for 25 min) to the total colony-forming units. *soj*$^+$ *spo0J*$^+$ (AK239), *soj*$^+$ *spo0J*$^+$ Δ10*parS* (AK243), Δ*soj* (AK557), Δ*soj* Δ10*parS* (AK617), Δ*spo0J* (AK241), Δ*spo0J* Δ10*parS* (AK245), Δ*soj-spo0J* (AK559), Δ*soj-spo0J* Δ10*parS* (AK563).

4.4 The impact of *parS* on chromosome organization

During the early stages of *B. subtilis* spore development, the chromosome origin region is segregated towards the cell pole and trapped by the formation of an asymmetric septum (Chapter 1.4 and 1.8.1). Previous studies have shown that deletion of the eight origin-proximal *parS* sites impairs chromosome origin trapping in the forespore, and it was subsequently found that recruitment of condensin by Spo0J:*parS* nucleoprotein complexes is involved in organizing the chromosome origin to facilitate proper segregation (Gruber and Errington, 2009; Sullivan et al., 2009). Based on these previously published studies, as well as results shown in Chapter 3 where chromosome origin separation was impaired when Spo0J was redistributed away from origin-proximal *parS* sites, it was anticipated that chromosome organization and segregation would be impaired in a Δ10*parS* mutant.

To look at overall chromosome morphology and segregation, the nucleoid was visualized in single cells by staining DNA and membranes with fluorescent dyes. Unexpectedly, nucleoids appeared to be normally condensed in both Δ8*parS* and Δ10*parS* strains, and all cells contained DNA (Figure 4.4.1). These results indicate that under the growth conditions used (i.e. – in the absence of multifork replication when the replication elongation rate is thought to be slower) bulk DNA organization and segregation are largely maintained in the absence of Spo0J:*parS* nucleoprotein complexes.

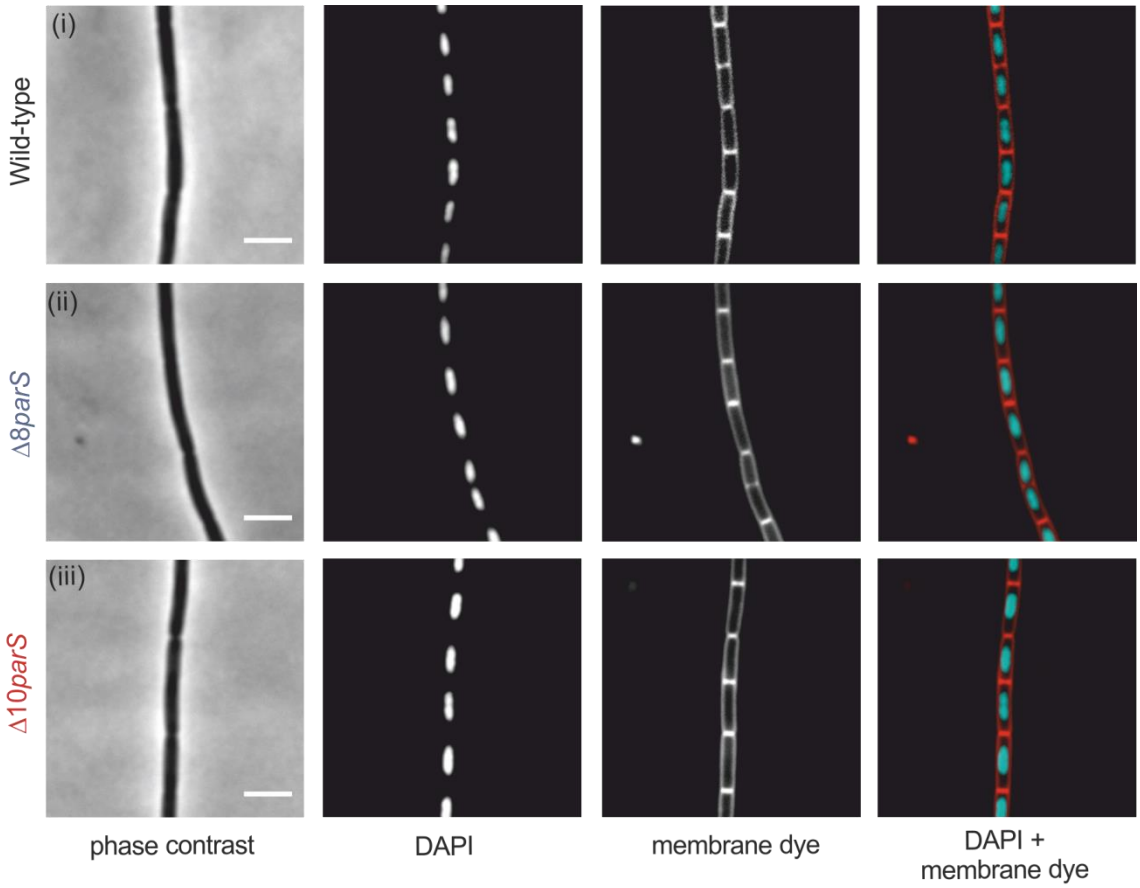

Figure 4.4.1: The Δ10*parS* strain was not affected in overall chromosome organization

DAPI staining in a wild-type strain and the Δ10*parS* mutant. Cells were grown in 2% glucose minimal media supplemented with 200 µg/ml casein hydrolysate at 37˚ until early exponential phase. Cell membranes were stained with FM-595 dye to distinguish individual cells and morphology was determined using epifluorescence microscopy (Scale bar = 3 µm). Approximately 500 cells were visualized for each strain and typical cells are shown. (i) Wild-type (AK239), (ii) Δ8*parS* (BNS1657), (iii) Δ10*parS* (AK243).

4.5 Chromosome origin segregation and positioning are not affected in the absence of *parS* sites

Although bulk chromosome segregation was not defective in the Δ10*parS* mutant, I hypothesized that the strain might display a more subtle defect in chromosome origin separation, as was observed when Spo0J was redistributed away from origin-proximal *parS* sites (Chapter 3). To test this model, the origin region was tagged with an array of *tetO* operators which were bound by a fluorescent TetR reporter protein (TetR-GFP) (Figure 4.5.1A) and the number of origins per cell in the Δ10*parS* mutant was determined. Again it was surprising to observe that chromosome origin segregation was not affected and that the majority of cells contained two TetR-GFP foci similar to the wild-type strain (Figure 4.5.1Bi; red bars). There was an increase in the number of cells with three or four foci in the Δ10*parS* mutant, which is consistent with the Δ10*parS* mutant over initiating DNA replication (Figure 4.3.1). Analysis of the Δ*spo0J* mutant revealed a broad distribution ranging from 1-5 TetR-GFP foci per cell regardless of the presence of *parS* sites (Figure 4.5.1Bii), which again is in agreement with the over replication phenotype observed by quantitative PCR analysis (Figure 4.3.1).

Since origin separation was not affected, I next determined whether chromosome origin positioning was altered. The average origin position was determined in cells that contain two spatially resolved foci along the length of the cell (Figure 4.5.2A; schematic diagram describing measurement and Chapter 2.9). Under the experimental conditions used (Figure 4.5.2B and 4.5.2Ci), wild-type origins are positioned near the cell quarter position at 27.0% ± 1.2% and the interfocal distance between the two origins relative to the cell length is 46.1% ± 2.0%. The position of the replicated sister origins in a Δ*spo0J*

null mutant appears to be closer with the interfocal distance at 41.5% ± 2.0%. These results are in agreement with a previous study, indicating that the chromosomes in vegetative growing *B. subtilis* cells are linearly positioned with the two chromosomes aligned side by side (Lee et al., 2003; Wang et al., 2014a). Surprisingly in the ∆10*parS* mutant, replication origin regions appear to be positioned normally at the cell quarter positions (27.5% ± 1.5%) with the distance between sister origins at 45.0% ± 2.2% (Figure 4.5.2B; red and 4.5.2Cii). Again in the mutant lacking both Spo0J and *parS* sites, the origins are positioned closer together at 40.1% ± 1.9%.

Taken together, these results suggest that under the growth conditions used, deletion of all *parS* sites does not significantly affect either chromosome organization or replication origin segregation and positioning.

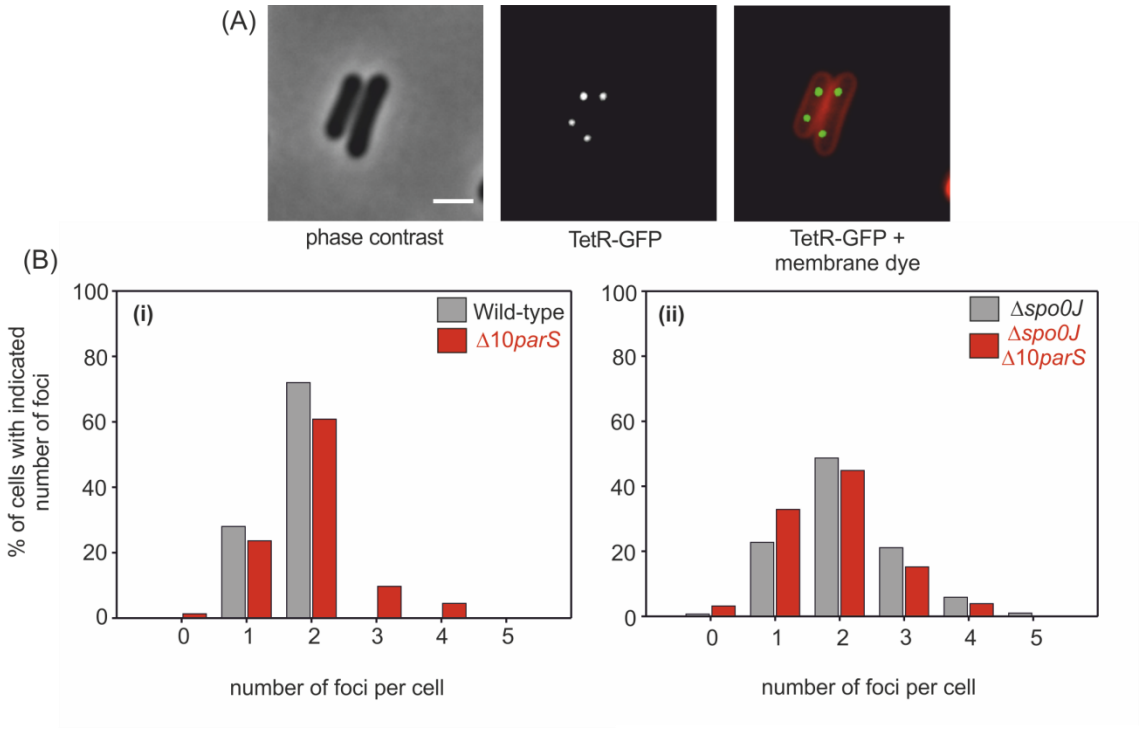

Figure 4.5.1: Chromosome segregation was not affected in the Δ10*parS* strain

(A) Origin localization in wild-type *B. subtilis.* The *oriC* region was labelled with an array of *tetO* operators bound by TetR-GFP. *soj*$^{+}$ *spo0J*$^{+}$ (AK181) (Scale bar = 3 μm). **(B)** Origin counting in wild-type and Δ10*parS* mutant in the presence and absence of Spo0J. Cells were grown in 2% succinate minimal media at 37˚ until early exponential phase. Cell membranes were stained with FM-595 dye to distinguish individual cells and the number of fluorescent TetR-GFP foci per cell was determined using epifluorescence microscopy. Bar charts showing the results from chromosome origin counts. The strain information is shown in the top right hand corner of each graph. An approximate of 500 cells was counted for each strain. (i) *soj*$^{+}$ *spo0J*$^{+}$ wild-type (AK181), *soj*$^{+}$ *spo0J*$^{+}$ Δ10*parS* (AK225), (ii) Δ*spo0J* (AK183), Δ*spo0J* Δ10*parS* (AK227).

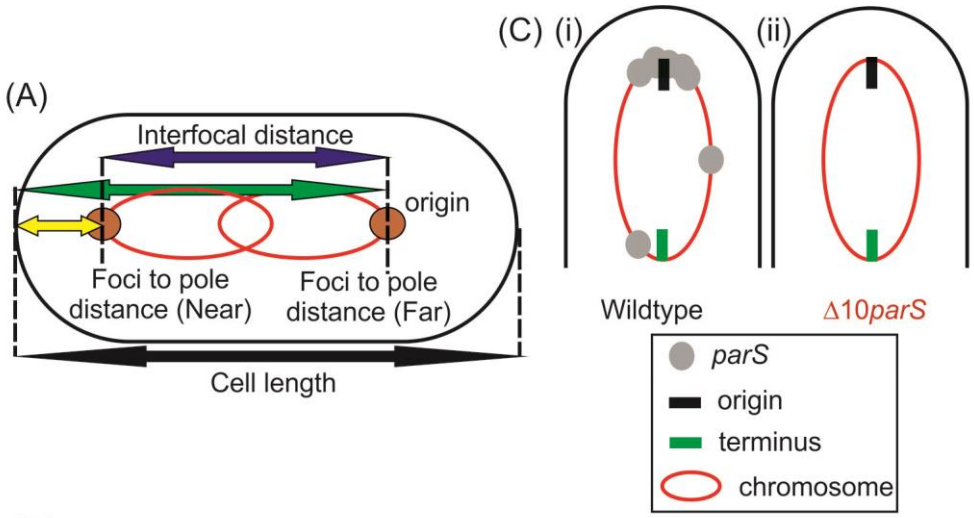

(B)

Strain	Genotype	% of cell length ± 95% CI		
		Interfocal distance	Average position	No. of cells analysed
AK181	*soj*$^+$ *spo0J*$^+$	46.1 ± 2.0	27.0 ± 1.2	105
AK183	Δ*spo0J*	41.5 ± 2.0	29.3 ± 1.3	105
AK225	Δ10*parS*	45.0 ± 2.2	27.5 ± 1.5	104
AK227	Δ*spo0J* Δ10*parS*	40.1 ± 1.9	30.0 ± 1.3	105

Figure 4.5.2: Origin positioning was not affected in the Δ10*parS* strain

(A) Schematic diagram showing the measurement of focus position in cells with two foci. Please refer to Chapter 2.9 for a detailed explanation. **(B)** Origin position within the cell. The *oriC* region was labelled with an array of *tetO* operators bound by TetR-GFP. Cells were grown in 2% succinate minimal media at 37˚C until early exponential phase. Cell membranes were stained with FM-595 dye to distinguish individual cells and the number of fluorescent TetR-GFP foci per cell was determined using epifluorescence microscopy. An approximate of 100 cells was measured for each strain. The 95% confidence intervals for the mean were calculated. (i) *soj*$^+$ *spo0J*$^+$ (AK181), *soj*$^+$ *spo0J*$^+$ Δ10*parS* (AK225), (ii) Δ*spo0J* (AK183), Δ*spo0J* Δ10*parS* (AK227). **(C)** Schematic diagram showing the positioning of the origin in (i) *soj*$^+$ *spo0J*$^+$ (AK181), *soj*$^+$ *spo0J*$^+$ Δ10*parS* (AK225).

4.6 Chapter 4 Discussion

4.6.1 Soj regulation by the Spo0J:*parS* complex

In this chapter a *B. subtilis* strain lacking all 10 *parS* sites was constructed. GFP-Soj localization studies and quantitative PCR analysis indicate that regulation of Soj by Spo0J was disrupted. Importantly therefore, it suggests that Spo0J nucleoprotein complex formation at *parS* sites is necessary for Spo0J to efficiently regulate Soj.

Although regulation of Soj by Spo0J was clearly perturbed by the deletion of *parS* sites, the defects observed were not as severe as in a Δ*spo0J* null mutant, suggesting that regulation was not fully abolished. In support of this interpretation, single cell analysis of GFP-Soj showed that Soj is still able to display localization patterns associated with the protein in its monomeric form, indicating that weak regulation by Spo0J was present. Furthermore, stimulation of DnaA activity by Soj in the Δ10*parS* strain was not detected in a sporulation assay. I propose that nonspecific binding of Spo0J dimers onto the chromosome is responsible for the observed residual regulation of Soj.

4.6.2 Impact of *parS* on global chromosome origin segregation, positioning and organization

Spo0J localizing at *oriC* and recruiting condensin to the origin region was proposed to be important for proper chromosome organization and segregation (Gruber and Errington, 2009; Sullivan et al., 2009; Wang et al., 2014b). Interestingly, under the growth conditions utilized, the chromosomes of the Δ8*parS* and Δ10*parS* strains appear to be largely normal. This is in contrast to earlier published data where the Δ8*parS* chromosomes are less condensed and form anucleate cells (Sullivan et al., 2009). I suspect that these differences in results were due to differences in the growth media used in the experiments (ie- fast growth media was used by Sullivan and colleagues). My data is consistent with previously published results indicating that in the absence of multifork replication when replication elongation rates are slower in a slow growth media, deletion of *parS* sites does not significantly affect overall nucleoid organization (Gruber et al., 2014).

In addition, although chromosome origin segregation and positioning were not affected in the absence of *parS* sites, it appears that Spo0J is still important under these conditions since sister origins appear to be closer together in the Δs*po0J* Δ10*parS* strain. It is possible that even in the absence of *parS* sites, the residual localization of Spo0J is important to load condensin onto DNA, thereby promoting proper overall chromosome organization and segregation. Potentially related to this, the observation that origin separation is impaired when Spo0J is redistributed to ectopic *parS* sites (Chapter 3.7) but is relatively unaffected when *parS* sites are deleted, suggests that in the former cases the redistribution of condensin away from the origin may be responsible for the severe segregation defect.

4.7 Chapter 4 Future work

4.7.1 ChIP-seq to investigate Spo0J enrichment in Δ10*parS* strain

In the absence of *parS* sites, Spo0J was unable to efficiently regulate Soj activity, consistent with the model that *parS*-dependent Spo0J nucleoprotein complexes are required to regulate Soj activity, however, closer examination of the marker frequency analysis revealed that the degree of overinitiation was not as severe as in the absence of Spo0J (Figure 4.3.1) and together with the GFP-Soj localization data (Figure 4.2.1), suggested that some residual Spo0J activity still remains.

However it remains unclear whether this residual activity was due to unspecific binding of Soj dimers to DNA and/or Spo0J forming short nucleoprotein complexes that were not detectable by looking at Spo0J-GFP foci formation (Figure 4.1.2). To investigate this further, ChIP-seq will be performed to analyse Spo0J on the *B. subtilis* genome in the absence of *parS* sites and whether any enrichment of Spo0J might be observed, which may indicates other not yet discovered *parS* sites, that may also explain the less severe overinitiation observed.

4.7.2 GFP-Soj and Spo0J-GFP localization in the absence of *parS* at 359˚

ChIP-chip studies have shown that the *parS* site located within the *spo0J* gene, near the origin at 359˚ showed the highest affinity for Spo0J binding (Breier and Grossman, 2007; Lin and Grossman, 1998). Therefore it was conceivable that mutating the *parS* binding site in *spo0J* without affecting the sequence of the Spo0J protein could have reduced or abolished the ability for Spo0J-GFP to form the nucleoprotein complexes (Figure 4.2.1), which in turn disrupted Spo0J ability to regulate Soj activity (Figure 4.2.1; GFP-Soj localization and Figure 4.3.1; marker frequency analysis).

As a more direct test for the importance of the *parS* at 359˚ for Spo0J nucleoprotein complex formation, a Δ1*parS* stain containing the mutated *parS* at 359˚ will be constructed (as described in Chapter 4.1) to look at Spo0J-GFP localization within this mutant. Likewise, GFP-Soj localization will also be investigated in the same Δ1*parS* background (as described in Chapter 4.2), to rule out the possibility that removal of this *parS* was responsible for the Soj localization pattern observed in the Δ10*parS* stain (Figure 4.2.1).

However it is highly unlikely that *parS* at 359˚ was responsible for these results because systematically removing *parS* will enrich Spo0J to the remaining *parS* sites and because these *parS* sites around the origin have relatively high affinity for Spo0J, it is likely that Spo0J-GFP will still form a foci at the origin (Breier and Grossman, 2007; Lin and Grossman, 1998; Livny et al., 2007). In support of this, my data have also shown that a single consensus *parS* is sufficient for Spo0J-GFP to form a foci (Figure 5.1.2) and this in turn is able to regulate Soj activity as judged by GFP-Soj localization (Figure 5.2.1) and DnaA regulation (Figure 5.3.1; marker frequency analysis).

Chapter 5: A single *parS* site is necessary and sufficient for Spo0J to regulate Soj

Chapter 5 Introduction

I showed in Chapter 4 that deletion of all ten chromosomal *parS* sites renders Spo0J unable to properly regulate Soj activity. Conversely, I showed in Chapter 3 that redistribution of Spo0J away from origin-proximal *parS* sites had no effect on the regulation of Soj. Based on these results, I hypothesized that a single *parS* site located anywhere in the cell would likely be sufficient to promote regulation of Soj by Spo0J.

To specifically investigate the importance of *parS* site localization for Spo0J to regulate Soj, a single consensus *parS* site from 359° was re-introduced into the Δ10*parS* mutant either on the chromosome at different locations or on a low copy-number plasmid. The data shows that only a single *parS* site is necessary and sufficient for the proper regulation of Soj activity by Spo0J, regardless of its genetic location.

In addition it was found that *parS* location affects overall chromosome organization, although this did not impair chromosome segregation. Furthermore, *parS* sites were recruited to the cell quarter position.

Chapter 5 Results

5.1 Insertion of a single *parS* into different region of the chromosome

All ten *parS* sites showed different affinity for Spo0J, therefore to ensure Spo0J affinity to *parS* is uniform among the Δ9*parS* mutants, the consensus *parS* sequence 5'-TGTTCCACGTGAAACA-3' which showed the highest affinity for Spo0J and is located within the *spo0J* gene, near the origin at 359˚ was chosen (Breier and Grossman, 2007; Lin and Grossman, 1998).

To re-introduce a single *parS* site into either the right arm of the chromosome at 90˚, the left arm at 270˚, or near the origin at 359˚, plasmids containing a single *parS* consensus sequence were individually integrated into the Δ10*parS* strain by double crossover (Figure 5.1.1A, 90˚ purple, 270˚ green, 359˚ brown dot).

To integrate *parS* onto the right arm of the chromosome at 90˚ (Figure 5.1.1A, purple dot), the same plasmid that was used to construct the Δ10*parS* strain was modified (see chapter 4.1). As before, the native $parS^{90}$ located within the coding sequence of the *yhaX* gene was modified by site directed mutagenesis to maintain the amino acid sequence coding for the protein. Subsequently, a consensus *parS* sequence was inserted directly after the stop codon of the *yhaX* gene (Figure 5.1.1B).

Next, to construct a strain with a single *parS* on the left arm of the chromosome at 270˚ (Figure 5.1.1A, green dot), the consensus *parS* sequence was inserted into an integration plasmid next to an antibiotic resistance cassette, and the new *parS* was to be inserted into the non-coding sequence between the two convergent genes *ytcC* and *ytxO* (Figure 5.1.1C).

Finally a plasmid containing the *soj-spo0J* locus was integrated into the Δ10*parS* mutant to re-introduce the native consensus *parS* site within *spo0J* at 359˚ (Figure 5.1.1A, brown dot and Figure 5.1.1D). Proper integration of all plasmids was verified by PCR and DNA sequencing (data not shown).

To confirm that the reintroduced *parS* sequences were functional, localization of Spo0J-GFP was visualized by epifluorescence microscopy. It should be noted that in the strains containing Δ9$parS^{+90}$ and Δ9$parS^{+270}$, the plasmid used to create the *spo0J-gfp* fusion contained a mutated $parS^{359}$ sequence (while maintaining the amino acid coding sequence for the Spo0J protein) (See chapter 4.1).

As discussed in Chapter 4.1, in the Δ10*parS* mutant Spo0J-GFP was delocalized and associated with the nucleoid as a weak diffuse signal (Figure 5.1.2ii). In strains containing single *parS* sites, Spo0J-GFP formed bright foci within the cell (Figure 5.1.2iii-v). These results are consistent with Spo0J binding to *parS* to form a nucleoprotein complex. Interestingly, in comparison to the discrete Spo0J-GFP foci formed when a single *parS* was present, in the wild-type background Spo0J-GFP foci appeared slightly jagged (Figure 5.1.2i). I suspect that this is due to Spo0J-GFP binding to multiple *parS* sites.

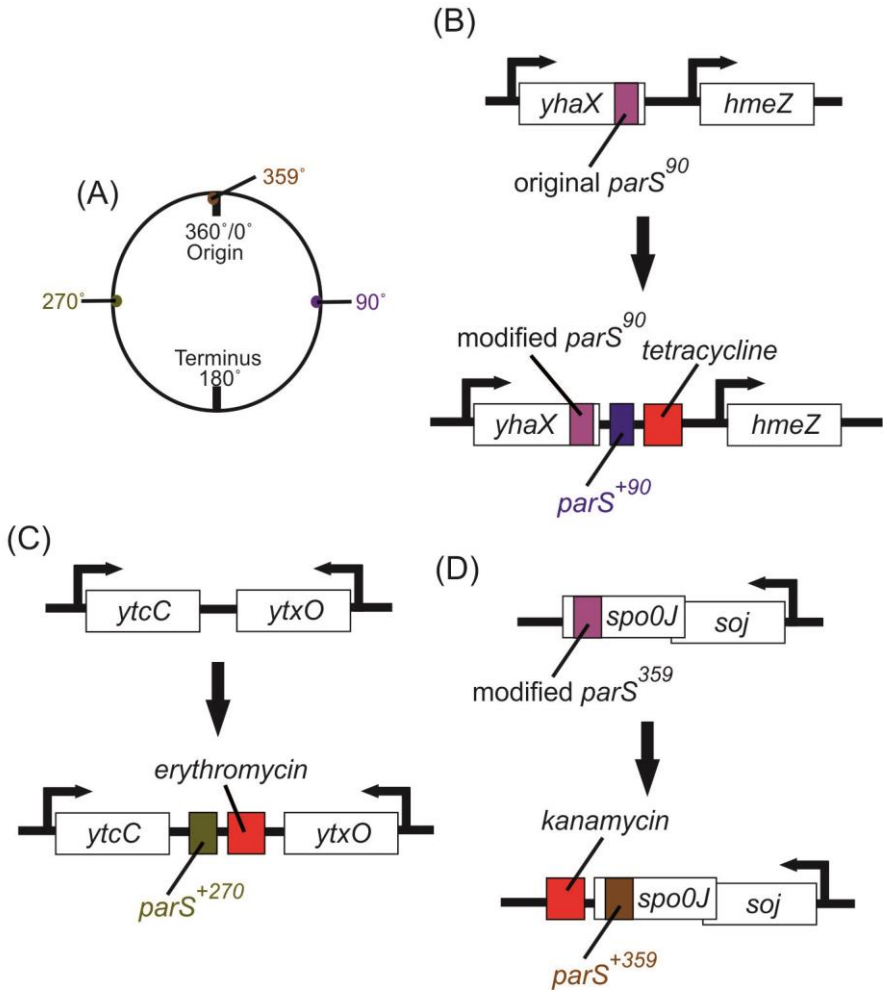

Figure 5.1.1: Insertion of a single *parS* onto the chromosome

(A) Schematic diagram showing a Δ10*parS* strain with a single *parS* sequence inserted into 90˚, 270˚ and 359˚ (purple, green, brown dot respectively). **(B)** Schematic diagram showing the replacement of $parS^{90}$ linked to an antibiotic resistance cassette (tetracycline; red bar) in *yhaX*. **(C)** Schematic diagram showing insertion of $parS^{270}$ linked to an antibiotic resistance cassette (erythromycin; red bar) between two convergent genes *ytcC* and *ytxO*. **(D)** Schematic diagram showing the re-introduction of $parS^{359}$ linked to antibiotic resistance cassette (kanamycin; red bar) into *spo0J* of the Δ10*parS* strain.

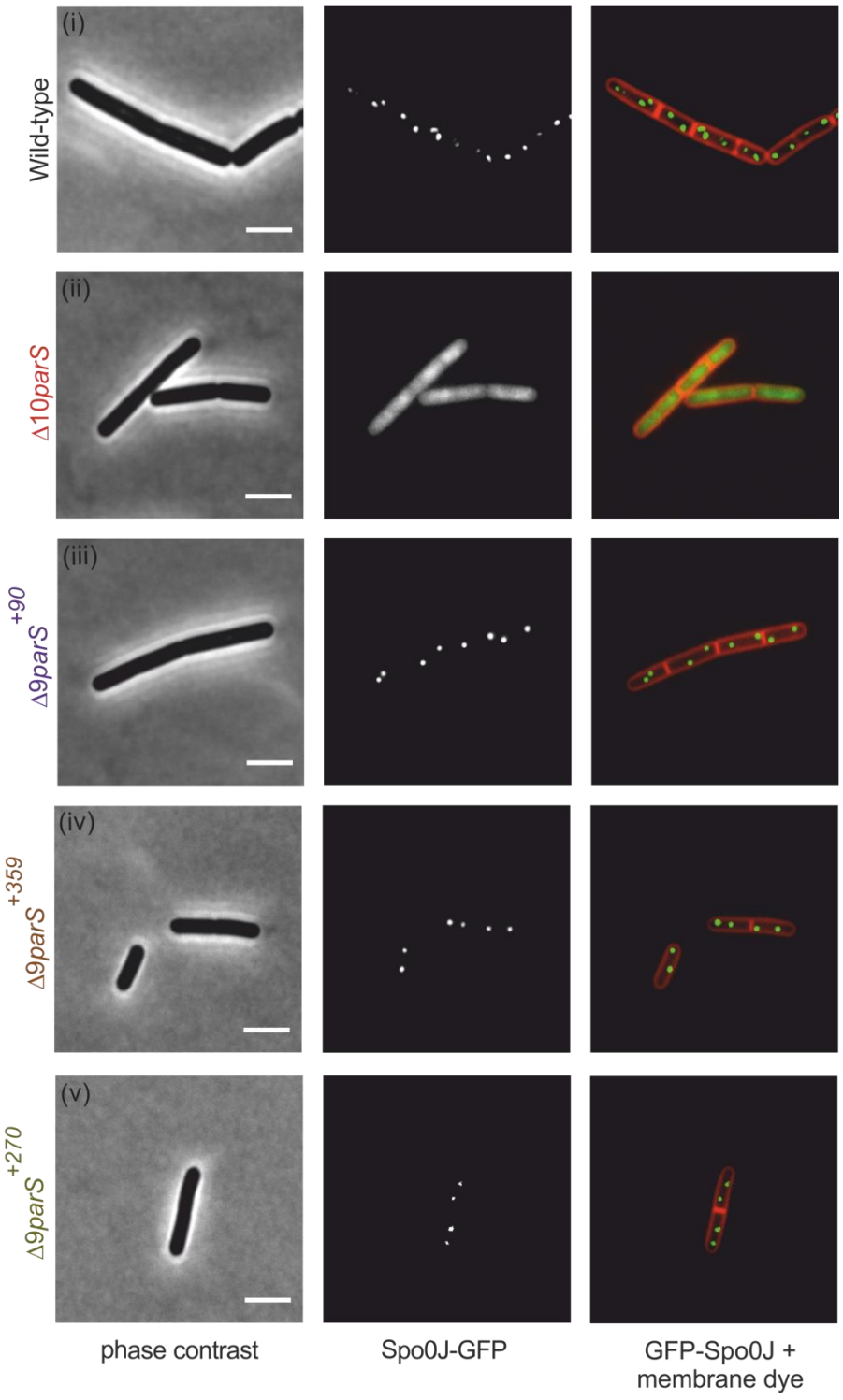
(i)
Wild-type
(ii)
Δ10parS
(iii)
Δ9parS+90
(iv)
Δ9parS+359
(v)
Δ9parS+270
phase contrast
Spo0J-GFP
GFP-Spo0J +
membrane dye

Figure 5.1.2: Spo0J-GFP localization in wild-type and single *parS* strains

Spo0J-GFP localization of wild-type and *parS* mutants. Cells were grown in 2% succinate minimal media at 37˚ until early exponential phase. Membranes were stained with FM-595 dye to distinguish cells and visualized using epifluorescence microscopy (Scale bar = 3 μm). Approximately 500 cells were visualized for each strain and typical cells are shown. (i) Wild-type (AK367), (ii) Δ10*parS* (AK369), (iii) Δ9*parS*$^{+90}$ (AK373), (iv) Δ9*parS*$^{+270}$ (AK597), (v) Δ9*parS*$^{+359}$ (AK593).

5.2 GFP-Soj localization is partially restored in the presence of a *parS* site

To investigate Soj activity directly within single cells, the *soj* gene was fused to *gfp* under the control of its native promoter and GFP-Soj was visualized using epifluorescence microscopy.

As described in Chapters 3.2, 3.6 and 4.2, wild-type GFP-Soj binds to septa (Figure 5.2.1i, arrow) and forms a faint focus with the origin (Figure 5.2.1i, asterisk). In the absence of Spo0J, GFP-Soj is associated with the nucleoid (Figure 5.2.1.ii, circle). In the absence of chromosomal *parS* sites, GFP-Soj localization adopted a localization pattern most closely resembling the Soj dimer bound to the nucleoid (Figure 5.2.1iii).

The reintroduction of a single *parS* site, regardless of its position in the chromosome, shifted the GFP-Soj localization pattern to most closely resemble that of the monomeric protein. In these strains, GFP-Soj continues to form faint cytoplasmic foci (Figure 5.2.1v, vii and ix, asterisk), and bind to septa (Figure 5.2.1v, vii and ix, arrow), suggesting that a single *parS* site is sufficient to promote significant control of Soj activity by Spo0J. However, GFP-Soj was also occasionally observed to accumulate as small patches adjacent to septa (Figure 5.2.1v, vii and ix, circle). I suspect that these patches represent GFP-Soj binding to DNA located proximal to a cell pole (see Chapter 7).Taken together, these observations indicate that while a single *parS* site is necessary and sufficient to promote regulation of Soj by Spo0J, single sites may be less efficient compared to the multiple *parS* sites distributed throughout the wild-type chromosome.

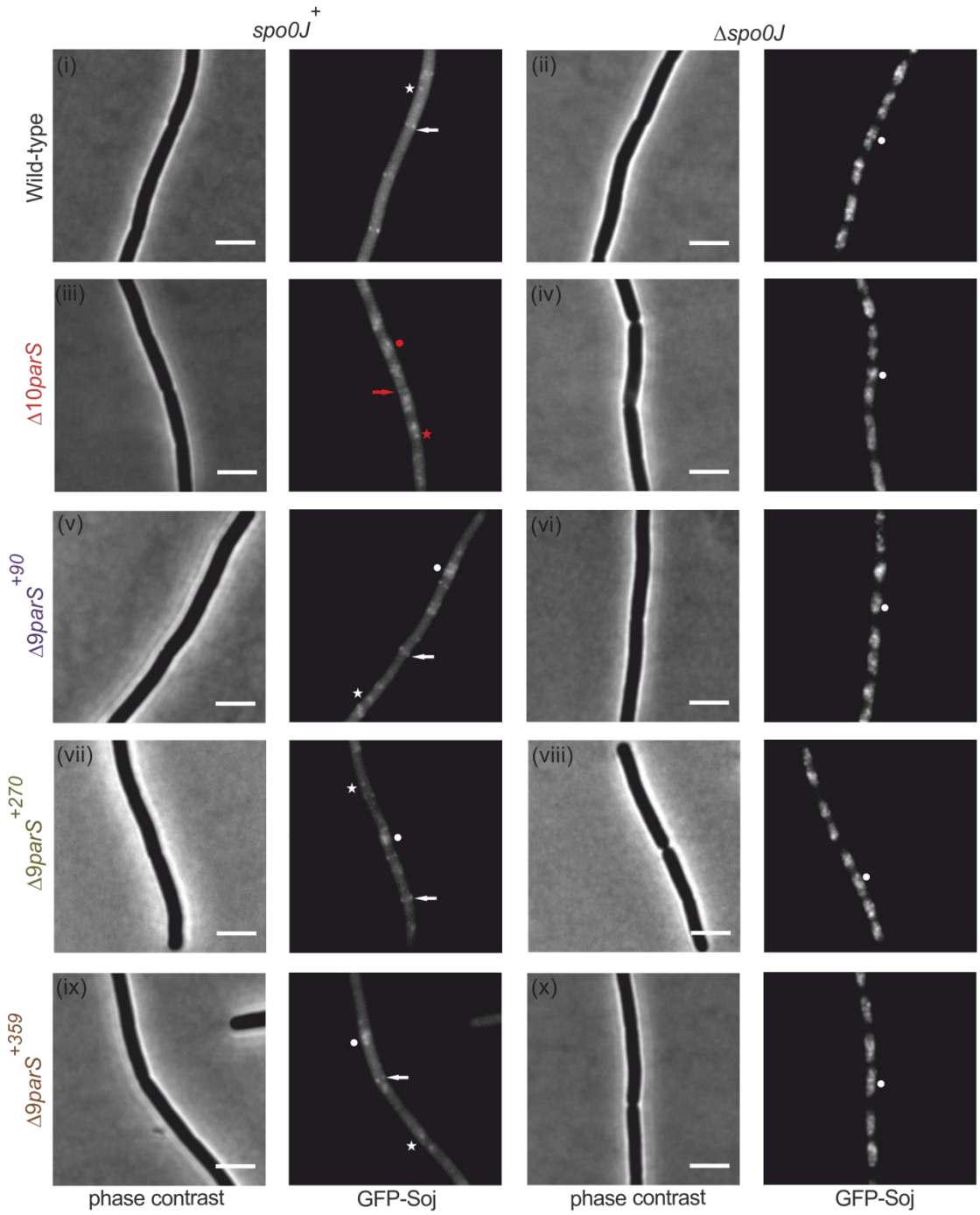
spo0J+
Δspo0J
(i)
(ii)
Wild-type
(iii)
(iv)
Δ10parS
(v)
(vi)
Δ9parS+90
(vii)
(viii)
Δ9parS+270
(ix)
(x)
Δ9parS+359
phase contrast
GFP-Soj
phase contrast
GFP-Soj

Figure 5.2.1: Soj localization was restored in the presence of a single *parS* site

GFP-Soj localization of wild-type and *parS* mutants in the presence and absence of Spo0J. Cells were grown in 2% glucose minimal media at 37˚ until early exponential phase. GFP-Soj localization was determined by epifluorescence microscopy. An arrow (→) denotes localization at a septum, an asterisk (*) indicates localization as a focus and a circle (●) denotes nucleoid binding (Scale bar = 3 μm). Approximately 500 cells were visualized for each strain and typical cells are shown. (i) *soj*$^{+}$ *spo0J*$^{+}$ (AK277), (ii) Δ*spo0J* (AK279), (iii) *soj*$^{+}$ *spo0J*$^{+}$ Δ10*parS* (AK281), (iv) Δ*spo0J* Δ10*parS* (AK283), (v) *soj*$^{+}$ *spo0J*$^{+}$ Δ9*parS* $^{+90}$ (AK399), (vi) Δ*spo0J* Δ9*parS* $^{+90}$ (AK325), (vii) *soj*$^{+}$ *spo0J*$^{+}$ Δ9*parS* $^{+270}$ (AK599), (viii) Δ*spo0J* Δ9*parS* $^{+270}$ (AK601), (ix) *soj*$^{+}$ *spo0J*$^{+}$ Δ9*parS* $^{+359}$ (AK305), (ix) Δ*spo0J* Δ9*parS* $^{+359}$ (AK307).

5.3 Control of DNA replication is restored in the presence of a *parS* site

As described in Chapter 4, in the absence of chromosomal *parS* sites Soj accumulates in its dimeric form to activate DnaA, resulting in an increase in the DNA replication initiation frequency. Therefore, I next determined whether a single *parS* site was sufficient to modulate Soj regulation of DnaA. A range of Δ9*parS* strains containing a single *parS* site at various chromosomal locations were created, and into these backgrounds Δ*soj* and/or Δ*spo0J* mutants were introduced. Strains were checked by Western blot and PCR analysis to confirm correct construction (Chapter 2.13.4 and data not shown).

When a single *parS* site was re-introduced anywhere in the chromosome, marker frequency analysis showed that DNA replication initiation frequency was restored to the wild-type level ($Spo0J^+$, Soj^+ Figure 5.3.1). The effect on DNA replication was due to proper regulation of Soj by Spo0J, since in all of the parental strains Soj-dependent overinitiation was observed in a *spo0J* mutant (Figure 5.3.1, 3.3.1, 3.6.2 and 4.3.1). These results are consistent with the localization of GFP-Soj within strains that harbour a single *parS* site (Figure 5.2.1).

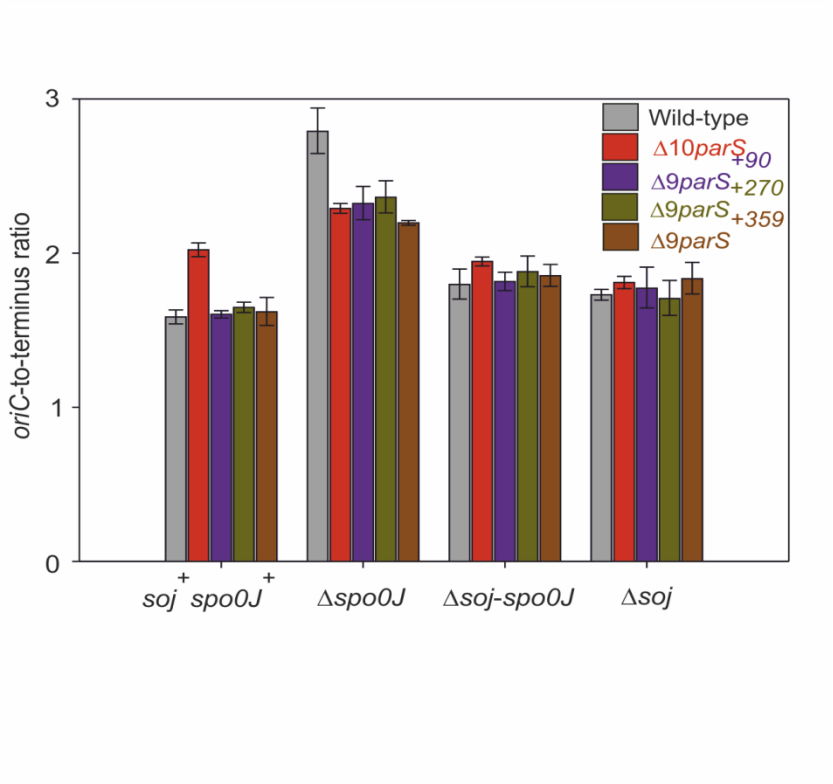

Figure 5.3.1: Control of DNA replication was restored in the Δ9*parS* strain in the presence of Spo0J nucleoprotein complex formation

The rate of replication initiation was restored by a single *parS* site. Cells were grown in 2% succinate minimal media at 37˚ until early exponential phase. Genomic DNA was harvested from cells and the *oriC*-to-terminus ratio of each mutant in a wild-type strain (grey), Δ10*parS* (red), $parS^{90}$ (purple), $parS^{270}$ (greed), $parS^{359}$ (brown) was determined using marker frequency analysis. The results are shown as the average ± standard deviation from three technical replicates. soj^{+} $spo0J^{+}$ (AK239), soj^{+} $spo0J^{+}$ Δ10*parS* (AK243), soj^{+} $spo0J^{+}$ $parS^{+90}$ (AK323), soj^{+} $spo0J^{+}$ $parS^{+270}$ (AK603), soj^{+} $spo0J^{+}$ $parS^{+359}$ (AK259), Δ*spo0J* (AK241), Δ*spo0J* Δ10*parS* (AK245), Δ*spo0J* $parS^{+90}$ (AK325), Δ*spo0J* $parS^{+270}$ (AK605), Δ*spo0J* $parS^{+359}$ (AK261), Δ*soj-spo0J* (AK559), Δ*soj-spo0J* Δ10*parS* (AK563), Δ*soj-spo0J* $parS^{+90}$ (AK553), Δ*soj-spo0J* $parS^{+270}$ (AK607), Δ*soj-spo0J* $parS^{+359}$ (AK561), Δ*soj* (AK557), Δ*soj* Δ10*parS* (AK617), Δ*soj* $parS^{+90}$ (AK555), Δ*soj* $parS^{+270}$ (AK649), Δ*soj* $parS^{+359}$ (AK669).

5.4 Spo0J spreading is required for the proper control of Soj activity

It has been proposed that the specific binding of Spo0J to *parS* promotes lateral spreading followed by long-distance bridging interactions to construct nucleoprotein complexes (Broedersz et al., 2014; Graham et al., 2014). To investigate whether the effect of a *parS* site on Soj activity is dependent upon Spo0J forming a nucleoprotein complex, two *spo0J* alleles were analysed, *spo0J*^{G77S} and *spo0J*^{R149A}. Both of these *spo0J* mutants bind specifically to *parS* *in vitro* but fail to spread and form observable nucleoprotein complexes (Graham et al., 2014).

To introduce the *spo0J*^{G77S} and *spo0J*^{R149A} mutations into both the wild-type and Δ9*parS* $^{+90}$ background, plasmids were constructed that contain either the native *soj-spo0J* locus or the *soj-spo0J* locus without the *parS*^{359} site (as not to re-introduce *parS*^{359} back into the Δ9*parS* $^{+90}$ mutant) to allow integration into the chromosome by double-crossover. As previously noted because *parS*^{359} is located within the coding sequence of the *spo0J* gene, site directed mutagenesis was used to mutate the *parS*^{359} sequence while maintaining the amino acid coding sequence for the Spo0J protein. A strain containing the *spo0J*^{G77S} allele (Breier and Grossman, 2007) and the plasmid containing the *spo0J*^{R149A} allele (Autret et al., 2001) were used as templates for PCR and construction of the integrating plasmids. The resulting strains (wild-type and Δ9*parS* $^{+90}$ containing the *spo0J*^{G77S} and *spo0J*^{R149A} alleles) were sequenced to confirm the presence all desired changes.

Marker frequency analysis shows that spreading-deficient Spo0J mutants overinitiate DNA replication but the rates of overinitiation were lower as compared to the complete absence of Spo0J, suggesting that Spo0J dimers binding to DNA still retained some capacity to regulate Soj (Figure 5.4.1).

Alternatively, these spreading-deficient mutants might still be able to form short Spo0J nucleoprotein complexes that still regulated Soj abet less efficiently. These results are consistent with the idea that binding of Spo0J dimers to DNA is insufficient to control Soj activity and that lateral spreading and/or bridging activity by Spo0J to form the extended nucleoprotein complexes is necessary to regulate Soj.

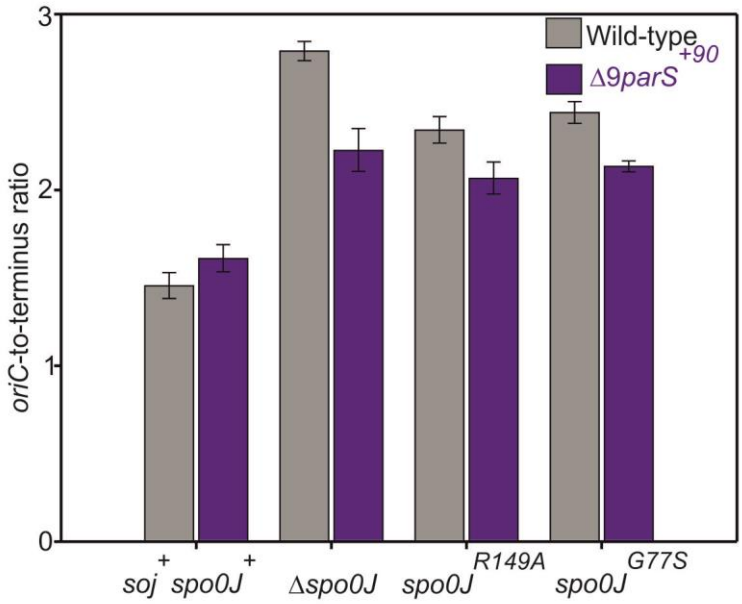

Figure 5.4.1: Control of DNA replication requires Spo0J spreading to form the extended nucleoprotein complex

Spo0J:*parS* nucleoprotein assembly is required for proper control of DNA replication initiation. Cells were grown in 2% succinate minimal media at 37˚ until early exponential phase. Genomic DNA was harvested from cells and the *oriC*-to-terminus ratio of each mutant was determined using marker frequency analysis. The results are shown as the average ± standard deviation from three technical replicates. *soj*$^{+}$ *spo0J*$^{+}$ (AK239), *soj*$^{+}$ *spo0J*$^{+}$ *parS*^{90} (AK323), Δ*spo0J* (AK241), Δ*spo0J parS*^{90} (AK325), *spo0J*^{R149A} (AK249), *spo0J*^{R149A} *parS*^{90} (AK417), *spo0J*^{G77S} (AK251), *spo0J*^{G77S} *parS*^{90} (AK419).

5.5 Low-copy plasmid containing a single *parS*

The experiments described above indicate that a single *parS* site, regardless of its position on the chromosome, is sufficient for Spo0J to form a nucleoprotein complex competent of regulating Soj (Figure 5.2.1 and 5.3.1). Next, I wondered whether Spo0J nucleoproteins complexes on plasmids would be capable of regulating Soj activity in the absence of chromosomal *parS* sites (Δ10*parS* mutant).

To investigate this, the multi-copy plasmid containing a single consensus *parS* site (described in Chapter 3.5) was transformed into the Δ10*parS* background. Although transformants could be obtained, growth of the resulting strains was severely compromised. This suggests that in the presence of a large excess of *parS* sites *in trans*, *parS* sites on the chromosome are important for cell survival because in earlier experiments, the strains harbouring the multi-copy plasmids were viable when *parS* sites were present within the chromosome (Chapter 3).

To circumvent the multi-copy plasmid problem, a single consensus *parS* site was inserted into the low copy-number plasmid pLOSS (~1-3 copy per chromosome) (Claessen et al., 2008; Tanaka and Koshikawa, 1977) (Figure 5.5.1A). The plasmid was sequenced to ensure that the *parS* sequence was present. In this case transformants were easily obtained and all strains grew normally. To assess whether the *parS* site on the plasmid was functional, epifluorescence microscopy was used to examine Spo0J-GFP localization. In a Δ10*parS* strain containing the *parS*$^{+}$ pLOSS plasmid, Spo0J-GFP formed discrete foci within the cell that were generally well separated and arranged into an orderly pattern (Figure 5.5.1iv). In a wild-type background there was a slight increase in the number of Spo0J-GFP foci per cell, likely reflecting

nucleoprotein complexes forming both on the chromosome and the plasmid (Figure 5.5.1iii). Importantly however, this pattern was clearly different from the nucleoid associated distribution observed when the multi-copy *parS*$^{+}$ plasmids were used (Figure 3.5.1Bii). There was no effect on Spo0J-GFP localization in the presence of the control plasmid lacking the *parS* site (Figure 5.5.1i-ii). These results are consistent with the idea that pLOSS exists as a low-copy number plasmid within the cell and that Spo0J-GFP is forming nucleoprotein complexes at *parS* sites *in trans*.

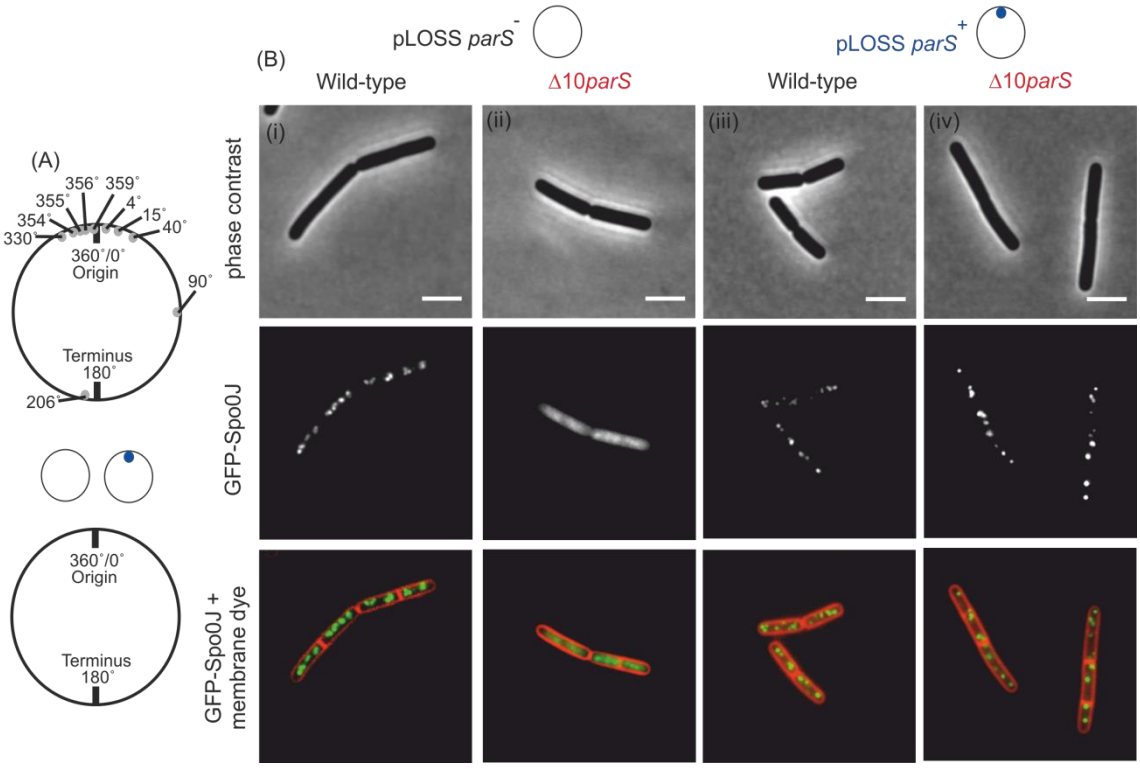

Figure 5.5.1: Spo0J-GFP localization in the presence of a low-copy plasmid containing a single *parS* site

(A) Schematic diagram showing a low-copy plasmid harbouring a single *parS* site in a strain with all ten endogenous *parS* as shown by grey dots (4˚, 15˚, 40˚, 90˚, 206˚, 330˚, 354˚, 355˚, 356˚ and 359˚) and a strain without all ten *parS.* **(B)** Spo0J-GFP foci formation in strain harbouring the control or *parS* plasmids. Cells were grown in 2% succinate minimal media at 37˚ supplemented with spectinomycin (50 µg/ml) until early exponential phase. Cell membranes were stained with FM-595 dye to distinguish individual cells and fluorescent Spo0J-GFP foci per cell were determined using epifluorescence microscopy (Scale bar = 3 µm). Approximately 500 cells were visualized for each strain and typical cells are shown. (i) *parS*$^{-}$ pLOSS wild-type (AK457), (ii) *parS*$^{-}$ pLOSS Δ10*parS* (AK461), (iii) *parS*$^{+}$ pLOSS wild-type (AK455), (iv) *parS*$^{+}$ pLOSS Δ10*parS* (AK459).

5.6 A single *parS* on a low-copy plasmid is able to restore Soj regulation by Spo0J

Multiple assays were used to determine whether *parS*$^+$ pLOSS in the Δ10*parS* mutant is able to restore regulation of Soj by Spo0J. GFP-Soj localization in the Δ10*parS* mutant containing *parS*$^+$ pLOSS was similar to wild-type with clear septal localization and the formation of faint cytoplasmic foci (Figure 5.6.1vii, arrow and asterisk respectively). In the presence of the control plasmid lacking the *parS* site, GFP-Soj localization in theΔ10*parS* was mostly nucleoid associated, consistent with the protein accumulating as a dimer (Figure 5.6.1v, circle). Marker frequency analysis (Figure 5.6.2) showed that regulation of DnaA by Soj was restored to wild-type levels in the Δ10*parS* mutant containing *parS*$^+$ pLOSS (Western blot was performed for correct strain construction; Figure 2.13.5). These results indicate that Spo0J is able to interact with *parS in trans* to form nucleoprotein complexes capable of efficiently regulating Soj activity.

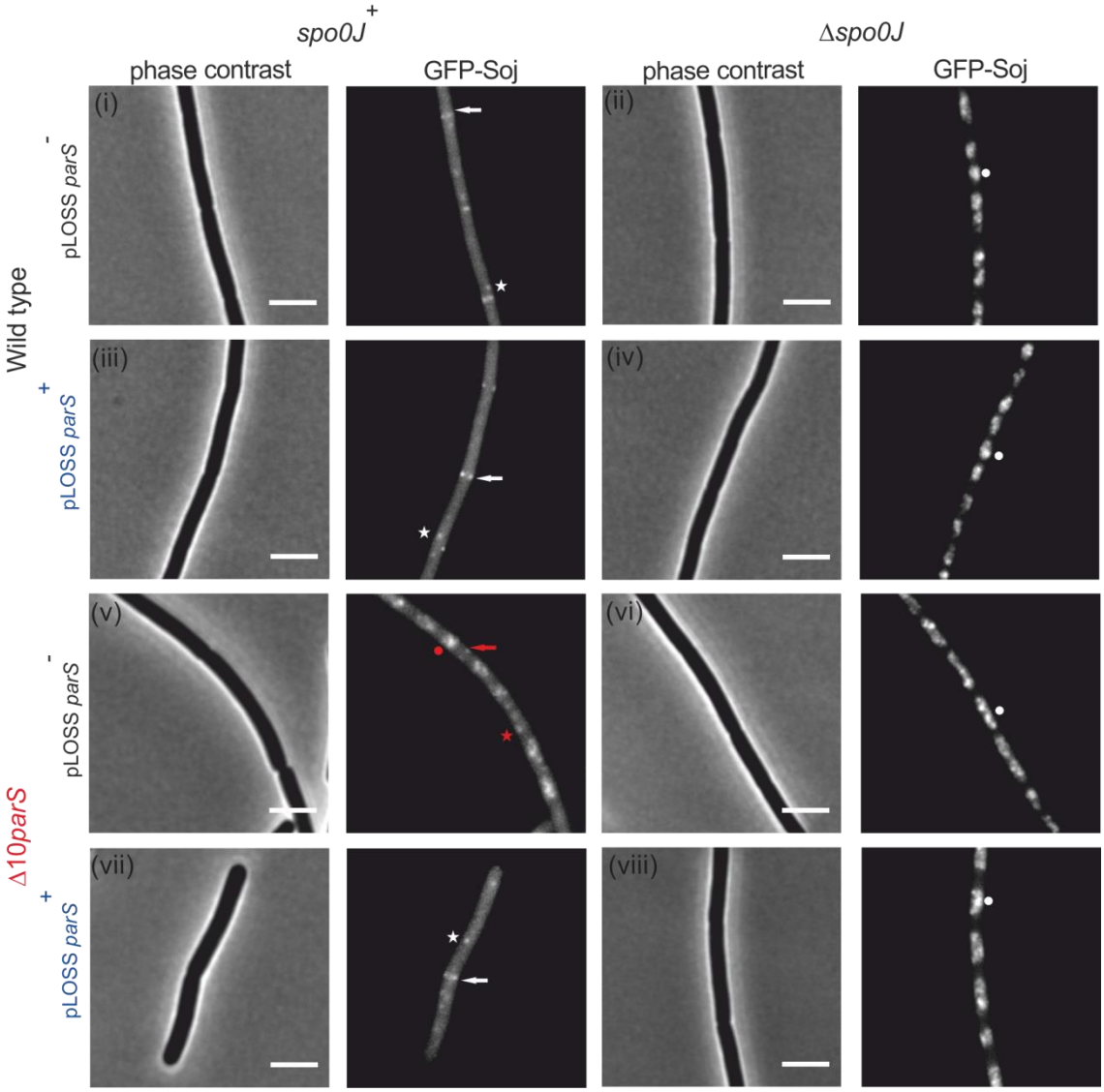
spo0J+
Δspo0J
phase contrast
GFP-Soj
phase contrast
GFP-Soj
Wild type
Δ10parS
pLOSS parS -
pLOSS parS +
pLOSS parS -
pLOSS parS +
(i)
(ii)
(iii)
(iv)
(v)
(vi)
(vii)
(viii)

Figure 5.6.1: GFP-Soj localization in the presence of ectopic *parS* sites

GFP-Soj localization in the wild-type and *parS* mutants in the presence of the control or *parS* plasmids. Cells were grown in 2% glucose minimal media at 37˚ supplemented with spectinomycin (50 µg/ml) until early exponential phase. GFP-soj localization was determined by epifluorescence microscopy. An arrow (→) denotes localization at a septum, an asterisk (*) indicates localization as a focus and a circle (●) denotes nucleoid binding (Scale bar = 3 µm). Approximately 500 cells were visualized for each strain and typical cells are shown. (i) *parS*$^{-}$ pLOSS wild-type (AK465), (ii) ∆spo0J *parS*$^{-}$ pLOSS wild-type (AK469), (iii) *parS*$^{+}$ pLOSS wild-type (AK463), (iv) ∆spo0J *parS*$^{+}$ pLOSS wild-type (AK467), (v) *parS*$^{-}$ pLOSS ∆10*parS* (AK473), (vi) ∆spo0J *parS*$^{-}$ pLOSS ∆10*parS* (AK477), (vii) *parS*$^{+}$ pLOSS ∆10*parS* (AK471), ∆spo0J *parS*$^{+}$ pLOSS ∆10*parS* (AK475).

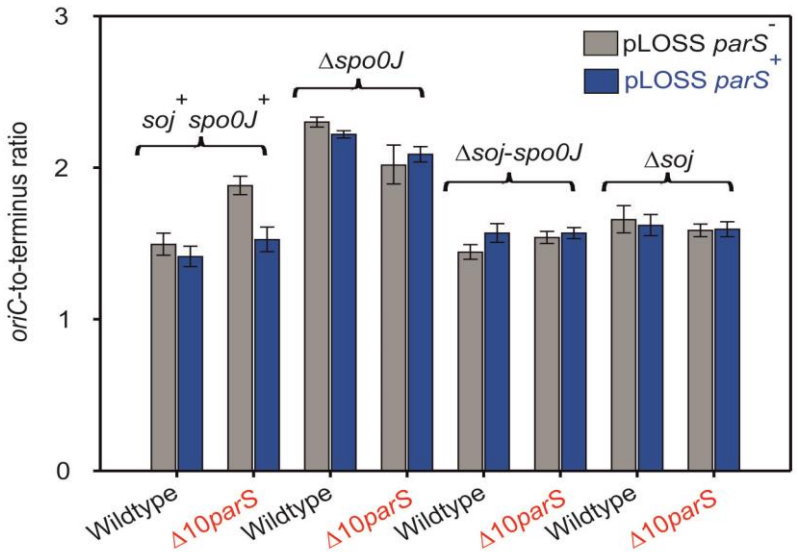

Figure 5.6.2: DNA replication initiation was restored by ectopic *parS*

DNA replication initiation was restored by the low-copy plasmid in a Δ10*parS* mutant. Cells were grown in 2% succinate minimal media at 37˚ supplemented with spectinomycin (50 µg/ml) until early exponential phase. Genomic DNA was harvested from cells and the *oriC*-to-terminus ratio of each mutant containing *parS*$^-$ pLOSS (grey) or *parS*$^+$ pLOSS (blue) was determined using marker frequency analysis. The results are shown as the average ± standard deviation from three technical replicates. *parS*$^-$ pLOSS wild-type (AK429), *parS*$^-$ pLOSS Δ10*parS* (AK437), *parS*$^+$ pLOSS wild-type (AK427), *parS*$^+$ pLOSS Δ10*parS* (AK435), Δspo0J *parS*$^-$ pLOSS wild-type (AK433), Δspo0J *parS*$^-$ pLOSS Δ10*parS* (AK441), Δspo0J *parS*$^+$ pLOSS wild-type (AK431), Δspo0J *parS*$^+$ pLOSS Δ10*parS* (AK439), Δ*soj-spo0J parS*$^-$ pLOSS wild-type (AK625), Δ*soj-spo0J parS*$^-$ pLOSS Δ10*parS* (AK629), Δ*soj-spo0J parS*$^+$ pLOSS wild-type (AK623), Δ*soj-spo0J parS*$^+$ pLOSS Δ10*parS* (AK627), Δ*soj parS*$^-$ pLOSS wild-type (AK621), Δ*soj parS*$^-$ pLOSS Δ10*parS* (AK633), Δ*soj parS*$^+$ pLOSS wild-type (AK619), Δ*soj parS*$^+$ pLOSS Δ10*parS* (AK631).

5.7 A single ectopic *parS* on the chromosome affects overall chromosome organization and segregation

As discussed in Chapter 4, non-specific residual binding of either Spo0J or condensin to the DNA may explain the almost identical overall chromosome morphology and origin segregation/positioning of the Δ10*parS* mutant compared to wild-type. Therefore, I next explored how enriching Spo0J at ectopic positions on the chromosome by inserting a single *parS* site into the Δ10*parS* mutant (Δ9*parS*$^{+90}$, Δ9*parS*$^{+270}$, Δ9*parS*$^{+359}$) would affect chromosome organization.

First the overall chromosome morphology was determined by visualizing nucleoids within single cells; DNA was stained with DAPI and the cell membrane was stained with FM-595. Interestingly, in cells with a single *parS* site, the nucleoid appeared to be less condensed (Figure 5.7.1ii-iv). This defect in nucleoid morphology was more severe in strains with a *parS* site located away from the origin at 90˚ and 270˚ (Figure 5.7.1ii-iii). In addition, these strains appears to be elongated and produced ~1-2% of stumpy cells (data not shown), indicating a defect in the coordination of DNA replication and segregation. Taken together with the results of previous Chapters 3 and 4, this indicates that Spo0J:*parS* nucleoprotein complexes located away from the origin impair chromosome organization, likely through the inappropriate recruitment of condensin. It is not clear why a *parS* site located near *oriC* also causes the nucleoid to decondense.

I suspected that strains with a single *parS* site located away from *oriC* might be affected in chromosome origin segregation, as was observed when Spo0J was redistributed away from origin-proximal *parS* sites (Chapter 3.7). I tested this hypothesis by visualizing the number of origins per cell (as described in Chapter 3.7 and 4.5) in the Δ9*parS*$^{+90}$ and Δ9*parS*$^{+359}$ strains (Figure 5.7.2A).

Chromosome origin separation was largely unaffected when *parS* is present near the origin at 359˚, with the majority of cells containing two TetR-GFP foci (Figure 5.7.2Bi; brown bar). Strikingly, when a *parS* site is located away from *oriC* there was a sharp increase in cells containing only a single focus (Figure 5.7.2Bi; purple bar). This is in agreement with previous results when Spo0J (and likely condensin) was redistributed away from the origin using *parS* arrays and *parS*$^{+}$ plasmids (Chapter 3.7), and is consistent with published results that condensin has to be recruited to *oriC* for proper origin segregation (Wang et al., 2014b). In a Δ*spo0J* mutant the number of foci per cell greatly increased, consistent with marker frequency analysis (Figure 5.3.1) indicating increased DNA replication initiation. Taken together these results show that a single *parS* must be located near *oriC* to elicit proper chromosome organization and origin separation.

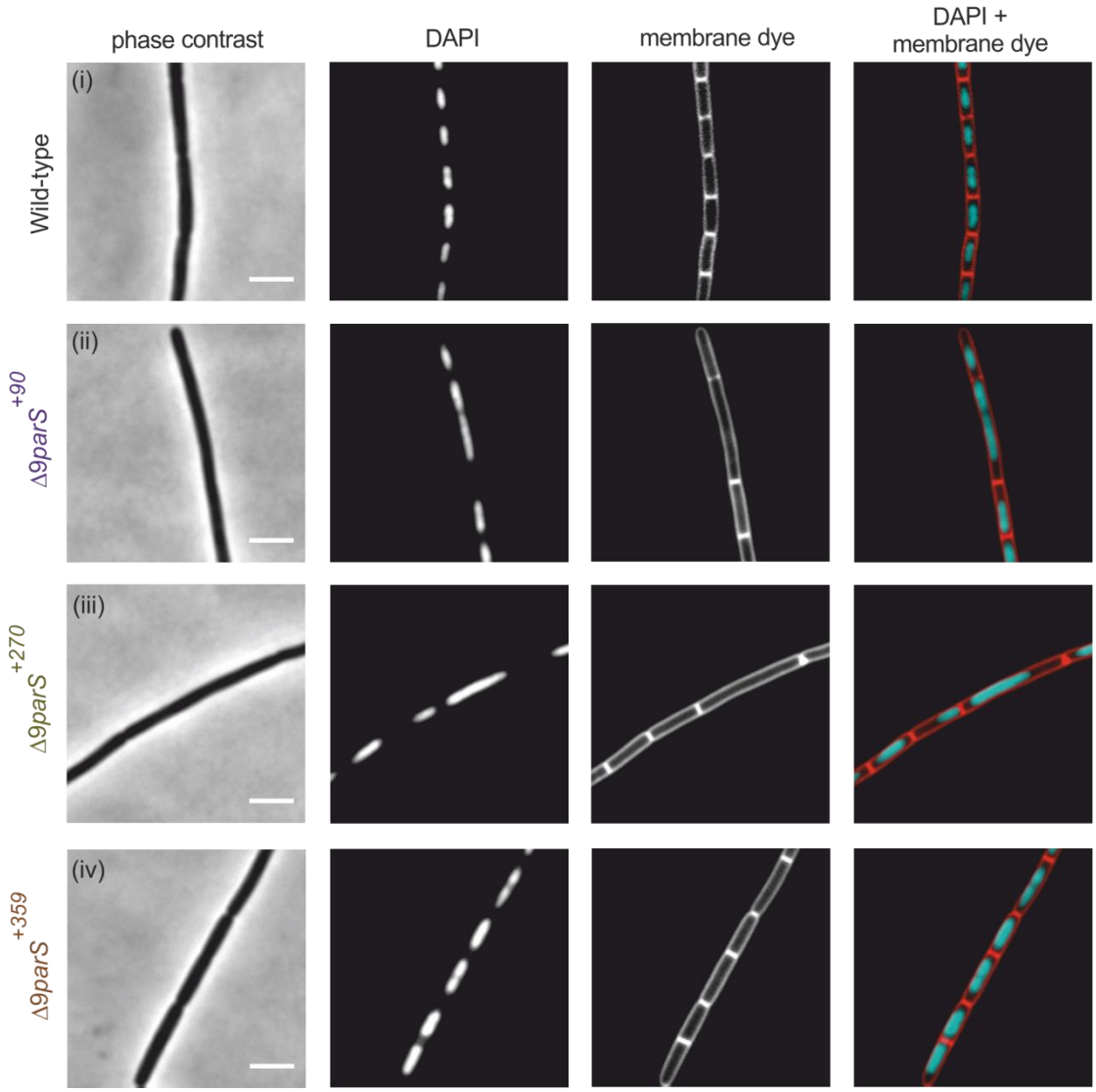

Figure 5.7.1: Overall chromosome organization is affected when *parS* is located away from the origin

Nucleoid of *parS* mutants are affected. Cells were grown in 2% glucose minimal media supplemented with 200 µg/ml casein hydrolysate at 37˚ until early exponential phase. DNA was visualized by DAPI (cyan colour) and membranes were stained with FM-595 dye (Scale bar = 3 µm). Approximately 500 cells were visualized for each strain and typical cells are shown. (i) Wild-type (AK239), (ii) Δ9*parS*$^{+90}$ (AK323), (iii) Δ9*parS*$^{+270}$ (AK603), (iv) Δ9*parS*$^{+359}$ (AK259).

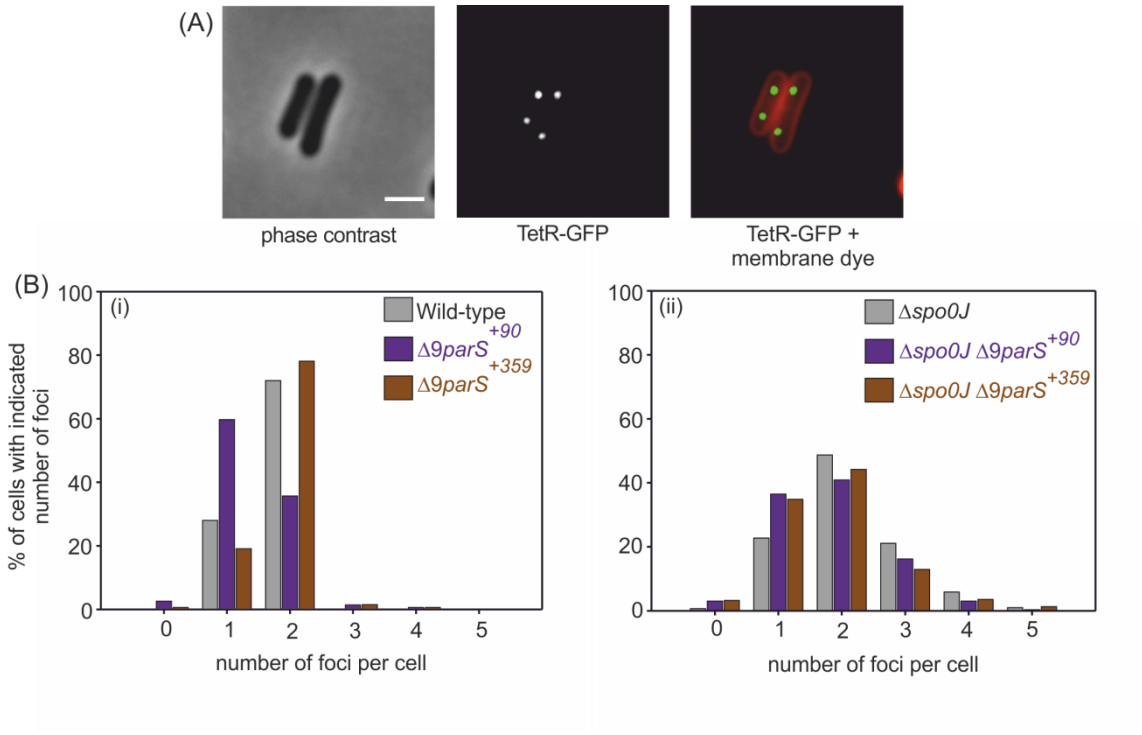

Figure 5.7.2: Segregation and positioning of replicated sister is affected when *parS* is located away from the origin

(A) Origin localization in wild-type *B. subtilis.* The *oriC* region was labelled with an array of *tetO* operators bound by TetR-GFP. *soj*$^{+}$ *spo0J*$^{+}$ (AK181) (Scale bar = 3 μm). **(B)** Origin counting in wild-type (grey), Δ9*parS*$^{+90}$ (purple), Δ9*parS*$^{+359}$ (brown) in the presence and absence of Spo0J. Cells were grown in 2% succinate minimal media at 37˚ until early exponential phase. Cell membranes were stained with FM-595 dye to distinguish individual cells and the number of fluorescent TetR-GFP foci per cell was determined using epifluorescence microscopy. Bar charts showing the results from chromosome origin counts. The strain information is shown in the top right hand corner of each graph. An approximate of 300 cells was counted for each strain. *soj*$^{+}$ *spo0J*$^{+}$ (AK181), *soj*$^{+}$ *spo0J*$^{+}$ Δ9*parS*$^{+90}$ (AK405), *soj*$^{+}$ *spo0J*$^{+}$ Δ9*parS*$^{+359}$ (AK591), Δ*spo0J* (AK183), Δ*spo0J* Δ9*parS*$^{+90}$ (AK615), Δ*spo0J* Δ9*parS*$^{+359}$ (AK639).

5.8 *parS* may be involved in chromosome orientation

As shown above, redistribution of Spo0J to ectopic *parS* sites affected origin separation and chromosome morphology. Therefore, I wondered whether origin positioning would also be affected when Spo0J (and likely condensin) are enriched at ectopic locations. To investigate this, origin position relative to the cell length was measured as described in Chapter 4.5 and 2.9. Strikingly, the origin appears to deviate from wild-type position in the presence of an ectopic *parS* site, suggesting that *parS* is influencing chromosome organization (Figure 5.8.1A-B). Again in the Δ*spo0J* mutant the origins are positioned closer together (Figure 5.8.1A).

To investigate *parS* localization, the position of Spo0J-GFP in strains containing a single *parS* site was measured (as described in Chapter 4.5 and 2.9). Spo0J-GFP foci were always found at the cell quarter position similar to wild-type, independent of where the *parS* sites were integrated into the chromosome (Figure 5.8.2A-B). This localization was dependent upon Soj because in the mutant background, Spo0J-GFP foci were located closer together (Figure 5.8.2A). Taken together, these results indicate that *parS* may be recruited to the cell quarter position through Spo0J and Soj and that when *parS* is located away from *oriC* this result in reorientation of the chromosome.

(A)

Strain	Genotype	% of cell length ± 95% CI: Interfocal distance	% of cell length ± 95% CI: Average position	No. of cells analysed
AK181	*soj*$^{+}$ *spo0J*$^{+}$	46.1 ± 2.0	27.0 ± 1.2	105
AK183	Δ*spo0J*	41.5 ± 2.0	29.3 ± 1.3	105
AK405	Δ9*parS*$^{+90}$	38.3 ± 2.3	30.9 ± 1.5	105
AK615	Δ*spo0J* Δ9*parS*$^{+90}$	41.5 ± 1.9	31.3 ± 1.3	105
AK591	Δ9*parS*$^{+359}$	52.5 ± 2.9	24.1 ± 1.7	105
AK639	Δ*spo0J* Δ9*parS*$^{+359}$	43.1 ± 1.9	28.5 ± 1.2	105

(B)

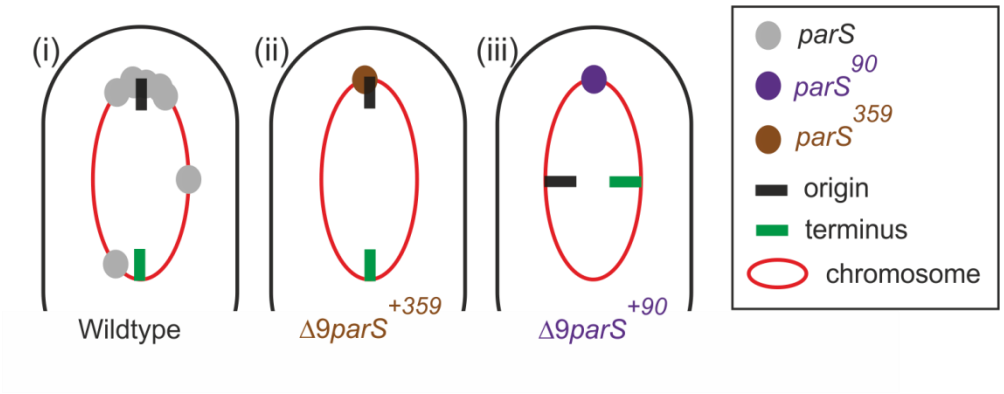

Figure 5.8.1: Origin was repositioned in the presence of ectopic *parS*

(A) The origin was repositioned when a single ectopic *parS* was introduced into the Δ10*parS* strain. The *oriC* region was labelled with an array of *tetO* operators bound by TetR-GFP. Cells were grown in 2% succinate minimal media at 37˚ until early exponential phase. Cell membranes were stained with FM-595 dye to distinguish individual cells and fluorescent TetR-GFP was visualized using epifluorescence microscopy. An approximate of 100 cells was measured for each strain. The 95% confidence intervals for the mean were calculated. *soj*$^{+}$ *spo0J*$^{+}$ (AK181), Δ*spo0J* (AK183), *soj*$^{+}$ *spo0J*$^{+}$ Δ9*parS*$^{+90}$ (AK405), Δ*spo0J* Δ9*parS*$^{+90}$ (AK615), *soj*$^{+}$ *spo0J*$^{+}$ Δ9*parS*$^{+359}$ (AK591), Δ*spo0J* Δ9*parS*$^{+359}$ (AK639). **(B)** Schematic diagram showing the position of the origin within the cell. (i) *soj*$^{+}$ *spo0J*$^{+}$ (AK181), (ii) *soj*$^{+}$ *spo0J*$^{+}$ Δ9*parS*$^{+359}$ (AK591), (iii) *soj*$^{+}$ *spo0J*$^{+}$ Δ9*parS*$^{+90}$ (AK405).

(A)

Strain	Genotype	% of cell length ± 95% CI: Interfocal distance	% of cell length ± 95% CI: Average position	No. of cells analysed
AK367	*soj*$^{+}$ *spo0J*$^{+}$	47.9 ± 1.8	26.1 ± 1.3	99
AK421	Δ*soj*	54.2 ± 2.2	24.7 ± 1.7	102
AK373	Δ9*parS*$^{+90}$	48.0 ± 2.2	26.0 ± 1.4	102
AK425	Δ*soj* Δ9*parS*$^{+90}$	35.9 ± 2.9	32.1 ± 1.9	102
AK597	Δ9*parS*$^{+270}$	45.6 ± 2.5	27.2 ± 1.6	102
AK643	Δ*soj* Δ9*parS*$^{+270}$	31.7 ± 3.5	34.1 ± 1.6	102
AK593	Δ9*parS*$^{+359}$	50.7 ± 2.6	24.6 ± 1.8	102
AK641	Δ*soj* Δ9*parS*$^{+359}$	37.6 ± 3.3	32.2 ± 1.9	102

(B)

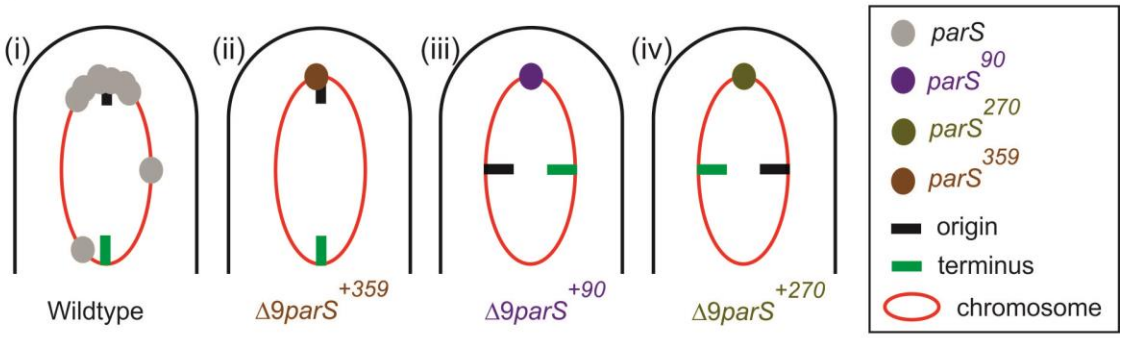

Figure 5.8.2: Spo0J-GFP foci was positioned at the cell quarter

(A) Ectopic *parS* on the chromosome was repositioned to the cell quarter. Cells were grown in 2% succinate minimal media at 37˚ until early exponential phase. Membranes were stained with FM-595 dye to distinguish cells and visualized using epifluorescence microscopy. *soj*$^{+}$ *spo0J*$^{+}$ (AK367), Δ*soj* (AK421), *soj*$^{+}$ *spo0J*$^{+}$ Δ9*parS*$^{+90}$ (AK373), Δ*soj* Δ9*parS*$^{+90}$ (AK425), *soj*$^{+}$ *spo0J*$^{+}$ Δ9*parS*$^{+270}$ (AK597), Δ*soj* Δ9*parS*$^{+270}$ (AK643), *soj*$^{+}$ *spo0J*$^{+}$ Δ9*parS*$^{+359}$ (AK593), Δ*soj* Δ9*parS*$^{+359}$ (AK641). **(B)** Schematic diagram showing the position of the overall Spo0J-GFP localization within the cell. (i) *soj*$^{+}$ *spo0J*$^{+}$ (AK367), (ii) *soj*$^{+}$ *spo0J*$^{+}$ Δ9*parS*$^{+359}$ (AK593), (iii) *soj*$^{+}$ *spo0J*$^{+}$ Δ9*parS*$^{+90}$ (AK373), (iv) *soj*$^{+}$ *spo0J*$^{+}$ Δ9*parS*$^{+270}$ (AK597).

5.9 Chapter 5 Discussion

5.9.1 Soj regulation by Spo0J requires a single *parS* site either *in cis* or *in trans*

In Chapter 3 it was shown that increasing the number of *parS* sites and redistributing Spo0J did not compromise regulation of Soj. In Chapter 4 it was shown that regulation of Soj by Spo0J was severely perturbed in the absence of all *parS* sites. Here in Chapter 5 single *parS* sites were re-introduced to the Δ10*parS* strain at different locations. Soj activity assays showed that regulation by Spo0J was restored close to wild-type levels in these strains. These results indicate that only a single Spo0J:*parS* nucleoprotein complex is required to regulate Soj.

Interestingly, when a multi-copy plasmid containing *parS* was transformed into the ∆10*parS* mutant, the strain was transformable but subsequent propagation was severely compromised. It is likely that in this scenario, without any origin proximal *parS* sites to recruit Spo0J, Spo0J (and condensin) was strongly titrated away from the chromosome leading to a severe segregation defect that inhibited cell viability (see below for more explanation).

Finally, close inspection of Soj-GFP localization in the range of ∆9*parS* mutants revealed small patches of Soj accumulating near the septum. It may be that reducing the efficiency of Spo0J to stimulate Soj ATPase activity has revealed an intermediate stage in Soj localization. This observed behaviour is reminiscent of ParA in both *C. crescentus* and *V. cholerae* where the dimeric forms of the proteins display a cloud-like localization pattern over the nucleoid to capture and pull the ParB/*parS* complex towards the cell pole (Fogel and Waldor, 2006; Ptacin et al., 2010; Schofield et al., 2010; Shebelut et al., 2010).

Thus, Soj dimers may also preferentially accumulate near the cell pole where they could influence the localization/positioning of Spo0J:*parS* complexes and/or the activity of DnaA. A similar enrichment of Soj dimers near the cell pole was observed when GFP-Soj was artificially overexpressed in a merodiploid strain with the wild-type *soj* gene at its native position and a xylose-inducible *gfp-soj* fusion elsewhere on the chromosome. (Autret and Errington, 2003).

5.9.2 Chromosome origin organization and segregation was affected by ectopic *parS*

It was shown in Chapter 4 that nucleoid morphology was not affected in the absence of *parS* sites and I speculated that the residual binding of condensin onto DNA is sufficient to maintain overall chromosome organization. To investigate whether actively recruiting Spo0J, and thus condensin, away from the origin would have any effect on organization, nucleoids were stained with DAPI and visualized in a range of Δ9*parS* mutants. Strikingly, strains Δ9*parS*$^{+90}$ and Δ9*parS*$^{+270}$ appear to form elongated cells with less condensed nucleoids. These strains also generated cells that contained spaces devoid of DNA, suggesting that cell division was also being affected, likely as an indirect consequence of the chromosome organization defect. Furthermore, these mutants also exhibited a clear defect in origin segregation. In contrast, origin segregation was largely unaffected in the Δ9*parS*$^{+359}$, consistent with the notion that origin proximal Spo0J recruiting condensin to *oriC* is necessary for proper chromosome segregation.

5.9.3 *B. subtilis* chromosome is dynamic

Vegetative growing *B. subtilis* cells have been found to adopt an *ori-ter* orientation with both chromosome arms lying side by side in a linear fashion and with their position along the chromosome corresponding with distinct distances along the cell length (Lee et al., 2003; Teleman et al., 1998; Wang et al., 2014a). Furthermore, the entire *B. subtilis soj-spo0J* locus containing *parS* is required for efficient maintenance of an unstable plasmid and remarkably these plasmids are localized to the cell quarter position (Lin and Grossman, 1998; Yamaichi and Niki, 2000). My data has revealed that Spo0J-GFP foci were recruited towards the cell quarter position regardless of the location of the inserted *parS* site, thereby suggesting that the chromosome is flexible and re-orientates when a *parS* site is positioned towards the cell pole. In addition, visualizing the origin by tagging it with the *tetO*/TetR-GFP system further revealed that this region appears to be displaced away from its normal position within the cell when an ectopic *parS* is present. These observations suggest that *B. subtilis* chromosome orientation may be defined in part by origin proximal *parS* sites, although more detailed experiments have to be performed (see Chapter 6). In support of this model, published data have shown that removing endogenous *parS* in *C. crescentus* and *V. cholerae* and replacing it with an ectopic *parS* lead to global rearrangement of the chromosome (David et al., 2014; Umbarger et al., 2011). However, it should be noted that both *C. crescentus* and *V. cholerae* ParB/*parS* complex is anchored to the cell pole, while *B. subtilis* chromosome is not anchored to the cell pole during vegetative growth.

5.10 Chapter 5 Future work

5.10.1 Combining the *spo0J*^{R206C} DNA binding-deficient mutation with the spreading-deficient mutation

Both the spreading-deficient Spo0J mutants and the Δ10*parS* mutant overinitiate DNA replication, but the degree of overinitiation was not as severe as in the complete absence of Spo0J (Figure 5.3.1 and Figure 5.4.1). It is possible that unspecific Spo0J dimers binding to DNA still retained some capacity to regulate Soj or that these mutants might still be able to form short transient Spo0J nucleoprotein complexes that were capable of regulating Soj less efficiently.

Therefore to investigate whether the DNA binding activity was causing this lower degree in overinitiation, the DNA binding-deficient mutation *spo0J*^{R206C} (Autret et al., 2001) will be combined with the spreading-deficient mutation *spo0J*^{G77S} or *spo0J*^{R149A} in the Δ9*parS* and Δ10*parS* background. I speculate that the degree of overinitiation in these mutants will be close to the Δ*spo0J* mutant because now both the DNA binding and spreading activities have been abolished.

Chapter 6: Final Discussion

6.1 The assembly of the Spo0J nucleoprotein complexes in regulating Soj

During the majority of the *B. subtilis* cell cycle, Soj has been proposed to act as an inhibitor of DnaA, being maintained in its monomeric form through efficient regulation by Spo0J nucleoprotein complexes (Murray and Errington, 2008; Scholefield et al., 2011). This is in line with the data I have presented in this thesis, namely that a single *parS* site is necessary and sufficient for the assembly of a Spo0J nucleoprotein complex capable of controlling Soj activity.

My data show that the regulation of Soj by Spo0J was perturbed by the deletion of *parS* sites*,* but the defects observed were not as severe as in a Δ*spo0J* null mutant, suggesting that Spo0J still retain some regulatory capacity. Furthermore, a single *parS*, regardless of the location, restored the ability for Spo0J to regulate Soj. And that to fully restore Soj regulation, Spo0J have to form the nucleoprotein complexes through spreading and/or bridging from the *parS* site. This is in line with the *in vitro* data that a single *parS* is sufficient for Spo0J to stimulate maximum ATPase activity of Soj (Scholefield et al., 2011). More importantly, this suggests that the lower initiation frequency observed in the Δ10*parS* mutant could be due to Spo0J binding to unspecific DNA and/or forming short transient Spo0J nucleoprotein complex that retained some capacity to regulate Soj (see future work).

Interestingly, when Spo0J was not present in the Δ10*parS* strain, the degree of overinitiation was again not as severe as in a Δ*spo0J* mutant. This similar pattern of overinitiation was observed even when a single *parS* is present in the range of the Δ*spo0J* Δ9*parS* strains. I do not know why this pattern of overinitiation was observed, but I suspect that Spo0J binding to origin

proximal *parS* and through spreading and bridging, will form the nucleoprotein complexes that may change the local conformation of the DNA. In addition, condensin recruitment to the origin and the nucleoid associated protein, Hbsu may also facilitate in changing the DNA conformation around the origin, thereby facilitating DnaA binding to DnaA-Boxes to initiate DNA replication initiation. It is also possible that these changes in DNA conformation might have affected Soj and Spo0J expression levels. Alternatively, Spo0J and /or *parS* might facilitate in recruiting or stabilising DnaA oligomerization at the origin to initiate DNA replication because ChIP-chip analysis of *B. subtilis* genome have shown that areas of Spo0J enrichment corresponds with DnaA enrichment at the origin (Ishikawa et al., 2007). And a recent paper has shown that in *C. crescentus*, DnaA bind to sites surrounding *parS* sequence (Mera et al., 2014). Other possibilities such as during the construction of the Δ8*parS* strain (Sullivan et al., 2009), site-directed mutagenesis to remove the *parS* site located within protein coding sequences could have altered the expression or activity of these proteins, or other undiscovered factors might be interacting with Spo0J and/or *parS* sites.

In the Δ*soj* and Δ(*soj-spo0J*) double mutant, the initiation frequency was restored to a level near wild-type (slight overinitiation was observed), regardless of the number and location of the *parS*, suggesting that it is Soj-dependent. This slight degree in overinitiation likely reflects the effects of other regulatory mechanisms that may serve as a backup system in the event of the loss of one regulatory system. One such system is the dual role of YabA in regulating DnaA activity by inhibiting DnaA helix formation and tethering DnaA to the replisome to titrate DnaA away from the origin (for more regulatory mechanisms during vegetative growth, look at Chapter 1.3).

Taken together, I hypothesize that formation of the Spo0J nucleoprotein complexes increases the local concentration of Spo0J through lateral spreading and bridging (Graham et al., 2014). This will increase the chances/ability of Spo0J to contact a Soj dimer and stimulate its ATPase activity. Alternatively, assembly of a Spo0J nucleoprotein complex may cause the chromosome to adopt a conformation that is optimum for Spo0J to interact with Soj. These possibilities are not mutually exclusive and could involve other (unknown) regulatory mechanisms and factors.

6.2 Spo0J nucleoprotein complexes in chromosome segregation

Condensin recruitment to the replication origin region by Spo0J is essential for proper chromosome segregation (Gruber and Errington, 2009; Sullivan et al., 2009; Wang et al., 2014b). The data that I have presented in this thesis is consistent with the idea, as redistributing Spo0J to ectopic location dramatically affected origin segregation. I hypothesize that in a normal cell, following DNA replication initiation the replicated origins are immediately organized by condensin to promote segregation. In the situation when condensin was redistributed onto the chromosome away from the origin (i.e. – *parS* sites at either 90 º or 270º) DNA replication still proceeds normally, however, instead of immediately separating the replicated origins these regions remain in close proximity until the sites of ectopic condensin enrichment are replicated. Organization and segregation will then occur around these ectopic regions, thus affecting proper chromosome conformation. Additionally, other mechanisms may also be affected by the ectopic positioning of Spo0J, such as the partitioning activity of Soj which contributes to *parS* site segregation and localization, DnaA localization to the origin may contribute to origin segregation

and the enrichment of condensin to several location on the left and right arms of the chromosome that contain highly expressed genes (Gruber and Errington, 2009; Ireton et al., 1994; Mera et al., 2014; Sharpe and Errington, 1996; Sullivan et al., 2009; Wang et al., 2014a).

Nevertheless, this leads to an interesting question as to the function of the two *parS* sites at 90˚ and 270˚ that are located away from the origin region. I propose that during vegetative growth when *B. subtilis* chromosome oscillate between the left-*ori*-right and *ori-ter* pattern (Wang et al., 2014a), Spo0J forming nucleoprotein complexes at *parS* (90˚) will bridge the left and right arms of the chromosome, maintaining it in the *ori-ter* conformation. On the other hand, a recent study using super-resolution microscopy and chromosome-capture technologies have revealed that *B. subtilis* forms two macro domains, one at the replication origin and the other at the terminus that adopts specific sub-cellular location within the cell. The formation of the terminus macro domain requires both Spo0J nucleoprotein complex and condensin at *parS* (206˚) (Submitted) (Marbouty et al., 2014). In addition, these two *parS* sites appear to have the lowest affinity for Spo0J (Breier and Grossman, 2007), therefore I suggest that at least for the interaction at 90˚, Spo0J nucleoprotein complexes may be less stable and this will allow the chromosome arms to rapidly move apart as it switches between the *ori-ter to* left-*ori*-right orientation during period of high growth rates.

6.3 Soj may coordinate the initiation of DNA replication and chromosome segregation

Soj and Spo0J belong to the family of the type I plasmid partition system. Segregation of plasmids by this system is thought to occur when ParA/SopA forms either a filament or a cloud-like structure over the nucleoid that pushes or pulls the plasmid towards the cell pole, respectively (Ebersbach and Gerdes, 2001, 2004; Erzberger et al., 2006; Hatano et al., 2007; Lim et al., 2005; Ringgaard et al., 2009). *B. subtilis* Soj does not form a filament (Scholefield et al., 2012). However, my data has revealed that GFP-Soj can accumulate near the septum when only a single *parS* site is present in the genome. I hypothesize that this localization pattern may represent dimeric Soj interacting with the nucleoid, consistent with enrichment of GFP-Soj near the cell pole when the protein is artificially overexpressed in a *soj* merodiploid strain (Autret and Errington, 2003).

I thereby propose a model for *B. subtilis* origin segregation based mainly on the previously described DNA relay mechanism (Lim et al., 2014). In this model, dimeric Soj binds to the nucleoid (Murray and Errington, 2008; Scholefield et al., 2011), creating a Soj gradient extending over the nucleoid (Figure 6.3.1i-ii). Following DNA replication initiation , Spo0J forms nucleoprotein complexes through lateral spreading and DNA bridging with origin proximal *parS* sites located at mid-cell and the chromosome adopting a *left*-ori-*right* pattern (Breier and Grossman, 2009; Graham et al., 2014; Lin and Grossman, 1998; Livny et al., 2007; Murray et al., 2006; Wang et al., 2014a).

To generate movement for the origin, origin proximal Spo0J:*parS* complexes will progressively associate and disassociate with the nucleoid bound Soj dimers (Vecchiarelli et al., 2013). This interaction between Spo0J

and Soj will stimulate the ATPase activity of Soj, causing it to disassociate from the nucleoid as a monomer and inhibiting DnaA activity to repress DNA replication initiation during chromosome segregation (Figure 6.3.1iii) (Scholefield et al., 2011). The dissociated Soj monomer will then accumulate at the septum in a MinD-dependent manner (Figure 6.3.1iv) (Autret and Errington, 2003; Murray and Errington, 2008). As the origins separate, the chromosome will reorientate itself to adopt the *ori-ter* pattern (Lee et al., 2003; Wang et al., 2014a).

Through either a passive or an active process, monomeric Soj proteins will bind ATP to regenerate the dimeric form of the protein. Because Soj monomers are enriched at the cell pole, I propose that the resulting increase in the local concentration of Soj proteins will promote dimerization in this region of the cell. Accumulation of Soj dimers could then act to transiently overwhelm the ability of the origin proximal Spo0J nucleoprotein complexes to stimulate nucleotide exchange (Figure 6.3.1v). Note it was recently shown that DNA replication initiates when the origin is located at the edge of the nucleoid and proximal to the cell pole (Wang et al., 2014a). Thus, the proposed increase in Soj dimers near the cell pole could act to spatially regulate DNA replication initiation. Following DNA replication initiation (Figure 6.3.1vi) the duplicated origins are moved in tandem to mid cell by condensin (Figure 6.3.1vii), and this repositioning will allow regeneration of the gradient of Soj dimers on the nucleoid (Figure 6.3.1i-ii). The replicated origins will again be segregated through repartition of the process (Figure 6.3.1i-vii).

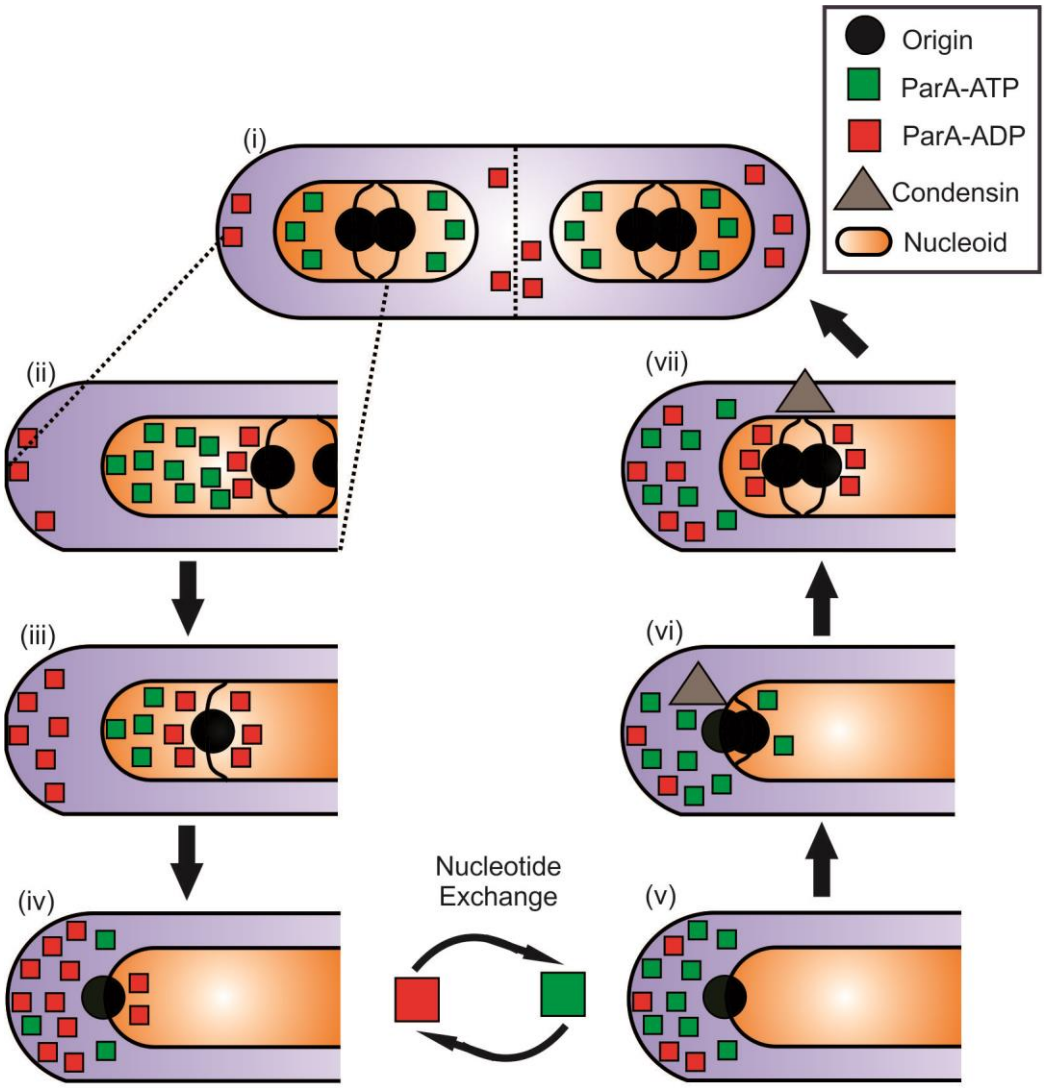

Figure 6.3.1: Soj model in initiation of DNA replication and chromosome segregation

Cartoon representation of the model describing Soj coordinating DNA replication initiation and chromosome segregation. (i-ii) Soj dimer forms a gradient over the nucleoid. (iii) Origin-proximal Spo0J:*parS* complexes stimulate Soj ATPase activity to generate movement while monomeric Soj inhibits DnaA activity during chromosome segregation. (iv) The origin translocates to the edge of the nucleoid with monomeric Soj accumulating at the septum. (v) Soj nucleotide exchange leads to increase in Soj dimer at the cell pole. (vi) DNA replication initiate at the cell quarter. (viii) The origins are translocated to the mid cell by condensin.

Chapter 7: Future work

7.1 The relationship between initiation of DNA replication and chromosome segregation by Spo0J, Soj, and condensin

Spo0J:*parS* complexes interact with Soj and condensin at the origin (Breier and Grossman, 2007; Graham et al., 2014; Gruber and Errington, 2009; Lin and Grossman, 1998; Livny et al., 2007; Murray et al., 2006; Sullivan et al., 2009). However, it remains unclear whether condensin recruitment by Spo0J might influence Soj regulation or vice-versa. To investigate this, mutants should be identified that block specific interaction of various complexes. Some examples of these are available (Figure 7.1.1), such as the *spo0J*^{L5H} allele that cannot interact with Soj but does recruit condensin, while the converse is true for the *spo0J*^{N112S} and *spo0J*^{R149G} alleles. The *dnaA*^{L294R}, *dnaA*^{V323D} and *dnaA*^{A341V} alleles that do not interact with Soj but allow Spo0J to both recruit condensin and regulate Soj, the *soj*^{D66A} allele that abolish Soj interaction with Spo0J but allows interaction with DnaA, and the *soj*^{K201A} allele that do not localize to the septum but still interacts with Spo0J and DnaA (Bartosik et al., 2014; Gruber and Errington, 2009; Scholefield et al., 2012). Both forward and reverse genetic approaches could be used to identify more mutants.

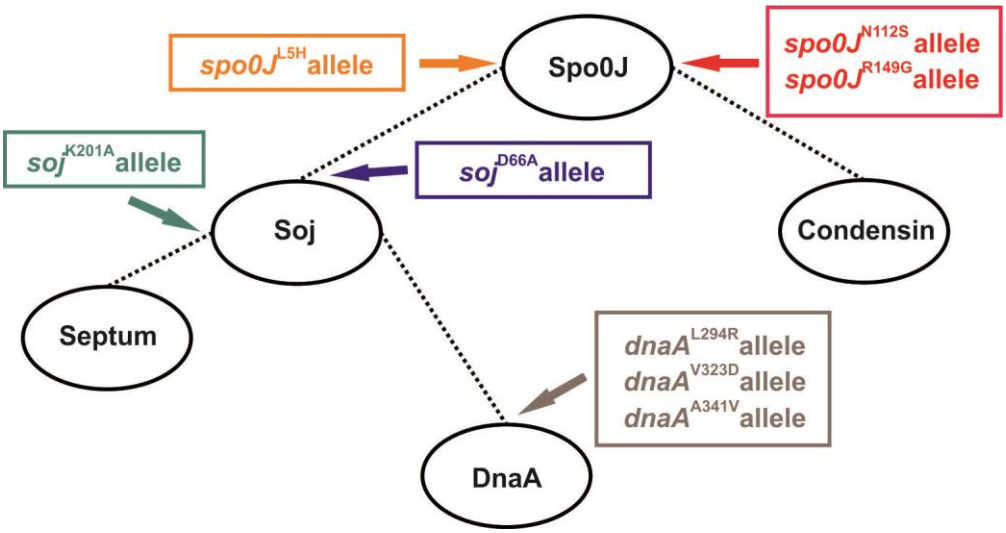

Figure 7.1.1: Flow chart showing Spo0J, Soj, condensin and DnaA interaction

Schematic diagram showing the various known alleles that affect interaction between complexes.

7.2 The role of Soj and Spo0J in chromosome segregation and organization

In *C. crescentus* and *V. cholerae*, segregation of the newly replicated chromosome requires the dimeric form of ParA to form a gradient over the nucleoid to capture and pull the ParB/*parS* complex towards the cell pole (Fogel and Waldor, 2006; Ptacin et al., 2010). Although in *B. subtilis*, Soj neither forms a filament nor the ParA gradient (Scholefield et al., 2012), however my data show that in the presence of a single *parS* site, GFP-Soj was observed to accumulate as small patches adjacent to septa and this was suspected to represent GFP-Soj binding to DNA located proximal to a cell pole (Figure 5.2.1).

To test this idea of GFP-Soj binding to the nucleoid, the Δ9*parS* strains will be stained either with the non-specific DNA fluorescent dye, DAPI or with HU-RFP to confirm whether the small patches do indeed accumulate over the nucleoid mass. Furthermore, to more directly test whether DNA binding property is required, localization studies using the DNA binding mutant GFP-Soj^{R189A} in the context of the Δ9*parS* strains will be performed.

In addition, because the small patches appears to be reminiscent of the ParA cloud-like structure in *C. crescentus* and *V. cholerae*, it will be interesting to investigate whether a similar mechanism exist in *B. subtilis.* Time-lapse microscopy using either Spo0J-YFP or visualizing the origin with the TetR-YFP/*tetO* reporter system in the context of CFP-Soj patches in the 9*parS*$^{+359}$ mutant will be performed. I speculate that if the mechanism is similar to the plasmid type I system, then both the TetR-YFP and Spo0J-YFP focus should be at the edge of the receding Soj-CFP patch as it translocate across the nucleoid.

Likewise, to further understand Soj and Spo0J in driving chromosome segregation, a similar reconstituted cell free system used by Vecchiarelli and

colleagues to study F and P1 plasmid movement *in vitro*, using total internal reflection fluorescent microscopy (TIRFM) will be performed (Vecchiarelli et al., 2013; Vecchiarelli et al., 2014).

Finally my data also suggests that *parS* in *B. subtilis* may play a part in chromosome positioning. To more accurately investigate this, colocalization experiments will be utilized to visualize multiple regions of the chromosome in single cells using the strains described in this thesis. TetR-YFP/*tetO* and LacI-CFP/*lacO* arrays could be integrated into various regions of the chromosome, and additionally DNA could be visualized using HU-RFP.

7.3 The involvement of condensin in origin segregation

The chromosome of the Δ8*parS* mutant when grown in rich media appeared to be less condensed with an increased frequency of anucleate cells formation, suggesting a defect in chromosome segregation (Sullivan et al., 2009). However my data showed that chromosome organization and segregation in the Δ8*parS* and Δ10*parS* mutant appeared to be largely normal when grown in minimal media (Figure 4.4.1 and Figure 4.5.1), consistent with published data that lowering the replication fork velocity bypass the defect in origin segregation in the absence of condensin (Gruber et al., 2014).

To reconcile these differences, the Δ10*parS* mutant will be grown in rich media and both the origin counting assay and DAPI staining will be employed to clarify the involvement of condensin. Relating to this, when the multi-copy $parS^+$ plasmid was transformed into the Δ10*parS* background, the transformants were severely compromised (Chapter 5.5). I speculate this might be due to the inappropriate recruitment of condensin to the $parS^+$ plasmid, therefore to investigate this, tranformants will be maintained in minimal media plates instead of LB plates (rich media).

References

Abe, Y., Jo, T., Matsuda, Y., Matsunaga, C., Katayama, T., and Ueda, T. (2007). Structure and function of DnaA N-terminal domains - Specific sites and mechanisms in inter-DnaA interaction and in DnaB helicase loading on oriC. J Biol Chem *282*, 17816-17827.

Ah-Seng, Y., Lopez, F., Pasta, F., Lane, D., and Bouet, J.Y. (2009). Dual Role of DNA in Regulating ATP Hydrolysis by the SopA Partition Protein. J Biol Chem *284*, 30067-30075.

Ali, B.M.J., Amit, R., Braslavsky, I., Oppenheim, A.B., Gileadi, O., and Stavans, J. (2001). Compaction of single DNA molecules induced by binding of integration host factor (IHF). P Natl Acad Sci USA *98*, 10658-10663.

Autret, S., and Errington, J. (2003). A role for division-site-selection protein MinD in regulation of internucleoid jumping of Soj (ParA) protein in Bacillus subtilis. Molecular microbiology *47*, 159-169.

Autret, S., Nair, R., and Errington, J. (2001). Genetic analysis of the chromosome segregation protein Spo0J of Bacillus subtilis: evidence for separate domains involved in DNA binding and interactions with Soj protein. Molecular microbiology *41*, 743-755.

Aylett, C.H.S., and Lowe, J. (2012). Superstructure of the centromeric complex of TubZRC plasmid partitioning systems. P Natl Acad Sci USA *109*, 16522-16527.

Aylett, C.H.S., Wang, Q., Michie, K.A., Amos, L.A., and Lowe, J. (2010). Filament structure of bacterial tubulin homologue TubZ. P Natl Acad Sci USA *107*, 19766-19771.

Badrinarayanan, A., Lesterlin, C., Reyes-Lamothe, R., and Sherratt, D. (2012). The Escherichia coli SMC complex, MukBEF, shapes nucleoid organization independently of DNA replication. Journal of bacteriology *194*, 4669-4676.

Barilla, D., Carmelo, E., and Hayes, F. (2007). The tail of the ParG DNA segregation protein remodels ParF polymers and enhances ATP hydrolysis via an arginine finger-like motif. P Natl Acad Sci USA *104*, 1811-1816.

Barilla, D., and Hayes, F. (2003). Architecture of the ParF center dot ParG protein complex involved in prokaryotic DNA segregation. Molecular microbiology *49*, 487-499.

Barilla, D., Rosenberg, M.F., Nobbmann, U., and Hayes, F. (2005). Bacterial DNA segregation dynamics mediated by the polymerizing protein ParF. Embo J *24*, 1453-1464.

Bartosik, A.A., Glabski, K., Jecz, P., Lasocki, K., Mikosa, M., Plochocka, D., Thomas, C.M., and Jagura-Burdzy, G.T. (2014). Dissection of the region of Pseudomonas aeruginosa ParA that is important for dimerization and interactions with its partner ParB. Microbiology, 2406-2420.

Bath, J., Wu, L.J., Errington, J., and Wang, J.C. (2000). Role of Bacillus subtilis SpoIIIE in DNA transport across the mother cell-prespore division septum. Science *290*, 995-997.

Ben-Yehuda, S., Fujita, M., Liu, X.S., Gorbatyuk, B., Skoko, D., Yan, J., Marko, J.F., Liu, J.S., Eichenberger, P., Rudner, D.Z., *et al.* (2005). Defining a centromere-like element in Bacillus subtilis by Identifying the binding sites for the chromosome-anchoring protein RacA. Mol Cell *17*, 773-782.

Ben-Yehuda, S., Rudner, D.Z., and Losick, R. (2003). RacA, a bacterial protein that anchors chromosomes to the cell poles. Science *299*, 532-536.

Bongers, R.S., Veening, J.W., Van Wieringen, M., Kuipers, O.P., and Kleerebezem, M. (2005). Development and characterization of a subtilin-regulated expression system in

Bacillus subtilis: Strict control of gene expression by addition of subtilin. Applied and environmental microbiology *71*, 8818-8824.
Bonilla, C.Y., and Grossman, A.D. (2012). The primosomal protein DnaD inhibits cooperative DNA binding by the replication initiator DnaA in Bacillus subtilis. Journal of bacteriology *194*, 5110-5117.
Boonstra, M., de Jong, I.G., Scholefield, G., Murray, H., Kuipers, O.P., and Veening, J.W. (2013). Spo0A regulates chromosome copy number during sporulation by directly binding to the origin of replication in Bacillus subtilis. Molecular microbiology *87*, 925-938.
Bowman, G.R., Comolli, L.R., Zhu, J., Eckart, M., Koenig, M., Downing, K.H., Moerner, W.E., Earnest, T., and Shapiro, L. (2008). A polymeric protein anchors the chromosomal origin/ParB complex at a bacterial cell pole. Cell *134*, 945-955.
Bramhill, D., and Kornberg, A. (1988a). Duplex Opening by Dnaa Protein at Novel Sequences in Initiation of Replication at the Origin of the Escherichia-Coli Chromosome. Cell *52*, 743-755.
Bramhill, D., and Kornberg, A. (1988b). A Model for Initiation at Origins of DNA-Replication. Cell *54*, 915-918.
Braun, R.E., O'Day, K., and Wright, A. (1985). Autoregulation of the DNA replication gene dnaA in E. coli K-12. Cell *40*, 159-169.
Breier, A.M., and Grossman, A.D. (2007). Whole-genome analysis of the chromosome partitioning and sporulation protein Spo0J (ParB) reveals spreading and origin-distal sites on the Bacillus subtilis chromosome. Molecular microbiology *64*, 703-718.
Breier, A.M., and Grossman, A.D. (2009). Dynamic Association of the Replication Initiator and Transcription Factor DnaA with the Bacillus subtilis Chromosome during Replication Stress. Journal of bacteriology *191*, 486-493.
Britton, R.A., Lin, D.C., and Grossman, A.D. (1998). Characterization of a prokaryotic SMC protein involved in chromosome partitioning. Genes & development *12*, 1254-1259.
Broedersz, C.P., Wang, X.D., Meir, Y., Loparo, J.J., Rudner, D.Z., and Wingreen, N.S. (2014). Condensation and localization of the partitioning protein ParB on the bacterial chromosome. P Natl Acad Sci USA *111*, 8809-8814.
Burbulys, D., Trach, K.A., and Hoch, J.A. (1991). Initiation of Sporulation in Bacillus-Subtilis Is Controlled by a Multicomponent Phosphorelay. Cell *64*, 545-552.
Burkholder, W.F., Kurtser, I., and Grossman, A.D. (2001). Replication initiation proteins regulate a developmental checkpoint in Bacillus subtilis. Cell *104*, 269-279.
Campbell, C.S., and Mullins, R.D. (2007). In vivo visualization of type II plasmid segregation: bacterial actin filaments pushing plasmids. The Journal of cell biology *179*, 1059-1066.
Castilla-Llorente, V., Munoz-Espin, D., Villar, L., Salas, M., and Meijer, W.J.J. (2006). Spo0A, the key transcriptional regulator for entrance into sporulation, is an inhibitor of DNA replication. Embo J *25*, 3890-3899.
Chen, Y.D., and Erickson, H.P. (2008). In vitro assembly studies of FtsZ/Tubulin-like proteins (TubZ) from Bacillus plasmids - Evidence for a capping mechanism. J Biol Chem *283*, 8102-8109.
Cho, E., Ogasawara, N., and Ishikawa, S. (2008). The functional analysis of YabA, which interacts with DnaA and regulates initiation of chromosome replication in Bacillus subtils. Genes Genet Syst *83*, 111-125.
Claessen, D., Emmins, R., Hamoen, L.W., Daniel, R.A., Errington, J., and Edwards, D.H. (2008). Control of the cell elongation-division cycle by shuttling of PBP1 protein in Bacillus subtilis. Molecular microbiology *68*, 1029-1046.

Collier, J., and Shapiro, L. (2009). Feedback Control of DnaA-Mediated Replication Initiation by Replisome-Associated HdaA Protein in Caulobacter. Journal of bacteriology *191*, 5706-5716.
Crisona, N.J., Strick, T.R., Bensimon, D., Croquette, V., and Cozzarelli, N.R. (2000). Preferential relaxation of positively supercoiled DNA by E-coli topoisomerase IV in single-molecule and ensemble measurements. Genes & development *14*, 2881-2892.
Cunningham, K.A., and Burkholder, W.F. (2009). The histidine kinase inhibitor Sda binds near the site of autophosphorylation and may sterically hinder autophosphorylation and phosphotransfer to Spo0F. Molecular microbiology *71*, 659-677.
Dame, R.T., Wyman, C., and Goosen, N. (2000). H-NS mediated compaction of DNA visualised by atomic force microscopy. Nucleic Acids Res *28*, 3504-3510.
Danilova, O., Reyes-Lamothe, R., Pinskaya, M., Sherratt, D., and Possoz, C. (2007). MukB colocalizes with the oriC region and is required for organization of the two Escherichia coli chromosome arms into separate cell halves. Molecular microbiology *65*, 1485-1492.
David, A., Demarre, G., Muresan, L., Paly, E., Barre, F.X., and Possoz, C. (2014). The two Cis-acting sites, parS1 and oriC1, contribute to the longitudinal organisation of Vibrio cholerae chromosome I. Plos Genet *10*, e1004448.
Duderstadt, K.E., Chuang, K., and Berger, J.M. (2011). DNA stretching by bacterial initiators promotes replication origin opening. Nature *478*, 209-U291.
Ebersbach, G., Briegel, A., Jensen, G.J., and Jacobs-Wagner, C. (2008). A self-associating protein critical for chromosome attachment, division, and polar organization in caulobacter. Cell *134*, 956-968.
Ebersbach, G., and Gerdes, K. (2001). The double par locus of virulence factor pB171: DNA segregation is correlated with oscillation of ParA. Proc Natl Acad Sci U S A *98*, 15078-15083.
Ebersbach, G., and Gerdes, K. (2004). Bacterial mitosis: partitioning protein ParA oscillates in spiral-shaped structures and positions plasmids at mid-cell. Molecular microbiology *52*, 385-398.
Erzberger, J.P., Mott, M.L., and Berger, J.M. (2006). Structural basis for ATP-dependent DnaA assembly and replication-origin remodeling. Nat Struct Mol Biol *13*, 676-683.
Erzberger, J.P., Pirruccello, M.M., and Berger, J.M. (2002). The structure of bacterial DnaA: implications for general mechanisms underlying DNA replication initiation. Embo J *21*, 4763-4773.
Felczak, M.M., and Kaguni, J.M. (2004). The box VII motif of Escherichia coli DnaA protein is required for DnaA oligomerization at the E. coli replication origin. J Biol Chem *279*, 51156-51162.
Fiebig, A., Keren, K., and Theriot, J.A. (2006). Fine-scale time-lapse analysis of the biphasic, dynamic behaviour of the two Vibrio cholerae chromosomes. Molecular microbiology *60*, 1164-1178.
Fogel, M.A., and Waldor, M.K. (2005). Distinct segregation dynamics of the two Vibrio cholerae chromosomes. Molecular microbiology *55*, 125-136.
Fogel, M.A., and Waldor, M.K. (2006). A dynamic, mitotic-like mechanism for bacterial chromosome segregation. Genes & development *20*, 3269-3282.
Fujikawa, N., Kurumizaka, H., Nureki, O., Terada, T., Shirouzu, M., Katayama, T., and Yokoyama, S. (2003). Structural basis of replication origin recognition by the DnaA protein. Nucleic Acids Res *31*, 2077-2086.

Fujimitsu, K., Senriuchi, T., and Katayama, T. (2009). Specific genomic sequences of E. coli promote replicational initiation by directly reactivating ADP-DnaA. Genes & development *23*, 1221-1233.
Fujita, M., Gonzalez-Pastor, J.E., and Losick, R. (2005). High- and low-threshold genes in the Spo0A regulon of Bacillus subtilis. Journal of bacteriology *187*, 1357-1368.
Garner, E.C., Campbell, C.S., and Mullins, R.D. (2004). Dynamic instability in a DNA-segregating prokaryotic actin homolog. Science *306*, 1021-1025.
Garner, E.C., Campbell, C.S., Weibel, D.B., and Mullins, R.D. (2007). Reconstitution of DNA segregation driven by assembly of a prokaryotic actin homolog. Science *315*, 1270-1274.
Garner, J., and Crooke, E. (1996). Membrane regulation of the chromosomal replication activity of E-coli DnaA requires a discrete site on the protein. Embo J *15*, 2313-2321.
Gatlin, J.C., and Bloom, K. (2010). Microtubule motors in eukaryotic spindle assembly and maintenance. Seminars in cell & developmental biology *21*, 248-254.
Gayathri, P., Fujii, T., Moller-Jensen, J., van den Ent, F., Namba, K., and Lowe, J. (2012). A bipolar spindle of antiparallel ParM filaments drives bacterial plasmid segregation. Science *338*, 1334-1337.
Gerdes, K., Larsen, J.E., and Molin, S. (1985). Stable inheritance of plasmid R1 requires two different loci. Journal of bacteriology *161*, 292-298.
Glaser, P., Sharpe, M.E., Raether, B., Perego, M., Ohlsen, K., and Errington, J. (1997). Dynamic, mitotic-like behavior of a bacterial protein required for accurate chromosome partitioning. Genes & development *11*, 1160-1168.
Gorbatyuk, B., and Marczynski, G.T. (2001). Physiological consequences of blocked Caulobacter crescentus dnaA expression, an essential DNA replication gene. Molecular microbiology *40*, 485-497.
Gorbatyuk, B., and Marczynski, G.T. (2005). Regulated degradation of chromosome replication proteins DnaA and CtrA in Caulobacter crescentus. Molecular microbiology *55*, 1233-1245.
Graham, T.G., Wang, X., Song, D., Etson, C.M., van Oijen, A.M., Rudner, D.Z., and Loparo, J.J. (2014). ParB spreading requires DNA bridging. Genes & development.
Gruber, S., and Errington, J. (2009). Recruitment of Condensin to Replication Origin Regions by ParB/SpoOJ Promotes Chromosome Segregation in B. subtilis. Cell *137*, 685-696.
Gruber, S., Veening, J.W., Bach, J., Blettinger, M., Bramkamp, M., and Errington, J. (2014). Interlinked sister chromosomes arise in the absence of condensin during fast replication in B. subtilis. Curr Biol *24*, 293-298.
Hatano, T., Yamaichi, Y., and Niki, H. (2007). Oscillating focus of SopA associated with filamentous structure guides partitioning of F plasmid. Molecular microbiology *64*, 1198-1213.
Hayes, F. (2000). The partition system of multidrug resistance plasmid TP228 includes a novel protein that epitomizes an evolutionarily distinct subgroup of the ParA superfamily. Molecular microbiology *37*, 528-541.
Higgins, D., and Dworkin, J. (2012). Recent progress in Bacillus subtilis sporulation. FEMS microbiology reviews *36*, 131-148.
Higgins, N.P., Peebles, C.L., Sugino, A., and Cozzarelli, N.R. (1978). Purification of Subunits of Escherichia-Coli DNA Gyrase and Reconstitution of Enzymatic-Activity. P Natl Acad Sci USA *75*, 1773-1777.
Hoch, J.A., and Mathews, J.L. (1973). Chromosomal Location of Pleiotropic Negative Sporulation Mutations in Bacillus-Subtilis. Genetics *73*, 215-228.

Hranueli, D., Piggot, P.J., and Mandelstam, J. (1974). Statistical estimate of the total number of operons specific for Bacillus subtilis sporulation. Journal of bacteriology *119*, 684-690.
Ireton, K., Gunther, N.W.t., and Grossman, A.D. (1994). spo0J is required for normal chromosome segregation as well as the initiation of sporulation in Bacillus subtilis. Journal of bacteriology *176*, 5320-5329.
Ishigo-Oka, D., Ogasawara, N., and Moriya, S. (2001). DnaD protein of Bacillus subtilis interacts with DnaA, the initiator protein of replication. Journal of bacteriology *183*, 2148-2150.
Ishikawa, S., Ogura, Y., Yoshimura, M., Okumura, H., Cho, E., Kawai, Y., Kurokawa, K., Oshima, T., and Ogasawara, N. (2007). Distribution of stable DnaA-binding sites on the Bacillus subtilis genome detected using a modified ChIP-chip method. DNA research : an international journal for rapid publication of reports on genes and genomes *14*, 155-168.
Itaya, M. (1992). Construction of a Novel Tetracycline Resistance Gene Cassette Useful as a Marker on the Bacillus-Subtilis Chromosome. Biosci Biotech Bioch *56*, 685-686.
Iyer, L.M., Leipe, D.D., Koonin, E.V., and Aravind, L. (2004). Evolutionary history and higher order classification of AAA+ ATPases. Journal of structural biology *146*, 11-31.
Jacob, F., Brenne, S., and Cuzin, F. (1963). On the regulation of DNA replication in bacteria. Cold Spring Harbor Symposia on Quantitative Biology *28*, 329-348.
Jameson, K.H., Rostami, N., Fogg, M.J., Turkenburg, J.P., Grahl, A., Murray, H., and Wilkinson, A.J. (2014). Structure and interactions of the Bacillus subtilis sporulation inhibitor of DNA replication, SirA, with domain I of DnaA. Molecular microbiology.
Jensen, R.B., and Shapiro, L. (1999). The Caulobacter crescentus smc gene is required for cell cycle progression and chromosome segregation. Proc Natl Acad Sci U S A *96*, 10661-10666.
Jensen, R.B., and Shapiro, L. (2003). Cell-cycle-regulated expression and subcellular localization of the Caulobacter crescentus SMC chromosome structural protein. Journal of bacteriology *185*, 3068-3075.
Jonas, K., Liu, J., Chien, P., and Laub, M.T. (2013). Proteotoxic Stress Induces a Cell-Cycle Arrest by Stimulating Lon to Degrade the Replication Initiator DnaA. Cell *154*, 623-636.
Kalliomaa-Sanford, A.K., Rodriguez-Castaneda, F.A., McLeod, B.N., Latorre-Rosello, V., Smith, J.H., Reimann, J., Albers, S.V., and Barilla, D. (2012). Chromosome segregation in Archaea mediated by a hybrid DNA partition machine. P Natl Acad Sci USA *109*, 3754-3759.
Kato, J., and Katayama, T. (2001). Hda, a novel DnaA-related protein, regulates the replication cycle in Escherichia coli. Embo J *20*, 4253-4262.
Kawakami, H., Keyamura, K., and Katayama, T. (2005). Formation of an ATP-DnaA-specific initiation complex requires DnaA arginine 285, a conserved motif in the AAA plus protein family. J Biol Chem *280*, 27420-27430.
Kawakami, H., Ozaki, S., Suzuki, S., Nakamura, K., Senriuchi, T., Su'etsugu, M., Fujimitsu, K., and Katayama, T. (2006). The exceptionally tight affinity of DnaA for ATP/ADP requires a unique aspartic acid residue in the AAA+ sensor 1 motif. Molecular microbiology *62*, 1310-1324.
Kitagawa, R., Ozaki, T., Moriya, S., and Ogawa, T. (1998). Negative control of replication initiation by a novel chromosomal locus exhibiting exceptional affinity for Escherichia coli DnaA protein. Genes & development *12*, 3032-3043.
Kunst, F., Ogasawara, N., Moszer, I., Albertini, A.M., Alloni, G., Azevedo, V., Bertero, M.G., Bessieres, P., Bolotin, A., Borchert, S., *et al.* (1997). The complete genome sequence of the Gram-positive bacterium Bacillus subtilis. Nature *390*, 249-256.

Kurokawa, K., Mizumura, H., Takaki, T., Ishii, Y., Ichihashi, N., Lee, B.L., and Sekimizu, K. (2009). Rapid Exchange of Bound ADP on the Staphylococcus aureus Replication Initiation Protein DnaA. J Biol Chem *284*, 34201-34210.
Larsen, R.A., Cusumano, C., Fujioka, A., Lim-Fong, G., Patterson, P., and Pogliano, J. (2007). Treadmilling of a prokaryotic tubulin-like protein, TubZ, required for plasmid stability in Bacillus thuringiensis. Genes & development *21*, 1340-1352.
Lau, I.F., Filipe, S.R., Soballe, B., Okstad, O.A., Barre, F.X., and Sherratt, D.J. (2003). Spatial and temporal organization of replicating Escherichia coli chromosomes. Molecular microbiology *49*, 731-743.
Laub, M.T., Chen, S.L., Shapiro, L., and McAdams, H.H. (2002). Genes directly controlled by CtrA, a master regulator of the Caulobacter cell cycle. P Natl Acad Sci USA *99*, 4632-4637.
Le, T.B., Imakaev, M.V., Mirny, L.A., and Laub, M.T. (2013). High-resolution mapping of the spatial organization of a bacterial chromosome. Science *342*, 731-734.
Leaver, M., Dominguez-Cuevas, P., Coxhead, J.M., Daniel, R.A., and Errington, J. (2009). Life without a wall or division machine in Bacillus subtilis. Nature *457*, 849-853.
LeDeaux, J.R., Yu, N., and Grossman, A.D. (1995). Different roles for KinA, KinB, and KinC in the initiation of sporulation in Bacillus subtilis. Journal of bacteriology *177*, 861-863.
Lee, P.S., and Grossman, A.D. (2006). The chromosome partitioning proteins Soj (ParA) and Spo0J (ParB) contribute to accurate chromosome partitioning, separation of replicated sister origins, and regulation of replication initiation in Bacillus subtilis. Molecular microbiology *60*, 853-869.
Lee, P.S., Lin, D.C.H., Moriya, S., and Grossman, A.D. (2003). Effects of the chromosome partitioning protein Spo0J (ParB) on oriC positioning and replication initiation in Bacillus subtilis. Journal of bacteriology *185*, 1326-1337.
Lenarcic, R., Halbedel, S., Visser, L., Shaw, M., Wu, L.J., Errington, J., Marenduzzo, D., and Hamoen, L.W. (2009). Localisation of DivIVA by targeting to negatively curved membranes. Embo J *28*, 2272-2282.
Leonard, T.A., Butler, P.J., and Lowe, J. (2004). Structural analysis of the chromosome segregation protein Spo0J from Thermus thermophilus. Molecular microbiology *53*, 419-432.
Leonard, T.A., Butler, P.J., and Lowe, J. (2005). Bacterial chromosome segregation: structure and DNA binding of the Soj dimer--a conserved biological switch. Embo J *24*, 270-282.
Lesley, J.A., and Shapiro, L. (2008). SpoT regulates DnaA stability and initiation of DNA replication in carbon-starved Caulobacter crescentus. Journal of bacteriology *190*, 6867-6880.
Li, Y., Stewart, N.K., Berger, A.J., Vos, S., Schoeffler, A.J., Berger, J.M., Chait, B.T., and Oakley, M.G. (2010). Escherichia coli condensin MukB stimulates topoisomerase IV activity by a direct physical interaction. Proc Natl Acad Sci U S A *107*, 18832-18837.
Lim, G.E., Derman, A.I., and Pogliano, J. (2005). Bacterial DNA segregation by dynamic SopA polymers. Proc Natl Acad Sci U S A *102*, 17658-17663.
Lim, H.C., Surovtsev, I.V., Beltran, B.G., Huang, F., Bewersdorf, J., and Jacobs-Wagner, C. (2014). Evidence for a DNA-relay mechanism in ParABS-mediated chromosome segregation. eLife *3*, e02758.
Lin, D.C.H., and Grossman, A.D. (1998). Identification and characterization of a bacterial chromosome partitioning site. Cell *92*, 675-685.

Lin, D.C.H., Levin, P.A., and Grossman, A.D. (1997). Bipolar localization of a chromosome partition protein in Bacillus subtilis. P Natl Acad Sci USA *94*, 4721-4726.
Livny, J., Yamaichi, Y., and Waldor, M.K. (2007). Distribution of centromere-like parS sites in bacteria: insights from comparative genomics. Journal of bacteriology *189*, 8693-8703.
Lu, M., Campbell, J.L., Boye, E., and Kleckner, N. (1994). SeqA: a negative modulator of replication initiation in E. coli. Cell *77*, 413-426.
Marbouty, M., Le Gall, A., Cattoni, D.I., Koh, A., Caournac, A., Fiche, J.B., Mozziconacci, J., Murray, H., Koszul, R., and Nollmann, M. (2014). 3D Folding Mechanisms and Function of Higher-order Chromatin Domains. Submitted.
Marston, A.L., and Errington, J. (1999). Dynamic movement of the ParA-like soj protein of B-subtilis and its dual role in nucleoid organization and developmental regulation. Mol Cell *4*, 673-682.
McGarry, K.C., Ryan, V.T., Grimwade, J.E., and Leonard, A.C. (2004). Two discriminatory binding sites in the Escherichia coli replication origin are required for DNA strand opening by initiator DnaA-ATP. P Natl Acad Sci USA *101*, 2811-2816.
McGrath, P.T., Iniesta, A.A., Ryan, K.R., Shapiro, L., and McAdams, H.H. (2006). A dynamically localized protease complex and a polar specificity factor control a cell cycle master regulator. Cell *124*, 535-547.
Mera, P.E., Kalogeraki, V.S., and Shapiro, L. (2014). Replication initiator DnaA binds at the Caulobacter centromere and enables chromosome segregation. Proc Natl Acad Sci U S A *111*, 16100–16105.
Merrikh, H., and Grossman, A.D. (2011). Control of the replication initiator DnaA by an anti-cooperativity factor. Molecular microbiology *82*, 434-446.
Messer, W. (2002). The bacterial replication initiator DnaA. DnaA and oriC, the bacterial mode to initiate DNA replication. FEMS microbiology reviews *26*, 355-374.
Micka, B., and Marahiel, M.A. (1992). The DNA-Binding Protein Hbsu Is Essential for Normal Growth and Development in Bacillus-Subtilis. Biochimie *74*, 641-650.
Miller, D.T., Grimwade, J.E., Betteridge, T., Rozgaja, T., Torgue, J.J., and Leonard, A.C. (2009). Bacterial origin recognition complexes direct assembly of higher-order DnaA oligomeric structures. Proc Natl Acad Sci U S A *106*, 18479-18484.
Mohl, D.A., and Gober, J.W. (1997). Cell cycle-dependent polar localization of chromosome partitioning proteins in Caulobacter crescentus. Cell *88*, 675-684.
Moller-Jensen, J., Borch, J., Dam, M., Jensen, R.B., Roepstorff, P., and Gerdes, K. (2003). Bacterial mitosis: ParM of plasmid R1 moves plasmid DNA by an actin-like insertional polymerization mechanism. Mol Cell *12*, 1477-1487.
Moller-Jensen, J., Jensen, R.B., Lowe, J., and Gerdes, K. (2002). Prokaryotic DNA segregation by an actin-like filament. Embo J *21*, 3119-3127.
Molt, K.L., Sutera, V.A., Moore, K.K., and Lovett, S.T. (2009). A Role for Nonessential Domain II of Initiator Protein, DnaA, in Replication Control. Genetics *183*, 39-49.
Montabana, E.A., and Agard, D.A. (2014). Bacterial tubulin TubZ-Bt transitions between a two-stranded intermediate and a four-stranded filament upon GTP hydrolysis. P Natl Acad Sci USA *111*, 3407-3412.
Mott, M.L., and Berger, J.M. (2007). DNA replication initiation: mechanisms and regulation in bacteria. Nat Rev *5*, 343-354.
Murray, H., and Errington, J. (2008). Dynamic Control of the DNA Replication Initiation Protein DnaA by Soj/ParA. Cell *135*, 74-84.
Murray, H., Ferreira, H., and Errington, J. (2006). The bacterial chromosome segregation protein Spo0J spreads along DNA from parS nucleation sites. Molecular microbiology *61*, 1352-1361.

Ni, L.S., Xu, W.J., Kumaraswami, M., and Schumacher, M.A. (2010). Plasmid protein TubR uses a distinct mode of HTH-DNA binding and recruits the prokaryotic tubulin homolog TubZ to effect DNA partition. P Natl Acad Sci USA *107*, 11763-11768.
Nicolas, E., Upton, A.L., Uphoff, S., Henry, O., Badrinarayanan, A., and Sherratt, D. (2014). The SMC complex MukBEF recruits topoisomerase IV to the origin of replication region in live Escherichia coli. Mbio *5*, e01001-01013.
Nievera, C., Torgue, J.J.C., Grimwade, J.E., and Leonard, A.C. (2006). SeqA blocking of DnaA-oriC interactions ensures staged assembly of the E-coli Pre-RC. Mol Cell *24*, 581-592.
Niki, H., Jaffe, A., Imamura, R., Ogura, T., and Hiraga, S. (1991). The new gene mukB codes for a 177 kd protein with coiled-coil domains involved in chromosome partitioning of E. coli. Embo J *10*, 183-193.
Nishida, S., Fujimitsu, K., Sekimizu, K., Ohmura, T., Ueda, T., and Katayama, T. (2002). A nucleotide switch in the Escherichia coli DnaA protein initiates chromosomal replication - EVidence from a mutant DnaA protein defective in regulatory ATP hydrolysis in vitro and in vivo. J Biol Chem *277*, 14986-14995.
Noirot-Gros, M.F., Dervyn, E., Wu, L.J., Mervelet, P., Errington, J., Ehrlich, S.D., and Noirot, P. (2002). An expanded view of bacterial DNA replication. Proc Natl Acad Sci U S A *99*, 8342-8347.
Noirot-Gros, M.F., Velten, M., Yoshimura, M., McGovern, S., Morimoto, T., Ehrlich, S.D., Ogasawara, N., Polard, P., and Noirot, P. (2006). Functional dissection of YabA, a negative regulator of DNA replication initiation in Bacillus subtilis. P Natl Acad Sci USA *103*, 2368-2373.
Nolivos, S., and Sherratt, D. (2014). The bacterial chromosome: architecture and action of bacterial SMC and SMC-like complexes. FEMS microbiology reviews *38*, 380-392.
Nozaki, S., Yamada, Y., and Ogawa, T. (2009). Initiator titration complex formed at datA with the aid of IHF regulates replication timing in Escherichia coli. Genes Cells *14*, 329-341.
Ogura, Y., Imai, Y., Ogasawara, N., and Moriya, S. (2001). Autoregulation of the dnaA-dnaN operon and effects of DnaA protein levels on replication initiation in Bacillus subtilis. Journal of bacteriology *183*, 3833-3841.
Ogura, Y., Ogasawara, N., Harry, E.J., and Moriya, S. (2003). Increasing the ratio of Soj to Spo0J promotes replication initiation in Bacillus subtilis. Journal of bacteriology *185*, 6316-6324.
Okumura, H., Yoshimura, M., Ueki, M., Oshima, T., Ogasawara, N., and Ishikawa, S. (2012). Regulation of chromosomal replication initiation by oriC-proximal DnaA-box clusters in Bacillus subtilis. Nucleic Acids Res *40*, 220-234.
Ptacin, J.L., Gahlmann, A., Bowman, G.R., Perez, A.M., von Diezmann, A.R.S., Eckart, M.R., Moerner, W.E., and Shapiro, L. (2014). Bacterial scaffold directs pole-specific centromere segregation. P Natl Acad Sci USA *111*, E2046-E2055.
Ptacin, J.L., Lee, S.F., Garner, E.C., Toro, E., Eckart, M., Comolli, L.R., Moerner, W.E., and Shapiro, L. (2010). A spindle-like apparatus guides bacterial chromosome segregation. Nature cell biology *12*, 791-798.
Quisel, J.D., Lin, D.C.H., and Grossman, A.D. (1999). Control of development by altered localization of a transcription factor in B-subtilis. Mol Cell *4*, 665-672.
Quon, K.C., Yang, B., Domian, I.J., Shapiro, L., and Marczynski, G.T. (1998). Negative control of bacterial DNA replication by a cell cycle regulatory protein that binds at the chromosome origin. P Natl Acad Sci USA *95*, 120-125.
Rahn-Lee, L., Gorbatyuk, B., Skovgaard, O., and Losick, R. (2009). The Conserved Sporulation Protein YneE Inhibits DNA Replication in Bacillus subtilis. Journal of bacteriology *191*, 3736-3739.

Rahn-Lee, L., Merrikh, H., Grossman, A.D., and Losick, R. (2011). The sporulation protein SirA inhibits the binding of DnaA to the origin of replication by contacting a patch of clustered amino acids. Journal of bacteriology *193*, 1302-1307.
Real, G., Autret, S., Harry, E.J., Errington, J., and Henriques, A.O. (2005). Cell division protein DivIB influences the Spo0J/Soj system of chromosome segregation in Bacillus subtilis. Molecular microbiology *55*, 349-367.
Ringgaard, S., van Zon, J., Howard, M., and Gerdes, K. (2009). Movement and equipositioning of plasmids by ParA filament disassembly. Proc Natl Acad Sci U S A *106*, 19369-19374.
Rokop, M.E., Auchtung, J.M., and Grossman, A.D. (2004). Control of DNA replication initiation by recruitment of an essential initiation protein to the membrane of Bacillus subtilis. Molecular microbiology *52*, 1757-1767.
Rozgaja, T.A., Grimwade, J.E., Iqbal, M., Czerwonka, C., Vora, M., and Leonard, A.C. (2011). Two oppositely oriented arrays of low-affinity recognition sites in oriC guide progressive binding of DnaA during Escherichia coli pre-RC assembly. Mol Microbiol *82*, 475-488.
Schofield, W.B., Lim, H.C., and Jacobs-Wagner, C. (2010). Cell cycle coordination and regulation of bacterial chromosome segregation dynamics by polarly localized proteins. Embo J *29*, 3068-3081.
Scholefield, G., Errington, J., and Murray, H. (2012). Soj/ParA stalls DNA replication by inhibiting helix formation of the initiator protein DnaA. Embo J *31*, 1542-1555.
Scholefield, G., and Murray, H. (2013). YabA and DnaD inhibit helix assembly of the DNA replication initiation protein DnaA. Molecular microbiology *90*, 147-159.
Scholefield, G., Whiting, R., Errington, J., and Murray, H. (2011). Spo0J regulates the oligomeric state of Soj to trigger its switch from an activator to an inhibitor of DNA replication initiation. Molecular microbiology *79*, 1089-1100.
Schwartz, M.A., and Shapiro, L. (2011). An SMC ATPase mutant disrupts chromosome segregation in Caulobacter. Molecular microbiology *82*, 1359-1374.
Seitz, H., Weigel, C., and Messer, W. (2000). The interaction domains of the DnaA and DnaB replication proteins of Escherichia coli. Molecular microbiology *37*, 1270-1279.
Sharpe, M.E., and Errington, J. (1996). The Bacillus subtilis soj-spo0J locus is required for a centromere-like function involved in prespore chromosome partitioning. Molecular microbiology *21*, 501-509.
Shebelut, C.W., Guberman, J.M., van Teeffelen, S., Yakhnina, A.A., and Gitai, Z. (2010). Caulobacter chromosome segregation is an ordered multistep process. P Natl Acad Sci USA *107*, 14194-14198.
Simmons, L.A., Felczak, M., and Kaguni, J.M. (2003). DnaA protein of Escherichia coli: oligomerization at the E-coli chromosomal origin is required for initiation and involves specific N-terminal amino acids. Molecular microbiology *49*, 849-858.
Skoko, D., Yoo, D., Bai, H., Schnurr, B., Yan, J., McLeod, S.M., Marko, J.F., and Johnson, R.C. (2006). Mechanism of chromosome compaction and looping by the Escherichia coli nucleoid protein Fis. J Mol Biol *364*, 777-798.
Smits, W.K., Goranov, A.I., and Grossman, A.D. (2010). Ordered association of helicase loader proteins with the Bacillus subtilis origin of replication in vivo. Molecular microbiology *75*, 452-461.
Smits, W.K., Merrikh, H., Bonilla, C.Y., and Grossman, A.D. (2011). Primosomal proteins DnaD and DnaB are recruited to chromosomal regions bound by DnaA in Bacillus subtilis. Journal of bacteriology *193*, 640-648.
Soppa, J. (2001). Prokaryotic structural maintenance of chromosomes (SMC) proteins: distribution, phylogeny, and comparison with MukBs and additional prokaryotic and eukaryotic coiled-coil proteins. Gene *278*, 253-264.

Soufo, C.D., Soufo, H.J., Noirot-Gros, M.F., Steindorf, A., Noirot, P., and Graumann, P.L. (2008). Cell-cycle-dependent spatial sequestration of the DnaA replication initiator protein in Bacillus subtilis. Dev Cell *15*, 935-941.
Steinmetz, M., and Richter, R. (1994). Plasmids Designed to Alter the Antibiotic-Resistance Expressed by Insertion Mutations in Bacillus-Subtilis, through in-Vivo Recombination. Gene *142*, 79-83.
Su'etsugu, M., and Errington, J. (2011). The Replicase Sliding Clamp Dynamically Accumulates behind Progressing Replication Forks in Bacillus subtilis Cells. Mol Cell *41*, 720-732.
Su'etsugu, M., Shimuta, T.R., Ishida, T., Kawakami, H., and Katayama, T. (2005). Protein associations in DnaA-ATP hydrolysis mediated by the Hda-replicase clamp complex. J Biol Chem *280*, 6528-6536.
Sullivan, N.L., Marquis, K.A., and Rudner, D.Z. (2009). Recruitment of SMC by ParB-parS Organizes the Origin Region and Promotes Efficient Chromosome Segregation. Cell *137*, 697-707.
Tadesse, S., Mascarenhas, J., Kosters, B., Hasilik, A., and Graumann, P.L. (2005). Genetic interaction of the SMC complex with topoisomerase IV in Bacillus subtilis. Microbiology *151*, 3729-3737.
Tanaka, T., and Koshikawa, T. (1977). Isolation and characterization of four types of plasmids from Bacillus subtilis (natto). Journal of bacteriology *131*, 699-701.
Tang, M., Bideshi, D.K., Park, H.W., and Federici, B.A. (2006). Minireplicon from pBtoxis of Bacillus thuringiensis subsp. israelensis. Applied and environmental microbiology *72*, 6948-6954.
Teleman, A.A., Graumann, P.L., Lin, D.C.H., Grossman, A.D., and Losick, R. (1998). Chromosome arrangement within a bacterium. Curr Biol *8*, 1102-1109.
Toro, E., Hong, S.H., McAdams, H.H., and Shapiro, L. (2008). Caulobacter requires a dedicated mechanism to initiate chromosome segregation. Proc Natl Acad Sci U S A *105*, 15435-15440.
Toro, E., and Shapiro, L. (2010). Bacterial Chromosome Organization and Segregation. Csh Perspect Biol *2*.
Umbarger, M.A., Toro, E., Wright, M.A., Porreca, G.J., Bau, D., Hong, S.H., Fero, M.J., Zhu, L.J., Marti-Renom, M.A., McAdams, H.H., *et al.* (2011). The three-dimensional architecture of a bacterial genome and its alteration by genetic perturbation. Mol Cell *44*, 252-264.
Vecchiarelli, A.G., Hwang, L.C., and Mizuuchi, K. (2013). Cell-free study of F plasmid partition provides evidence for cargo transport by a diffusion-ratchet mechanism. Proc Natl Acad Sci U S A *110*, E1390-1397.
Vecchiarelli, A.G., Neuman, K.C., and Mizuuchi, K. (2014). A propagating ATPase gradient drives transport of surface-confined cellular cargo. Proc Natl Acad Sci U S A *111*, 4880-4885.
Veening, J.W., Murray, H., and Errington, J. (2009). A mechanism for cell cycle regulation of sporulation initiation in Bacillus subtilis. Genes & development *23*, 1959-1970.
Velten, M., McGovern, S., Marsin, S., Ehrlich, S.D., Noirot, P., and Polard, P. (2003). A two-protein strategy for the functional loading of a cellular replicative DNA helicase. Mol Cell *11*, 1009-1020.
Viollier, P.H., Thanbichler, M., McGrath, P.T., West, L., Meewan, M., McAdams, H.H., and Shapiro, L. (2004). Rapid and sequential movement of individual chromosomal loci to specific subcellular locations during bacterial DNA replication. Proc Natl Acad Sci U S A *101*, 9257-9262.

Wagner, J.K., Marquis, K.A., and Rudner, D.Z. (2009). SirA enforces diploidy by inhibiting the replication initiator DnaA during spore formation in Bacillus subtilis. Molecular microbiology *73*, 963-974.
Waldminghaus, T., and Skarstad, K. (2009). The Escherichia coli SeqA protein. Plasmid *61*, 141-150.
Wang, S.C., and Shapiro, L. (2004). The topoisornerase IV ParC subunit colocalizes with the Caulobacter replisome and is required for polar localization of replication origins. P Natl Acad Sci USA *101*, 9251-9256.
Wang, X., Montero Llopis, P., and Rudner, D.Z. (2014a). Bacillus subtilis chromosome organization oscillates between two distinct patterns. Proc Natl Acad Sci U S A.
Wang, X., Tang, O.W., Riley, E.P., and Rudner, D.Z. (2014b). The SMC condensin complex is required for origin segregation in Bacillus subtilis. Curr Biol *24*, 287-292.
Wang, X.D., Llopis, P.M., and Rudner, D.Z. (2013). Organization and segregation of bacterial chromosomes. Nat Rev Genet *14*, 191-203.
Wu, L.J., and Errington, J. (1994). Bacillus subtilis SpoIIIE protein required for DNA segregation during asymmetric cell division. Science *264*, 572-575.
Wu, L.J., and Errington, J. (1997). Septal localization of the SpoIIIE chromosome partitioning protein in Bacillus subtilis. Embo J *16*, 2161-2169.
Wu, L.J., and Errington, J. (2002). A large dispersed chromosomal region required for chromosome segregation in sporulating cells of Bacillus subtilis. Embo J *21*, 4001-4011.
Wu, L.J., and Errington, J. (2003). RacA and the Soj-Spo0J system combine to effect polar chromosome segregation in sporulating Bacillus subtilis. Molecular microbiology *49*, 1463-1475.
Yamaichi, Y., Bruckner, R., Ringgaard, S., Moll, A., Cameron, D.E., Briegel, A., Jensen, G.J., Davis, B.M., and Waldor, M.K. (2012). A multidomain hub anchors the chromosome segregation and chemotactic machinery to the bacterial pole. Genes & development *26*, 2348-2360.
Yamaichi, Y., Fogel, M.A., McLeod, S.M., Hui, M.P., and Waldor, M.K. (2007a). Distinct centromere-like parS sites on the two chromosomes of Vibrio spp. Journal of bacteriology *189*, 5314-5324.
Yamaichi, Y., Fogel, M.A., and Waldor, M.K. (2007b). par genes and the pathology of chromosome loss in Vibrio cholerae. Proc Natl Acad Sci U S A *104*, 630-635.
Yamaichi, Y., and Niki, H. (2000). Active segregation by the Bacillus subtilis partitioning system in Escherichia coli. P Natl Acad Sci USA *97*, 14656-14661.
Youngman, P.J., Perkins, J.B., and Losick, R. (1983). Genetic Transposition and Insertional Mutagenesis in Bacillus-Subtilis with Streptococcus-Faecalis Transposon Tn917. P Natl Acad Sci-Biol *80*, 2305-2309.
Zhang, W., Machon, C., Orta, A., Phillips, N., Roberts, C.J., Allen, S., and Soultanas, P. (2008). Single-molecule atomic force spectroscopy reveals that DnaD forms scaffolds and enhances duplex melting. J Mol Biol *377*, 706-714.

Appendices

Poster 1: SGM autumn conference 2012

Poster 2: Conference on Gram positive microorganisms 2013

Publication 1: Murray, H., and Koh, A. (2014). Multiple regulatory systems coordinate DNA replication with cell growth in Bacillus subtilis. Plos Genet *10*.

The role of *Bacillus subtilis* Soj/ParA in chromosome origin separation

Alan Koh and Heath Murray
Centre for Bacterial Cell Biology, Institute for Cell & Molecular Biosciences
Newcastle University, Newcastle Upon Tyne, United Kingdom
E-mail: s.c.a.koh@newcastle.ac.uk

Centre For Bacterial Cell Biology

Newcastle University

1

Proper replication and segregation of chromosomes is important for all cells. The model organsim *Bacillus subtilis* contains a single circular chromosome containing a sole replication origin (*oriC*). As the cell cycle progresses, initiation of DNA replication will occur at *oriC* and proceed bi-directionally until the entire genome is duplicated. Concomitant with this process the replicated chromosomes will be segregated and finally the cell division machinery will localise at mid cell to form a new cell pole leading to the formational of two identical daughter cells.

Soj (ParA) is a dynamic Walker-type ATPase that can either inhibit or activate the initiation of DNA replication through DnaA (the DNA replication initiator protein), depending on its nucleotide bound state (Murray and Errington, 2008; Scholefield *et al.*, 2011, 2012). Soj is regulated by Spo0J (ParB) (Ireton *et al*, 1994; Murray and Errington, 2008), a DNA binding protein that bind to *parS* sites and forms a nucleoprotein along the DNA (Murray *et al* 2006; Breier and Grossman, 2007). In *B. subtilis* eight of the ten *parS* sites are located near the origin of replication (Lin and Grossman, 1998). Besides being involved in DNA replication initiation, Spo0J also interacts with the SMC complex and recruits it to replicated sister origins to facilitate chromosome segregation (Gruber & Errington, 2009; Sullivan *et al* 2009). Soj has also been implicated in the separation of replicated sister chromosome origins (Lee and Grossman, 2006).

We are interested in the properties of Soj that are involved in the separation of replicated sister origins, and we are investigating this question by using a single-cell origin separation assay to study the effects of mutations that alter Soj activity.

2 The activity cycle of Soj

Genetic and structural analyses have yielded Soj variants with different amino-acid substitutions that inhibit specific properties of the protein (Leonard *et al*. 2005; Hester and Lutkenhaus, 2007; Scholefield and Murray, 2011). The Soj^{K16A} (Fig. 1A) substitution inhibits ATP binding, while the Soj^{G12V} (Fig. 1B) substitution allows ATP binding but is defective in dimerization due to a steric clash in the dimer interface. The Soj^{R189A} (Fig. 1C) and Soj^{D40A} (Fig. 1D) substitutions allow ATP dependent dimerization, but inhibit DNA binding activity of the former and inhibit ATP hydrolysis in the latter. Related to Soj^{D40A}, the Spo0J^{L5H} mutant (Fig. 1E) is unable to interacts with the Soj dimer and therefore cannot stimulate the ATP hydrolysis activity of Soj.

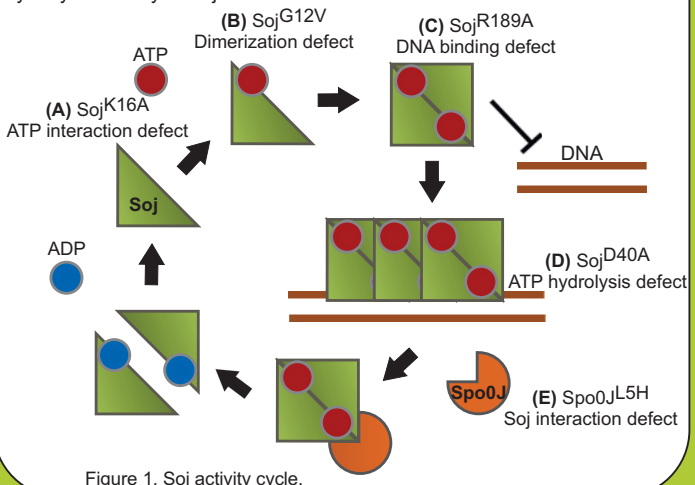

Figure 1. Soj activity cycle.

3 The Origin separation assay

In order to determine whether replicated sister origins have separated, we visualised *oriC* and an origin distal region simultaneously using two markers as first described in (Lee and Grossman, 2006). The *tetO* array was inserted at 359˚ near the replication origin and was visualized using TetR-YFP, while the *lacO* array was inserted at 345˚ (~150 kb downstream of the *tetO* array on the same chromosome arm) and was visualized using LacI-CFP. This reporter strain was then grown in slow growth media to avoid overlapping rounds of DNA replication and observed using epifluorescence microscopy.

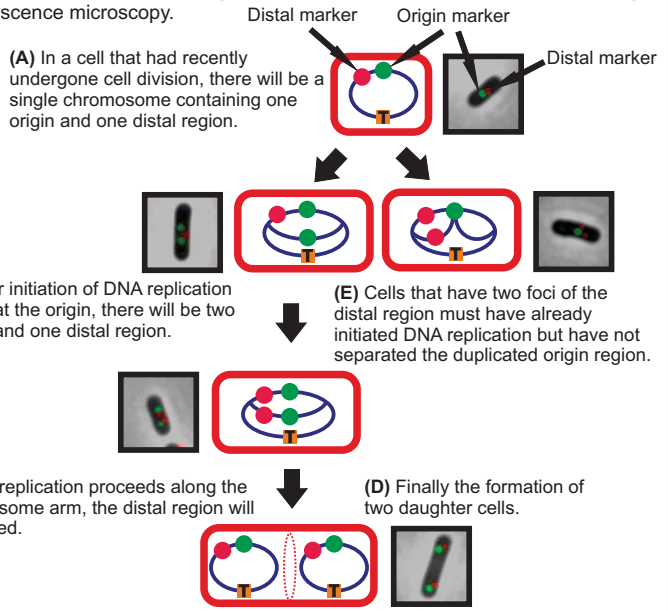

Figure 2. The origin separation assay showing two classes of cells.Strains were grown at 30˚C in minimal medium and samples were taken for microscopy during exponential growth. Green circle denotes origin marker, red circle denotes distal marker and orange box denotes terminus. (A) Cell just undergo cell division (B) Cell initiate DNA replication (C) Replication proceed (D) Formation of two identical daughter cells (E) Separation of sister origin defect.

4 The results

We have found that 1.9% of cells in the wild-type strain had fewer foci of the origin region than the distal region. Of all the Soj variants tested, the dimeric *soj*^{D40A} mutant, which activates DNA replication initiation, showed the greatest defect in origin separation. Consistent with this observation a *spo0J*^{L5H} mutant, which cannot stimulate the ATPase activity of the Soj dimer, was also defective in origin separation. To determine whether overinitiation of DNA replication could affect sister origin separation a Δ*yabA* mutant was tested, and again a defect in origin separation was observed.

Initiation Frequency a

Genotype	Separation defect (%)	Separation defect (normalized)
soj^{G12V}	2.3%	1.2
soj^{R189A}	2.7%	1.4
Wild-type	1.9%	1.0
soj^{K16A}	3.2%	1.7
Δ*soj*	3.0%	1.6
soj^{D40A}	6.7%	3.5
Δ*yabA*	6.1%	3.2
spo0J^{L5H}	11.4%	6.0

Table 1. Relative numbers of foci of an origin (359˚) and distal (345˚) region of the chromosome.
(a) Initiation frequency by marker frequency analysis. Previously published results (Murray and Errington, 2008; Scholefield and Murray, 2011) and unpublished results (Koh and Murray).

5 Conclusion and Future work

Our comprehensive analysis of mutant Soj proteins shows that the greatest defect in chromosome origin separation is caused by the dimeric Soj^{D40A} protein which activates DNA replication initiation. A mutant Spo0J protein that cannot stimulate Soj ATPase activity showed a similar defect, as did a *yabA* mutant, both of which cause an increase in the rate of DNA replication initiation. Taken together, these results suggest that overinitiation of DNA replication leads to a defect in sister origin separation. We speculate that this phenotype could be due to insufficient chromosome segregation machinery present in the cell to cope with the increase in replicated origins, or it could be due to uncoupling of coordinated DNA replication and segregation activities. These hypotheses are currently being investigated.

6 References

1. Murray, H., and Errington, J. (2008) Dynamic control of the DNA replication initiation protein DnaA by Soj/ParA. Cell. 135, 74-84.
2. Scholefield, G., Whiting, R., Errington, J., and Murray, H. (2011) SpoOJ regulates the oligomeric state of Soj to trigger its switch from an activator to an inhibitor of DNA replication initiation. Mol Microbiol. 79, 1089-1100.
3. Scholefield, G., Errington, J., and Murray, H. (2012) Soj/ParA stalls DNA replication by inhibiting helix formation of the initiator protein DnaA. EMBO. 31, 1542-1555.
4. Ireton, K., Iv, N.W.G., and Grossman, A.D. (1994) Spo0J is required for normal chromosome segregation as well as the initiation of sporulation in *Bacillus subtilis*. J. Bacteriol. 176, 5320-5329.
5. Murray, H., Ferreira, H., and Errington, J. (2006) The bacterial chromosome segregation protein Spo0J spreads along DNA from *parS* nucleation sites. Mol Microbiol. 61, 1352-1361
6. Breier, A.M., and Grossman, A.D. (2007) Whole-genome analysis of the chromosome partitioning and sporulation protein Spo0J (ParB) reveals spreading and origin-distal sites on *Bacillus subtilis* chromosome. Mol Microbiol. 64, 703-718.
7. Lin, D.Chi-Hong., and Grossman, A.D. (1998) Identification and characterization of a bacterial chromosome partitioning site. Cell. 92, 675-685.
8. Gruber, S., and Errington, J. (2009) Recruitment of condensin to replication origin regions by ParB/SpoOJ promotes chromosome segregation in *B. subtilis*. Cell. 137, 685-696.
9. Sullivan, N.L., Marquis, K.A., and Rudner, D.Z. (2009) Recruitment of SMC to the origin by ParB-parS organises the origin and promotes efficient chromosome segregation. Cell. 137, 697-707.
10. Lee, P.S., and Grossman, A.D. (2006) The chromosome partitioning proteins Soj (ParA) and Spo0J (ParB) contribute to accurate chromosome partitioning, separation of replicated sister origins, and regulation of replication initiation in *Bacillus subtilis*. Mol Microbiol. 60, 853-869.
11. Leonard, T.A., Butler, P.J., and Löwe, J. (2005) Bacterial chromosome segregation: Structure and DNA binding of the Soj dimer - a conserved biological switch. EMBO. 24, 270-282.
12. Hester, C.M., and Lutkenhaus, J. (2007) Soj (ParA) DNA binding is mediated by conserved arginines and is essential for plasmid segregation. PNAS. 104, 20326-20331.

A single chromosomal *parS* site is necessary and sufficient for Spo0J to regulate Soj in *Bacillus subtilis*

Alan Koh and Heath Murray
Centre for Bacterial Cell Biology, Institute for Cell & Molecular Biosciences
Newcastle University, Newcastle Upon Tyne, United Kingdom
E-mail: s.c.a.koh@newcastle.ac.uk

Centre For Bacterial Cell Biology

Newcastle University

1

The viability of an organism is reliant on proper transmission of the genetic material from parent to progeny and therefore requires coordination of DNA replication with chromosome segregation. The model organism *Bacillus subtilis* contains a single circular chromosome with a defined replication origin (*oriC*). As the cell cycle progresses, DNA replication initiates at *oriC* and proceeds bidirectionally until the entire genome is duplicated. Concomitant with this process the replicated chromosome is actively segregated. Finally, the cell divisionary machinery will localise at midcell to form the new cell pole, leading to the formation of two identical daughter cells.

The ParABS system was first identified for its role ensuring faithful inheritance of low copy-number plasmids (Gerdes *et al.*, 2000), and it is now appreciated that the majority of bacterial species harbour orthologues of the *par* genes in their chromosome(s) (Livny *et al.*, 2007). Par systems are composed of three components: the DNA binding site *parS*, the *parS* binding protein ParB (Spo0J), and the ATPase ParA (Soj) that interacts with the ParB:*parS* nucleoprotein complexes (Gerdes *et al.*, 2000; Murray *et al.*, 2006; Breier *et al.*, 2007). In *B. subtilis* eight of the ten *parS* sites are located near the origin of replication (Lin *et al.*, 1998; Breier *et al.*, 2007). There are at least two independent functions performed by Spo0J. First it is involved in chromosome origin segregation by binding to *parS* sites to recruit condensin (SMC-ScpAB) to the origin region (Stephan *et al.*, 2009; Sullivan *et al.*, 2009). Second, it is involved in regulating DNA replication initiation via Soj (Murray *et al.*, 2008).

Soj is a dynamic protein that, depending upon its oligomeric state, will either inhibit or activate DNA replication initiation by directly regulating the master initiation protein DnaA (Murray *et al.*, 2008; Scholefield *et al.*, 2011, 2012). It has been shown that Spo0J regulates Soj by directly stimulating its ATPase activity, thereby promoting dissociation of the ATP-dependent Soj dimer (Scholefield *et al.*, 2011). However, it has not been determined whether the localization of Spo0J near the replication origin is required to regulate Soj.

Utilizing several approaches we have investigated whether the regulation of Soj by Spo0J is dependent on the number or/and locality of *parS* sites in *B. subtilis*.

2

Construction of the *parS* mutants

The Δ8*parS* strain was previously constructed by Sullivan *et al.* (2009), where eight of the origin-proximal *parS* sites were removed by allelic replacement. The Δ10*parS* strain was constructed by integrating an antibiotic cassette into the *parS* sites at 90° and 206°. The Δ9*parS* was constructed by integrating a plasmid harbouring either the native *soj-spo0J* or a Δ*spo0J* mutant by double crossover into the Δ10*parS* strain.

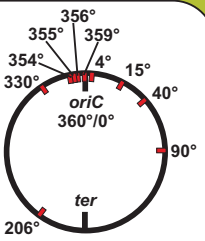

Figure 1: Schematic diagram of the ten identified Spo0J binding sites (*parS*) in the *B. subtilis* chromosome.

3

Spo0J and *parS* are required for the localization of Soj

In a wild-type stain that does not overinitiate DNA replication, GFP-Soj is observed to form foci in the cytoplasm and localize to the septa (Figure 2A). This localization pattern is dependent on Spo0J, and in a Δ*spo0J* mutant GFP-Soj relocalizes to the nucleoid (Figure 2B). To test whether *parS* is required for Spo0J to regulate Soj, a strain was constructed with all ten *parS* sites deleted. In this mutant strain GFP-Soj was relocalized to the nucleoid, while also remaining present at septa (Figure 2E). As expected, in the absence of Spo0J GFP-Soj localizes exclusively with the nucleoid (Figure 2F). In contrast, when a single origin-proximal *parS* site was reintroduced into the chromosome, the localization pattern of GFP-Soj was indistinguishable from the wild-type strain (Figures 2C, 2D). These results suggest that Spo0J requires at least one *parS* site to properly regulate the localization of GFP-Soj.

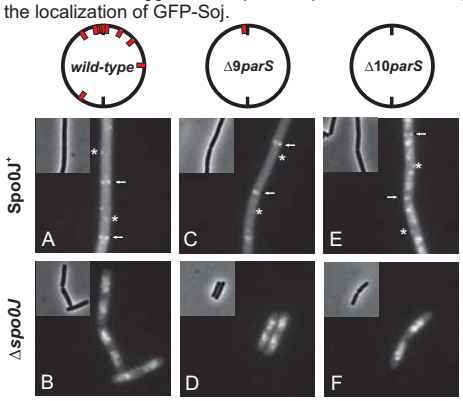

Figure 2: Localization of wild-type GFP-Soj in the various *parS* mutants, both in the presence and absence of Spo0J. The localization of GFP-Soj was observed using epifluorescence microscopy. Cells were grown in minimal medium at 37° to exponential phase. An asterick (*) denotes localization as a focus and an arrow (→) indicates localization at a septum. (A) Wild-type, (B) Δ*spo0J,* (C) Δ9*parS,* (D)Δ9*parS* Δ*spo0J,* (E) Δ10*parS*, (F) Δ10*parS* Δ*spo0J.*

4

A *parS* site is required for Spo0J to control Soj's activity regulating DNA replication initiation

Soj is a key regulator of DNA replication by acting directly on the master initiator protein, DnaA. Marker frequency analysis (MFA) was used to determine the ability of Spo0J to regulate Soj in the absence of *parS* sites. Quantitative PCR was used to measure the DNA sites near the origin and terminus of replication. In the absence of the regulator Spo0J, there is an increase in the rate of DNA replication initiation in the wild-type strain. The Δ10*parS* mutant displayed an appreciable increase in *ori/ter* ratio, indicating an increase in the rate of DNA replication initiation. When a single *parS* was reintroduced, the *ori/ter* ratio was reduced to the wild-type level. Interestingly, when a high-copy number plasmid containing a single *parS* was introduced into the Δ10*parS* mutant, the initiation rate remained elevated. Taken together, these results suggest that Spo0J requires one *parS* site on the chromosome for Spo0J to properly regulate Soj.

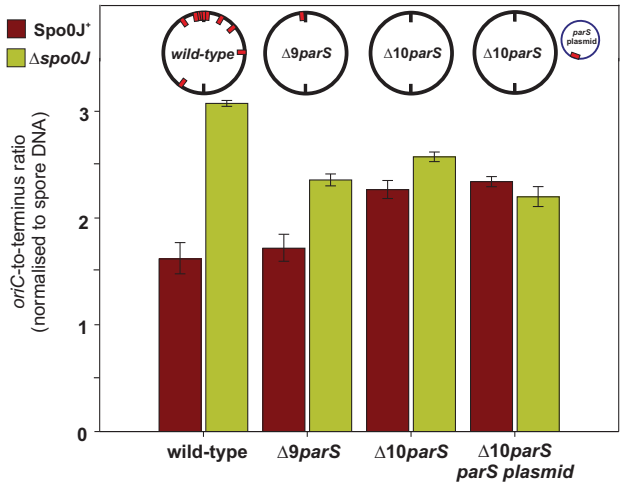

Figure 3: The *oriC*-to-terminus ratio of various *parS* mutants in the presence or absence of Spo0J. Cells were grown at 37°C in minimal medium to exponential phase. Values were normalized to the spore DNA, and the results are shown as the average ± standard deviation (n=3).

5

A *parS* site is required for Spo0J to control Soj's activity regulating sporulation

In the absence of Spo0J, Soj accumulate as a dimer and stimulates DnaA activity, which in turn activates the sporulation checkpoint protein Sda to transiently inhibit sporulation. In the Δ10*parS* mutant a decrease in sporulation frequency was observed as compared to the wild-type strain. In contrast, when a single *parS* was reintroduced into the chromosome the sporulation frequency was restored.

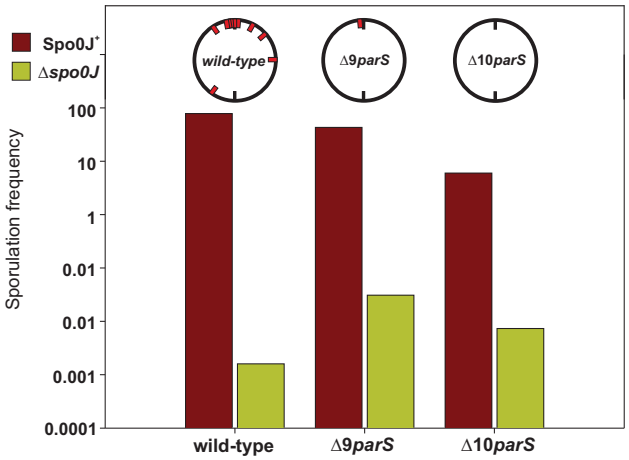

Figure 4: The sporulation frequency of various *parS* mutants in the presence or absence of Spo0J. Cells were growth in Schaeffer's medium at 37°C until late exponential growth, before diluting down into fresh medium and allowed to grow for a further 48hrs. The sporulation frequencies were determined by calculating the ratio of heat-resistance colony-forming units (80°C for 25 mins) to the total colony-forming units.

6

Conclusion

We have shown that in *B. subtilis* Spo0J requires one *parS* site for the efficient regulation of Soj and that this *parS* site is only functional in *cis* (i.e. - when integrated into the bacterial chromosome). We speculate that the single active *parS* site needs to be in the proximity of the replication origin for the proper regulation of Soj by Spo0J. This question is currently being investigated.

7

References

1. Gerdes, K., Møller-Jensen, J., and Jensen, R.B. (2000). Plasmid and chromosome partitioning: surprises from phylogeny. Mol. Microbiol. *37*, 455-466.
2. Livny, J., Yamaichi, Y., and Waldor, M.K. (2007). Distribution of centromere-like parS sites in bacteria: insights from comparative genomics. J. bacteriol. *189*, 8693-8703.
3. Murray, H., Ferreira, H., and Errington, J. (2006). The bacterial chromosome segregation protein Spo0J spreads along DNA from parS nucleation sites. Mol. Microbiol. *61*, 1352-1361.
4. Breier, A.M., and Grossman, A.D. (2007). Whole-genome analysis of the chromosome partitioning and sporulation protein Spo0J (ParB) reveals spreading and origin-distal sites on the Bacillus subtilis chromosome. Mol. Microbiol. *64*, 703-718.
5. Lin, D.C, and Grossman, A.D. (1998). Identification and characterization of a bacterial chromosome partitioning site. Cell. *92*, 675-685.
6. Murray, H., and Errington. J. (2008). Dynamic control of the DNA replication initiation protein DnaA by Soj/ParA. Cell. *135*, 74-84.
7. Scholefield, G., Whiting, R., Errington, J., and Murray, H. (2011). Spo0J regulates the oligomeric state of Soj to trigger its switch from an activator to an inhibitor of DNA replication initiation. Mol. Microbiol. *79*, 1089-1100.
8. Scholefield, Errington, J., and Murray, H. (2012). Soj/ParA stalls DNA replication by inhibiting helix formation of the initiator protein DnaA. EMBO Journal. *31*, 1542-1555.
9. Sullivan, N.L., Marquis, K.A., and Rudner, D.Z. (2009). Recruitment of SMC by ParB-parS organizes the origin region and promotes efficient chromosome segregation. Cell. *137*, 697-707.
10. Gruber, S., and Errington. J. (2009). Recruitment of condensin to replication origin regions by ParB/Spo0J promotes chromosome segregation in B. subtilis. Cell. *137*, 685-696.

OPEN ACCESS Freely available online

PLOS | GENETICS

Multiple Regulatory Systems Coordinate DNA Replication with Cell Growth in *Bacillus subtilis*

Heath Murray*, Alan Koh

Centre for Bacterial Cell Biology, Institute for Cell and Molecular Biosciences, Newcastle University, Newcastle Upon Tyne, United Kingdom

Abstract

In many bacteria the rate of DNA replication is linked with cellular physiology to ensure that genome duplication is coordinated with growth. Nutrient-mediated growth rate control of DNA replication initiation has been appreciated for decades, however the mechanism(s) that connects these cell cycle activities has eluded understanding. In order to help address this fundamental question we have investigated regulation of DNA replication in the model organism *Bacillus subtilis*. Contrary to the prevailing view we find that changes in DnaA protein level are not sufficient to account for nutrient-mediated growth rate control of DNA replication initiation, although this regulation does require both DnaA and the endogenous replication origin. We go on to report connections between DNA replication and several essential cellular activities required for rapid bacterial growth, including respiration, central carbon metabolism, fatty acid synthesis, phospholipid synthesis, and protein synthesis. Unexpectedly, the results indicate that multiple regulatory systems are involved in coordinating DNA replication with cell physiology, with some of the regulatory systems targeting *oriC* while others act in a *oriC*-independent manner. We propose that distinct regulatory systems are utilized to control DNA replication in response to diverse physiological and chemical changes.

Citation: Murray H, Koh A (2014) Multiple Regulatory Systems Coordinate DNA Replication with Cell Growth in *Bacillus subtilis*. PLoS Genet 10(10): e1004731. doi:10.1371/journal.pgen.1004731

Editor: William F. Burkholder, A*STAR, Singapore

Received March 4, 2014; **Accepted** September 3, 2014; **Published** October 23, 2014

Funding: This work was supported by a Royal Society University Research Fellowship to HM. The funders had no role in study design, data collection and analysis, decision to publish, or preparation of the manuscript.

Competing Interests: The authors have declared that no competing interests exist.

* Email: heath.murray@newcastle.ac.uk

Introduction

DNA replication must be coordinated with the cell cycle to ensure proper genome inheritance. For many bacteria cellular physiology dictates the rate of growth and division. In nutrient-rich media that support rapid growth rates, bacteria synthesize DNA more rapidly by increasing the frequency of DNA replication initiation [1–3]. This control system is termed nutrient-mediated growth rate regulation and although it has been appreciated for decades, the molecular mechanisms that connect cell physiology with DNA replication initiation remain debatable.

Historically it has been thought that there is a constant cell mass or cell size at the time of bacterial DNA replication initiation and it has been proposed that a positive regulator would accumulate in a growth-dependent manner to trigger DNA replication initiation when cells attained a critical size [4]. However, modern quantitative analysis of single bacterial cells within steady-state populations has shown that the relationship between DNA replication initiation and cell mass is variable, indicating that the control for timing of DNA replication initiation is not governed by a direct connection with mass accumulation [5].

DnaA is the master bacterial DNA replication initiator protein and is a candidate factor to connect cell physiology with DNA synthesis. DnaA is a member of the AAA+ family of ATPases and shares homology with archaeal and eukaryotic initiator proteins. DnaA directly stimulates DNA replication initiation from a single defined origin of replication (*oriC*) once per cell cycle. Multiple ATP-bound DnaA molecules bind to an array of recognition sequences (DnaA-box 5′-TTATCCACA-3′) within *oriC* where they assemble into a helical filament that promotes duplex DNA unwinding [6,7].

Studies in *Escherichia coli* have suggested that the amount of ATP-bound DnaA dictates the rate of DNA replication initiation. Artificial overexpression of DnaA increases the frequency of DNA replication initiation [8,9]. Conversely, decreasing the amount of DnaA per cell by synthetically promoting early cell division delays DNA replication initiation and modest increases in DnaA levels alleviate this delay, supporting the view that growth-dependent accumulation of DnaA is the trigger for replication initiation in *E. coli* [10]. However, it remains uncertain whether the amount of ATP-bound DnaA is the primary regulator that coordinates DNA replication initiation with cell growth in wild-type *E. coli* cells [11].

In contrast to *E. coli*, studies in *Bacillus subtilis* have suggested that the amount of DnaA may not dictate the rate of DNA replication initiation. Artificially decreasing cell size by stimulating cell division (thereby lowering the amount DnaA per cell to ~70% of wild-type) did not affect DNA replication initiation [10]. Moreover, results from overexpression of DnaA in *B. subtilis* are not clear. Increased expression of DnaA alone causes cell elongation, cell growth inhibition, and induction of the SOS DNA damage response due to depletion of DnaN because of autoregulation of the *dnaA-dnaN* operon by DnaA [12]. To circumvent this problem DnaA was co-overexpressed with DnaN, and under this condition DNA replication initiation does increase [12]. However, subsequent experiments demonstrated that over-expression of DnaN alone increases DNA replication initiation by

Author Summary

DNA replication must be coordinated with cellular physiology to ensure proper genome inheritance. Model bacteria such as the soil-dwelling *Bacillus subtilis* can achieve a wide range of growth rates in response to nutritional and chemical signals. In order to match the rate of DNA synthesis to the rate of nutrient-mediated cell growth, bacteria regulate the initiation frequency of DNA replication. This control of bacterial DNA replication initiation was first observed over forty years ago, however the molecular basis for this regulation has remained hotly debated. In this paper we test one of the leading models for nutrient-mediated growth rate regulation in bacteria, namely that the abundance of the master DNA replication initiation protein DnaA dictates the frequency of DNA replication events. Critically, our results show that changes in DnaA protein level are not sufficient to account for nutrient-mediated growth rate regulation of DNA replication initiation in *B. subtilis*. We then go on to show that there are strong connections between DNA replication and several essential cellular activities, which unexpectedly indicates that there is likely more than one single regulatory pathway involved in coordinating DNA replication with cell physiology. We believe that our work changes thinking regarding this long-standing biological question and reinvigorates the search for the molecular basis of these critical regulatory systems.

repressing the activity of the regulatory protein YabA (an inhibitor of DnaA)[13], suggesting that this could account for the effect on DNA replication initiation when DnaA and DnaN were co-overexpressed.

In this study we have investigated nutrient-mediated growth rate control of DNA replication initiation in *B. subtilis*. We find that changes in DnaA protein level are not sufficient to account for nutrient-mediated growth rate regulation of DNA replication initiation, although this regulation does require both DnaA and *oriC*. We then present evidence suggesting that multiple regulatory systems are involved in coordinating DNA synthesis with cell physiology, and that depending on the nature of the growth limitation, control of DNA replication acts through either *oriC*-dependent or *oriC*-independent mechanisms.

Results

Changes in DnaA levels cannot account for nutrient-mediated growth rate regulation of DNA replication initiation in *B. subtilis*

Steady-state bacterial growth rates can be manipulated by culturing cells in media that contain differing amounts of nutrients, with rich media supporting faster growth because resources are not required to synthesize cellular building blocks *de novo*. In response to different nutrient-mediated steady-state growth rates, bacteria control DNA synthesis by varying the frequency of DNA replication initiation while maintaining a constant speed of elongation [1–3,14]. The rate of DNA replication initiation can be determined by marker frequency analysis (i.e. - measuring the ratio of DNA at the replication origin (*ori*) versus the replication terminus (*ter*) using quantitative PCR), and Figure 1A shows the positive correlation between DNA replication initiation and nutrient-mediated growth rates (cell doublings per hour measured using spectrophotometry). It is important to state that experimental approaches which change bacterial growth rates without altering the chemical composition of the cell (e.g. – varying temperature) do not influence the rate of DNA replication initiation (Figures 1B, S1; [15,16]). Thus, varying nutrient availability modulates bacterial physiology, in turn affecting cell growth and DNA replication initiation [3].

It has been reported that DnaA protein level determines the frequency of DNA replication initiation in *E. coli* [8,9], therefore we wondered whether the amount of DnaA could account for nutrient-mediated growth rate regulation of DNA replication initiation in *B. subtilis* [14]. Western blot analysis shows that DnaA concentration increases with faster steady-state growth rates (Figure 1C; the tubulin homolog FtsZ was used as a loading control because its concentration is growth-rate independent [17,18]). Since *B. subtilis* cell size increases as a function of growth rate, the number of DnaA molecules would also be greater in larger cells formed during fast growth (Figure S2)[14]. This conclusion is in agreement with absolute quantification of DnaA proteins per cell determined at different growth rates using mass spectrometry (163-337 molecules at 0.5 doublings/hr; 875-1791 molecules at 1.0 doublings/hr)[18]. These results indicate that the amount of DnaA protein could account for nutrient-mediated growth rate regulation of DNA replication initiation in *B. subtilis*.

To directly test whether the amount of DnaA protein determines the rate of DNA replication initiation, the endogenous *dnaA* gene was placed under the control of an IPTG-inducible promoter (this also alleviated autoregulation of the *dnaA-dnaN* operon [12]). At near wild-type DnaA levels growth rates were normal, *ori:ter* ratios were unchanged, and the distribution of origin regions per cell visualized using a TetR-YFP/*tetO* reporter system was equivalent to wild-type (Figures 2A-C, S4A). In contrast, when the amount of DnaA fell significantly (between ~50–30% of wild-type, depending upon the media), growth rates slowed, *ori:ter* ratios dropped, DNA replication was inhibited as judged by origin region localization, and cells became elongated (Figures 2A–C, S4A). As noted above *dnaA* is located in an operon upstream of *dnaN* (encoding the sliding clamp component of the replisome) in *B. subtilis*, and Western blot analysis confirmed that the level of DnaN correlated with the level of DnaA (Figure S3B). Depletion of DnaN can cause replication fork stalling and induction of the SOS DNA damage response, which likely contributes to the slow growth and cell elongation phenotypes observed at low IPTG concentrations [12]. However, replication fork stalling would also be expected to cause an increase in the *ori:ter* ratio, suggesting that the observed decreases may be an overestimate of the true initiation frequency. We conclude that wild-type DnaA levels are necessary to achieve the proper frequency of DNA replication initiation at both slow and fast steady-state growth rates.

Only modest overexpression of DnaA could be achieved using the IPTG-inducible promoter (Figure 2A), much lower than the changes in DnaA concentration observed at different nutrient-mediated growth rates (Figure 1C). Therefore, to further increase DnaA protein levels a second copy of the *dnaA* gene was integrated at an ectopic locus under the control of a xylose-inducible promoter (again the endogenous *dnaA-dnaN* operon was expressed using an IPTG-inducible promoter to avoid autorepression). This strain was grown in media that supported a slow growth rate and varying amounts of xylose were added to induce DnaA (>10 fold overexpression was achieved, which was in the range observed for different nutrient-mediated growth rates; Figures 2E, 4D). When DnaA levels were elevated ~2–4 fold a modest increase in the *ori:ter* ratios was observed, although critically the resulting initiation frequencies remained well below the rate generated in rich media (Figures 2D, S4B). These results indicate that changes in DnaA protein levels are not sufficient to

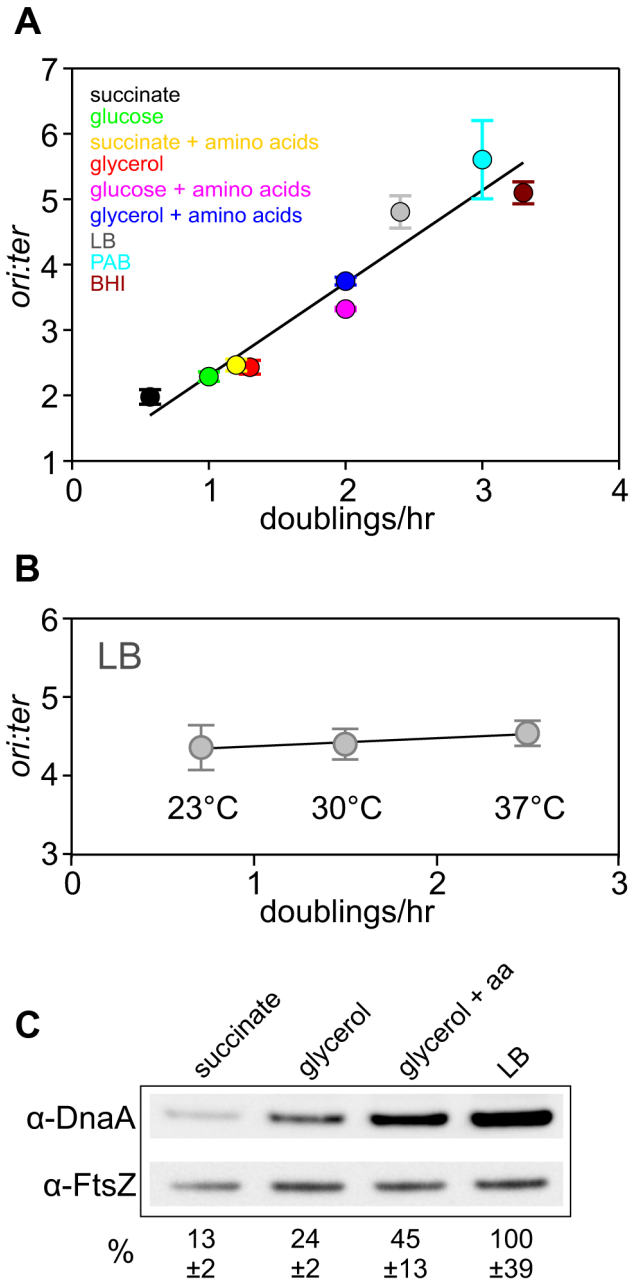

Figure 1. Nutrient-mediated growth rate regulation of DNA replication initiation in *B. subtilis*. (**A**) Culturing *B. subtilis* in a different media generates a range of steady-state growth rates and affects the frequency of DNA replication initiation. A wild-type strain (HM222) was grown overnight at 37°C in minimal media supplemented with succinate and amino acids (20 μg/ml). The culture was diluted 1:100 into various media to generate a range of steady-state growth rates and grown at 37°C until an A_{600} of 0.3–0.4. Genomic DNA was harvested from cells and marker frequency analysis was determined using qPCR. The *ori:ter* ratios are plotted versus growth rate (error bars indicate the standard deviation of three technical replicates). Representative data are shown from a single experiment; independently performed experiments are shown in Figures 4 and S5. (**B**) Culturing *B. subtilis* at different temperatures generates a range of steady-state growth rates but does not affect the frequency of DNA replication initiation. A wild-type strain (HM715) was grown overnight at 23°C in LB. The culture was diluted 1:100 into LB and incubated at different temperatures to generate a range of steady-state growth rates until an A_{600} of 0.2–0.3. Genomic DNA was harvested from cells and marker frequency analysis was determined using qPCR. The *ori:ter* ratios are plotted versus growth rate (error bars indicate the standard deviation of three technical replicates). Representative data are shown from a single experiment; an independently performed replicate of the experiment is shown in Figure S1. (**C**) Measurement of DnaA protein levels at various growth rates in wild-type *B. subtilis* (HM715). Cultures were grown at 37°C overnight as in (A) and diluted 1:100 into various media (succinate, glycerol, glycerol + amino acids, LB). to generate a range of steady-state growth rates until an A_{600} of 0.6–0.8. Cells were lysed and DnaA protein was detected using Western blot analysis (FtsZ protein was likewise detected and used as a loading control). For each culture media the average amount of DnaA (+/− standard deviation) from at least three biological replicates was determined using densitometry; values were normalized to LB.
doi:10.1371/journal.pgen.1004731.g001

account for nutrient-mediated growth rate regulation of DNA replication initiation in *B. subtilis*.

Surprisingly, further overexpression of DnaA lead to a dramatic decrease in the *ori:ter* ratios. To determine whether this inhibition was specific, DnaA was overexpressed in a strain where *oriC* was inactivated by partial deletion (Δ*oriC*), the endogenous *dnaA-dnaN* operon was expressed using a constitutive promoter to avoid autorepression, and genome replication was driven by a plasmid-derived replication origin (*oriN*; integrated ~1 kb to the left of *oriC*) that is recognized and activated by its cognate initiator protein (RepN). It is important to note that while initiation at *oriN* does not require either *oriC* or DnaA, the downstream *B. subtilis* initiation proteins DnaD, DnaB and DnaC (helicase) are necessary for *oriN* activity [19]. Therefore, if overexpression of DnaA was either inhibiting the expression of genes required for DNA replication (e.g. – nucleotide biosynthesis [20]) or sequestering essential replication factors, then DNA replication initiation from *oriN* would be expected to decrease. However, overexpression of DnaA in the Δ*oriC oriN*$^{+}$ background did not alter *ori:ter* ratios, showing that high overexpression of DnaA specifically inhibits DNA replication initiation at *oriC* (Figure S4C).

Neither Soj nor YabA nor (p)ppGpp are required for nutrient-mediated growth rate regulation of DNA replication initiation in *B. subtilis*

We hypothesized that nutrient-mediated growth rate control of DNA replication initiation could act via regulation of DnaA activity rather than protein abundance. There are two known trans-acting regulators of *B. subtilis* DnaA during steady-state growth, Soj and YabA. Soj is a dynamic protein that can act as either a negative or a positive regulator of DnaA, depending upon its quaternary state [21–23]. YabA is a negative regulator of DnaA that forms a protein bridge between the initiator DnaA and the DNA polymerase sliding clamp processivity factor, DnaN, and is thought to inhibit DNA replication by spatially sequestering DnaA away from the replication origin and by inhibiting DnaA oligomerization [24–27]. Interestingly, the number of both proteins per cell was found to positively correlate with growth rate [18].

To determine whether either of these regulatory proteins is required for nutrient-mediated growth rate regulation of DNA replication initiation, single knockout mutants were cultured in a range of media and analyzed using marker frequency analysis. It was found that both of the mutant strains retained the ability to coordinate DNA replication initiation with nutrient-mediated changes in growth rate (Figures 3A, S5A). To test whether Soj and YabA acted redundantly to control the nutrient-mediated activity of DnaA, the double mutant was constructed and analysed by marker frequency analysis. Again proper regulation of DNA

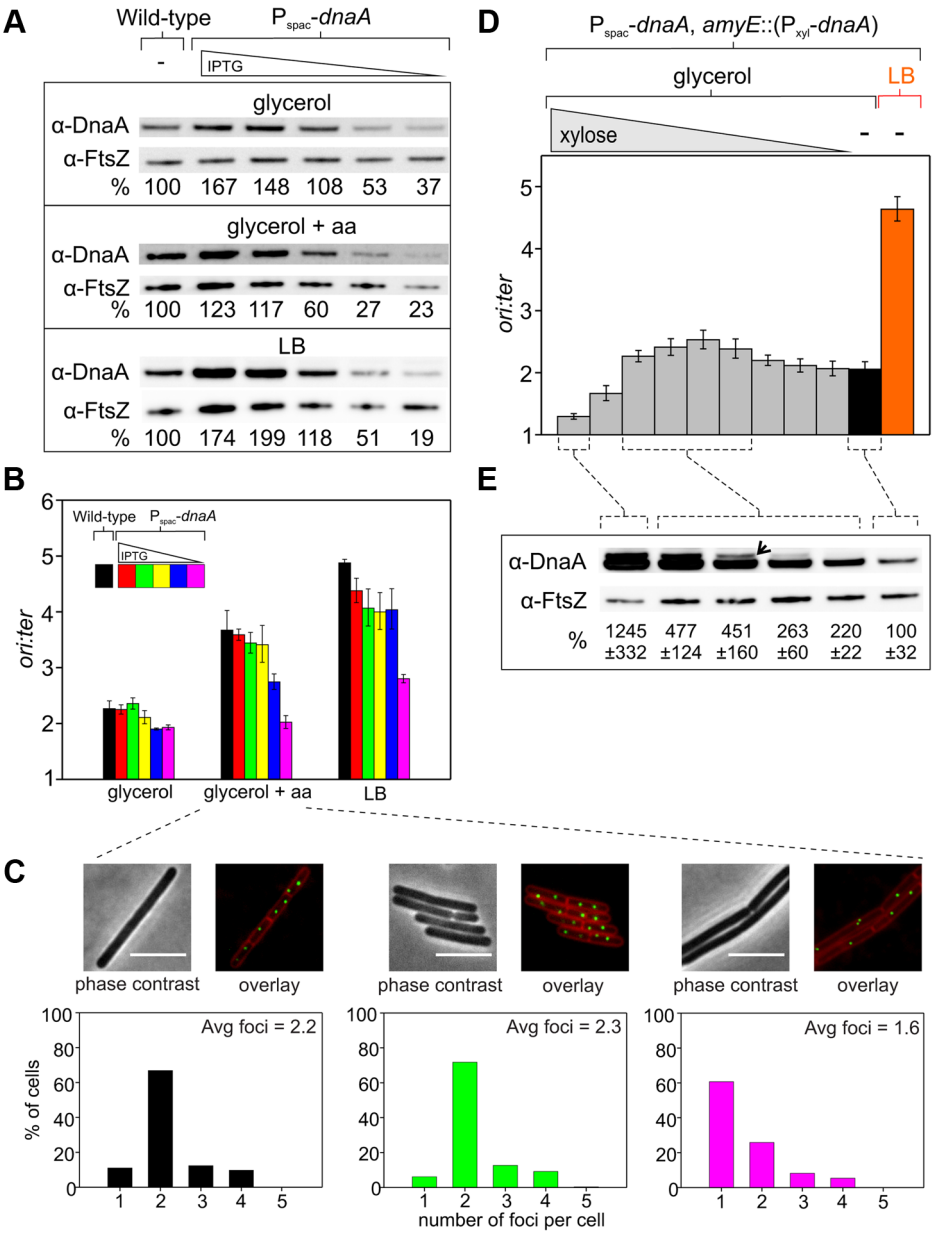

Figure 2. Changes in DnaA protein level are not sufficient to account for nutrient-mediated growth rate regulation of DNA replication initiation in *B. subtilis.* (**A**) The endogenous *dnaA* gene was placed under the control of the IPTG-inducible promoter P_{spac} to generate a range of DnaA protein levels. Strains were grown overnight at 37°C in minimal media supplemented with succinate and amino acids (20 μg/ml); IPTG (400 μM) and erythromycin was added to HM742. The cultures were diluted 1:100 into various media (glycerol, glycerol + amino acids, LB) to generate a range of steady-state growth rates and grown at 37°C until an A_{600} of 0.5–0.6; in each medium HM742 was supplemented with erythromycin and a range of IPTG (800, 400, 200, 100, 50 μM). Cells were lysed and DnaA protein was detected using Western blot analysis (FtsZ protein was likewise detected and used as a loading control). The amount of DnaA was determined using densitometry; values were normalized to wild-type. Wild-type (HM222), P_{spac}-*dnaA* (HM742). (**B**) DNA replication was measured at over a range of DnaA protein levels. Strains were grown as described in (A). Genomic DNA was harvested from cells and marker frequency analysis was determined using qPCR. For each growth media, the *ori:ter* ratios are plotted versus IPTG concentration (error bars indicate the standard deviation of three technical replicates). Representative data are shown from a single experiment; an independently performed replicate of the experiment is shown in Figure S4A. Wild-type (HM222), P_{spac}-*dnaA* (HM742). (**C**) Measurement of replication origins number per cell. An array of ~150 *tetO* sites was inserted near the replication origin and visualized using TetR-YFP. Strains were grown as described in (A), except that overnight cultures were only diluted into a single medium (glycerol + amino acids); AK652 was supplemented with erythromycin and a range of IPTG concentrations. Samples were taken at mid-exponential phase for microscopy and membranes were stained to identify single cells (scale bar = 5 μm). Histogram colour corresponds to the respective strain/IPTG concentration and the average number of origins per cell is indicated (n> 300). Wild-type (AK647), P_{spac}-*dnaA* (AK652). (**D**) To strongly overexpress DnaA the endogenous *dnaA* gene was placed under the control of P_{spac} and an ectopic copy of *dnaA* was integrated at the *amyE* locus under the control of the xylose inducible promoter P_{xyl} (HM745). The strain was grown overnight at 37°C in minimal media supplemented with glycerol, amino acids (20 μg/ml), IPTG (800 μM), and erythromycin. The culture was diluted 1:100 into media containing IPTG (800 μM), erythromycin, either glycerol minimal media supplemented with a range of xylose (1, 0.5, 0.25, 0.125, 0.063, 0.031, 0.016, 0.008, 0.004, 0%) or LB, and grown at 37°C until an A_{600} of 0.2–0.4. Genomic DNA was harvested from cells and marker frequency analysis was determined using qPCR. For each growth media, the *ori:ter* ratios are plotted versus xylose concentration (error bars indicate the standard deviation of three technical replicates). Representative data are shown from

a single experiment; an independently performed replicate of the experiment is shown in Figure S4B. (**E**) HM745 was grown as described in (D) until cultures reached an A_{600} of 0.6–0.9, cells were lysed, and DnaA protein was detected using Western blot analysis (FtsZ protein was likewise detected and used as a loading control). The open arrowhead highlights that overexpressed DnaA ran as a doublet (similar results have been observed for other overexpressed proteins in *B. subtilis*; HM). For each condition the average amount of DnaA (+/− standard deviation) from three biological replicates was determined using densitometry; values were normalized to the cultures without xylose.
doi:10.1371/journal.pgen.1004731.g002

replication initiation was maintained in the Δ*soj* Δ*yabA* mutant, indicating that neither regulatory protein is required (Figures 3A, S5B). Interestingly, both the single and double mutants displayed a reduced growth rate in rich media, suggesting that the burden of overactive DNA replication initiation may be exacerbated during multifork replication. In the case of the *soj* mutant it is also possible that the slow growth phenotype is related to its role in chromosome origin segregation [28–30].

We also determined whether the alarmone (p)ppGpp, a small molecule induced during nutrient limitation, is required for nutrient-mediated growth rate regulation of DNA replication initiation in *B. subtilis*. Marker frequency analysis was performed on a strain lacking the three known (p)ppGpp synthases (RelA, YwaC, YjbM). It was found that regulation of DNA replication initiation was unaffected by the absence of (p)ppGpp, suggesting that (p)ppGpp is not involved in the regulatory mechanisms coordinating DNA replication with nutrient availability during steady-state cell growth (Figures 3B, S5C).

DnaA and *oriC* are necessary for nutrient-mediated growth rate regulation of DNA replication initiation in *B. subtilis*

Since both overexpression of DnaA and deletion of DnaA regulatory proteins did not alter nutrient-mediated growth rate regulation of DNA replication initiation, it was unclear whether DnaA was actually a component of this system. To determine whether DnaA activity at *oriC* is required, marker frequency analysis was performed in a strain where *oriC* was inactivated (Δ*oriC*) and DNA replication initiates from the plasmid-derived *oriN*. It was found that *ori:ter* ratios remain constant over a wide range of growth rates in the Δ*oriC* mutant, indicating that nutrient-mediated growth rate regulation of DNA replication was lost (Figures 4A, S6A). Critically, DNA replication initiation from *oriC* is unaffected by the addition of *oriN* (Figures 4B, S6B). This shows that it is the absence of DnaA activity at *oriC*, rather than the presence of *oriN*, which accounts for the loss of nutrient-mediated growth rate regulation in the Δ*oriC* mutant.

However, it could not be concluded whether the Δ*oriC* mutation acted by removing replication origin function or by deleting a site that is required for the nutrient-mediated growth rate regulation. Therefore, a mutation was introduced into *dnaA* that alters the critical "arginine finger" residue ($Arg^{264}\rightarrow Ala$), thereby disabling DnaA filament assembly and initiation activity (note that a DnaA arginine finger mutant remains competent for DNA binding and ATP binding) [22,31]. Again the $dnaA^{R264A}$ mutant strain contains *oriN* in order to maintain viability. Like the Δ*oriC* mutant the $DnaA^{R264A}$ variant also lost growth rate regulation in response to nutrient availability, indicating that DnaA activity at *oriC* is necessary for growth rate regulation in *B. subtilis* (Figures 4C, S6C). Moreover, since the *ori:ter* ratios of the Δ*oriC* and $dnaA^{R264A}$ mutants remains constant during nutrient-mediated growth rate changes and since DNA replication elongation speed is independent of the nutrient-mediated growth rate [2,14], the results suggest that within a population of cells the average frequency of DNA replication initiation at *oriN* is independent of the nutrient-mediated growth rate.

Western blot analysis showed that in rich media there was less DnaA and DnaN in the Δ*oriC* strain, whereas conversely there was more DnaA and DnaN in the $dnaA^{R264A}$ mutant (Figure S3C). The latter result suggests that autoregulation of the *dnaA* promoter requires ATP-dependent filament formation by DnaA, however, the former result was more puzzling. To investigate this further the amount of DnaA in the Δ*oriC* strain was determined over a range of nutrient-mediated growth rates. While the concentration of DnaA was observed to increase as a function of growth rate in the wild-type strain, DnaA levels did not display the same correlation with growth rate in the Δ*oriC* mutant (Figure 4D). This suggests that in the Δ*oriC* mutant nutrient-mediated growth rate-dependent expression of DnaA is lost either because DNA replication initiation from *oriN* is constitutive or because the deletion within *oriC* affects *dnaA* expression (although this region is downstream of the *dnaA* gene).

The apparent decrease in growth rates observed for strains initiating DNA replication solely through *oriN*, particularly in rich media (Figures 4A, 4C, S6A, S6C), is likely due to the formation of cells lacking DNA as a direct consequence of decoupling DNA replication initiation from growth rate (Figure 4E). This result underscores the importance of growth rate regulation of DNA replication initiation to ensure bacterial fitness.

Slowing growth rate by limiting essential cellular activities inhibits DNA replication

Since nutrient-mediated growth rate regulation of DNA replication initiation did not appear to act through either DnaA protein accumulation or known DnaA regulators, we considered alternative possibilities for how DNA replication could be connected to cell physiology. One hypothesis was that this regulation could be linked to metabolism, either through the amount of a metabolic intermediate or the activity of a critical enzyme. Genetic evidence has suggested a relationship between several glycolytic enzymes and DNA replication in *B. subtilis* and *E. coli* [32,33], but it has not been established whether these connections act directly at the level of DnaA-dependent initiation. ATP would be another rational candidate since DnaA is an ATP-dependent protein, but it has been found that the concentration of ATP in *B. subtilis* (as well as in *E. coli*) is invariant over a wide range of growth rates (L. Krasny and R. Gourse, personal communication; [34,35]). Another hypothesis was that this regulation could be linked to the synthesis of an essential cellular complex, such as the ribosome or the cell membrane [36,37]. In this way a bacterial cell would integrate nutritional information based on the availability of multiple substrates required to construct such macromolecules.

In order to identify possible routes through which nutrient availability could impact DNA replication we analyzed a range of genetically altered strains, targeting respiration, central carbon metabolism, protein synthesis, fatty acid synthesis, and phospholipid synthesis (Table 1), that all manifest decreased steady-state growth rates in rich complex media. Genes were either disrupted by antibiotic cassettes or depleted using regulated expression systems; importantly, depletion of essential genes was not lethal under the experimental conditions used. Knock-out strains were compared to wild-type while depletion strains were analyzed

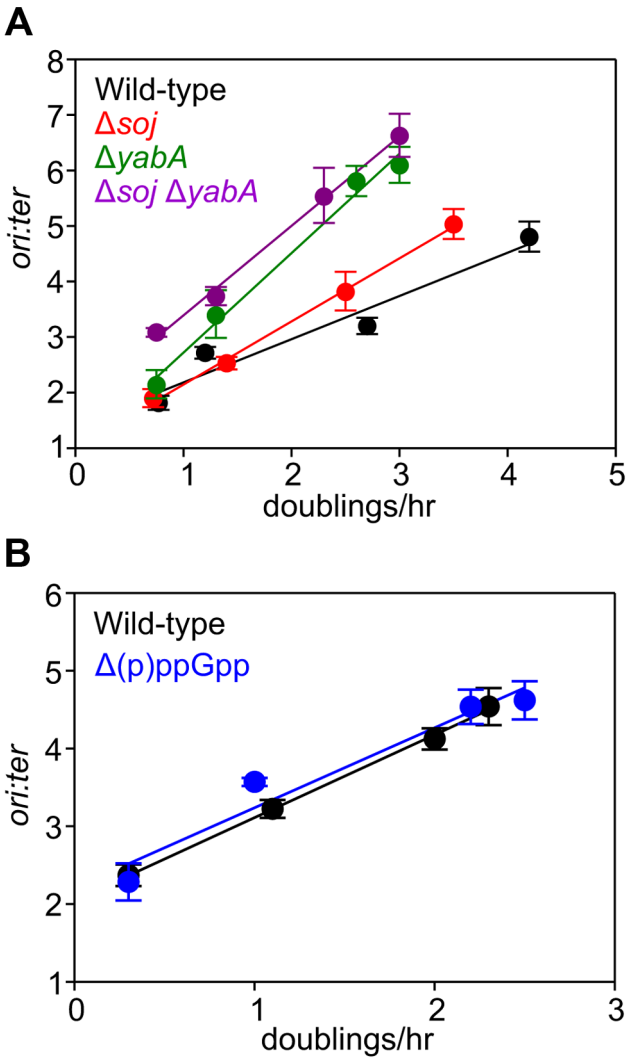

Figure 3. Nutrient-mediated growth rate regulation of DNA replication initiation is independent of Soj, YabA, and (p)ppGpp. (**A**) Growth rate regulation of DNA replication initiation is maintained in either Δ*soj* or Δ*yabA* mutants. Strains were grown overnight at 37°C in minimal media supplemented with succinate and amino acids (20 μg/ml). The culture was diluted 1:100 into various media (succinate, glycerol, glycerol + amino acids, LB) to generate a range of steady-state growth rates and grown at 37°C until an A_{600} of 0.3–0.4. Genomic DNA was harvested from cells and marker frequency analysis was determined using qPCR. The *ori:ter* ratios are plotted versus growth rate (error bars indicate the standard deviation of three technical replicates). Representative data are shown from a single experiment; an independently performed replicate of the experiment is shown in Figures S5A-B. Wild-type (HM222), Δ*soj* (HM227), Δ*yabA* (HM739), Δ*soj* Δ*yabA* (HM741). (**B**) Growth rate regulation of DNA replication initiation does not require (p)ppGpp. Strains were grown overnight at 37°C in minimal media supplemented with succinate and amino acids (200 μg/ml). The culture was diluted 1:100 into various media (succinate + amino acids, glycerol + amino acids, LB, PAB) to generate a range of steady-state growth rates and grown at 37°C until an A_{600} of 0.2–0.6. Genomic DNA was harvested from cells and marker frequency analysis was determined using qPCR. The *ori:ter* ratios are plotted versus growth rate (error bars indicate the standard deviation of three technical replicates). Representative data are shown from a single experiment; an independently performed experiment is shown in Figure S5C. Wild-type (HM222), Δ(p)ppGpp (HM1230).
doi:10.1371/journal.pgen.1004731.g003

without and with inducer (indicated in Figures 5, 6, S7, S8 with "-" and "+", respectively). DNA replication was measured using marker frequency analysis. Strikingly, in all of the strains examined the *ori:ter* ratio decreased to match the slower growth rates caused by gene disruption/depletion (Figures 5–6, S7–S8; black symbols).

Evidence for an *oriC*-independent response to changes in growth rate

The uniform response of DNA replication in slow growing mutants suggested that a single mechanism might account for this regulation, in accord with nutrient-mediated regulation of DNA replication initiation (Figures 4, S6). To examine this hypothesis the deletion and depletion strains were crossed into the Δ*oriC* strain that initiates DNA replication using *oriN*. For several mutants (*ndh*, *gapA*, *pdhB*, *fabHA*, *plsC* and *ltaS*) the *ori:ter* ratio was not significantly affected (≤1/10 of the percentage decrease observed for $oriC^+$), suggesting that the regulatory signal specifically targeted DNA replication initiation at *oriC* (Figures 5, S7; red symbols). However, there were a number of mutants (*pykA*, *pgsA*, and multiple ribosomal protein genes) that produced a marked decrease in the *ori:ter* ratio of the Δ*oriC* strain (≥1/2 of the percentage decrease observed for $oriC^+$), suggesting that in these cases DNA replication was being regulated through an *oriC*-independent mechanism (Figures 6A–C, S8A-C; red symbols). Interestingly, in some cases manipulation of different genes within a single biological pathway (e.g. – carbon metabolism or phospholipid synthesis) resulted in the regulation of DNA replication through the different regulatory systems.

Evidence for a DnaA-independent response to changes in growth rate

Since the Δ*oriC oriN*$^+$ strain does not require DnaA activity to initiate DNA replication, it suggested that the observed *oriC*-independent growth rate regulation might be DnaA-independent. To address this possibility the *oriC*-independent mutants (Figures 6A–C, S8A–C) were crossed into a Δ*dnaA* strain that initiates DNA replication using *oriN* (Figure S3C). When PykA was depleted in the Δ*dnaA* mutant the *ori:ter* ratio no longer decreased, indicating that DnaA was required for this response, although apparently not for its role in origin recognition and DNA unwinding (Figures 6D, S8D; green symbols). In contrast, when either ribosomal genes were deleted or PgsA was depleted in the Δ*dnaA* mutant the *ori:ter* ratios did decrease, suggesting that DnaA-independent mechanisms act under these conditions (Figures 6E–F, S8E–F; green symbols). Taken together, the genetic analysis reveals that in *B. subtilis* there is likely more than one regulatory system linking DNA replication with cell growth.

Slowing growth rate by targeting essential cellular activities with small molecules inhibits DNA replication initiation

The importance of growth rate regulation of DNA replication in response to nutrient availability is self-evident, but the biological relevance of growth rate regulation of DNA replication in response to genetic manipulations is less clear. To address this issue we evaluated the response of DNA replication to sublethal concentrations of antibiotics that produced slow steady-state growth rates. We chose small molecules that inhibit either fatty acid synthesis (cerulenin) or protein synthesis (chloramphenicol) because our genetic analyses indicated that the former regulated DNA replication through *oriC* while the latter acted independently of both *oriC* and DnaA. Incubation with either antibiotic caused a decrease in the *ori:ter* ratios in the wild-type strain, showing that

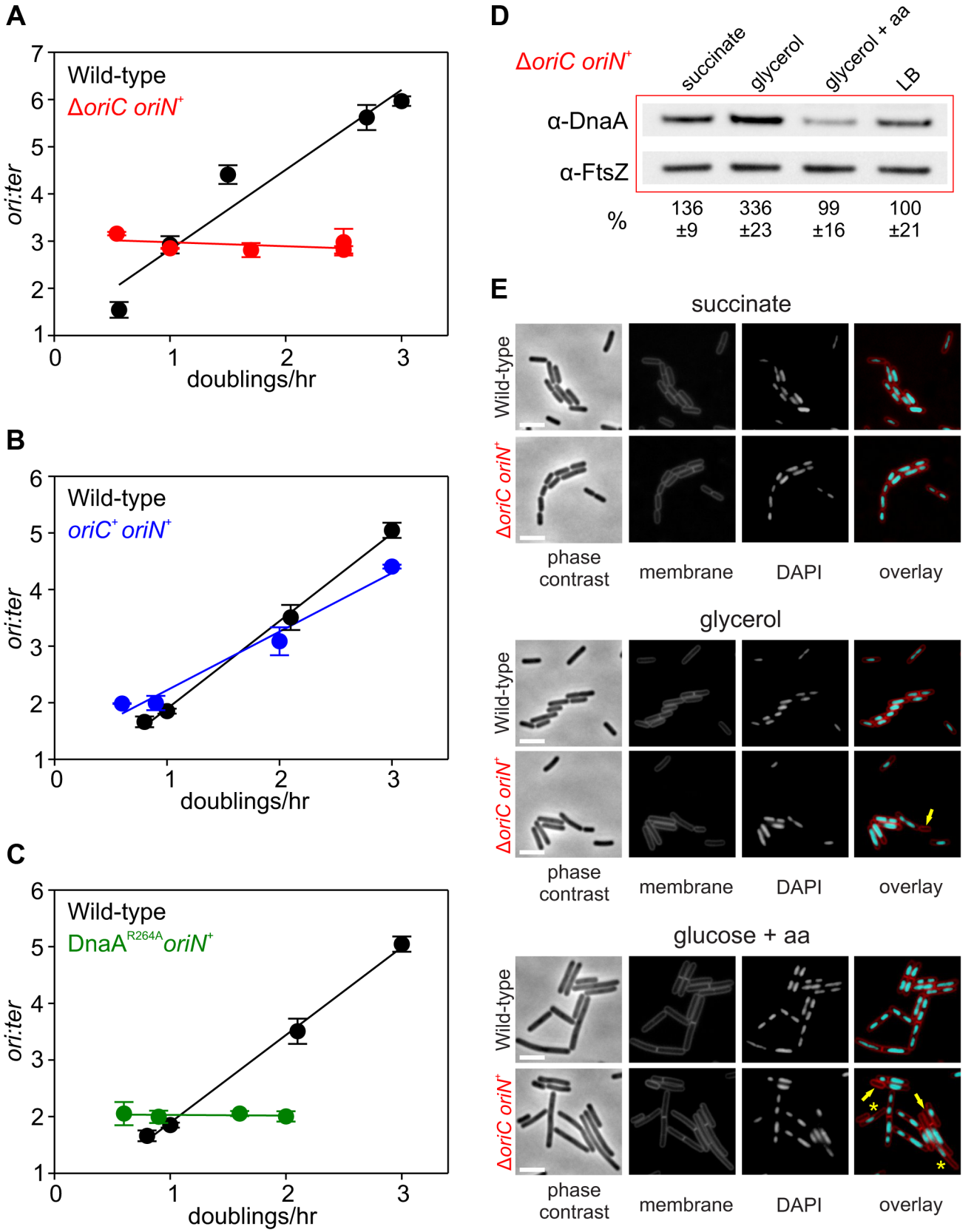

Figure 4. Nutrient-mediated growth rate regulation of DNA replication initiation requires *oriC* and DnaA. (**A**) *oriC* is required for growth rate regulation of DNA replication initiation. Strains were grown overnight at 37°C in minimal media supplemented with succinate and amino acids (20 μg/ml). The culture was diluted 1:100 into various media (succinate, glycerol, glycerol + amino acids, LB, PAB) to generate a range of steady-state growth rates and grown at 37°C until an A_{600} of 0.3–0.4. Genomic DNA was harvested from cells and marker frequency analysis was determined using

qPCR. The *ori:ter* ratios are plotted versus growth rate (error bars indicate the standard deviation of three technical replicates). Representative data are shown from a single experiment; an independently performed replicate of the experiment is shown in Figure S6A. Wild-type (HM222), Δ*oriC oriN*$^+$ (HM228). (**B**) Integration of *oriN* into the *B. subtilis* chromosome does not eliminate growth rate regulation of DNA replication initiation. Strains were grown as in (A) and the overnight culture was diluted 1:100 into various media (succinate, glycerol, glycerol + amino acids, LB). Genomic DNA was harvested from cells and marker frequency analysis was determined using qPCR. The *ori:ter* ratios are plotted versus growth rate (error bars indicate the standard deviation of three technical replicates). Representative data are shown from a single experiment; an independently performed replicate of the experiment is shown in Figure S6B. Wild-type (HM715), *oriC*$^+$ *oriN*$^+$ (HM949). (**C**) DnaA activity is required for growth rate regulation of DNA replication initiation. Strains were grown as in (B). Genomic DNA was harvested from cells and marker frequency analysis was determined using qPCR. The *ori:ter* ratios are plotted versus growth rate (error bars indicate the standard deviation of three technical replicates). Representative data are shown from a single experiment; an independently performed replicate of the experiment is shown in Figure S6C. Wild-type (HM715), DnaA^{R264A} *oriN*$^+$ (HM1122). (**D**) Measurement of DnaA protein levels at various growth rates in a Δ*oriC oriN*$^+$ strain (HM950). Cultures were grown as described in (B). Cells were lysed and DnaA protein was detected using Western blot analysis (FtsZ protein was likewise detected and used as a loading control). For each culture media the average amount of DnaA (+/− standard deviation) from at least three biological replicates was determined using densitometry; values were normalized to LB. (**E**) Subcellular localization of DNA over a range of growth rates in the wild-type (HM715) and Δ*oriC oriN*$^+$ (HM950) strains. Cells were grown as in (B) and the overnight culture was diluted 1:100 into various media (succinate, glycerol, or glucose + amino acids). Samples were taken at an A_{600} of 0.3–0.5 at which point membranes and DNA were stained. Arrows indicate cells without DNA and asterisks indicate space within the cell that does not contain DNA. Scale bar represents 3 μm.
doi:10.1371/journal.pgen.1004731.g004

growth rate regulation of DNA replication in response to genetic perturbations of essential cellular activities is physiologically relevant (Figures 7A–B, S9A–B; black symbols).

To further assess whether changes in DNA replication caused by these small molecules reflected the results using genetic approaches, the Δ*oriC oriN*$^+$ strain was analyzed. Only chloramphenicol elicited a significant decrease in the *ori:ter* ratios in the Δ*oriC* strain (Figures 7A–B, S9A–B; red symbols). Finally, the Δ*dnaA oriN*$^+$ strain was analyzed in the presence of chloramphenicol and again the *ori:ter* ratio decreased (Figures 7B, S9B). This result is fully consistent with the data from ribosomal gene deletions and indicates that regulation of DNA replication in response to perturbed ribosome activity is DnaA-independent.

Discussion

We have found that nutrient-mediated growth rate regulation of DNA replication initiation in *B. subtilis* requires both DnaA and *oriC*. To our knowledge this is the first time that a specific DNA replication initiation protein has been shown to play an essential role in this regulatory system, and because DnaA is the earliest acting initiation factor we propose that DnaA is the target for the nutrient-mediated growth rate regulatory system. Critically however, we show that changes in DnaA protein level are not sufficient to account for nutrient-mediated growth rate regulation of DNA replication initiation in *B. subtilis*. This is in contrast to the generally accepted mechanism for control of bacterial DNA replication initiation based on work using *E. coli* [8,9].

B. subtilis contains a bipartite origin that flanks the *dnaA* gene (*incA* and *incB* regions containing the *dnaA* promoter lie 1.3 kb upstream of the *incC* region which contains the DNA unwinding element) [38]. When the expression of the *dnaA-dnaN* operon was placed under the control of the inducible P_{spac} promoter in order to test the effect of DnaA overexpression on DNA replication initiation, a ~9kb plasmid was recombined upstream of *dnaA* by single cross-over. Therefore, integration of this vector resulted in the considerable displacement of the two origin regions from one another without any significant consequence. It will be extremely interesting to determine the maximum and minimum distances that the *inc* regions can be moved, as well as ascertaining the role of the upstream region in DNA replication initiation.

We have shown that neither of the known DnaA regulatory proteins present during vegetative growth, Soj and YabA, are required for nutrient-mediated growth rate regulation of DNA replication initiation. We have also determined that the alarmone (p)ppGpp is not required for this regulation, consistent with a previous report that induction of the stringent response inhibits DNA replication elongation but not initiation in *B. subtilis*

Table 1. Genes manipulated to limit essential cellular processes.

Gene	Protein	Cellular Activity
ndh	NADH dehydrogenase	respiration
gapA	glyceraldehyde-3-P dehydrogenase	central carbon metabolism
pykA	pyruvate kinase	central carbon metabolism
pdhB	pyruvate dehydrogenase (E1 β subunit)	central carbon metabolism
fabHA	β-ketoacyl-acyl carrier protein synthase III	fatty acid synthesis
ltaS	lipoteichoic acid synthase	lipoteichoic acid synthesis
plsC	acyl-ACP:1-acylglycerolphosphate acyltransferase	phospholipid synthesis
pgsA	phosphatidylglycerophosphate synthase	phospholipid synthesis
rpsU	ribosomal protein S21	protein synthesis
rplA	ribosomal protein L1	protein synthesis
rplW	ribosomal protein L23	protein synthesis
rpmJ	ribosomal protein L36	protein synthesis

doi:10.1371/journal.pgen.1004731.t001

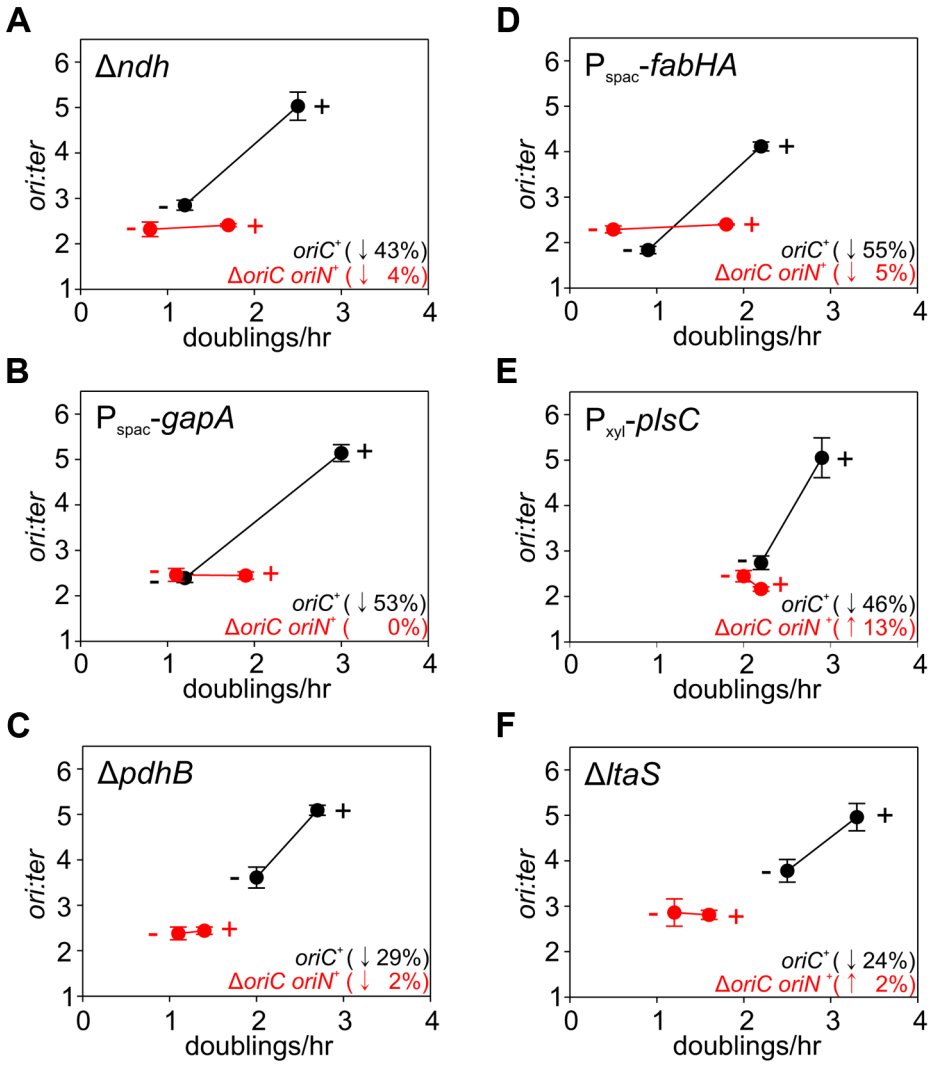

Figure 5. Analysis of *oriC*-dependent growth rate regulation through genetic targeting of essential cellular activities. Strains were grown overnight at 37°C in LB medium; strains harbouring plasmids integrated into the genome by single-crossover were supplemented with appropriate antibiotics and inducer (0.1 mM IPTG or 0.1% xylose). Overnight cultures were diluted 1:1000 into fresh LB medium and grown at 37°C until they reached an A_{600} of 0.3–0.5; strains harbouring plasmids integrated by single-crossover were supplemented with appropriate antibiotics either without or with the appropriate inducer (1 mM IPTG or 1% xylose). For datapoints "+" indicates the presence of either the wild-type gene (when comparing with knockout mutants) or the inducer; "−" indicates the absence of either the gene (when comparing with wild-type) or the inducer. Genomic DNA was harvested from cells and marker frequency analysis was determined using qPCR. The *ori:ter* ratios are plotted versus growth rate and the percentage change in the *ori:ter* ratios comparing each deletion/depletion is indicated (error bars indicate the standard deviation of three technical replicates). Representative data are shown from a single experiment; an independently performed replicate of the experiment is shown in Figure S7. (**A**) Wild-type (HM715), Δ*ndh* (HM1318), Δ*oriC oriN*$^+$ (HM957), Δ*ndh* Δ*oriC oriN*$^+$ (HM1319); (**B**) P_{spac}-*gapA* (HM1208), P_{spac}-*gapA* Δ*oriC oriN*$^+$ (HM1221); (**C**) Cultures were supplemented with 0.2% sodium acetate. Wild-type (HM715), Δ*pdhB* (HM1248), Δ*oriC oriN*$^+$ (HM950), Δ*pdhB* Δ*oriC oriN*$^+$ (HM1266); (**D**) P_{spac}-*fabHA* (HM964), P_{spac}-*fabHA* Δ*oriC oriN*$^+$ (HM966); (**E**) P_{xyl}-*plsC* (HM1080), P_{xyl}-*plsC* Δ*oriC oriN*$^+$ (HM1086); (**F**) Wild-type (HM715), Δ*ltaS* (HM1168), Δ*oriC oriN*$^+$ (HM957), Δ*ltaS* Δ*oriC oriN*$^+$ (HM1244).
doi:10.1371/journal.pgen.1004731.g005

[39,40]. This result marks an apparent distinction between the role of (p)ppGpp in *B. subtilis* and in proteobacteria such as *E. coli* and *Caulobacter crescentus* where (p)ppGpp has been shown to regulate DNA replication initiation [41,42].

The use of genetic manipulations and small molecule inhibitors presented here reinforce and extend previously observed connections for bacterial DNA replication with central carbon metabolism [32,33] and with phospholipid synthesis [43,44]. In addition our work identifies new links for *B. subtilis* DNA replication with respiration, fatty acid synthesis, lipoteichoic acid synthesis, and ribosome biosynthesis. The results indicate that growth rate regulation of DNA replication in *B. subtilis* can be controlled through either *oriC*-dependent, *oriC*-independent/DnaA-dependent, or *oriC*-independent/DnaA-independent mechanisms (summarized in Figure 7C). Based on these novel findings we propose that multiple systems coordinate DNA replication with bacterial cell growth, with distinct regulators responding to diverse physiological and chemical changes. This model deviates from the long-standing concept of a single universal cellular property utilized to link bacterial DNA replication with cell growth [4].

Since nutrient-mediated growth rate regulation of DNA replication initiation requires DnaA activity at *oriC*, this suggests

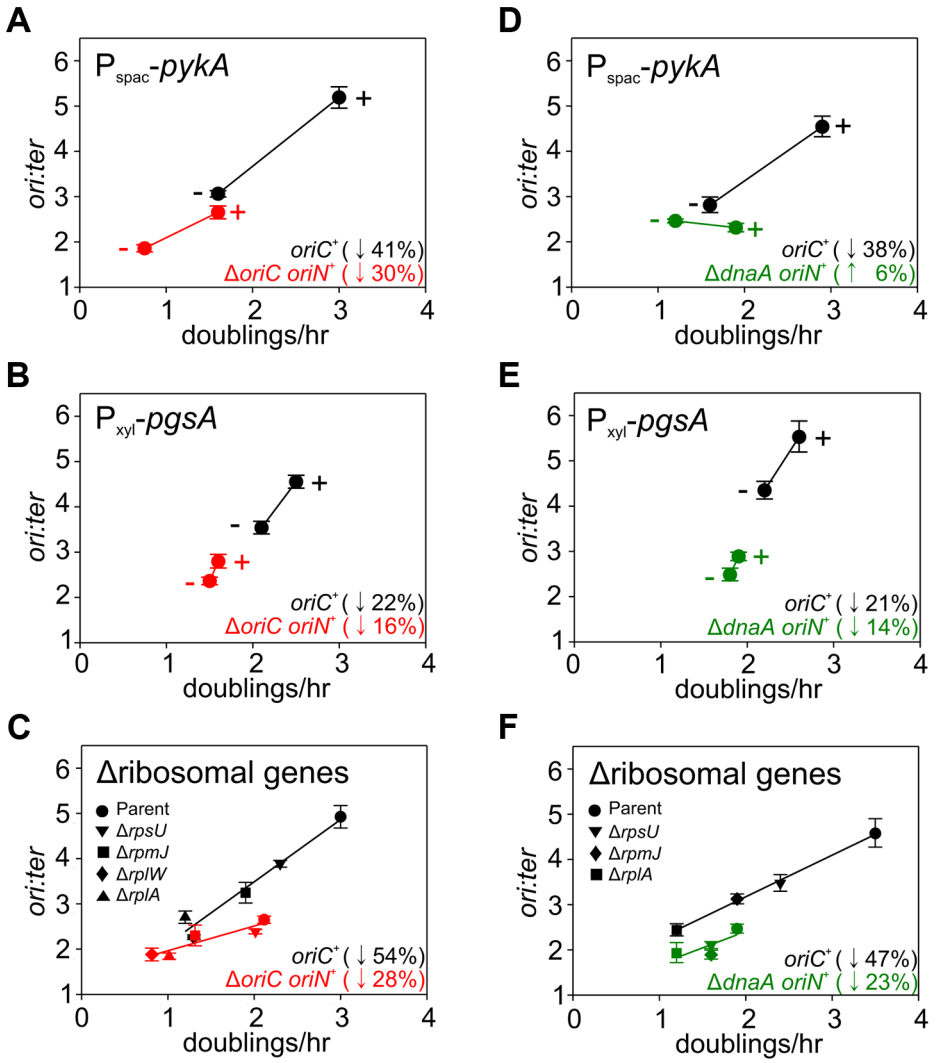

Figure 6. Analysis of *oriC*-independent growth rate regulation through genetic targeting of essential cellular activities. Strains were grown and data presented as described for Figure 5, except that the depletion of PgsA required supplementation with 1 mM IPTG to overexpress the xylose repressor. The *ori:ter* ratios are plotted versus growth rate and the percentage change in the *ori:ter* ratios comparing each deletion/depletion is indicated (error bars indicate the standard deviation of three technical replicates). Representative data are shown from a single experiment; an independently performed replicate of the experiment is shown in Figure S8. (**A**) P_{spac}-*pykA* (HM1176), P_{spac}-*pykA* Δ*oriC oriN*$^+$ (HM1186); (**B**) P_{xyl}-*pgsA* (HM1365), P_{xyl}-*pgsA* Δ*oriC oriN*$^+$ (HM1374); (**C**) Wild-type (HM715), Δ*rpsU* (HM1150), Δ*rplA* (HM1151), Δ*rplW* (HM1152), Δ*rpmJ* (HM1154), Δ*oriC oriN*$^+$ (HM950), Δ*rpsU* Δ*oriC oriN*$^+$ (HM1156), Δ*rplA* Δ*oriC oriN*$^+$ (HM1157), Δ*rplW* Δ*oriC oriN*$^+$ (HM1158), Δ*rpmJ* Δ*oriC oriN*$^+$ (HM1160). (**D**) P_{spac}-*pykA* (HM1176), P_{spac}-*pykA* Δ*dnaA oriN*$^+$ (HM1425); (**E**) P_{xyl}-*pgsA* (HM1365), P_{xyl}-*pgsA* Δ*dnaA oriN*$^+$ (HM1433); (**F**) Wild-type (HM715), Δ*rpsU* (HM1150), Δ*rplA* (HM1151), Δ*rpmJ* (HM1154), Δ*dnaA oriN*$^+$ (HM1423), Δ*rpsU* Δ*dnaA oriN*$^+$ (HM1429), Δ*rplA* Δ*dnaA oriN*$^+$ (HM1430), Δ*rpmJ* Δ*dnaA oriN*$^+$ (HM1432).
doi:10.1371/journal.pgen.1004731.g006

that factors affecting DNA synthesis through an *oriC*-independent mechanism (PykA, PgsA, and ribosomal proteins) are unlikely to be responsible for the nutrient sensing system. We suspect that nutrient-mediated regulation may be influenced by more than one control system, thereby forming a robust network capable of integrating information from multiple metabolic and cellular sources.

We note that for deletion/depletion mutants regulating DNA replication through *oriC*-dependent and *oriC*-independent/DnaA-dependent mechanisms, *ori:ter* ratios either remained constant or slightly increased in the Δ*oriC* and Δ*dnaA* strains, respectively (Figures 5, 6D, S7, S8D). Because the average initiation frequency of *oriN* appears to be growth rate independent (Figures 4A, 4C, S6A, S6C), the measured *ori:ter* ratios of these strains indicates that replication elongation speeds are either not being affected or are slightly decreasing. Therefore, for both *oriC*-dependent and *oriC*-independent/DnaA-dependent regulatory mechanisms, the observed decrease in *ori:ter* ratios in the *oriC*$^+$ strain most likely reflects inhibition of DNA replication initiation. In contrast, for the *oriC*-independent/DnaA-independent mutants where the *ori:ter* ratio was decreased when DNA replication initiated from *oriN*, this difference could be due to a change in DNA replication elongation (although this would mean that the elongation speed was increased).

Our current aim is to determine the molecular mechanisms underlying each system that coordinates DNA replication with cell growth. We hypothesize that the *oriC*-dependent regulatory system targets DnaA activity at *oriC*. We speculate that the *oriC*-independent/DnaA-dependent regulatory system could influence DNA replication initiation by affecting the abundance or

activity of a downstream replication initiation factor. For example, DnaA is also a transcription factor that is thought to directly regulate the expression of>50 genes, including *dnaB* [20,45]. Alternatively, DnaA could act by titrating initiation factors away from *oriN*. Lastly, in the case of the *oriC*-independent/DnaA-independent regulatory system it needs to be established whether DNA replication is affected at the step of initiation or elongation, after which the role of appropriate candidate proteins can be investigated.

Materials and Methods

Strains and plasmids

Strains are listed in Table S1. Plasmids are listed in Table S2 and Table S3.

Media and chemicals

Nutrient agar (NA; Oxoid) was used for routine selection and maintenance of both *B. subtilis* and *E. coli* strains. For experiments in *B. subtilis* cells were grown using a range of media (using the following concentrations unless otherwise noted): Luria-Bertani (LB) medium, Antibiotic 3 (PAB) medium, Brain-Heart Infusion (Bacto), or defined minimal medium base (Spizizen minimal salts supplemented with Fe-NH_4-citrate (1 μg/ml), $MgSO_4$ (6 mM), $CaCl_2$ (100 μM), $MnSO_4$ (130 μM), $ZnCl_2$ (1 μM), thiamine (2 μM)) supplemented with casein hydrolysate (200 μg/ml) and/or various carbon sources (succinate (1%), glycerol (0.5%), glucose (0.5%)). Supplements were added as required: tryptophan (20 μg/ml), phenylalanine (40 μg/ml), chloramphenicol (5 μg/ml), erythromycin (1 μg/ml), kanamycin (2 μg/ml), spectinomycin (50 μg/ml), tetracycline (10 μg/ml), zeocin (10 μg/ml). Unless otherwise stated all chemicals and reagents were obtained from Sigma-Aldrich.

Marker frequency analysis

Sodium azide (0.5%; Sigma) was added to exponentially growing cells to prevent further metabolism. Chromosomal DNA was isolated using a DNeasy Blood and Tissue Kit (Qiagen). The DNA replication origin (*oriC*) region was amplified using primers 5′-GAATTCCTTCAGGCCATTGA-3′ and 5′-GATTTCTGGCGAATTGGAAG-3′; the DNA replication terminus (*ter*) region was amplified using primers 5′-TCCATATCCTCGCTCCTACG-3′ and 5′-ATTCTGCTGATGTGCAATGG-3′. Either Rotor-Gene SYBR Green (Qiagen) or GoTaq (Promega) qPCR mix was used for PCR reactions. Q-PCR was performed in a Rotor-Gene Q Instrument (Qiagen). By use of crossing points (C_T) and PCR efficiency a relative quantification analysis ($\Delta\Delta C_T$) was performed using Rotor-Gene Software version 2.0.2 (Qiagen) to determine the origin:terminus

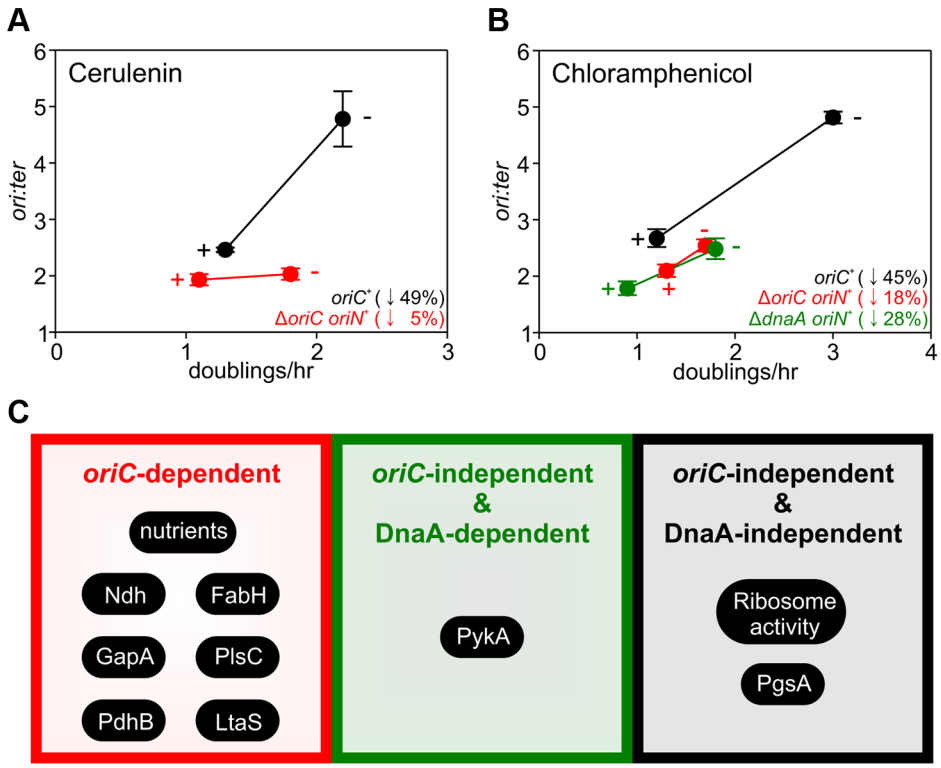

Figure 7. Analysis of *oriC*-dependent and *oriC*-independent growth rate regulation through small molecule targeting of fatty acid synthesis and protein synthesis. Strains were grown overnight at 37°C in LB medium. Overnight cultures were diluted 1:1000 into fresh LB medium either without or with antibiotics (2 μg/ml cerulenin (**A**), 1 μg/ml chloramphenicol (**B**)) and grown at 37°C until they reached an A_{600} of 0.3–0.5. For datapoints "+" indicates the presence of the small molecule inhibitor and "−" indicates the absence. Genomic DNA was harvested from cells and marker frequency analysis was determined using qPCR. The *ori:ter* ratios are plotted versus growth rate and the percentage change in the *ori:ter* ratios comparing each deletion/depletion is indicated (error bars indicate the standard deviation of three technical replicates). Representative data are shown from a single experiment; an independently performed replicate of the experiment is shown in Figure S9. Wild-type (HM715), Δ*oriC oriN*$^+$ (HM950), Δ*dnaA oriN*$^+$ (HM1423). (**C**) Summary of growth rate control systems affecting DNA replication described in this report.
doi:10.1371/journal.pgen.1004731.g007

(*ori:ter*) ratio of each sample. These results were normalized to the *ori:ter* ratio of a DNA sample from *B. subtilis* spores which only contain one chromosome and thus have an *ori/ter* ratio of 1.

Microscopy

To visualize cells during exponential growth starter cultures were grown overnight and then diluted 1:100 into fresh medium and allowed to achieve at least three doublings before observation. Cells were mounted on ~1.2% agar pads (0.25× minimal medium base) and a 0.13–0.17 mm glass coverslip (VWR) was placed on top. To visualize individual cells the cell membrane was stained with either 2 μg/ml Nile Red (Sigma) or 0.4 μg/ml FM5-95 (Molecular Probes). To visualize nucleoids DNA was stained with 2 μg/ml 4′-6-diamidino-2-phenylindole (DAPI) (Sigma). Microscopy was performed on an inverted epifluorescence microscope (Nikon Ti) fitted with a Plan-Apochromat objective (Nikon DM 100x/1.40 Oil Ph3). Light was transmitted from a 300 Watt xenon arc-lamp through a liquid light guide (Sutter Instruments) and images were collected using a CoolSnap HQ^2 cooled CCD camera (Photometrics). All filters were Modified Magnetron ET Sets from Chroma and details are available upon request. Digital images were acquired and analysed using METAMORPH software (version V.6.2r6). Analysis was performed using ImageJ software: foci counting utilized the particle analysis plugin; cell lengths and widths were measured using the ObjectJ plugin.

Western blot analysis

Proteins were separated by electrophoresis using a NuPAGE 4-12% Bis-Tris gradient gel run in MES buffer (Life Technologies) and transferred to a Hybond-P PVDF membrane (GE Healthcare) using a semi-dry apparatus (Hoefer Scientific Instruments). Proteins of interest were probed with polyclonal primary antibodies and then detected with an anti-rabbit horseradish peroxidase-linked secondary antibody using an ImageQuant LAS 4000 mini digital imaging system (GE Healthcare). Quantification was determined by densitometry using Image J software. Figure S3A shows that detection of DnaA, FtsZ and DnaN was within a linear range.

Supporting Information

Figure S1 Culturing *B. subtilis* at different temperatures generates a range of steady-state growth rates but does not affect the frequency of DNA replication initiation. A wild-type strain (HM715) was grown overnight at 23°C in LB. The culture was diluted 1:100 into LB and incubated at different temperatures to generate a range of steady-state growth rates until an A_{600} of 0.2-0.3. Genomic DNA was harvested from cells and marker frequency analysis was determined using qPCR. The *ori:ter* ratios are plotted versus growth rate (error bars indicate the standard deviation of three technical replicates). Representative data are shown from a single experiment; an independently performed replicate of the experiment is shown in Figure 1B.
(PDF)

Figure S2 Cell measurements as a function of nutrient-mediated growth rate. **(A)** Measurement of replication origins per cell. An array of ~25 *tetO* sites was inserted near the replication origin and was visualized using TetR-GFP. Strain AK47 was grown overnight at 37°C in minimal media supplemented with succinate (2%), amino acids (0.2%), spectinomycin (50 μg/ml) and erythromycin (1 μg/ml). Cultures were washed twice and diluted 1:100 into various chemically defined media supplemented with either succinate (2%), glucose (1.5%), or glucose (1.5%) with amino acids (200 μg/ml) and grown at 37°C until they reached an A_{600} of 0.3–0.5. Samples were taken for microscopy and membranes were stained. Scale bar represents 3 μm. **(B)** Quantification of the number of origins per cell at different growth rates. The average number of origins per cell is indicated above each histogram. **(C,E)** Cell lengths were grouped according to the number of origins, measurements were binned in 0.5 μm steps, and data plotted as a percentage within each population. **(D,F)** The average cell lengths and widths (+/− standard deviation) were grouped according to the number of origins per cell.
(PDF)

Figure S3 Western blot analysis of wild-type, *oriN*, and P_{spac}-*dnaA-dnaN* strains. Strains were grown overnight at 37°C in LB medium. Overnight cultures were diluted 1:1000 into fresh LB medium and grown at 37°C until an A_{600} of 0.5-0.7 was attained. Cells were lysed and proteins were detected using Western blot analysis. **(A)** A two-fold dilution series of a cell lysate was used to determine the linear range for each antibody. **(B)** The endogenous *dnaA-dnaN* operon was placed under the control of the IPTG-inducible promoter P_{spac} to generate a range of expression levels. HM742 was supplemented with IPTG (400 μM) and erythromycin. The cultures were diluted 1:100 into LB and grown at 37°C until an A_{600} of 0.5–0.6; HM742 was supplemented with erythromycin and a range of IPTG (800, 400, 200, 100, 50 μM). Cells were lysed and DnaN protein was detected using Western blot analysis (FtsZ protein was likewise detected and used as a loading control). The amount of DnaN was determined using densitometry; values were normalized to wild-type. Wild-type (HM222), P_{spac}-*dnaA-dnaN* (HM742). **(C)** Analysis of *oriN* strains. Wild-type (HM715), $oriC^+$ $oriN^+$ (HM949), Δ*oriC* $oriN^+$ (HM957), Δ*dnaA* $oriN^+$ (HM1423), $dnaA^{R264A}$ $oriN^+$ (HM1122).
(PDF)

Figure S4 Changes in DnaA protein level are not sufficient to account for nutrient-mediated growth rate regulation of DNA replication initiation in *B. subtilis*. **(A)** The endogenous *dnaA* gene was placed under the control of the IPTG-inducible promoter P_{spac} to generate a range of DnaA protein levels. Strains were grown overnight at 37°C in minimal media supplemented with succinate and amino acids (20 μg/ml); IPTG (400 μM) and erythromycin was added to HM742. The cultures were diluted 1:100 into various media (glycerol, glycerol + amino acids, LB) to generate a range of steady-state growth rates and grown at 37°C until an A_{600} of 0.5–0.6; in each medium HM742 was supplemented with erythromycin and a range of IPTG (800, 400, 200, 100, 50 μM). Genomic DNA was harvested from cells and marker frequency analysis was determined using qPCR. For each growth media, the *ori:ter* ratios are plotted versus IPTG concentration (error bars indicate the standard deviation of three technical replicates). Representative data are shown from a single experiment; an independently performed replicate of the experiment is shown in Figure 2B. Wild-type (HM222), P_{spac}-*dnaA* (HM742). **(B)** To strongly overexpress DnaA the endogenous *dnaA* gene was placed under the control of P_{spac} and an ectopic copy of *dnaA* was integrated at the *amyE* locus under the control of the xylose inducible promoter P_{xyl} (HM745). The strain was grown overnight at 37°C in minimal media supplemented with glycerol, amino acids (20 μg/ml), IPTG (800 μM), and erythromycin. The culture was diluted 1:100 into media containing IPTG (800 μM), erythromycin, either glycerol minimal media supplemented with a range of xylose (1, 0.5, 0.25, 0.125, 0.063, 0.031, 0.016, 0.008, 0.004, 0%) or LB, and grown at 37°C until an A_{600} of 0.2–0.4. Genomic DNA was harvested from cells and marker frequency analysis was determined using qPCR. For each growth media, the *ori:ter* ratios are plotted versus xylose concentration

(error bars indicate the standard deviation of three technical replicates). Representative data are shown from a single experiment; an independently performed replicate of the experiment is shown in Figure 2D. **(C)** To determine whether overexpression of DnaA specifically inhibits DNA replication initiation from *oriC*, the endogenous *dnaA* gene was placed under the control of P_{spac}, an ectopic copy of *dnaA* was integrated at the *amyE* locus under the control of the xylose inducible promoter P_{xyl}, *oriC* was inactivated by partial deletion (Δ*incAB*), and DNA replication was driven by *oriN* (HM1467). The strain was grown overnight at 37°C in minimal media supplemented with glycerol, amino acids (20 μg/ml), IPTG (800 μM), and erythromycin. The culture was diluted 1:100 into glycerol minimal media containing IPTG (800 μM), erythromycin, supplemented with a range of xylose (1, 0.5, 0.25, 0.125, 0.063, 0.031, 0.016, 0.008, 0.004, 0%), and grown at 37°C until an A_{600} of 0.2–0.4. Genomic DNA was harvested from cells and marker frequency analysis was determined using qPCR. The *ori:ter* ratios are plotted versus xylose concentration (error bars indicate the standard deviation of three technical replicates).
(PDF)

Figure S5 Nutrient-mediated growth rate regulation of DNA replication initiation is independent of Soj, YabA, and (p)ppGpp. **(A)** Growth rate regulation of DNA replication initiation is maintained in either Δsoj or ΔyabA mutants. Strains were grown overnight at 37°C in minimal media supplemented with succinate and amino acids (20 μg/ml). The culture was diluted 1:100 into various media (succinate, glycerol, glycerol + amino acids, LB) to generate a range of steady-state growth rates and incubated at 37°C until an A_{600} of 0.3–0.4. Genomic DNA was harvested from cells and marker frequency analysis was determined using qPCR. The *ori:ter* ratios are plotted versus growth rate (error bars indicate the standard deviation of three technical replicates). Representative data are shown from a single experiment; an independently performed replicate of the experiment is shown in Figure 3A. Wild-type (HM222), Δ*soj* (HM227), Δ*yabA* (HM739). **(B)** Growth rate regulation of DNA replication initiation is maintained in a Δ*soj* Δ*yabA* double mutant. Cells were grown as in (A). Genomic DNA was harvested from cells and marker frequency analysis was determined using qPCR. The *ori:ter* ratios are plotted versus growth rate (error bars indicate the standard deviation of three technical replicates). Representative data are shown from a single experiment; an independently performed replicate of the experiment is shown in Figure 3A. Wild-type (HM222), Δ*soj* Δ*yabA* (HM741). **(C)** Growth rate regulation of DNA replication initiation does not require (p)ppGpp. Strains were grown overnight at 37°C in minimal media supplemented with succinate and amino acids (200 μg/ml). The culture was diluted 1:100 into various media (succinate + amino acids, glycerol + amino acids, LB) to generate a range of steady-state growth rates and incubated at 37°C until an A_{600} of 0.2–0.6. Genomic DNA was harvested from cells and marker frequency analysis was determined using qPCR. The *ori:ter* ratios are plotted versus growth rate (error bars indicate the standard deviation of three technical replicates). Representative data are shown from a single experiment; an independently performed experiment is shown in Figure 3B. Wild-type (PY79), Δ(p)ppGpp (bSS186).
(PDF)

Figure S6 Nutrient-mediated growth rate regulation of DNA replication initiation requires *oriC* and DnaA. **(A)** *oriC* is required for growth rate regulation of DNA replication initiation. Strains were grown overnight at 37°C in minimal media supplemented with succinate and amino acids (20 μg/ml). The culture was diluted 1:100 into various media (succinate, glycerol, glycerol + amino acids, LB) to generate a range of steady-state growth rates and incubated at 37°C until an A_{600} of 0.3–0.4. Genomic DNA was harvested from cells and marker frequency analysis was determined using qPCR. The *ori:ter* ratios are plotted versus growth rate (error bars indicate the standard deviation of three technical replicates). Representative data are shown from a single experiment; an independently performed replicate of the experiment is shown in Figure 4A. Wild-type (HM715), Δ*oriC oriN*$^+$ (HM950). **(B)** Integration of *oriN* into the *B. subtilis* chromosome does not eliminate growth rate regulation of DNA replication initiation. Strains were grown as in (A). Genomic DNA was harvested from cells and marker frequency analysis was determined using qPCR. The *ori:ter* ratios are plotted versus growth rate (error bars indicate the standard deviation of three technical replicates). Representative data are shown from a single experiment; an independently performed replicate of the experiment is shown in Figure 4B. Wild-type (HM715), *oriC*$^+$ *oriN*$^+$ (HM949). **(C)** DnaA activity is required for growth rate regulation of DNA replication initiation. Strains were grown as in (B). Genomic DNA was harvested from cells and marker frequency analysis was determined using qPCR. The *ori:ter* ratios are plotted versus growth rate (error bars indicate the standard deviation of three technical replicates). Representative data are shown from a single experiment; an independently performed replicate of the experiment is shown in Figure 4C. Wild-type (HM715), $DnaA^{R264A}$ *oriN*$^+$ (HM1122).
(PDF)

Figure S7 Analysis of *oriC*-dependent growth rate regulation through genetic targeting of essential cellular activities. Strains were grown overnight at 37°C in LB medium; strains harbouring plasmids integrated into the genome by single-crossover were supplemented with appropriate antibiotics and inducer (0.1 mM IPTG or 0.1% xylose). Overnight cultures were diluted 1:1000 into fresh LB medium and grown at 37°C until they reached an A_{600} of 0.3–0.5; strains harbouring plasmids integrated by single-crossover were supplemented with appropriate antibiotics either without or with the appropriate inducer (1 mM IPTG or 1% xylose). For datapoints "+" indicates the presence of either the wild-type gene (when comparing with knockout mutants) or the inducer; "−" indicates the absence of either the gene (when comparing with wild-type) or the inducer. Genomic DNA was harvested from cells and marker frequency analysis was determined using qPCR. The *ori:ter* ratios are plotted versus growth rate and the percentage change in the *ori:ter* ratios comparing each deletion/depletion is indicated (error bars indicate the standard deviation of three technical replicates). Representative data are shown from a single experiment; an independently performed replicate of the experiment is shown in Figure 5. **(A)** Wild-type (HM715), Δ*ndh* (HM1318), Δ*oriC oriN*$^+$ (HM957), Δ*ndh* Δ*oriC oriN*$^+$ (HM1319); **(B)** P_{spac}-*gapA* (HM1208), P_{spac}-*gapA* Δ*oriC oriN*$^+$ (HM1221); **(C)** Cultures were supplemented with 0.2% sodium acetate. Wild-type (HM715), Δ*pdhB* (HM1248), Δ*oriC oriN*$^+$ (HM950), Δ*pdhB* Δ*oriC oriN*$^+$ (HM1266); **(D)** P_{spac}-*fabHA* (HM964), P_{spac}-*fabHA* Δ*oriC oriN*$^+$ (HM966); **(E)** P_{xyl}-*plsC* (HM1364), P_{xyl}-*plsC* Δ*oriC oriN*$^+$ (HM1373); **(F)** Wild-type (HM715), Δ*ltaS* (HM1168), Δ*oriC oriN*$^+$ (HM957), Δ*ltaS* Δ*oriC oriN*$^+$ (HM1244).
(PDF)

Figure S8 Analysis of *oriC*-independent growth rate regulation through genetic targeting of essential cellular activities. Strains were grown and data presented as described for Figure S7, except

that the depletion of PgsA required supplementation with 1 mM IPTG to overexpress the xylose repressor. Genomic DNA was harvested from cells and marker frequency analysis was determined using qPCR. The *ori:ter* ratios are plotted versus growth rate and the percentage change in the *ori:ter* ratios comparing each deletion/depletion is indicated (error bars indicate the standard deviation of three technical replicates). Representative data are shown from a single experiment; an independently performed replicate of the experiment is shown in Figure 6. **(A)** P_{spac}-*pykA* (HM1176), P_{spac}-*pykA* Δ*oriC oriN*$^+$ (HM1186); **(B)** P_{xyl}-*pgsA* (HM1365), P_{xyl}-*pgsA* Δ*oriC oriN*$^+$ (HM1374); **(C)** Wild-type (HM715), Δ*rpsU* (HM1150), Δ*rplA* (HM1151), Δ*rplW* (HM1152), Δ*rpmJ* (HM1154), Δ*oriC oriN*$^+$ (HM950), Δ*rpsU* Δ*oriC oriN*$^+$ (HM1156), Δ*rplA* Δ*oriC oriN*$^+$ (HM1157), Δ*rplW* Δ*oriC oriN*$^+$ (HM1158), Δ*rpmJ* Δ*oriC oriN*$^+$ (HM1160). **(D)** P_{spac}-*pykA* (HM1176), P_{spac}-*pykA* Δ*dnaA oriN*$^+$ (HM1425); **(E)** P_{xyl}-*pgsA* (HM1365), P_{xyl}-*pgsA* Δ*dnaA oriN*$^+$ (HM1433); **(F)** Wild-type (HM715), Δ*rpsU* (HM1150), Δ*rplA* (HM1151), Δ*rpmJ* (HM1154), Δ*dnaA oriN*$^+$ (HM1423), Δ*rpsU* Δ*dnaA oriN*$^+$ (HM1429), Δ*rplA* Δ*dnaA oriN*$^+$ (HM1430), Δ*rpmJ* Δ*dnaA oriN*$^+$ (HM1432).
(PDF)

Figure S9 Analysis of *oriC*-dependent and *oriC*-independent growth rate regulation through small molecule targeting of fatty acid synthesis and protein synthesis. Strains were grown overnight at 37°C in LB medium. Overnight cultures were diluted 1:1000 into fresh LB medium either without or with antibiotics (2 μg/ml cerulenin **(A)**, 1 μg/ml chloramphenicol **(B)**) and grown at 37°C until they reached an A_{600} of 0.3-0.5. For datapoints "+" indicates the presence of the small molecule inhibitor and "-" indicates the absence. Genomic DNA was harvested from cells and marker frequency analysis was determined using qPCR. The *ori:ter* ratios are plotted versus growth rate and the percentage change in the *ori:ter* ratios comparing each deletion/depletion is indicated (error bars indicate the standard deviation of three technical replicates). Representative data are shown from a single experiment; independently performed replicates of the experiments are shown in Figures 7A–B. Wild-type (HM715), Δ*oriC oriN*$^+$ (HM950), Δ*dnaA oriN*$^+$ (HM1423).
(PDF)

Table S1 Strain list.
(PDF)

Table S2 Plasmid list.
(PDF)

Table S3 Description of plasmids constructed and primers used.
(PDF)

Text S1 Supplementary references.
(PDF)

Acknowledgments

We thank Yoshikazu Kawai and Romain Mercier for the generous gift of strains and for comments on the manuscript. We thank Simon Syvertsson for strains. We thank Henrik Strahl, Nadia Rostami, Graham Scholefield, and Jeff Errington for useful discussions. We also thank the Editors and the anonymous Reviewers for constructive criticisms and suggestions.

Author Contributions

Conceived and designed the experiments: HM AK. Performed the experiments: HM AK. Analyzed the data: HM AK. Contributed reagents/materials/analysis tools: HM AK. Wrote the paper: HM AK.

References

1. Cooper S, Helmstetter CE (1968) Chromosome replication and the division cycle of *Escherichia coli* B/r. J Mol Biol 31: 519–540.
2. Helmstetter CE, Cooper S (1968) DNA synthesis during the division cycle of rapidly growing *Escherichia coli* B/r. J Mol Biol 31: 507–518.
3. Schaechter M, Maaloe O, Kjelgaard NO (1958) Dependency on medium and temperature on cell size and chemical coposition during balanced growth of *Salmonella typhimurium*. J Gen Microbiol 19: 592–606.
4. Donachie WD (1968) Relationship between cell size and time of initiation of DNA replication. Nature 219: 1077–1079.
5. Wold S, Skarstad K, Steen HB, Stokke T, Boye E (1994) The initiation mass for DNA replication in *Escherichia coli* K-12 is dependent on growth rate. EMBO J 13: 2097–2102.
6. Leonard AC, Grimwade JE (2011) Regulation of DnaA Assembly and Activity: Taking Directions from the Genome. Annu Rev Microbiol 65: 19–35.
7. Duderstadt KE, Chuang K, Berger JM (2011) DNA stretching by bacterial initiators promotes replication origin opening. Nature 478: 209–213.
8. Atlung T, Lobner-Olesen A, Hansen FG (1987) Overproduction of DnaA protein stimulates initiation of chromosome and minichromosome replication in *Escherichia coli*. Mol Gen Genet 206: 51–59.
9. Lobner-Olesen A, Skarstad K, Hansen FG, von Meyenburg K, Boye E (1989) The DnaA protein determines the initiation mass of *Escherichia coli* K-12. Cell 57: 881–889.
10. Hill NS, Kadoya R, Chattoraj DK, Levin PA (2012) Cell size and the initiation of DNA replication in bacteria. PLoS Genetics 8: e1002549.
11. Boye E, Nordstrom K (2003) Coupling the cell cycle to cell growth. EMBO Rep 4: 757–760.
12. Ogura Y, Imai Y, Ogasawara N, Moriya S (2001) Autoregulation of the dnaAzdnaN operon and effects of DnaA protein levels on replication initiation in *Bacillus subtilis*. J Bacteriol 183: 3833–3841.
13. Goranov AI, Breier AM, Merrikh H, Grossman AD (2009) YabA of *Bacillus subtilis* controls DnaA-mediated replication initiation but not the transcriptional response to replication stress. Mol Microbiol 74: 454–466.
14. Sharpe ME, Hauser PM, Sharpe RG, Errington J (1998) *Bacillus subtilis* cell cycle as studied by fluorescence microscopy: constancy of the cell length at initiation of DNA replication and evidence for active nucleoid partitioning. J Bacteriol 180: 547–555.
15. Lark KG, Maaloe O (1956) Nucleic acid synthesis and the division cycle of Salmonella typhimurium. Biochim Biophys Acta 21: 448–458.
16. Lark KG, Maaloe O, Rostock O (1955) Cytological studies of nuclear division in *Salmonella typhimurium*. J Gen Microbiol 13: 318–326.
17. Weart RB, Levin PA (2003) Growth rate-dependent regulation of medial FtsZ ring formation. J Bacteriol 185: 2826–2834.
18. Muntel J, Fromion V, Goelzer A, Maabeta S, Mader U, et al. (2014) Comprehensive absolute quantification of the cytosolic proteome of *Bacillus subtilis* by data independent, parallel fragmentation in liquid chromatography/mass spectrometry (LC/MS(E)). Mol Cell Proteomics 13: 1008–1019.
19. Hassan AK, Moriya S, Ogura M, Tanaka T, Kawamura F, et al. (1997) Suppression of initiation defects of chromosome replication in *Bacillus subtilis dnaA* and *oriC*-deleted mutants by integration of a plasmid replicon into the chromosomes. J Bacteriol 179: 2494–2502.
20. Goranov AI, Katz L, Breier AM, Burge CB, Grossman AD (2005) A transcriptional response to replication status mediated by the conserved bacterial replication protein DnaA. Proc Natl Acad Sci U S A 102: 12932–12937.
21. Murray H, Errington J (2008) Dynamic control of the DNA replication initiation protein DnaA by Soj/ParA. Cell 135: 74–84.
22. Scholefield G, Errington J, Murray H (2012) Soj/ParA stalls DNA replication by inhibiting helix formation of the initiator protein DnaA. EMBO J 31: 1542–1555.
23. Ogura Y, Ogasawara N, Harry EJ, Moriya S (2003) Increasing the ratio of Soj to Spo0J promotes replication initiation in *Bacillus subtilis*. J Bacteriol 185: 6316–6324.
24. Soufo CD, Soufo HJ, Noirot-Gros MF, Steindorf A, Noirot P, et al. (2008) Cell-cycle-dependent spatial sequestration of the DnaA replication initiator protein in *Bacillus subtilis*. Dev Cell 15: 935–941.
25. Merrikh H, Grossman AD (2011) Control of the replication initiator DnaA by an anti-cooperativity factor. Mol Microbiol 82: 434–446.
26. Scholefield G, Murray H (2013) YabA and DnaD inhibit helix assembly of the DNA replication initiation protein DnaA. Mol Microbiol 90: 147–159.
27. Noirot-Gros MF, Dervyn E, Wu LJ, Mervelet P, Errington J, et al. (2002) An expanded view of bacterial DNA replication. Proc Natl Acad Sci USA 99: 8342–8347.
28. Lee PS, Grossman AD (2006) The Chromosome partitioning proteins Soj (ParA) and Spo0J (ParB) contribute to accurate chromosome partitioning, separation of replicated sister origins, and regulation of replication initiation in *Bacillus subtilis*. Mol Microbiol 60: 853–869.

29. Wang X, Tang OW, Riley EP, Rudner DZ (2014) The SMC Condensin Complex Is Required for Origin Segregation in *Bacillus subtilis*. Curr Biol 24: 287–292.
30. Wang X, Montero Llopis P, Rudner DZ (2014) *Bacillus subtilis* chromosome organization oscillates between two distinct patterns. Proc Natl Acad Sci USA 10.1073/pnas.1407461111.
31. Kawakami H, Keyamura K, Katayama T (2005) Formation of an ATP-DnaA-specific initiation complex requires DnaA Arginine 285, a conserved motif in the AAA+ protein family. J Biol Chem 280: 27420–27430.
32. Janniere L, Canceill D, Suski C, Kanga S, Dalmais B, et al. (2007) Genetic evidence for a link between glycolysis and DNA replication. PloS One 2: e447.
33. Maciag M, Nowicki D, Janniere L, Szalewska-Palasz A, Wegrzyn G (2011) Genetic response to metabolic fluctuations: correlation between central carbon metabolism and DNA replication in *Escherichia coli*. Microb Cell Fact 10: 19.
34. Schneider DA, Gourse RL (2004) Relationship between growth rate and ATP concentration in *Escherichia coli*: a bioassay for available cellular ATP. J Biol Chem 279: 8262–8268.
35. Petersen C, Moller LB (2000) Invariance of the nucleoside triphosphate pools of *Escherichia coli* with growth rate. J Biol Chem 275: 3931–3935.
36. Saxena R, Fingland N, Patil D, Sharma AK, Crooke E (2013) Crosstalk between DnaA protein, the initiator of *Escherichia coli* chromosomal replication, and acidic phospholipids present in bacterial membranes. Int J Mol Sci 14: 8517–8537.
37. Sikora AE, Zielke R, Wegrzyn A, Wegrzyn G (2006) DNA replication defect in the *Escherichia coli cgtA(ts)* mutant arising from reduced DnaA levels. Arch Microbiol 185: 340–347.
38. Moriya S, Fukuoka T, Ogasawara N, Yoshikawa H (1988) Regulation of initiation of the chromosomal replication by DnaA-boxes in the origin region of the *Bacillus subtilis* chromosome. EMBO J 7: 2911–2917.
39. Levine A, Vannier F, Dehbi M, Henckes G, Seror SJ (1991) The stringent response blocks DNA replication outside the *ori* region in *Bacillus subtilis* and at the origin in *Escherichia coli*. J Mol Biol 219: 605–613.
40. Wang JD, Sanders GM, Grossman AD (2007) Nutritional control of elongation of DNA replication by (p)ppGpp. Cell 128: 865–875.
41. Lesley JA, Shapiro L (2008) SpoT regulates DnaA stability and initiation of DNA replication in carbon-starved *Caulobacter crescentus*. J Bacteriol 190: 6867–6880.
42. Schreiber G, Ron EZ, Glaser G (1995) ppGpp-mediated regulation of DNA replication and cell division in *Escherichia coli*. Current Microbiol 30: 27–32.
43. Sekimizu K, Kornberg A (1988) Cardiolipin activation of DnaA protein, the initiation protein of replication in *Escherichia coli*. J Biol Chem 263: 7131–7135.
44. Xia W, Dowhan W (1995) *In vivo* evidence for the involvement of anionic phospholipids in initiation of DNA replication in *Escherichia coli*. Proc Natl Acad Sci USA 92: 783–787.
45. Breier AM, Grossman AD (2009) Dynamic association of the replication initiator and transcription factor DnaA with the *Bacillus subtilis* chromosome during replication stress. J Bacteriol 191: 486–493.